DISSERTATIONES
MEDICINAE
UNIVERSITATIS
TARTUENSIS
345

MAARJALIIS PAAVO

Short-Wavelength and Near-Infrared Autofluorescence Imaging in Recessive Stargardt Disease, Choroideremia, *PROM1*-Macular Dystrophy and Ocular Albinism

DISSERTATIONES MEDICINAE UNIVERSITATIS TARTUENSIS
345

DISSERTATIONES MEDICINAE UNIVERSITATIS TARTUENSIS
345

MAARJALIIS PAAVO

Short-Wavelength and Near-Infrared Autofluorescence Imaging in Recessive Stargardt Disease, Choroideremia, *PROM1*-Macular Dystrophy and Ocular Albinism

UNIVERSITY OF TARTU
Press
1632

Department of Ophthalmology, University of Tartu, Tartu, Estonia

Dissertation accepted for the commencement of the degree of Doctor of Philosophy in Medicine on April 19th, 2023 by the Council of the Faculty of Medicine, University of Tartu, Estonia.

Supervisors: Kuldar Kaljurand, MD, PhD, Department of Ophthalmology, Faculty of Medicine, University of Tartu, Estonia

Professor Janet R. Sparrow, PhD, Department of Ophthalmology and Department of Pathology & Cell Biology, Columbia University, USA

Reviewers: Eeva-Marja Sankila, MD, PhD, Department of Ophthalmology, Helsinki University Hospital, Helsinki, Finland

Kalev Nõupuu, MD, PhD, Department of Ophthalmology, Faculty of Medicine, University of Tartu, Estonia

Opponent: Professor Carel Hoyng, MD, PhD, Radboud University Medical Centre, Nijmegen, the Netherlands

Commencement: 19th of June 2023

ISSN 1024-395X (print)
ISBN 978-9916-27-208-4 (print)

ISSN 2806-240X (pdf)
ISBN 978-9916-27-209-1 (pdf)

University of Tartu Press
www.tyk.ee

TABLE OF CONTENTS

LIST OF ORIGINAL PUBLICATIONS

I. **Paavo M**, Zhao J, Kim HJ, Lee W, Zernant J, Cai C, Allikmets R, Tsang SH, Sparrow JR. **Mutations in GPR143/OA1 and ABCA4 Inform Interpretations of Short-Wavelength and Near-Infrared Fundus Autofluorescence**. Invest Ophthalmol Vis Sci. 2018 May 1;59(6):2459–2469. doi: 10.1167/iovs.18-24213. PMID: 29847651; PMCID: PMC5959512.

II. **Paavo M**, Carvalho JRL Jr, Lee W, Sengillo JD, Tsang SH, Sparrow JR. **Patterns and Intensities of Near-Infrared and Short-Wavelength Fundus Autofluorescence in Choroideremia Probands and Carriers**. Invest Ophthalmol Vis Sci. 2019 Sep 3;60(12):3752–3761. doi: 10.1167/iovs.19-27366. PMID: 31499530; PMCID: PMC6735265.

III. **Paavo M**, Lee W, Allikmets R, Tsang S, Sparrow JR. **Photoreceptor cells as a source of fundus autofluorescence in recessive Stargardt disease**. J Neurosci Res. 2019 Jan;97(1):98–106. doi: 10.1002/jnr.24252. Epub 2018 Apr 27. PMID: 29701254; PMCID: PMC6532423.

IV. **Paavo M,** Lee W, Parmann R, Lima de Carvalho-Jr J, Zernant J, Tsang S, Allikmets R. **Insights into PROM1-Macular Disease Using Multimodal Imaging**. – Accepted by *IOVS* March 2023

Contribution of the author to the preparation of the original publications:

Article I: Collecting the clinical material, participation in the design of the study, patient recruitment, retinal imaging, data analysis and interpretation, preparing the illustrations and participation in the manuscript writing process. Experiments with mice were carried out and analyzed in prof. Janet R. Sparrow laboratory

Article II: Collecting clinical material, proposing the research idea, planning the study design, analyzing the phenotypic and clinical data, preparing the figures and writing the manuscript.

Article III: Collecting clinical material, analyzing the data, preparing the figures and participation in writing the manuscript.

Article IV: Collecting clinical material, retinal imaging, planning the study design, analyzing the phenotypic and clinical data, preparing the figures and writing the manuscript.

ABBREVIATIONS

ABCA4	Retinal-specific ATP-binding cassette transporter
ABCA4	A gene which encodes the ABCA4 transporter
AF	Autofluorescence
FAF	Fundus autofluorescence
A2E	N-retinylidene-N-retinylethanolamine
BCVA	Best corrected visual acuity
CHM	Choroideremia
CI	Confidence interval
CRISPR	Clustered regularly interspaced short palindromic repeats
Cas9	CRISPR-associated protein 9
cSLO	Confocal scanning laser ophthalmoscope
ELM	External limiting membrane
EZ	Ellipsoid zone
Ff ERG	Full-field electroretinography
GCL	Ganglion cell layer
GPR143	G protein-coupled receptor 143
GL	Grey level
HPLC	High-performance liquid chromatography
ILM	Internal limiting membrane
INL	Inner nuclear layer
IPL	Inner plexiform layer
IRD	Inherited retinal disease
IR-R	Infrared reflectance
IS	Inner segment
IZ	Interdigitation zone
MRP	Melanin-related protein
NFL	Nerve fibre layer
NIR-AF	Near-infrared autofluorescence
NRPE	N-retinylidene-phosphatidylethanolamine
OA1	Ocular albinism type 1
ONL	Outer nuclear layer
OPL	Outer plexiform layer
ORT	Outer retinal tubulation
OS	Outer segment
PE	Phosphatidylethanolamine
PEDF	Pigment epithelial derived factor
PMEL	Premelanosome protein
Rab	Ras-associated-binding
RDH8	Retinol dehydrogenase 8
REP-1	Rab escort protein
RPE	Retinal pigment epithelium
SD-OCT	Spectral-domain optical coherence tomography

STGD1	Stargardt disease type 1
STGD4	Stargardt disease type 4
SW-AF	Short-wavelength autofluorescence
VEGF	Vascular endothelial growth factor

1. INTRODUCTION

Inherited retinal diseases are the leading cause of visual impairment among the working age-group in the developed countries. To date over 300 genes (https://web.sph.uth.edu/RetNet/) have been associated with different retinal dystrophies. Separately each of these diseases are very rare and in most cases disease mechanisms are still not fully understood.

Because of genetic and phenotypical heterogeneity diagnosis of inherited retinal disease has been challenging. The human eye is a complex and delicate organ and it is not feasible to take tissue samples from human retina for diagnosis and research. Therefore retinal imaging studies which are noninvasive, are an invaluable source of information under a variety of retinal conditions and are being widely used in the clinical setting. Retinal imaging techniques have evolved a lot over the decades. Traditional fundus camera allowed us to capture what the ophthalmologist sees when viewing the fundus with the biomicroscope. The addition of lasers into imaging systems opened another dimension by allowing us to see the invisible by creating cross-sections visualizing retinal layers or making use of the autofluorescence emitted from retinal natural fluorophores. These imaging techniques have developed from early research methods to unreplacable diagnostic tools in everyday ophthalmology.

Correct interpretation of the imaging data is also important. Different imaging techniques can detect abnormalities in retinal structure but also reveal changes in biological processes of the retina. Major advances have been made over the last decades in developing new therapeutic interventions for inherited retinal disease leading to the approval of first gene augmentation therapy for *RPE65*-related retinal dystrophy. However most of retinal dystrophies still need further studying and development of suitable treatment options. In the light of new therapeutic interventions, imaging studies also offer valuable outcome measures in evaluating treatment efficiency.

This study aims to provide insights into fundus autofluorescence imaging. We analyzed short-wavelength and near-infared autofluorescence qualitatively and quantitatively in cases of genetically confirmed recessive Stargardt disease, choroideremia, *PROM1*-macular disease and ocular albinism to better understand the sources of fundus autofluorescence. We also aimed at finding new clinical implications for autofluorescence imaging in evaluating inherited retinal disease.

2. LITERATURE REVIEW

2.1. The fundus of the human eye

The fundus is the interior surface of the eye. Vision is our primary sense of perception and most of stimuli we receive come through the retina. Topographically retina is composed of the macula, which is the central part of retina and peripheral retina. The fovea provides high acuity vision and structurally presents as a depression in the center of the macula situated 2,5 mm lateral to the optic disc (Ross and Pawlina 2016) and is composed mainly of cone photoreceptors. The dense packing of the cells is responsible for sharp vision (Kolb, Fernandez, and Nelson 1995; Bringmann et al. 2018). Fovea is further divided into three parts. Fovea centralis, also known as foveal pit, has the highest portion of cones, but lacks rod photoreceptors and is an avascular zone (Kolb, Fernandez, and Nelson 1995). During the fetal development of fovea, the inner retinal layers are displaced to the side forming the foveal depression and foveal maturation continues even after birth until early adolescence (Hendrickson et al. 2012; Bringmann et al. 2018). The other parts are parafovea, which extends about 1–3 mm from central fovea and perifovea, which is located at about 3–5 mm from the foveal pit. Nasal to the macula is the optic disc with retinal arteries and veins passing through. The peripheral part of retina is mostly made up of rod photoreceptors (Ross and Pawlina 2016) which are responsible for night vision (**Figure 1, A)**.

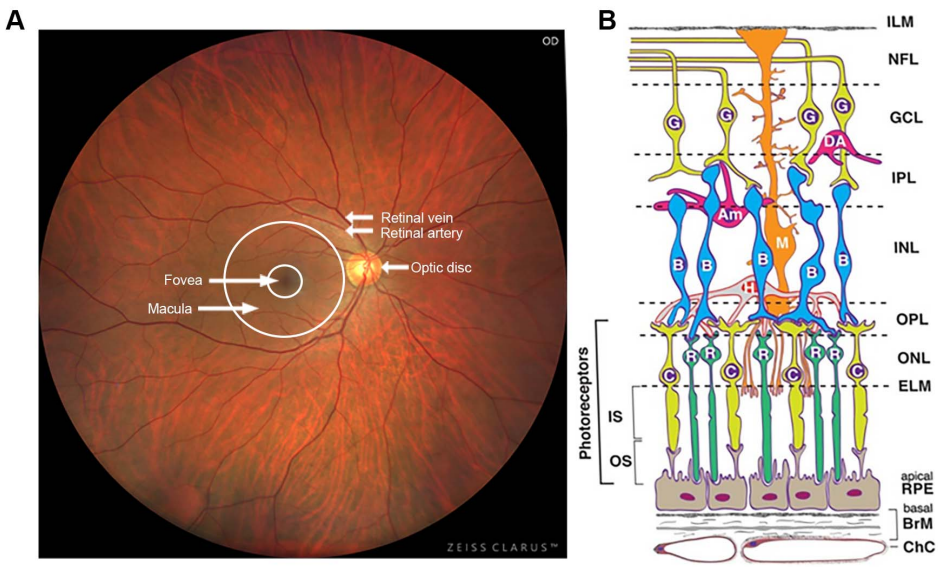

Figure 1. Healthy eye. **A.** Color fundus photograph demonstrating fovea, macula, optic disc and blood vessels. **B**. A schematic drawing of retina and the choroid. RPE, retinal pigment epithelium. C, cone photoreceptor; R, rod photoreceptor; H, horizontal cell

(interneuron); B, bipolar cell (interneuron); M, Müller cell; Am, amacrine cell (interneuron); DA, displaced amacrine cell (interneuron); G, ganglion cell. Layers: ChC, choriocapillaris; BrM, Bruch's membrane; ELM, external limiting membrane; ONL, outer nuclear layer; OPL, outer plexiform layer; INL, inner nuclear layer; IPL, inner plexiform layer; GCL, ganglion cell layer; NFL, nerve fiber layer (ganglion cell axons); ILM, inner limiting membrane. Ref: (Zheng et al. 2012).

2.1.1. Retinal structure and cell types

The retina is the innermost layer of the posterior pole of the eye. The photoreceptor cells of the retina are responsible for converting the light into electrical impulses that are sent to the brain. The retina can be divided into neurosensory or neural retina and retinal pigment epithelium (RPE) together with Bruch's membrane.

Histologically, neurosensory retina is made up of 9 layers: photoreceptor layer, the external limiting membrane (ELM), the outer nuclear layer (ONL), the outer plexiform layer (OPL), the inner nuclear layer (INL), the inner plexiform layer (IPL), the ganglion cell layer (GCL), the nerve fiber layer (NFL) and the inner limiting membrane (ILM) (Ross and Pawlina 2016) (**Figure 1, B**).

The retinal pigment epithelium is a monolayer of cuboidal pigmented cells that is situated on the Bruch's membrane. The apical extensions of the RPE surround the photoreceptor outer segments. The photoreceptor layer is composed of highly specialized neurons: rods make up the majority of retinal photoreceptor cells, while cones account for only 3–5% of photoreceptors. Topographically the fovea is a rod-free zone but has a very high density of cones (Sung and Chuang 2010). The cone system offers the highest visual acuity and resolution due to the fact that each foveal cone is connected to only one bipolar and one ganglion cell, whereas in the rest of the retina each bipolar and ganglion cell has to serve multiple photoreceptors (Sung and Chuang 2010). Photoreceptors consist of an outer segment (OS), connecting stalk and the inner segment (IS) (**Figure 1, B**); the latter is divided into outer ellipsoid and inner myoid part. The OS is made up of flattened membranous structures called discs within which the light absorbing rod and cone opsin visual pigments are housed. The IS is responsible for protein synthesis and energy production. The ELM is not a true membrane, but is formed from Müller cell's apical ends that are attached to rods and cones. The ONL contains the nuclei of photoreceptor cells and the OPL is formed by the processes of photoreceptors and interneuron cells (horizontal, plexiform, amacrine and bipolar cells), where the electrical signal is transmitted via synapses. The nuclei of interneuron cells together with Müller's cells are located in the INL. Müller's cells have long processes that extend form ELM to ILM throughout the retina. The IPL is where the connections of interneuron cells and ganglion cells form. The GCL consists of large multipolar neurons with long axons that pass into the NFL and merge into the optic nerve. The innermost layer ILM is made up of basal lamina of Müller cells (Ross and Pawlina 2016; Hendrickson et al. 2012) (**Figure 1, B**).

Posterior to the retina is the pigmented vascular layer known as the choroid; the latter is situated between the RPE and sclera (**Figure 2, B**). Choroidal vessels provide the outer retina with nutrients and oxygen whereas the inner part of retina gets its blood supply from intraretinal vascular plexuses originating from the central ophthalmic artery. The vessels in the choroid decrease in size closer to the retina and the adjacent layer to the RPE is called the choriocapillary layer which is responsible for the exchange of nutrients and metabolites with retina. The perivascular space consists of choroidal melanocytes, connective tissue, immune system cells, lymphatic channels and smooth muscle cells (Ross and Pawlina 2016) (**Figure 1, B)**.

2.1.2. Photoreceptors and the visual cycle

Photoreceptors are specialized neurons that initiate the visual perception process. Human retina is composed of mainly rods with a ratio of 95:5 between rods and cones, however the fovea is made up of only densely packed cone photoreceptors (Ross and Pawlina 2016; Sung and Chuang 2010; Kolb, Fernandez, and Nelson 1995).

Rod photoreceptors can detect dim light and produce monochromatic vision whereas cone photoreceptors are responsible for bright light function and color vision (Fu and Yau 2007; Kefalov 2012). Rod pigments absorb light at a maximum of 496 nm, while cones can be divided into classes: L, M and S meaning long- (588 nm), middle- (521) and short-wavelength (420) sensitivity (Ross and Pawlina 2016; Kolb, Fernandez, and Nelson 1995).

Phototransduction is a complex process in the retina where light is turned into electrical impulses. Light is absorbed by photoreceptor visual pigments: rhodopsin in rods and iodopsin in cones. In that process the light absorbing chromophore vitamin A derivative 11-*cis*-retinal, bound to cone and rod opsin proteins, is isomerized to the all-*trans*-retinal configuration and released from opsin – this process is known as bleaching (Wald 1968; Leibrock, Reuter, and Lamb 1998; Kefalov 2012). The all-*trans*-retinal is subsequently reduced to all-*trans*-retinol and transported to the RPE and Müller cells where through a multistep conversion all-*trans*-retinal is recycled back to 11-*cis*-retinal that allows the visual pigment to regain light sensitivity (Fulton and Rando 1987; Ross and Pawlina 2016; Saari 2000) **(Figure 2).** Cones can regain sensitivity within 3–4 minutes while rods take over 30 minutes to restore light sensitivity. This difference is attributable to an additional pathway for recycling the 11-*cis* chromophore to cones that is not dependent on RPE. Specifically Müller cells provide cones with 11-*cis*-retinol for the synthesis of cone chromophore (Mata et al. 2002; Saari 2012; Ross and Pawlina 2016; Leibrock, Reuter, and Lamb 1998).

Defects in different proteins and enzymes that participate in the visual cycle lead to various retinal conditions ranging from stationary visual deficits to severe forms of progressive retinal dystrophies (Travis et al. 2007).

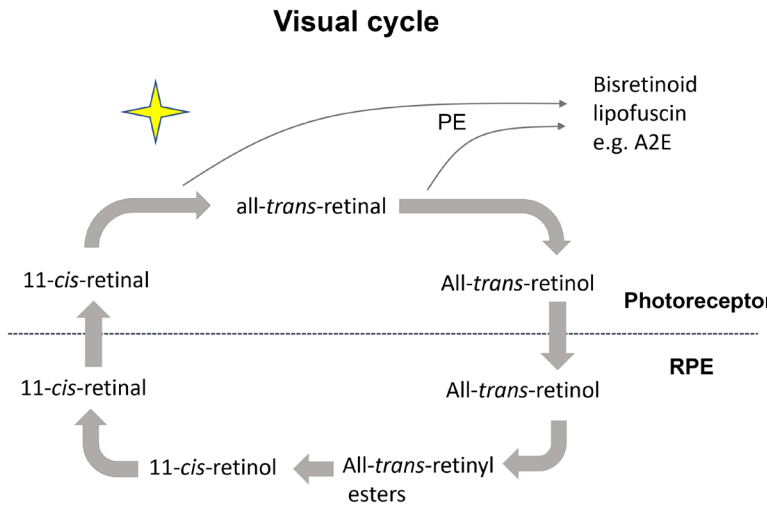

Figure 2. Visual cycle. Light is absorbed by the chromophore 11-*cis*-retinal, a vitamin A derivative; 11-*cis*-retinal is then isomerized to all trans-retinal. The all-*trans*-retinal is subsequently reduced to all-*trans*-retinol and transported to the RPE where all-trans-retinol is recycled back to 11-*cis*-retinal in a multistep process that allows the visual pigment to regain light sensitivity. Bisretinoid fluorophores such as A2E are formed in photoreceptors when all-*trans* retinal and 11-*cis*-retinal react non-enzymatically with phosphatidylethanolamine (PE).

2.1.3. Retinal pigment epithelium

Retinal pigment epithelium (RPE) is a polarized layer of cells that is situated posterior to neural retina and is essential to the functioning of neuroretina. The RPE is a monolayer of cells that maintains the outer blood-retinal barrier by forming tight junctions. This restricts the passage of molecules between neural retina and choroid. The apical side of RPE cells faces the photoreceptor outer segments. Microvilli extending from apical side of the RPE envelope the photoreceptor outer segments. Correct anatomical positioning of RPE-neurosensory retina is important since photoreceptors rely on RPE cells for functioning (Sparrow, Hicks, and Hamel 2010; Boulton and Dayhaw-Barker 2001; Anderson and Fisher 1979; Spaide and Curcio 2011).

Besides aforementioned blood-retinal barrier and restoring of photosensitivity in the visual cycle, the RPE has other prominent roles. These functions include the absorption of stray light and the transport of fluid, ions and nutrients to the retina. RPE is responsible for the transport and storing of retinoids that are needed for the visual cycle (Bok 1990; Saari 2012). Another major role of the RPE is the phagocytosis and degradation of photoreceptor outer segments, which are renewed approximately every 7–12 days (Young 1971; Young and Droz 1968; Sung and Chuang 2010). Consequently, the bisretinoid fluorophores

that form in photoreceptor outer segments accumulate in RPE rather than in photoreceptor cells. Bisretinoids are sensitive to light and can oxidatively damage proteins and lipids (S.R. Kim et al. 2006).

2.1.4. Bisretinoid lipofuscin

The bisretinoid lipofuscin that accumulates in RPE is unique in terms of the spectral qualities, mode of formation and composition. Lipofuscin pigments in RPE originate from photoreceptor cell outer segments (Katz et al. 1986) and are formed by random inadvertent reactions of vitamin A aldehyde (all-*trans*-retinaldehyde; 11-*cis*-retinal) of the visual cycle (Katz, Eldred, and Robison 1987) (**Figure 2**). After absorbing a photon of light, the 11-*cis*-retinal chromophore of rhodopsin and cone pigment undergoes isomerization to all-*trans*-retinaldehyde. Released retinaldehyde reacts with phosphatidylethanolamine (PE) in the outer segment disc membrane and forms a reversible Schiff base adduct, N-retinylidene-PE (NRPE) (Ahn, Wong, and Molday 2000; L.L. Molday, Rabin, and Molday 2000; H. Sun, Molday, and Nathans 1999). The ATP-binding cassette (ABC) transporter ABCA4 that is expressed by photoreceptor cells (Illing, Molday, and Molday 1997; H. Sun and Nathans 2001, 1997) is responsible for flipping the NRPE from the interior of outer segment discs to the cytoplasmic space. Most of retinaldehyde is reduced to a less reactive alcohol (all-*trans*-retinol) by the cytoplasmic retinol dehydrogenase (Rdh). However some retinaldehyde escapes this reduction allowing two retinaldehydes to condense with PE nonenzymatically. As a result bisretinoid fluorophores are irreversibly formed in the outer segment compartments of the photoreceptor cells (Parish et al. 1998; Liu et al. 2000; S.R. Kim, He, et al. 2007).

In a healthy retina there is constant renewal of photoreceptor outer segments, so bisretinoid compounds are kept to a minimum in photoreceptor cells by means of daily shedding of outer segment membrane followed by RPE-mediated phagocytic clearance. If these light-absorbing fluorophores were to collect in outer segments, they could interfere with photon absorbance by cone and rod visual pigments. Consequently, the bisretinoid compounds are deposited as lipofuscin in the lysosomes of the RPE cells (Sparrow et al. 2008; Tsybovsky, Molday, and Palczewski 2010; Ben-Shabat et al. 2002).

The heterogeneous mixture of bisretinoid fluorophores includes A2-GPE (A2-glycero-phosphoethanolamine), A2-DHP-PE (A2-dihydropyridine-phosphatidylethanolamine), all-*trans*-retinal dimer-PE (all-*trans*-retinal dimer phosphatidylethanolamine), and the most well known one A2E (Fishkin et al. 2005; Parish et al. 1998; Yamamoto et al. 2011; H.J. Kim and Sparrow 2018).

These various bisretinoids account for the fundus autofluorescence (AF) signal with the excitation maximum in the blue (~470 nm) and emission maximum in the yellow-orange spectrum range (~600 nm) (Sparrow et al. 2010). These bisretinoids have slightly different absorbance maxima yet they all fluoresce in response to blue 488 nm excitation and have similar emission spectra (Fishkin et al. 2005; Parish et al. 1998; Sparrow et al. 1999). Interestingly visual

cycle mediators like all-*trans*-retinal and all-*trans*-retinyl ester do not show any fluorescence (Sparrow et al. 2010).

Vitamin A intake and serum retinol levels can affect bisretinoid formation in RPE (Radu et al. 2005; Katz and Norberg 1992). The accumulation of bisretinoid lipofuscin in RPE with age has been well documented (Feeney 1978; Feeney-Burns, Hilderbrand, and Eldridge 1984; Weiter et al. 1986). Bisretinoid lipofuscin accumulation is the highest in the macular area and lower in the fovea which correlates with the distribution of rod photoreceptors suggesting that phagocytized rod outer segments are the main source for bisretinoid lipofuscin (Feeney 1978). A2E is a major bisretinoid compound which has been studied more extensively and has been shown to cause inflammatory and cytotoxic changes in RPE cells leading to degeneration (De and Sakmar 2002; Sparrow, Vollmer-Snarr, et al. 2003). Accumulation of bisretinoid lipofuscin and exposure to short-wavelength visible light has also been shown to increase oxidative stress and trigger apoptosis in RPE cells (Wassell et al. 1999; Sparrow et al. 1999).

2.1.5. Ocular melanin

Melanin is found in various cells in the human body. Brown/black eumelanin and red pheomelanin are present in the eye and skin, while neuromelanin is only present in the brain. In the eye melanin can be found in the uveal melanocytes and in the pigmented epithelial cells like RPE, iris pigment epithelium and ciliary pigment epithelium. (Hu, Simon, and Sarna 2008)

Melanin in the RPE originates from the neuroectoderm, while the melanin in uveal and skin melanocytes develops from neural crest. Uveal and skin melanocytes show continual synthesis of melanin during life, but in the RPE the majority of melanosomes are formed during the fetal period and adult RPE contains only adult melanosomes where the biosynthesis of melanin is either absent or very low (Simon, Hong, and Peles 2008). RPE contains mainly eumelanin, which is the most common type of melanin (Weiter et al. 1986; Hu, Simon, and Sarna 2008), but pheomelanin is also present. Those two melanins originate from different precursors in melanogenesis: eumelanins are derived from the oxidation of tyrosine by tyrosinase, while pheomelanins go through subsequent reaction with cysteine (Hu, Simon, and Sarna 2008; Simon, Hong, and Peles 2008).

Melanosomes are organelles for melanin synthesis, storage and transport. Melanosomes mature in stages: The first stage is formation of an endosome. In the second stage endosomes develop longitudinal pre-melanosome protein fibrils without melanin. In the third stage there are clear pigmented fibrils. In the fourth stage melanosomes reach maturity and are densely filled with melanin (Watt et al. 2009).

Melanin in the uveal melanocytes varies with race and eye color, whereas the melanin in RPE is considered to be independent on those factors (Weiter et al. 1986). Uveal melanocytes contain eumelanin and pheomelanin. In dark

colored eyes, the ratio of eumelanin is higher in relation to pheomelanin and in light colored eyes the vice versa (Wielgus and Sarna 2005; Wakamatsu et al. 2008). The role of melanin in the eye is to prevent light scattering to optimize visual acuity, but it also has antioxidant properties. Both melanins – eumelanin and pheomelanin, are protective against free radicals, but eumelanin is thought to be less photoreactive and therefore less cytotoxic (Ortonne 2002), which could also explain why dark-colored eyes have less age-related macular degeneration and uveal melanoma (Hu et al. 2005; Group 2000).

2.1.6. Topography and distribution of RPE melanin and lipofuscin

RPE cells differ in shape topographically in the fundus: the peripheral cells are more flat, while the macular RPE cells are taller and contain more condensely packed melanin granules (Boulton and Dayhaw-Barker 2001). Melanin granules in the RPE melanosomes are situated apically in the cell whereas lipofuscin is located mostly basally, but with age they can also combine into melanolipofuscin complexes (Feeney 1978; Feeney-Burns, Hilderbrand, and Eldridge 1984). Weiter et al. showed by *ex vivo* optical measurements that the concentration of RPE melanin decreased from the periphery to posterior pole, but increased again in macular area. RPE lipofuscin content was lower in the periphery and higher in posterior pole, but showed a significant reduction in the foveal area (Weiter et al. 1986). Roughly said there is an inverse distribution of RPE melanin compared to lipofuscin. Choroidal melanin increased gradually from the periphery and submacular choroid showed the highest level of pigmentation (Feeney-Burns 1984, Weiter 1986).

Besides melanin and lipofuscin there are other pigments in the retina: macular pigment is a yellowish pigment that is composed of meso-zeaxanthin, lutein and zeaxanthin (Landrum and Bone 2001). Macular pigment aids visual performance by alleviating chromatic aberration through the absorption of blue light. Melanopsin, found in retinal ganglion cells belongs to a photopigment family together with rod and cone opsins, but does not participate in the visual sensation process; it instead regulates circadian rhythms (Hattar et al. 2002).

2.2. Retinal imaging

Retinal imaging has become a valuable tool in modern ophthalmology with various techniques and devices. A traditional fundus camera uses single bright flash to obtain a high-resolution 35 to 50 degree true color image. Fundus cameras also allow for autofluorescence imaging using blue light excitation (Park et al. 2013).

Confocal scanning laser ophthalmosocpy (cSLO) system is another widely used technique that creates fundus images by scanning the retina with two laser-beams. cSLO systems offer capturing of non-invasive pseudo-color (**Figure 1A)**,

reflectance, red-free, autofluorescence images, as well as invasive fluorescein angiography and indocyanine angiography (Hassenstein and Meyer 2009). While these imaging techniques offer *en face* images of the fundus, spectral domain optical coherence tomography (SD-OCT) offers a cross-sectional image of retinal layers and is often combined in the same camera together with cSLO. The development of cSLO cameras has allowed for imaging of not only central retina with 30° or 55° field, but also capturing wide-field images from the peripheral retina. Optical coherence tomography angiography (OCTA) has offered a non-invasive imaging method for retinal vessels. Adaptive optics is another modern imaging tenchology that allows us to assess ocular health in the microscopic level. As this study is focused on multimodal imaging using the cSLO and SD-OCT, these imaging methods will be described here in more detail.

2.2.1. Confocal scanning laser ophtalmoscopy

In modern ophthalmology cSLO is a widely used imaging technology. The first cSLO camera was introduced in 1980-s (Webb, Hughes, and Pomerantzeff 1980), but has advanced substantially over the decades. cSLO cameras use a point light source – a laserbeam that scans the retina at different points vertically and horizontally, the backscattered light is recorded as a greyscale image. cSLO has been used for various imaging modalities like fluorescein angiography, indocyanin green angiography and autofluorescence (Bille 2019).

Fundus camera systems use longer wavelength (530 to 580 nm) excitation compared to cSLO (488 nm) for AF imaging. While the fundus camera obtains a single image with a flash, the cSLO captures a series AF images using the short wavelength excitation light. Post-acquisition processing allows for the mean image to be calculated and pixel values are normalized in order to reduce background noise. The result is a greyscale image from values 0 to 256 with dark pixels presenting lower and light pixels presenting higher signal strength (Schmitz-Valckenberg et al. 2008). Compared to cSLO imaging the fundus camera AF signal is lower and is more susceptible to artefacts from anterior segment (Park et al. 2013).

The most widely used commercial device for cSLO, the HRA SD-OCT can be combined with the cSLO for simultaneous fundus and OCT recordings (**Figure 3)**.

The Heidelberg Spcetralis® HRA2 offers short-wavelength autofluorescence (SW-AF) by using 488 nm for excitation and a >500 nm filter for emission. Near-infrared autofluorescence is also possible by using a 787-nm excitation and >800 emission filter. Images are typically recorded either as a 30° × 30° or 55° × 55° field. The wavelength of the SD-OCT imaging system is 870 nm. This instrument has an axial resolution of approximately 7 μm (Heidelberg Engineering. Heidelberg HRA 2 retina angiograph – operation manual. Germany: Heidelberg Engineering GmbH; 2003).

2.2.2. SD-OCT and anatomical correlates

Spectral-domain optical coherence tomography offers a noninvasive visualization of the anatomy of the retina (**Figure 3, B**). SD-OCT systems use near-infrared light (centered at ~ 850 nm or ~ 1050 nm) to detect the back-scattered light from the retinal layers to generate cross-sectional images. The layers are formed as bands of higher and lower reflectivity based on their structural components and to some extent they correspond to the classical histological layers of retina. The outermost highly reflective band corresponds to the retinal pigment epithelium (RPE) and Bruch's membrane. The next hyperreflective band, that can be difficult to distinguish from RPE is the interdigitation zone (IZ) which is thought to be the RPE apical processes reaching around the cone outer segment tips. The next clearly distinguishable hyperreflective layer is the ellipsoid zone (EZ) that is thought to present the inner segment of photoreceptors and is packed with mitochondria (Spaide and Curcio 2011). A more delicate hyperreflective band anterior to the EZ is the external limiting membrane (ELM), where Müller cells' apical ends meet the photoreceptors. The next rather wide hyporeflective layer corresponds to the outer nuclear layer (ONL) with the photoreceptor cell bodies. The hyperreflective band on top of ONL is the outer plexiform layer (OPL). This is followed by the hyporeflective inner nuclear layer (INL) with interneuron and Müller cell bodies followed by the hyperreflective inner plexiform layer (IPL). The superficial layers of retina are made up of less reflective ganglion cell layer (GCL) and more reflective nerve fibre layer (NFL) (**Figure 3, B**) (Spaide and Curcio 2011; Staurenghi et al. 2014).

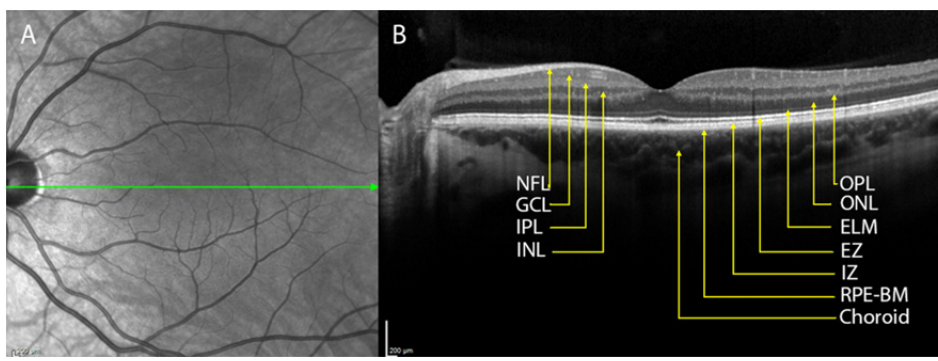

Figure 3 A. IR-R fundus image showing the topographic position of SD-OCT section **B**. SD-OCT scan through the fovea showing the hypo-and hyperreflective layers: NFL – nerve fibre layer. GCL – ganglion cell layer. IPL – inner plexiform layer. INL – inner nuclear layer. OPL – outer plexiform layer. ONL – outer nuclear layer. ELM – external limiting membrane. EZ – ellipsoid zone. IZ – interdigitation zone. RPE-BM – retinal pigment epithelium-Bruchs membrane complex. Choroid.

In routine clinical practice most SD-OCT images are acquired simultaneously with a near infrared reflectance fundus image (IR-R) which uses an excitation wavelength of 820 nm, whereas the barrier filters are completely removed (**Figure 3, A**) (Hassenstein and Meyer 2009; Elsner et al. 1996). The longer wavelength allows to detect changes in the retina, highly reflective structures at the subretinal and sub-RPE level are enhanced and better recognized. IR-R also has the ability to penetrate opaque media or cataracts as no flash is needed (Hassenstein and Meyer 2009).

2.2.3. Origins of fundus autofluorescence

Fluorescence is a well known physical concept where a molecule absorbs a photon of certain excitation wavelength, undergoes molecular energy transformations, and emits a lower energy photon of specific emission wavelength (F. C. Delori, Staurenghi, et al. 1995). The excitation wavelength is always shorter than the emission wavelength. Different molecular spectrums have a wavelength maximum at which the fluorophore results in greatest intensity of fluorescence. Similarly, the emission spectra exhibits a wavelength at which emission intensity is maximum.

Similar imaging concept is used in fluorescein angiography and indocyanine green angiography with the help of injecting a fluorescent dye intravenously. In fundus autofluorescence AF imaging naturally occurring endogenous retinal fluorophores are used as the source of fluorescence making this technique non-invasive. Fundus signal was first noted in the clinical setting about 50 years ago during angiography procedure before injecting the fluorescein dye (Bonnin, Passot, and Triolaire-Cotten 1976; Rabb et al. 1978).

The fundus AF of the human eye was first measured by introducing fundus spectrometer (François C. Delori 1992). Further in vivo studies showed that fundus autofluorescence had a peak emission at 630 nm and that autofluorescence increased with age (F. C. Delori, Dorey, et al. 1995).

While the term fundus AF has often been used to refer to short-wavelength autofluorescence, another major source of autofluofluorescence is based on melanin and accounts for near-infrared autolfluorescence signal (Keilhauer and Delori 2006).

More recent studies have also aimed at describing green-light autofluorescence that has become available in some commercial devices and operates at higher excitation wavelength compared to SW-AF. The exact contribution of fluorophores in green-light AF and its differences from SW-AF still need further research (Borrelli et al. 2020; Bittencourt et al. 2019).

2.2.4. Short-wavelength autofluorescence

Fundus short-wavelength autofluorescence (SW-AF) is an inherent signal originating predominantly from bisretinoid fluorophores. SW-AF can be elicited by excitation with a laserlight within the spectral range 400 and 590 nm, with a

peak excitation at 490–510 nm (F. C. Delori, Staurenghi, et al. 1995) and emission with a peak in the yellow–orange range 600–610 nm. Spectral characteristics as well as histopathological studies have confirmed that the cellular source of SW-AF is bisretinoid compounds (Eagle et al. 1980; F. C. Delori, Dorey, et al. 1995; Weiter et al. 1986; Sparrow et al. 2010; Wing, Blanchard, and Weiter 1978).

Bisretinoid lipofuscin is a mixture of more than 20 fluorophores, out of which the A2E is best known (Sparrow, Fishkin, et al. 2003). Bisretinoid fluorophores are formed in the outer segments of photoreceptors during a non-enzymatic reactions of vitamin A aldehyde and then deposited in the RPE cells as bisretinoid lipofuscin (F. C. Delori, Staurenghi, et al. 1995; Sparrow et al. 2010).

Delori et al. also demonstrated the topographic distribution of SW-AF in the healthy eye. The macular area within 7°–15° from fovea showing the highest and fovea the lowest SW-AF signal. The signal in the fovea is low because of attenuation by macular pigment, reduction of lipofuscin content and increased RPE melanin granules, the latter being positioned apically of lipofuscin in the RPE (**Figure 4, C**) (F. C. Delori, Dorey, et al. 1995; Robson, Moreland, et al. 2003). The SW-AF signal is relatively homogeneous outside the macular area and represents the distribution of RPE lipofuscin. (von Rückmann, Fitzke, and Bird 1995) Blood vessels appear dark due to blockage of the SW-AF signal while the optic disk is dark due to the absence of SW-AF emission because there are no RPE cells (**Figure 4, A)**.

The dominant source of SW-AF signal is located at the RPE-photoreceptor level, however the photopigments in the photoreceptors act as a barrier (Schmitz-Valckenberg et al. 2021). Bleaching of rod photopigment rhodopsin with blue-light can account for a 30% rise SW-AF signal compared to the dark-adapted state (Theelen et al. 2008).

Overall areas of increased SW-AF signal or hyperautofluorescence can result from increased concentration of fluorophores or unmasking of these compounds from outer retinal atrophy. In areas of hypoautofluorescence the reason can be reduced fluorophores in RPE cells or absence of RPE cells as in cases of atrophy or blockage of signal from e.g. retinal hemorrhage (von Rückmann, Fitzke, and Bird 1995).

An age-related increase in bisretinoid liposfuscin associated SW-AF signal has been described as well as higher levels of SW-AF in Caucasian population versus African-American or Asian ethnicities (Boulton et al. 1990; Greenberg et al. 2013). There are other factors that can also influence the SW-AF signal, like dense vitreous opacities or the aging human lens that can absorb blue-light and reduce autofluorescence (Ranjan and Beedu 2006; Gaillard et al. 2000).

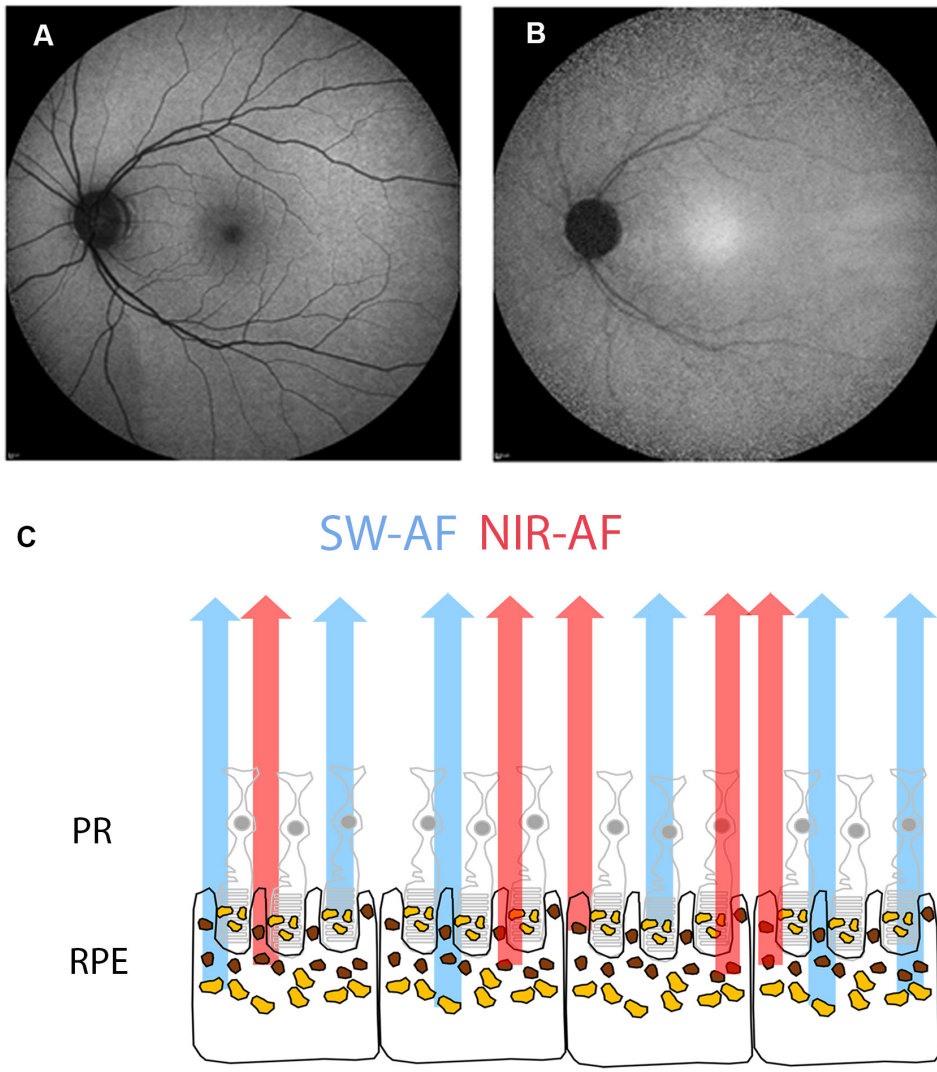

Figure 4. Short-wavelength autofluorescence (SW-AF) **A** and near-infrared autofluorescence (NIR-AF) **B** of a healthy eye (33 year-old white female). **C** schematic drawing of fundus autofluorescence signal originating from lipofuscin (yellow) and melanin (brown) granules.

2.2.5. Near-infrared autofluorescence

SW-AF imaging has become the cornerstone of fundus autofluorescence and is widely used in both research and clinical practice, however another less used major source of autofluorescence is melanin that accounts for near-infrared autofluorescence (NIR-AF).

Picolino et al. noticed pseudofluorescence at 805 nm before conducting indocyanine angiography (Piccolino et al. 1996). With the development of cSLO imaging techniques our understanding of NIR-AF has been advanced. The NIR-AF signal is known to originate primarily from melanin in the RPE cells and to lesser extent from the choroidal melanin and can be excited at 787 nm with the emission >800 nm. Melanin related signal is much weaker than that of bis-retinoid lipofuscin, even with significantly higher radiant power and detection sensitivity (Keilhauer and Delori 2006; Boulton et al. 1990). Therefore the NIR-AF image is usually of lower contrast compared to SW-AF image of the same eye (**Figure 4 A, B**).

In addition to the high foveal NIR-AF signal that corresponds to elevated melanin optical density in RPE (Keilhauer and Delori 2006; Weiter et al. 1986; U. Kellner, Kellner, and Weinitz 2010), it has been shown that NIR-AF signal is strong and bright in the case of full-thickness macular hole (Keilhauer and Delori 2006) and diminished in cases of RPE atrophy, confirming that RPE melanin is the major source of fundus NIR-AF signal (Duncker, Marsiglia, et al. 2014).

The choroidal contribution to the NIR-AF signal becomes more evident in choroidal nevi, which appear hyperautofluorescent in NIR-AF imaging (Keilhauer and Delori 2006; U. Kellner, Kellner, and Weinitz 2010).

In healthy eyes SW-AF signal is attenuated in the fovea and NIR-AF signal is the strongest in the fovea (Keilhauer and Delori 2006) which corresponds to the higher concentration of melanin in the RPE cells (Weiter et al. 1986). In ex vivo studies it has been shown that the optical density of melanin is highest in the foveal area, where the RPE cells are taller and contain more melanin (Weiter et al. 1986). More precisely the maximum intensity of NIR-AF signal in the fovea is located slightly nasal to the maximum of SW-AF signal, the latter being with higher contrast and exposure (Keilhauer and Delori 2006). While macular pigment absorbs SW-AF light accounting for the central macula hypoAF signal, the NIR-AF light is not affected by macular pigment and therefore allows better evaluation of central macula. Outside of the macular area both NIR-AF and SW-AF signal are rather uniform**.** As with SW-AF imaging, optic disc (lack of autofluorescent material) and blood vessels (absorbance of signal) have no SW-AF signal and are seen as hypoautofluorescent (**Figure 4 B**). As in SW-AF imaging, areas of RPE atrophy present with reduced NIR-AF signal due to the loss of RPE cells (Duncker, Marsiglia, et al. 2014).

Whereas increased lipofuscin concentration with age has been observed in RPE cells, melanin in the RPE cells decreases after 40 years of age (Feeney-Burns, Hilderbrand, and Eldridge 1984; Schmidt and Peisch 1986). Melanin in the choroid and iris melanosomes does not go through that change (Weiter et al. 1986). Photo-oxidation with blue light is thought to increase the autofluorescence of melanin (Kayatz et al. 2001), so that could slow down the reduction of NIR-AF levels with aging (Docchio et al. 1991).

NIR-AF signal originates mostly from melanin and its related compounds: melanolipofuscin, melanolysosomes and oxidized melanin. In the RPE cell me-

lanin is situated apically and lipofuscin basally (**Figure 4C**). With age RPE melanosomes containing melanin fuse with lysosomes and melanolipofuscin is formed through melanin degradation and remodeling (Docchio et al. 1991). Melanolipofuscin is a complex granule that has a melanin core and a lipofuscin shell (Feeney 1978; Biesemeier, Schraermeyer, and Eibl 2011).

2.2.6. Quantitative fundus autofluorescence

Fundus AF images can be valuable on their own, however additional information about the condition of retina can be acquired through quantitatively evaluating AF signal strength. In fundus AF images each pixel can be assigned a grey value level between 0 to 255 using e.g the Heidelberg Eye Explorer software. However that does not offer information if the values of AF signal are truly lower or higher and how they deviate from normal.

Early studies in human subjects to measure the level of SW-AF signal were carried out with the noninvasive spectrophotometry and showed the increase of RPE lipofuscin with an elevated AF signal in recessive Stragardt disease (F. C. Delori, Dorey, et al. 1995; F. Delori et al. 2011). Studies using the cSLO systems constructed linear profiles of AF intensities or in a predetermined area of pixels (Cideciyan et al. 2004; Lois et al. 2000; Lois et al. 2004; Lois et al. 1999; von Rückmann, Fitzke, and Bird 1995, 1997).

The quantitative autofluorescence (qAF) method was developed by Delori et al. to allow a standardized method for combining AF intensity measurements with spatial information (F. Delori et al. 2011). The images are acquired with the cSLO (HRA2, Spectralis HRA + OCT, Heidelberg Engineering, Heidelberg Germany), with a 30° × 30° field, 488 nm excitation, and emission capture from 500 to 680 nm. The camera is modified with the addition of a special reference bar that is seen on top of every qAF image (**Figure 5, B**), to account for variable detector sensitivity and variable laser power. Additional factors such as laser power, the laser off-set (zero signal provided by the instrument software), detector sensitivity, refractive errors, and variations in anterior media structures like lens opacities are also considered in the calculation formula. Pupils are dilated before recording the images, the photoreceptor visual pigment is bleached with SW-AF light for 20 seconds. Each image is acquired in high-speed video mode (8.9 frames/ second); two images are recorded, each being typically 9–12 frames. Images are then examined for quality and at least 6 of the 9–12 frames are selected. Selected frames are aligned and averaged and saved in non-normalized mode to avoid histogram stretching (F. Delori et al. 2011; Burke et al. 2014).

At eccentricities of 7–8° (2–2.3 mm) from the fovea the absorption by macular pigment is minimal (Bone et al. 1988) therefore calculation of qAF within concentric segments 7–9° eccentric to the fovea (as described below) is not affected by absorption. The qAF8 ring refers to 8 predetermined circular segments in that area that is mostly used to calculate qAF values, but qAF values can also be measured in other segments or manually selected areas. The software also allows for generation of qAF color coded maps, where cool colors like blue and

green illustrate lower and warm colors like yellow and red higher qAF values **(Figure 5**).

This method enables comparisons amongst serial images in the same or different subjects. Between session repeatability of qAF (95% confidence limits; method of Bland-Altmann) calculated in multiple studies has ranged from 7 to 10% (Burke et al. 2014; F. Delori et al. 2011; Duncker, Tsang, Woods, et al. 2015) indicating that qAF will only differ by more than 7–10%, 5% of the time. Quantitative autofluorescence levels exhibit a significant increase with age. In healthy eyes, qAF increases with increasing eccentricity up to 10–15◦ from the fovea with the highest values being superotemporally (Greenberg et al. 2013) **(Figure 5, B, C**). Furthermore, qAF values have been shown to be higher in females. In addition there may be ethnic differences: compared with Hispanics, qAF is significantly higher in whites and lower in Blacks and Asians (**Figure 5, A**) (Greenberg et al. 2013).

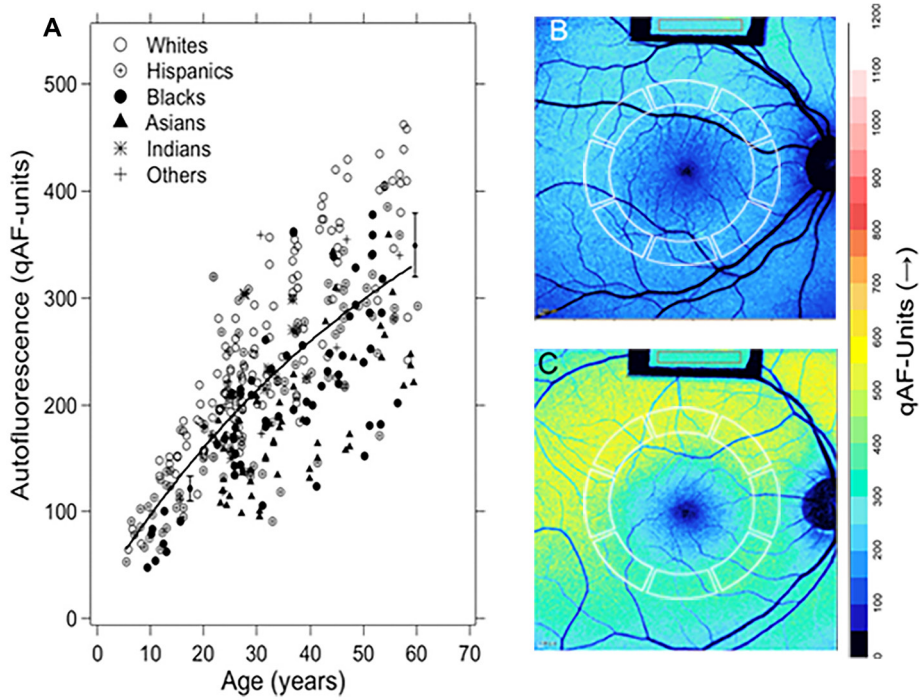

Figure 5: **A**. qAF intensities in healthy eyes by ethnicity plotted against age. (Greenberg et al. 2013)(Copyright 2013 The Association for Research in Vision and Ophthalmology, Inc).; **B**. qAF color map of a 30 y.o **C**. qAF color map of 50 y.o. with the classical qAF8 ring in eight segments.

2.3. Inherited retinal disease

Inherited retinal diseases (IRD) are a the main cause of visual impairment in pediatric and working age populations in developed countries (Liew, Michaelides, and Bunce 2014; Heath Jeffery et al. 2021; Solebo, Teoh, and Rahi 2017) and are thought to affect 1 in 2000 people worldwide (Sohocki et al. 2001).

Over 300 causative genes have been identified, with most forms of IRD mainly affecting photoreceptors but can also primarily affect the RPE or the inner retina (https://web.sph.uth.edu/RetNet/).

Until recently people diagnosed with IRD were faced with no prospect of treatment. With the approval of the first gene augmentation therapy for a rare form of Leber congenital amaurosis related with *RPE65* mutation in 2017 (X. Wang et al. 2020), the paradigm has changed on uncurable inherited retinal disease. In *RPE65* gene therapy the treatment restores the retinoid cycle that ultimately results in production of the 11- *cis*-retinal chromophore needed for a functioning visual pigment. Various therapeutic trials aimed at other retinal dystrophies are focused on gene augmentation, gene modification with CRISPR/Cas9 technology, but also other molecular therapies, stem cell-based therapies and retinal prostheses (da Costa et al. 2021; Kaczmarek, Kowalski, and Anderson 2017; Mead et al. 2015; Weiland and Humayun 2014). As many IRDs are caused by deficits in the visual cycle, resulting in either inadequate production of 11-*cis*-retinal or build-up of excess toxic retinoid, some drug trials are aimed at altering vitamin A metabolism in the visual cycle (Sundaramurthi et al. 2019).

While retinal imaging studies play an important role in timely and correct diagnosis (Boon et al. 2008; Yung, Klufas, and Sarraf 2016), they also offer invaluable information about disease process (Georgiou et al. 2020; Strauss et al. 2019) and can aid in finding new therapeutic targets. In assessing treatment efficacy in clinical trials, imaging studies can offer various end-points/outcome measures (Jolly, Bridge, and MacLaren 2019). Deviations in AF intensity and texture can be observed in nearly all inherited retinal degenerative diseases where an increase or decrease of AF signal or abnormal AF patterns are indicative of an abnormal visual cycle or disruption in the tissue architecture (Georgiou, Fujinami, and Michaelides 2020).

2.3.1. Recessive Stargardt disease

Autosomal recessive Stargardt disease (STGD1, OMIM 248200) is the most common juvenile macular dystrophy with the prevalence of 1:10 000 (Michaelides et al. 2003). The disease typically presents with central visual field disturbance in teens or early adulthood (Michaelides et al. 2003; Tanna et al. 2017), but late onset disease is also possible with milder symptoms in middle-aged subjects (Westeneng-van Haaften et al. 2012).

The disease is caused by mutations in the *ABCA4* gene which encodes the ATP-binding cassette transporter in the outer segments of cone and rod photoreceptors and is a vital player in the visual cycle (Allikmets 1997). ABCA4

transporter's role is to clear the photoreceptors from the excessive 11-*cis* and all-*trans* retinal, which are both reactive and potentially toxic to the photoreceptors (Cideciyan et al. 2004; Tsybovsky, Molday, and Palczewski 2010; Quazi, Lenevich, and Molday 2012; Quazi and Molday 2014).

With photon absorbance all-*trans*-retinal is released into rod and cone outer segments and most of it diffuses freely across the lipid bilayer to the cytoplasm where it is taken up by RDH8 and detoxified. But a fraction of all-*trans*-retinal forms a reversible Schiff base compound called phosphatidylethanol-N-retinylidene-phosphatidylethanolamine (NRPE) which is transported by ABCA4 to the cytoplasmic side of the membrane. That is where the role of ABCA4 transporter is essential in transporting NRPE to photoreceptor disc surface where it can be reduced to the less reactive alcohol (all-*trans*-retinol) (Tsybovsky, Molday, and Palczewski 2010). In the case of defective ABCA4 protein, an accumulation of NRPE allows a second retinaldehyde molecule to react and form a non-reversible bisretinoid molecule in the outer segments of photoreceptors which subsequently are deposited in the RPE (R.S. Molday and Zhang 2010). RPE cells participate in photoreceptor cell outer segment renewal by phagocytosis of shed outer segments and with that the excessive bisretinoid complexes accumulate in the RPE cells leading to cellular damage (Sparrow et al. 1999; Holz et al. 1999; Sparrow, Nakanishi, and Parish 2000; Sparrow, Zhou, and Cai 2003; Zhou et al. 2009) and degeneration of RPE-photoreceptor complex (Sparrow and Boulton 2005; Cideciyan et al. 2004; Burke et al. 2014; Sparrow et al. 2012). The accumulation of bisretinoid fluorophores in the retina has also been confirmed in a *Abca4* mouse model (Weng et al. 1999; Sparrow et al. 2013; Charbel Issa et al. 2013; S.R. Kim, Jang, et al. 2007). Studies on *Abca4* knockout mouse model have shown that photoreceptor cells degeneratate with photooxidation (Ueda et al. 2016; Radu et al. 2008; Sparrow, Zhou, and Cai 2003; Sparrow, Nakanishi, and Parish 2000; Sparrow et al. 2013). Besides this well-studied pathological pathway, there are also studies implying that low-level inflammation can have a part in STGD1 pathogenesis, because photooxidation of bisretinoid compounds could lead to complement activation (Zhou et al. 2009; Zhou et al. 2006) and microglia activation. (Radu et al. 2011; Kohno et al. 2013).

There has been some debate on the sequence of cellular involvement in the disease process. The primary event in STGD1 is thought to be the accumulation of bisretinoid in photoreceptor outer segments, that is transferred into RPE cells through phagocytosis. Excessive accumulation of bisretinoid lipofuscin leads to RPE dysfunction and cell loss. Photoreceptor cell loss happens subsequently because of pathological RPE (Cideciyan et al. 2004; Sparrow and Boulton 2005; Duncker, Marsiglia, et al. 2014; Fang et al. 2020; Greenstein et al. 2015). Other imaging studies have proposed photoreceptor layer to be the initial site of cell degeneration (Song et al. 2015; Gomes et al. 2009).

2.3.1.1. Genetic and clinical aspects

STGD1 is genetically heterogenous. Over 1200 different mutations have been associated with *ABCA4* related STGD1 (Allikmets et al. 1997; Zernant et al. 2011; Fujinami, Zernant, et al. 2013; F.P.M. Cremers et al. 2020). Depending of the severity of the mutation and the remaining function of ABCA4 protein affected, there is variability in disease severity.

The disease can be clinically categorized based on electrophysiology (ERG) findings: Group 1 shows abnormal pattern ERG with normal full-field(ff) ERG, group 2 shows cone dysfunction in ffERG and group 3 shows a more advanced loss of cone and rod function (Lois et al 2001). These groups are not different stages of a disease but have a prognostic value with group 1 having the best and group 3 the worst prognosis (Fujinami, Lois, et al. 2013).

Typically the disease starts in the first or second decade of life with disturbance of central vision and milder retinal changes either seen as abnormal foveal reflex, bull's eye maculopathy or small yellowish flecks in the fundus examination (Fishman 1976; Lois et al. 2001; Fujinami, Zernant, et al. 2013; F.P.M. Cremers et al. 2020). With high-quality retinal imaging it is possible to detect early changes in SD-OCT scans in the foveal area like ILM thickening or abnormal patterns in fundus AF images (W. Lee et al. 2014; Fujinami et al. 2014). RPE atrophy in macular area with or without foveal sparing and widespread confluent fleck patterns usually ensue with a loss of central vision later in adulthood (Lois et al. 2001; Fujinami, Zernant, et al. 2013; F.P.M. Cremers et al. 2020).

Genotype-phenotype correlation has been difficult to establish because of wide allelic heterogeneity and genotype may vary between different cases or even within the same pedigree. Two major disease-causing variants of *ABCA4*, p.(Gly1961Glu) and p.(Asn1868Ile) have been associated with mildest prognoses presenting with bull's eye maculopathy or optic gap phenotype (W. Lee et al. 2022; Burke et al. 2012; Cella et al. 2009; Fujinami, Zernant, et al. 2013; Nõupuu et al. 2014). *ABCA4* variants resulting in null alleles such as stop-gain, frameshift, canonical splice site, large copy number variants and some missense variants are more likely to present with severe phenotypes like cone-rod dystrophy, rapid-onset chorioretinopathy and generalized retinitis pigmentosa-like features (W. Lee et al. 2022; F.P.M. Cremers et al. 2020).

2.3.1.2. Retinal Imaging

Due to phenotypic heterogeneity, differential diagnosis of STGD1 remains challenging, as there are other retinal diseases with similar findings, e.g. *PRPH1*-related pattern dystrophy (Duncker, Tsang, Woods, et al. 2015), *ELOVL4*-associated STGD3 (A.O. Edwards et al. 1999; K. Zhang et al. 2001), *PROM1*-macular dystrophy also known as STGD4 (M.F. Kniazeva, Chiang, Cutting, et al. 1999), bulls eye maculopathies like hydroxychloroquine retinopathy (Nõupuu et al. 2016).

High-quality retinal imaging is an important tool in STGD1 diagnosis and management. SD-OCT imaging usually reveals changes in outer retinal layers corresponding to photoreceptors. ILM thickening can be seen in early STGD1 (W. Lee et al. 2014), whereas disruption of EZ and ONL thinning ensue as the disease progresses (Greenstein et al. 2015; Duncker, Marsiglia, et al. 2014; K.N. Khan, Kasilian, et al. 2018). White yellowish retinal flecks that are seen in the fundus usually correspond to hyperreflective material at the level of outer retinal layers. In later stages of photoreceptor and RPE atrophy the SD-OCT shows loss of photoreceptor attributable layers and RPE, with increased SD-OCT signal seen as hypertransmission (Sparrow et al. 2015). The areas of EZ loss corresponded to areas of reduced SW-AF and NIR-AF signal (Müller et al. 2019) and absence of SW-AF signal usually colocalizes with RPE atrophy in SD-OCT images. Cidecyan et al 2004 have proposed 6 stages of STGD1: Stage I as a normal retinal structure and function. Stage II, increased AF intensity but normal retinal function. Stage III is defined as an increase in the mean fundus AF intensity and AF texture. Stage IV with increased fundus AF texture with partial degeneration of photoreceptors; Stage V with reduction of the mean fundus AF intensity and reduction of visual function and stage VI as the end-stage is characterized as a complete loss of the RPE and photoreceptors (Cideciyan et al. 2004).

The excessive accumulation of bisretinoid fluorophores is what accounts for the increased SW-AF signal in STGD1 patients (F. Delori et al. 2011; Burke et al. 2014), which can help to differentiate it from other similar retinal diseases (Duncker, Tsang, Woods, et al. 2015; Duncker, Tsang, Lee, et al. 2015).

Previous studies with qAF have revealed that there is an increase in SW-AF signal even in areas with healthy looking retina (Burke et al. 2014) and functional studies have shown that increased level of AF does not necessarily correspond to reduced retinal function (Müller et al. 2019). Fleck-formations appear as mostly hyperautofluorescent foci in SW-AF imaging (Cideciyan et al. 2004; Sparrow et al. 2015) and have been spatially correlated with reduced retinal function (Verdina et al. 2012).

The excessive bisretinoid deposition eventually leads to RPE cell atrophy as demonstrated by decreased SW-AF and NIR-AF signal (Cideciyan et al. 2004; Duncker, Marsiglia, et al. 2014). However SW-AF and NIR-AF imaging can show different extent of atrophy in STGD1 patients with NIR-AF imaging showing a wider area with decreased signal (Duncker, Marsiglia, et al. 2014; Greenstein et al. 2015; Cicinelli et al. 2020; Parmann et al. 2022). The centrifugal progression of the disease observed in SW-AF imaging has been described, but the mechanism behind that is not yet fully understood (Cukras et al. 2012).

2.3.1.3. Therapeutic considerations

At the moment there are no approved treatment options for STGD1, however there are ongoing clinical trials of stem cell therapy, gene replacement therapy

and pharmacological approaches (Hussain et al. 2018; F.P.M. Cremers et al. 2020). Gene replacement therapy with adeno-associated-virus vector have been studied for various IRD, but in the case of STGD1 the large size of the *ABCA4* gene makes that approach challenging. Lentivirus-based transport mechanism in *ABCA4* gene augmentation therapy has been studied, but recently finished phase I/II phase trials showed that even though the treatment was well tolerated, patients showed no significant improvement in visual function (Parker et al. 2022).

Stem-cell based therapy aimed at restoring RPE monolayer is another approach, but it is unclear whether transplantation of RPE cells alone is enough or is it necessary to include photoreceptor cells. Mutation-specific therapies that mainly employ antisense oligonucleotides that are targeted at mutations that affect pre-mRNA splicing have shown promising results in some IRD clinical trials and are in the preclinical phase in regards of *ABCA4* disease. CRISPR/Cas9 technology also allows mutation specific corrections by single basepair substitutions with the wild-type nucleotide (F.P.M. Cremers et al. 2020). Studies on animals have shown a possible harmful effect of vitamin A with *ABCA4* deficiency, so the current guideline is to avoid vitamin A supplements in STGD1 patients (Federspiel, Bertelsen, and Kessel 2018). Another line of interventional trials have aimed at testing drugs that could reduce bisretinoid lipofuscin build-up in the RPE cells by administering a modified form of vitamin A which reduces abnormal vitamin A dimerization (J. Zhang et al. 2015; Saad and Washington 2016; Kaufman, Ma, and Washington 2011).

2.3.2. Ocular albinism

Albinism is a rare congenital and non-progressive genetic disorder, in which melanin biosynthesis is affected. That results in hypopigmentation of hair, skin and eyes (Lyle, Sangster, and Williams 1997). Different forms of oculocutaneous and ocular albinism have been described being either autosomal recessive or x-chomosome linked (Oetting and King 1999; Oetting 2002).

2.3.2.1. Genetic and molecular aspects

Ocular albinism type 1 or the X-linked ocular albinism (OA1, OMIM #300500) also known as Nettleship-Falls is the most common form of ocular albinism with prevalence of 1 in 60,000 to 1 in 150 000 (Rosenberg and Schwartz 1998; Tsang and Sharma 2018) https://www.orpha.net/consor/cgi-bin/OC_Exp.php?Expert=54&lng=EN) and was first described by Bassi et al. in 1995. It results from mutations in the G protein-coupled receptor 143 (*GPR143*) gene (Bassi et al. 1995), that is expressed in melanocytes and RPE cells (Palmisano et al. 2008; Garner and Jay 1980; Schnur et al. 1998). Various disease causing variants have been reported with point mutations being common, but pathogenic splicing mutations, small insertions and deletions as well as the deletion of entire exons and other complex mutations have been reported in the *GPR143* gene (Bueschbell, Manga, and Schiedel 2022).

GPR143 is responsible for the delivery of melanin-related protein (MRP) to mature melanosomes and regulates transcription of melanosome genes as well as melanosome size. GPR143 loss of function does not impair melanin synthesis through the activity of tyrosinase like in oculocutaneous albinism, but reduces the expression of premelanosome protein (PMEL), PMEL is a melanosomal structural protein that is responsible for providing melanosome fibrillar matrix during melanin polymerization. As PMEL activity is reduced in OA1, melanin is synthesized but melanosomes are grossly enlarged and reduced in number and the organization of melanin in the melanosomes is altered (Cortese et al. 2005; Schiaffino 2010; Falletta et al. 2014). Melanosome maturation has also been described in the introduction in the paragraph about ocular melanin.

GPR143 has also a role in retinal development through production of pigment epithelial derived factor (PEDF) and downregulation of vascular endothelial growth factor (VEGF) so that defective GPR143 will lead to foveal vascularization and abnormal structure (Falk et al. 2012; Bakker et al. 2022; McKay 2019). GPR143 possibly also has an effect on retinal development by regulating release of endosomes that are needed in cellular communication and trafficking (McKay 2019).

2.3.2.2. Clinical aspects of OA1

In the OA1 the RPE is hypopigmented because instead of normal melanosomes, there are fewer macromelanosomes and they are not evenly dispersed in the RPE cells (Cortese et al. 2005; Garner and Jay 1980). Affected males can have ocular findings like translucent iris, photophobia, foveal hypoplasia, nystagmus and miswiring of the optic tract (Schiaffino 2010; Chong et al. 2009). Extraocular pigmentation is usually normal, however macromelanosomes can also be found in the skin in addition to ocular structures (Schiaffino 2010). Patients present with subnormal vision since birth, but the pathology is non-progressive in nature (Creel, Summers, and King 1990; Lyle, Sangster, and Williams 1997; Zhong et al. 2021). Previously it has been shown that visual acuity is correlated with the level of melanin in fundus in albinism patients (Summers 1996). There is also reduced macular pigment in the fundus of albinism patients (Wolfson et al. 2016).

Females can be carriers of the mutation on one of their X chromosomes, but because of a second healthy X chromosome, they do not develop the same manifestations as affected males. However they usually do present with a typical fundus mosaicism, that is also seen in some other carriers of X-linked diseases like choroideremia and *RPGR*-related retinitis pigmentosa (K.N. Khan et al. 2016; K.N. Khan, Lord, et al. 2018; Wu et al. 2018). Lyonisation is a process where in females either the maternal or paternal X-chromosome is transcriptionally silenced during embryogenesis via random selection (Lyon 1972). Because of that females can present with a typical mosaic of fundus pigmentation where wild-type pigmented RPE cells are seen adjacent to hypopigmented cells where the mutated X-chromosome is activated. That can be recognized as a

typical radial mud-splatter pigmentation-depigmentation pattern and this retinal finding is considered benign and non-progressive (Charles et al. 1992; Moshiri et al. 2013). The radial pattern is thought to be a result of RPE cell peripheral migration during eye development (Kwan et al. 2012). During optic cup morphogenesis the mixed population of normal and mutated RPE precursors will undergo pinwheel movements and then spread peripherally characterized by a pigmented and nonpigmented mosaic pattern (Moshiri et al. 2013). Despite the abnormal fundus findings and occasional iris transillumination, ocular albinism female carriers have normal vision (Charles et al. 1992).

As ocular albinism is non-progressive condition present at birth not much research is focused on possible therapies. Some clinical trials for OCA have aimed at replacing the lack of L-DOPA or using nitisinone, an oral inhibitor of tyrosine degradation. No significant improvement in visual acuity was noted but the trials were not specifically targeting very young patients (Summers et al. 2014; Adams et al. 2019).

2.3.2.3. Retinal imaging

SD-OCT imaging can be challenging for albinism patients due to nystagmus. Persistance of nerve fibre and ganglion cell layer in the fovea with the absence of physiological foveal depression has been shown in SD-OCT studies (Chong et al. 2009). SW-AF imaging shows absence of foveal hypoautofluorescence due to the reduced macular pigment in patients with albinism (Wolfson et al. 2016).

Because of lack of nystagmus, OA1 carriers make better candidates for imaging studies. SD-OCT imaging in OA1 female carriers can show mild persistence of inner retinal layers at fovea while the radial pigmentation mosaic in the fundus is even better visualized with SW-AF imaging (K.N. Khan, Lord, et al. 2018; Welch, Li, and Shields 2018).

2.3.3. Choroideremia

Choroideremia (CHM, OMIM 303100) is another X-linked recessive disorder that affects 1 in 50,000 individuals (Zinkernagel and MacLaren 2015) with a high prevalence in Finland (Sankila et al. 1992). The disease is caused by pathogenic variants in the *CHM* gene, that encodes the Rab escort protein (REP-1), which is expressed in variety of tissues as well as in the retina, RPE and choroid (https://www.proteinatlas.org/ENSG00000188419-).

2.3.3.1. Molecular and clinical aspects

In 1990 Cremers and colleagues cloned the gene, *CHM* located on the X-chromosome (Xq13-q22) and described loss-of-function *CHM* variants as the cause for CHM (F.P. Cremers et al. 1990). Disease causing variants in *CHM* are mostly null or loss of function mutations (Simunovic et al. 2016). A recent

review by Zeits et al showed that majority (76%) of the CHM reported mutations are gene/exon deletions, indels and nonsense variants, while the minority were splice-sites and missense changes (Zeitz et al. 2021). Some disease causing variants may also be located in deep intronic (Carss et al. 2017) or promoter regions (Radziwon et al. 2017) and might be therefore missed with standard laboratory sequencing.

There is not substantial evidence of genotype-phenotype correlation in CHM (Freund, Sergeev, and MacDonald 2016; Simunovic et al. 2016) however, rare cases of a splicing defect c.940+3delA have been associated with notably slow disease progression (Fry et al. 2020).

REP1 is important in activation of Ras-associated-binding (Rab) proteins and participates in the lipid modification of Rab GTPases (Seabra, Ho, and Anant 1995; Corbeel and Freson 2008). Rabs are important regulators of vesicle formation, intracellular trafficking and organelle movement. REP-1 is essential for the prenylation of Rab27a, which regulates melanin transport within melanosomes and intracellular protein trafficking (Seabra, Ho, and Anant 1995). These Rabs participate in trafficking of rhodopsin and other proteins in the photoreceptors (Kwok et al. 2008; J. Wang and Deretic 2014).

Another isoform REP-2 is present in most cell types and can compensate for REP-1 loss elsewhere in the body but not in the retina (F.P. Cremers et al. 1994) and therefore REP1 deficiency leads to accumulation of unprenylated Rabs (Tolmachova et al. 1999; Seabra, Ho, and Anant 1995; Larijani et al. 2003). Disruption of vesicular transport and protein trafficking to the outer segments of photoreceptors, mainly rods, such as rhodopsin trafficking, can lead to an altered disc formation and cell death (Kwok et al. 2008; J. Wang and Deretic 2014). Cellular models and animal models suggest that pathogenic variants in REP1 results in underprenylation of Rabs and disturbed phagocytotic function of the RPE leads to RPE degeneration (Seabra, Brown, and Goldstein 1993; F.P. Cremers et al. 1994; Wavre-Shapton et al. 2013).

One of the Rabs affected in CHM is Rab27a, which is required for melanosome movement into the apical processes of RPE cells (Futter et al. 2004). It has been hypothesized that the degeneration of the RPE and its adjacent layers may be the result of deficient melanosome transport which leads to a lack of protection against harmful light exposure (Corbeel and Freson 2008).

Male patients affected with CHM usually report nyctalopia already in childhood. That is followed by peripheral visual field defects that can progress to legal blindness in mid-life (Sorsby et al. 1952; Coussa and Traboulsi 2012; K.N. Khan et al. 2016; Coussa, Kim, and Traboulsi 2012). Fundus examination usually reveals pigment mottling in the mid-periphery advancing centrally and peripherally with large chorioretinal atrophy areas forming as the disease advances. The areas of chorioretinal atrophy correspond to areas of visual loss. CHM patients present with pigment clumping that is different from bone spicules (T.K. Lee et al. 2003). Central vision can remain good for decades because the macular area is preserved until the late-stage of the disease (Coussa and Traboulsi 2012). ffERG is usually abnormal showing generalized photoreptor dys-

function with earlier and greater reduction in rod-specific responses (Sieving, Niffenegger, and Berson 1986; Renner et al. 2006).

Similarly to OA1, the female carriers of CHM can have a mosaic pattern of wild-type and mutated retinal cells, which is seen as a pattern of pigment mottling in fundus examination. As a difference to OA1, in CHM the retinal changes in females can be progressive and lead to retinal degeneration of varying severity (Murro et al. 2017; Huang, Kim, and Fawzi 2012).

While most female carriers are asymptomatic, multifocal ERGs can show a pattern of dysfunction consistent with mosaicism (Vajaranant et al. 2008). Some carriers might develop more severe chorioretinal degeneration with vision loss (T.L. Edwards et al. 2015). The reason for varying severity in carrier status of CHM is thought to be the result of skewed X chromosome inactivation. The degree of X-inactivation can vary in each individual and if it is skewed so that 75–90% of normal X chromosomes are inactivated, it can lead to a manifestation of an X-linked disease in females (Wuthisiri et al. 2013). A possible dominant negative effect has been reported in CHM carriers by Giosaffatte *et al*. which could also help to explain the varying severeness of carrier profile (Di Giosaffatte et al. 2022).

2.3.3.2. Retinal Imaging

In CHM probands fundus autofluorescence usually shows areas of chorioretinal atrophy as loss of SW-AF signal and areas of preserved retina with detectable SW-AF signal. However even in preserved retinal areas the SW-AF can be non-uniform. SD-OCT imaging of affected males has revealed zones of macular sparing bordered by the loss of IZ and EZ with ONL thinning, and increased signal transmission posterior to RPE/Bruch's membrane (Aleman et al. 2017; Huang, Kim, and Fawzi 2012; Jolly et al. 2017). Intraretinal tubulations are usually seen in SD-OCT images on the border of chorioretinal atrophy and preserved retina (L.W. Sun et al. 2016). Abnormalities of central retina have been detected even in the younger patients presenting with EZ-IZ abnormalities with the presence of intact RPE. End-stage disease show relative preservation of the inner retina in regions with otherwise severe outer retina, RPE and choroidal disease (Aleman et al. 2017). Loss of foveal SW-AF signal has been correlated with vision loss in CHM probands and carriers (Huang, Kim, and Fawzi 2012). Retinal degeneration develops mostly symmetrically in both eyes (Jolly 2016), but might become more asymmetric in older patients (Aleman et al. 2017). Carriers of CHM can also exhibit hyperreflective deposits in outer retina by SD-OCT corresponding to hyperautofluorescent foci in SW-AF (Huang, Kim, and Fawzi 2012).

2.3.3.3. Therapeutic considerations

The name choroideremia refers to a disease affecting primarily the choroid, however in the case of CHM there is still debate over whether the photoreceptors, RPE or choroid is the location for primary disease process.

It has been proposed that RPE degeneration could be the leading process with photoreceptors being affected subsequently (Hariri et al. 2017; L.W. Sun et al. 2016; Morgan et al. 2014; Tolmachova et al. 2010; Krock, Bilotta, and Perkins 2007; R. Syed et al. 2013). Another theory is that RPE and photoreceptor degeneration are separate/autonomous events (Jacobson et al. 2006). Tolmachova *et al* used a mouse model to show that degeneration of either RPE or photoreceptor layer does not predispose to the degeneration of the other layers (Tolmachova et al. 2006), however they later also showed that disease affected RPE can accelerate photoreceptor degeneration (Tolmachova et al. 2010). There are also reports indicating photoreceptor layer as the primary site of pathology (Aleman et al. 2017; van den Hurk et al. 1997), which is supported by the clinical aspect that night blindness is an early sign of the disease and ffERG usually shows rod dysfunction (N. Syed et al. 2001; Ponjavic et al. 1995; Aleman et al. 2017). A rather consistent observation is that the loss of choroidal tissue occurs secondary to the degeneration of RPE and photoreceptors rather than being the site of the primary changes (N. Syed et al. 2001; Flannery et al. 1990). However some results suggested that the choriocapillaris is unhealthy before the RPE and outer retina degenerates (Foote et al. 2019). Understanding the disease process and the site of pathogenetic process is important in developing new therapeutic approaches.

Gene augmentation therapy have been a promising option for CHM, given it is not a large gene and the macular region is preserved until advanced stages of the disease. Gene augmentation therapy with AAV-REP1 injected subretinally and targeting the macular region has been intensively studied (Lam, Davis, and Gregori 2021), with one study completing phase 3 (NCT03496012), however it did not meet its primary endpoint of visual improvement and did not demonstrate efficacy based on key secondary endpoints. Despite those results, gene augmentation therapy still holds future perspectives, but because of the progressive nature of CHM, the aim of future therapy could be focused more on slowing down the disease rather than curing it. Besides extensive clinical studies on gene augmentation, CRISPR/Cas9- mediated base-editing, prime-editing, nonsense-suppression and antisense oligonucleotide methods have also been explored for CHM in preclinical studies (Han et al. 2021).

2.3.4. *PROM1*-related macular dystrophy

PROM1-related macular dystrophy is also sometimes referred to as Stargardt disease 4 (STGD4), because of the phenotypical overlap with STGD1 (M. Kniazeva, Chiang, Morgan, et al. 1999). It is caused by mutations in the *PROM1* gene and is much more uncommon than STGD1. Prominin1 (PROM1;

OMIM604365) is a transmembrane glycoprotein that is widely expressed in various human tissues including both rods and cones of retina and participates in various physiological roles. PROM1 (CD133) is known as a stem cell marker and has been identified in the apical plasma membrane of epithelial cells of several tissues (Karim et al. 2014; Singer et al. 2019) Another isoform Prominin-2 (PROM2) shares 60% amino acid identities with PROM1 and because of the presence of PROM2 in most tissues except in the eye, PROM1-related disease is only expressed in retina (Fargeas et al. 2003). In retinal photoreceptors it has an important structural role. PROM1 has been localized to the outer segment and connecting cilium of photoreceptors (Maw et al. 2000) and it plays a central role in disc morphogenesis but is also associated with photopigment sorting and phototransduction (Yang, Chen, Lillo, Chien, Yu, Michaelides, Klein, Howes, Li, Kaminoh, Chen, Zhao, Al-Sheikh, et al. 2008; Zacchigna et al. 2009). Animal studies in *PROM1* knock-out mice have demonstrated severely disorganized outer segments, whereas other parts of the photoreceptors have been found largely intact (Dellett et al. 2014; Zacchigna et al. 2009).

Loss of PROM1 function results in cone and rod degeneration and leads to visual impairment (Maw et al. 2000). A more recent study with knock-out cultured RPE cells showed that autophagosome trafficking to the lysozyme was decreased through increased mTORC1 and mTORC2 signalling, whereas overexpression of PROM1 had the opposite effect, meaning PROM1 has a role in autophagy of RPE cells (Bhattacharya 2009).

PROM1-related disease can present as macular dystrophy (Yang, Chen, Lillo, Chien, Yu, Michaelides, Klein, Howes, Li, Kaminoh, Chen, Zhao, Chen, et al. 2008; Imani et al. 2018), cone-rod dystrophy (Birtel et al. 2018; Pras et al. 2009; Eidinger et al. 2015; A.O. Khan and Bolz 2015; Wawrocka et al. 2018) or retinitis pigmentosa (Q. Zhang et al. 2007; Maw et al. 2000). Recessive forms usually present with panretinal dystrophy and macular involvement starting at a younger age whereas dominant forms show milder changes mostly restricted to macular area and present later in adulthood (Cehajic-Kapetanovic et al. 2019; Del Pozo-Valero et al. 2019; Liang et al. 2019).

PROM1-associated macular dystrophy (STGD4) presents with a phenotype similar to *ABCA4*-related Stargardt disease 1 (STGD1) (Yang, Chen, Lillo, Chien, Yu, Michaelides, Klein, Howes, Li, Kaminoh, Chen, Zhao, Al-Sheikh, et al. 2008; M. Kniazeva, Chiang, Morgan, et al. 1999; J.M. Kim et al. 2017; Strauss et al. 2018). Retinal imaging of *PROM1*-macular dystrophy has shown outer retinal thinning in SD-OCT images with increased signal transmission to choroid in cases of RPE atrophy. Fundus AF imaging usually reveals mottled and patchy areas of hypoautofluorescence in central macula and often a ring of hyperautofluorescence surrounding it with occasional hyperautofluorescent flecks (J.M. Kim et al. 2017; Cehajic-Kapetanovic et al. 2019; Fujinami et al. 2020; Strauss et al. 2018). In *PROM1*-related macular disease ffERG is usually normal or shows variable reduction in cone responses (Michaelides et al. 2010).

2.3.5. Summary of the literature review

IRDs present a heterogenous group of rare diseases that all together present a significant disease burden on modern society. The eye is a unique organ for developing therapeutic approaches because of its immune privileged status, accessibility, transparent ocular media that allows for visualization and the fellow eye that can usually serve as a control in treatment trials. With the approval of the first gene augmentation therapy in 2017 for *RPE65*-associated retinal degeneration and other gene therapies in trial phase, IRDs are in the frontline of precision medicine. There is a need for adequate retinal imaging studies prior to developing a suitable therapeutic approach as well as for evaluating the therapeutic effect.

SW-AF imaging has become a standard method in diagnosing inherited retinal diseases, because there are often recognizable disease-specific patterns seen in the images, but also in evaluating viable retinal areas. NIR-AF imaging has not been so accessible and therefore there is also the need to advance the knowledge on how to interpret the images. Comparative studies using both methods in various retinal diseases are therefore valuable.

Recessive Stargardt disease has been rather extensively studied and excessive lipofuscin accumulation and increased SW-AF signal in the retina has been well documented by qAF. However NIR-AF signal in STGD1 has not been quantitatively studied before. Quantitative autofluorescence is an indirect measurement of retinal fluorophores and allows comparison to healthy eyes as well as to other retinal pathologies. qAF can serve as a means of exploring the pathophysiology of the disease as well as for differential diagnosis. *PROM1*-macular dystrophy also known as STGD4, is often compared to STGD1 because of its phenotypic similarity. However the levels of SW-AF signal in *PROM1*-patients have not been specifically studied and therefore it is not known whether these two diseases share the same disease mechanism of excessive bisretinoid lipofuscin accumulation.

OA1 female carrier status presents an interesting model where areas of RPE cells with normal pigmentation and hypopigmented areas form a typical mosaic pattern in the fundus. As opposed to choroideremia carriers, that mosaic in OA1 is stationary and non-degenerative. Analysing these pigmented and non-pigmented areas with SW-AF and NIR-AF imaging could bring insight into the contribution of bisretinoid lipofuscin and melanin in fundus AF signal.

Fundus autofluorescence is valuable in analysing degenerative processes in the retina. SW-AF has been used to discriminate preserved RPE from areas of degeneration. Bisretinoid lipofuscin is formed in the photoreceptors and then transerred to the RPE cells via phagocytosis of outer segments. As NIR-AF signal is thought to originate mostly from RPE, it could be assumed that it is a more sensitive biomarker for detecting abnormal cellular processes in the RPE level. In STGD1 flecks usually appear in the macular area progressing peripherally and later retinal atrophy ensues. In males affected with choroideremia the chorioretinal atrophy develops first in the periphery preserving a central retinal

island of intact RPE. Flecks in STGD1 and the central preserved retinal island in CHM present an interesting target to be analysed with SW-AF and NIR-AF imaging, both for understanding the disease process and designing therapeutic approaches.

3. AIMS OF THE STUDY

1. To advance the understanding of fundus autofluorescence sources and the contribution of bisretinoid lipofuscin and melanin using patients and animal models presenting with varying levels of fluorophores (Study 1, Study 2, Study 3).
2. To qualitatively and quantitavely describe autofluorescence findings of STGD1, CHM, albinism and *PROM1*-retinal disease (Study 1, Study 2, Study 3, Study 4).
3. To analyze benefits and clinical applications of SW-AF and NIR-AF in inherited retinal disease studying STGD1, choroideremia and *PROM1*-macular disease (Study 2, Study 3, Study 4).

4. MATERIALS AND METHODS

4.1. Patients, Clinical Evaluation, and Genetic Testing

OA1 carriers and patients with STGD1 (Study 1)

The first part of the study consisted of prospective analysis of fundus AF images of five carriers with mutations in the X-linked ocular albinism gene *GPR143/OA1* seen in the Edward S. Harkness Eye Institute at Columbia University Irving Medical Center. Three of the carriers (patient [P]1, 2, 3) were siblings of the same family where the father (P6) had been diagnosed with *GPR143/OA1*. The fourth and the fifth OA1 carriers (P4, P5) were not related to the aforementioned family. All subjects had a comprehensive ophthalmological examination by a retina specialist. Blood was collected from all patients for genetic testing and genomic DNA was extracted from blood lymphocytes using a standard protocol. Direct Sanger sequencing confirmed that the three sisters from the same family (P1, P2, P3) were all heterozygous carriers of a novel mutation c.461del_T (p.Ile154fs) in *GPR143/OA1*. All nine exons were amplified and directly sequenced, and no other variants were found. Sequence analysis of *GPR143/OA1* in P4 disclosed heterozygosity for the c.455+3A>G mutation. There was not genetic confirmation for P5; the clinical diagnosis was based on iris transillumination and typical RPE mosaicism in the fundus. P6 (father of P1, P2, P3) was hemizygous for the mutation c.461del_T (p.Ile154fs) in *GPR143/OA1*.

The second part was a prospective analysis of fundus AF images from 25 patients (age range 8.3–51.5 years) with clinically and genetically confirmed diagnosis of STGD1. Images of patients with advanced disease were not included. At least one known mutation in the *ABCA4* gene was detected in all patients by direct sequencing. The control group consisted of 15 individuals without a history of eye disease. The mean age was 34.9 years (range 12.7–52.7 years) and 10 subjects identified themselves as Caucasian, 3 as Hispanic, 1 Asian, and 1 African American. Both groups had a comprehensive eye examination by a retina specialist.

Clinical, demographic, and genetic data of OA1 and STGD1 subjects are presented in **Table 1.**

Study 1 also included an analysis of animal models**.** Albino *Abca4/Abca4* null mutant mice (*Abca4*$^{-}$/ *Abca4*$^{-}$), homozygous for Rpe65-Leu450, were reared and genotyped (Table 2). Agouti *Abca4*$^{-/-}$ (129S-Abca4tm1Ght/J; Rpe65-Leu450) and agouti *Abca4*$^{+/+}$ (129S1/SvImJ; Rpe65-Leu450) were purchased from The Jackson Laboratory (Bar Harbor, ME, USA) and bred in-house. Agouti *Rdh8*$^{-/-}$ *Abca4*$^{-/-}$mice (Rpe65-Leu450) were acquired as a gift from Krzysztof Palczewski, Case Western Reserve University (Cleveland, OH, USA). Black C57BL/6J, and albino C57BL/6J-c2j wild-type mice (Rpe65-Met450) were purchased from The Jackson Laboratory (**Table 2**).

Choroideremia probands and carriers (Study 2)
A retrospective analysis of fundus images acquired from patients presenting to the Edward S. Harkness Eye Institute at Columbia University Irving Medical Center was performed. All patients underwent a comprehensive ophthalmic examination by a retina specialist. The diagnosis of CHM in probands was based on clinical findings and subsequent genetic testing. Heterozygous female carriers were identified through affected probands (family members) and then screened for the causative heterozygous mutation. The cohort consisted of 16 CHM male probands and 9 female carriers. All affected patients were male with a mean age of 44.9 years (range, 10.2–77.2) at the time of examination. Nine heterozygous carriers were also included in the study (18 eyes). The mean age in the carrier group was 54 (29.3–75.5). Demographic, clinical, and genetic data along with familial relationships are summarized in the **Table 3.**

STGD1 patients (Study 3)
A prospective analysis of fundus images from 12 patients seen at the the Edward S. Harkness Eye Institute at Columbia University Irving Medical Center (6 female, 6 male; age 9 to 61 years) with clinical diagnosis of STGD1 and subsequent genetic confirmation. Disease-causing variants were detected by direct sequencing of the *ABCA4* locus as has been previously described (Zernant et al. 2011; Zernant et al. 2014). A selection of patients was done on the basis of the presence of flecks visible in fundus SW-AF images and the availability of NIR-AF and spectral domain optical coherence tomography (SD-OCT) images. Patients with extensive atrophy or poor image quality were excluded. Demographic, clinical and genetic information is presented in **Table 4.**

PROM1-Macular Disease patients (Study 4)
A prospective cross-sectional analysis of 18 patients presented to the Edward S. Harkness Eye Institute at Columbia University Irving Medical Center. All patients underwent a comprehensive ophthalmic examination by a retina specialist. Demographic, clinical and genetic information is presented in **Table 5**.

Electrophysiology
Full-field electroretinogram (ffERG) was recorded using a Diagnosys Espion Electrophysiology System (Diagnosys) in accordance with standard techniques recommended by the International Society for Clinical Electrophysiology of Vision (ISCEV) (McCulloch et al. 2015).

Statistics
Statistical analyses were performed on the Prism 5 software (GraphPad Software, La Jolla, CA, USA) and the statistical tests were done as indicated. Statistical significance was evaluated by comparing CIs and by Wilcoxon-Mann-Whitney Test as appropriate. The Bland-Altman analysis was used to assess interobserver agreement.

Ethics

All procedures adhered to the tenets of the Declaration of Helsinki and written informed consent was obtained from all patients in prospective studies after full explanation of the procedures. The studies were carried out with the approval of the Institutional Review Board of Columbia University, and all patients were enrolled in accordance with the tenets set out in the Declaration of Helsinki. The research involving mice was approved by the Institutional Animal Care and Use Committee and adhered to the ARVO Statement for the Use of Animals in Ophthalmic and Vision Research.

4.2. Retinal imaging

High-quality normalized SW-AF images were obtained with Heidelberg cSLO camera (HRA2, Spectralis HRA + OCT, Heidelberg Engineering, Heidelberg Germany) with excitation set on 488 nm and barrier filter 500 nm (30° X 30° and 55° X 55° field). For qAF imaging a special reference had been added to the camera to allow adjustment for changes in sensitivity setting and laser power. In the beginning of imaging photopigments are bleached for 20–30 seconds (F. Delori et al. 2011) and images are acquired in a high-speed video mode (8.9 frames per second, 9–12 frames, 30° X 30° field). Those videos are averaged and saved in non-normalized mode to avoid histogram stretching.

The qAF values are calculated using a custom software written in IGOR (Wavemetrics, Lake Oswego, OR) that has been previously described by Delori et al. that takes into account different factors such as laser power, the laser offset (zero signal provided by the instrument software), detector sensitivity, refractive errors, and whether the patient is phacic or aphacic (F. Delori et al. 2011; Duncker, Stein, et al. 2015; Burke et al. 2014). The normative database consisted of 374 eyes (age range, 5–65 years) and has been published before (Greenberg et al. 2013).

NIR-AF images were captured with Heidelberg retinal tomography 2-scanning laser ophthalmoscope (HRA2, Spectralis HRA + OCT, Heidelberg Engineering, Heidelberg Germany) with excitation set at 787-and emission at >830-nm (30° X 30° and 55° X 55° field). For NIR-AF quantification, non-normalized images were acquired at a fixed sensitivity of 96 (30° X 30°). Images were analyzed in an open source software (Fiji; National Institutes of Health, Bethesda, MD, USA), where pixel gray level values were measured along a horizontal line through the fovea at 0.25-mm intervals reaching from fovea 4 mm nasally and temporally. The NIR-AF gray level values were adjusted by subtracting the gray level offset value provided by Heidelberg software. In Study 1 the control group consisted of 15 individuals without a history of eye disease. The mean age was 34.9 years (range 12.7–52.7 years) and 10 subjects identified themselves as Caucasian, 3 as Hispanic, 1 Asian and 1 African American. The healthy cohort for study 3 and Study 4 consisted of 19 subjects without eye disease, the mean age was 35.3 years (range, 12.7–52.7 years), and

10 subjects identified themselves as Caucasian, 3 as Hispanic, 4 Asian, and 2 African American.

SD-OCT images were acquired as line and volume scans in high-resolution mode together with a simultaneous near-infared-reflectance image (NIR-R; 820 nm) using Spectralis HRA-OCT (Heidelberg Engineering). For Study 2 foveal thickness (FT) and subfoveal choroidal thickness (SFT) were measured manually with the caliper tool in the Heidelberg Explorer (HEYEX) software. FT was defined as the distance from the internal limiting membrane to the outer border of RPE-Bruch's membrane and SFT was measured from the outer border of the RPE-Bruch's membrane complex and the chorioscleral border under the fovea. The control group consisted of 51 females without diagnosis of eye disease (aged 7–55, mean age 29) of whom 10 identified as Asian, 7 African American, 7 Hispanic, 4 Indian, and 23 white.

Color fundus images were captured with a FF 450plus Fundus Camera (Carl Zeiss Meditec). Ultra-widefield high-resolution optomap images were also captured (Optos Daytona; Optos, Inc., Marlborough, MA, USA) in the composite color and AF (excitation 532 nm) mode.

In Study 3 fleck analysis was carried out. All images were registered and aligned using i2kRetina software (DualAlign LLC, Clifton Park, NY USA). For illustrative purposes some non-aligned images were used in figures. To delineate an area for fleck analysis, a square was drawn in superior hemiretina such that all sides were equal to the optic disc-fovea distance in the corresponding image. In SW-AF images 5 hyperautofluorescent flecks were chosen (total of 95 flecks; 19 eyes, 10 patients) and then scored according to appearance in NIR-AF images.

Study 1 included analysis of mouse models by investigators in the laboratory of professor Janet R. Sparrow. For retinal imaging mice were anesthetized with an intraperitoneal injection of ketamine (100 mg/kg) and xylazine (10 mg/kg). Protocols for positioning, pupillary dilation, temperature monitoring, and placement of contact lens have been described (Sparrow et al. 2013). After visual pigment bleaching, fundus images (558 lens) were acquired with a cSLO (Spectralis HRA-OCT) equipped with an incident laser beam of 0.98 mm and an internal fluorescence reference (Sparrow et al. 2013). Nine successive frames were acquired in high-speed mode (8.9 images/s), using a sensitivity of 95 to 100; the frames were averaged and saved in the non-normalized mode. Fundus SWAF images were analyzed as described (Sparrow et al. 2013) and qAF was calculated by calibrating grey levels (GL), in predetermined fundus segments, to the GL of the fluorescent reference (F. Delori et al. 2011). All mice were exposed to only a single occasion of imaging. High-resolution NIR-AF (787 nm excitation, >830 nm emission) images were acquired at a sensitivity of 105 and after averaging 100 frames with background subtraction, the images were saved in non-normalized mode. GLs were measured using ImageJ (http://imagej.nih.gov/ij/) Between-session coefficient of repeatability (Bland-Altman) of NIR-AF GL values was 3.5%.

Quantitative high performance liquid chromatography (HPLC)

Mouse eyecups (4–6 per sample) were homogenized and extracted for quantitation by HPLC (Alliance system, Waters, Corp, Milford, MA) as previously described (Ueda et al. 2016).

5. RESULTS

5.1. Mutations in GPR143/OA1 and ABCA4 Inform Interpretations of Short-Wavelength and Near-Infrared Fundus Autofluorescence (Study 1)

The study cohort included five female ocular albinism carriers (age range 13,5–34,6). Also included were 25 patients (age range 8.3–51.5 years) with clinically and genetically confirmed diagnosis of STGD1. **Table 1** presents clinical and genetic data for patients.

Specially bred mice with different pigmentation and RPE lipofuscin levels (**Table 2**) were imaged (Spectralis HRA+OCT) and analyzed (Sparrow et al. 2013) to further test the concepts of SW-AF and NIR-AF sources.

Table 1. Demographic, clinical and genetic summary of the ocular albinism and Stargardt disease patient cohort.

Patient	Age	Eye analysed	Ethnicity	BCVA*		Genetic variants	
OA1				OD	OS		
1	13.5	OA	Hispanic	0	0	heterozygous mutation GPR143/OA1 gene, c.461del_T (p.Ile154fs)	
2	17.3	OA	Hispanic	0	0	heterozygous mutation GPR143/OA1 gene, c.461del_T (p.Ile154fs)	
3	21.7	OA	Hispanic	0	0	heterozygous mutation GPR143/OA1 gene, c.461del_T (p.Ile154fs)	
4	34.6	OA	Asian	0	0	heterozygous mutation GPR143/OA1 gene, c.455+3A>G	
5	20.1	OA	Caucasian	0	0	not available	
6	43.1	OA	Hispanic	1	1	hemizygous mutation GPR143/OA1 gene, c.461del_T (p.Ile154fs)	
STGD1							
1	14.3	OD	Caucasian	0.7	1	p.G1961E	p.P1380L
2	8.3	OD	Indian	0.5	0.6	p.R653C	p.G1961E
3	12.9	OD	Caucasian	0.9	0.9	p.[L541P;A1038V]	p.L2027F
4	17.2	OD	Caucasian	0.1	0.1	p.R1108C	p.Q1412
5	17.7	OD	Caucasian	0.7	0.7	p.G1961E	p.C54Y †
6	18.5	OD	Caucasian	0.8	0.9	p.A1773V	p.G1961E
7	21.6	OD	Caucasian	0.7	0.7	p.G1961E	p.V1682_V1686del †
8	22.6	OD	Caucasian	0.3	0.2	p.R602W	p.N1868I
9	24.5	OD	Caucasian	0.9	0.4	p.G1961E	p.N96D
10	25.9	OS	Caucasian	0.7	0.7	p.G1961E	p.N1614del †
11	26.8	OS	Caucasian	1.17	1.17	p.G1961E	p.L541P
12	27.8	OD	Caucasian	0.7	0.6	p.G1961E	p.C2150R
13	29.9	OD	Caucasian	0.9	0.9	c.3050+5G>A	p.G1961E
14	31.6	OS	Afro Arab	0.1	0.1	p.R1300	p.R2106C
15	36.3	OD	Caucasian	0.7	0.1	p.N1799D	p.N1868I
16	45	OD	Caucasian	0.4	0.4	p.R2106C	p.[L541P;A1038V]
17	46.6	OD	Indian	0.3	0.6	p.T1526M	p.F1714S †
18	50.7	OD	Caucasian	0.4	0.4	p.R2077G	p.R2107H
19	51.5	OS	Caucasian	0.1	0.1	p.N1868I	p.P1380L
20	45.8	OS	Caucasian	0.17	0.17	p.G1961E	p.G1961E
21	21.9	OD	Caucasian	0.1	0.1	p.G1961E	p.N96D
22	25.4	OS	Caucasian	0.7	0.7	p.G1748E	p.R2106H
23	15.2	OS	Caucasian	0	0.1	p.G1961E	p.V615A
24	11.4	OD	Caucasian	1	1.3	p.[L541P;A1038V]	c.768+358C>T
25	13.5	OD	Caucasian	1	0.3	p.V989A	c. 2918+5G>A

*logMAR equivalent

† genotype for these patients has been updated since the original publication of this table (Paavo et al 2018, IOVS)

Table 2. Mouse strains used in the study

mouse line	melanin status	bisretinoid status	Rpe65-450 variant
Abca4$^{-/-}$	albino	elevated relative to albino *Abca4*$^{+/+}$	Leu-450*
Abca4$^{+/+}$	albino		Leu-450
Abca4$^{-/-}$	agouti	elevated relative to agouti *Abca4*$^{+/+}$	Leu-450
Abca4$^{+/+}$	agouti		
Rdh8$^{-/-}$ *Abca4*$^{-/-}$	agouti	elevated relative to agouti *Abca4*$^{-/-}$	Leu-450
C57BL/6J^{c2j}	albino	reduced relative to black C57BL/6J	Met-450**
C57BL/6J	*black*		*Met-450*

*Leucine at position 450; °°Methionine at position 450

5.1.1. Inversed pattern of SW-AF and NIR-AF signal of pigmentary mosaic in OA1 carriers

All five of the OA1 carriers were asymptomatic, but presented with a typical "mud-splatter" fundus where radial streaks of hypopigmented RPE cells stretched from macular area to the periphery as seen in fundus pseudocolor image (**Figure 6, A**). Closer examination showed that pigmented fundus areas (**Figure 6A,** blue arrows) corresponded to hypoautofluorescence in SW-AF imaging (**Figure 6B,** blue arrows) and areas of hypopigmentation to hyperautofluorescence **(Figure 6 A, B,** white arrows). Comparison of the two AF modalities revealed that the units of the mosaic exhibiting NIR-AF signal **(Figure 6 C, E**) were associated with lower SW-AF (**Figure 6 D,F**), whereas the hypopigmented areas in the NIR-AF image (**Figure 6, C,E**) corresponded to foci of readily detectable SW-AF **(Figure 6, D, F**).

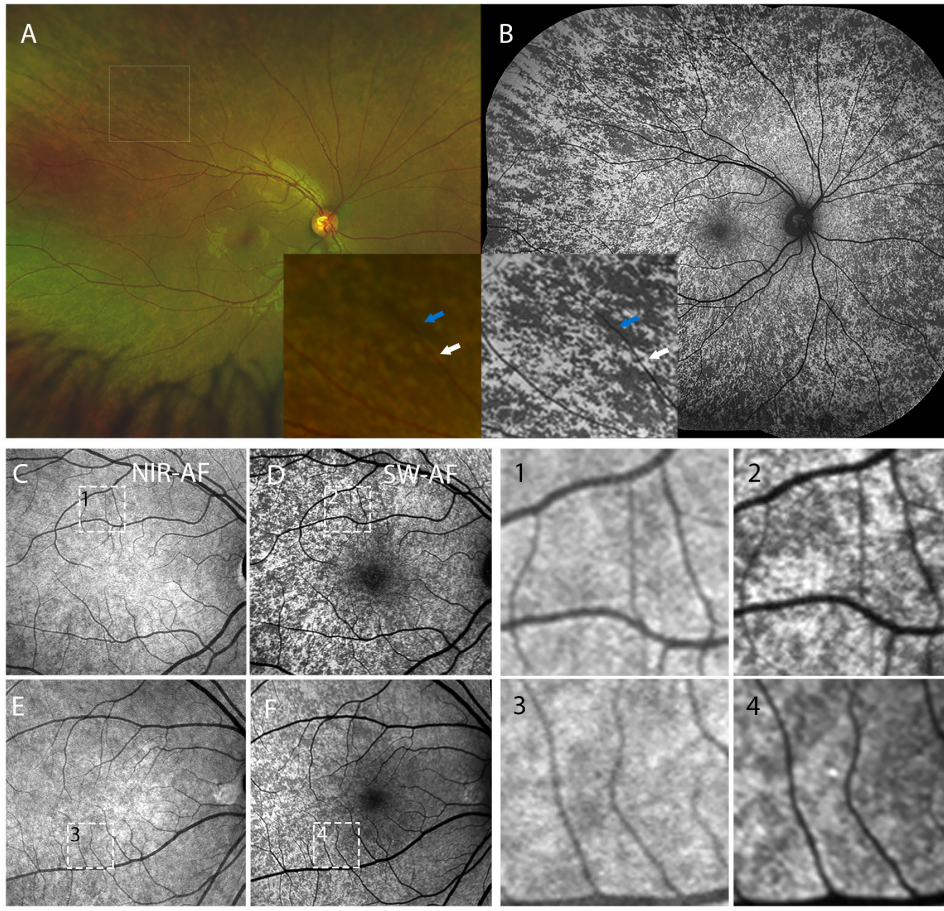

Figure 6. Multimodal imaging of OA1 carriers**.** Upper panel: Optos pseudocolor image (**A**) and SW-AF composite image (**B**) showing radial pattern of fundus hypopigmentation of P3**.** Lower panel: NIR-AF (787 nm) images (**C,E**) and SW-AF (488 nm) images (**D,F**) of GPR143/OA1 carriers. P3 (C,D) and P4 (E, F). (Spectralis, Heidelberg Engineering). Areas in the rectangles in are magnified in images in 1–4.

5.1.2. Quantitative Fundus AF and increased SW-AF signal from hypopigmented areas in OA1 carriers

To further understand the patterns of AF, we quantified SW-AF signal strength using the qAF method (Burke et al. 2014). Levels of qAF8 (7°–9° eccentricity from fovea) in OA1 carriers were within the 95% confidence intervals for age-matched healthy eyes (**Figure 7 B**). Comparison of OA1 carriers and age-matched healthy subjects using color-coded qAF maps scaled to a qAF range of 0 to 1200, revealed that in carriers, the pigmented units of the mosaic corresponded to the level of normal AF, whereas the hypopigmented areas exhibited significantly higher focal areas of SW-AF (**Figure 7, A)**.

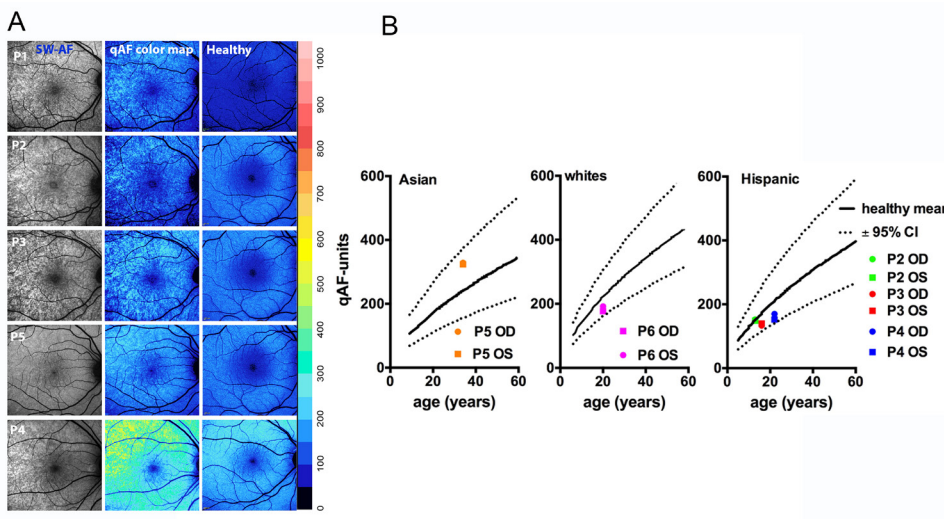

Figure 7. **A**. SW-AF (488 nm) images and color-coded qAF images of GPR143/OA1 carriers (P1–P5) and age-matched healthy eyes. The age-matched healthy subjects are aged 11.3 (P1), 20.1 (P2, P3, P5), and 32.6 (P4). Color codes are scaled from 0 to 1200 as indicated. **B.** qAF in Asian, white, and Hispanic GPR143/OA1 carriers (colored symbols) (P1–P5) and age-matched healthy subjects (mean, solid black line; and 95% confidence intervals, dashed lines). qAF was measured in eight circularly arranged segments, 7°–9° from the fovea (qAF8).

5.1.3. Increased NIR-AF Signal in STGD1

Previous studies have shown that subjects with *ABCA4*-related disease have higher SW-AF levels than healthy eyes (Burke et al. 2014). The contribution of excessive bisretinoid lipofuscin to NIR-AF signal has been discussed previously as observations made on the optic fissure in STGD1 and the hyperautofluorescent ring in retinitis pigmentosa (Duncker, Lee, et al. 2013; Duncker, Tabacaru, et al. 2013).

To further examine this issue, NIR-AF intensities were measured as GL intensities in STGD1 (**Figure 8 B**) and healthy retina **(Figure 8 A**) at 1-mm intervals (nine positions) along a horizontal axis starting at the fovea and proceeding temporally (0 to -4) and nasally (0 to +4) (**Figure 8 C).** Healthy eyes exhibited an increase in NIR-AF signal (**Figure 8 C**, blue graph) in a zone approximately 8° (2.3 mm from fovea) in diameter centered at the fovea as was expected. In that same area, NIR-AF signal was reduced in the STGD1 patients (**Figure 8C**, red graph) because of central atrophy. Outside the foveal area, GL values were consistently elevated in the STGD1 cohort, with the differences in GL values between the STGD1 and healthy eyes being statistically significant at all positions ($P < 0.05$, ANOVA and Sidak's multiple comparison test) (except at the 4-mm nasal position due to absent NIR-AF signal at the optic disc). The diffe-

rence was as much as 3-fold (2 mm nasal to fovea) (**Figure 8 C** blue versus red graph).

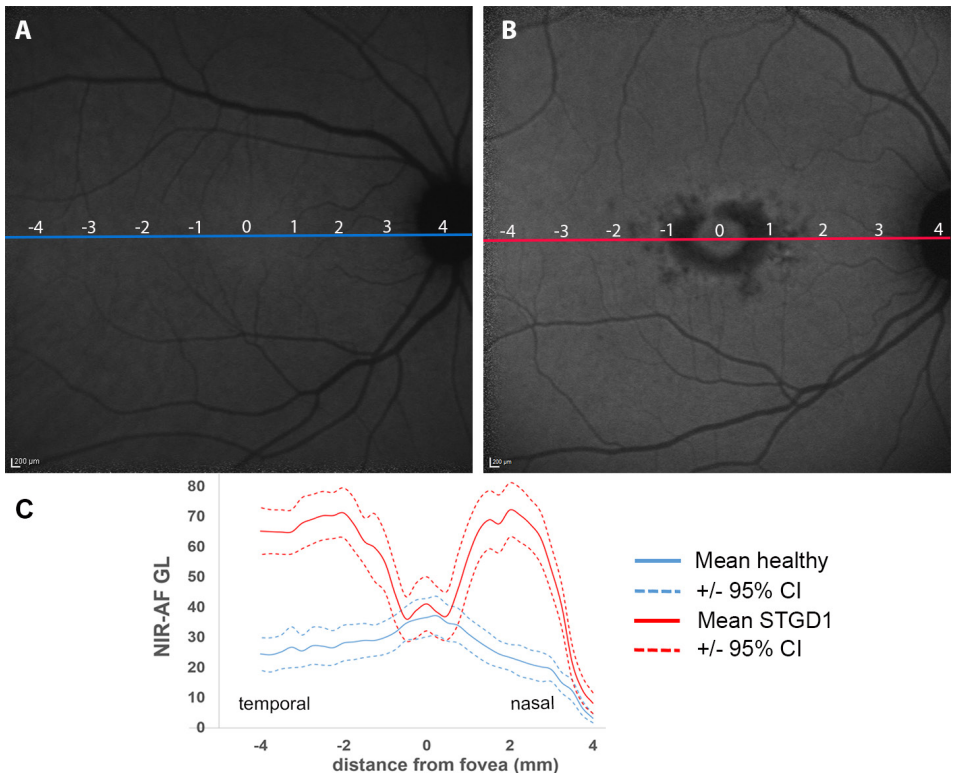

Figure 8. NIR-AF in STGD1. (**A, B**) NIR-AF images acquired from a healthy subject (age 48.3 years) (A) and STGD1 patient (31.6 years) (B). (**C**) NIR-AF intensity profiles presented as mean normalized GLs (solid lines) together with 95% confidence intervals (CIs) and plotted as a function of temporal-to-nasal distance along a horizontal line through the fovea in healthy subjects (n=15) and STGD1 patients (n=25).

5.1.4. Fundus AF in mice with different pigmentation and bisretinoid lipofuscin levels

Agouti *Abca4*$^{-/-}$ mice serve as a model of accelerated formation of bisretinoid lipofuscin (**Table 2**), which results in bisretinoid accumulation that is approximately 3-fold higher than in the wild type. The NIR-AF signal in the agouti *Abca4*$^{-/-}$ mice with elevated RPE lipofuscin (and therefore increased SW-AF) was greater than in agouti *Abca4*$^{+/+}$ mice (**Figure 9A**). Plots of NIR-AF versus SW-AF (age 2–9 months) in agouti *Abca4*$^{-/-}$ (72.4 +- 8, SE) versus *Abca4*$^{+/+}$ (156 +- 63, SE) mice revealed different slopes (t-test, P <0.05). Moreover, for

the same age interval, the greater change in SW-AF (x-axis) in the agouti *Abca4*$^{-/-}$ mice resulted in a greater change in NIR-AF (y-axis) than in the agouti *Abca4*$^{+/+}$ mice (**Figure 9 B**).

We also analyzed fundus AF levels in agouti *Rdh8*$^{-/-}$*Abca4*$^{-/-}$ double knockout mice (**Table 2**). In the absence of Rdh8 bisretinoid levels increase additionally compared to the single knockout *Abca4*$^{-/-}$ mice (Maeda et al. 2009; Flynn et al. 2014). The additive increase in SW-AF (qAF) in the agouti *Abca4*$^{+/+}$, *Abca4*$^{-/-}$, and *Rdh8*$^{-/-}$*Abca4*$^{-/-}$ mice was paralleled by increases in NIR-AF intensity (**Figure 9E**).

Albino *Abca4* $^{-/-}$ mice (**Table 2**) were used to test for NIR-AF signal in the absence of melanin. As it is known that NIR-AF signal originates from melanin, the signal was more robust in agouti *Abca4*$^{-/-}$ mice than in albino *Abca4*$^{-/-}$ mice (**Figure 9B versus Figure 9E**). However, despite the absence of melanin, the NIR-AF signal in the albino *Abca4*$^{-/-}$ mice increased together with the age-associated increase in the SW-AF signal (**Figure 9E**). Because in the hypopigmented areas of the fundus of OA1 carriers, SW-AF intensities were increased, we also compared qAF in albino mice. Consistent with observations in the OA1 carriers, SW-AF intensity (qAF) in the albino *Abca4*$^{-/-}$ mice was elevated relative to the age-matched agouti *Abca4*$^{-/-}$. This difference at first seemed discordant given our previous report that bisretinoid measured as A2E, is higher in the agouti (Ueda et al. 2016). For that reason, we also compared black *C57BL/6J* with albino *C57BL/6J-c2j* mice; black and albino mice are genetically identical except that the albino *C57BL/6J-c2j* harbour a homozygous mutation in the tyrosinase gene (c/c) **(Table 2**). qAF analysis showed that SW-AF signal was similar in black *C57BL/6J* and albino *C57BL/ 6J-c2j* mice (**Figure 9E**), even though we have also shown by chromatographic quantitation of the bisretinoid A2E, that the latter are present in lesser amounts in the albino eye (**Figure 9G**). Reduced HPLC quantified bisretinoid in the albino mice is due to loss associated with photooxidation and photodegradation (Sparrow et al. 2013). Therefore the stronger SW-AF signal in the albino would have to be due to the greater irradiance received by the RPE cell fluorophores in the eyes lacking melanin and due to light reflected by the sclera (Ueda et al. 2016). By plotting NIR-AF values as a function of SW-AF (age 4 and 6 months) for albino wild-type (*Abca4*$^{+/+}$, *C57BL/6Jc-2j*) and *Abca4*$^{-/-}$ mice, it was apparent that NIR-AF levels did not change when SW-AF intensity was limited to levels less than 1 qAF-unit. It is also notable that NIR-AF was more intense in mice having a black (i.e., *C57BL/6J*) versus agouti (*Abca4*$^{-/-}$) coat color (**Figure 9A** versus **F**).

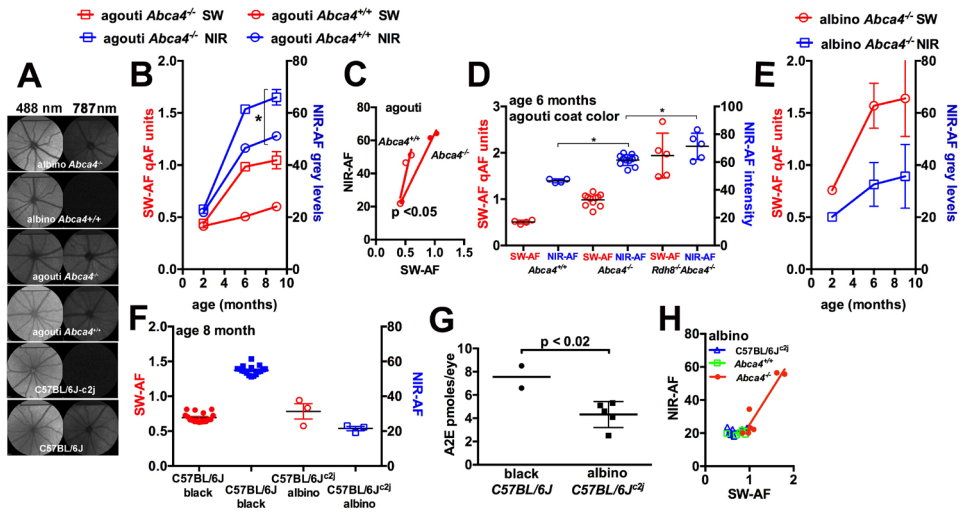

Figure 9. Fundus autofluorescence and HPLC analysis of mouse eyes. (**A**) Short-wavelength (SW-AF; 488 nm) and near infrared (NIR-AF; 787 nm) autofluorescence images of mouse fundus. *Abca4*$^{-/-}$ and wild-type (*Abca4*$^{+/+}$) albino mice and mice with an agouti coat color were imaged as indicated. The internal autofluorescent reference is visible in the top of the image. Note that in the case of the *Abca4*$^{+/+}$ mouse, the fundus has relatively high grey levels but the internal fundus AF reference is also brighter reflecting lower quantitative fundus autofluorescence (qAF) levels. **B-G**. Analysis of SW-AF and NIR-AF images acquired in mice at indicated ages. SW-AF is quantified as qAF-units and NIR-AF as grey levels. **B.** SW-AF and NIR-AF plotted as a function of age in agouti *Abca4*$^{-/-}$ and *Abca4*$^{+/+}$ mice. **C.** Plots of NIR-AF and SW-AF (age 2–9 months) in agouti *Abca4*$^{-/-}$ and *Abca4*$^{+/+}$ mice reveal different slopes (t-test, $p < 0.05$) indicating a greater increase in NIR-AF in mice exhibiting increased SW-AF (*Abca4*$^{-/-}$). **D.** SW-AF and NIR-AF in agouti *Abca4*$^{+/+}$, *Abca4*$^{-/-}$ and *Rdh*$^{-/-}$/ *Abca4*$^{-/-}$ mice indicating increases in NIR-AF intensity as SW-AF is elevated. **E**. SW-AF and NIR-AF plotted as a function of age in albino *Abca4-/-* mice. **F**. NIR-AF plotted versus SW-AF for black *C57BL/6J* and albino *C57BL/6J-c2j* mice (age 8 months). **G**. HPLC quantitation of the bisretinoid A2E in black *C57BL/6J* and *C57BL/6J-c2j* mice. **H**. Plotting of NIR-AF versus SW-AF for albino wild-type mice (*C57BL/6Jc2j, Abca4*$^{+/+}$) and *Abca4-/-* mice (age 4 and 6 months). Means +/- SEM are based on 2–11 mice.

5.2. Patterns of SW-AF and NIR-AF imaging in choroideremia probands and carriers (Study 2)

The choroideremia study cohort consisted of 16 affected male patients (31 eyes). The mean age was 44.9 years (range, 10.2–77.2) and BCVA ranged from 20/20 to 20/150. The study also included 9 female choroideremia carriers (18 eyes) mean age in the carrier group was 54 (29.3–75.5) and visual acuity ranged from 20/20 to 20/200. All images were evaluated independently by two investigators (MP, JRS).

Disease-causing mutations in the CHM gene were detected in all affected patients and carriers who underwent genetic screening. In the case of P9 and C4 the diagnosis was made based on clinical findings and a positive family history for CHM. Nineteen (19) unique variants were detected in the cohort, the majority of which were frameshifts (26.3%), large deletions (21.1%), and non-coding or intronic (26.3%). All intronic mutations occurred within canonical splice sites (+-1 and +-2) and are strongly predicted to result in skipping of the subsequent or adjacent exon. All missense variants are predicted to be pathogenic or previously associated with CHM (single nucleotide polymorphism). Demographic, clinical and genetic data is presented in **Table 3**.

Table 3. Demographic, Clinical and Genetic Characteristics of Affected Patients and Heterozygous Carriers of Choroideremia Study Cohort

Patient	Age	Gender	Race/Ethnicity	LogMAR BCVA		Study eye	*CHM* variant‡ cDNA (protein)	Zygosity	Relationship
				OD	OS				
P1	43	M	Caucasian	0.00	0.79	OU	c.877C>T (p.Arg293*)	Hemizygous	Proband
P2	52	M	African-American	0.30	0.30	OU	c.49+1G>A (p.?)	Hemizygous	Proband
P3	46	M	Caucasian	0.87	0.79	OU	c.1349G>T (p.Arg450Met)	Hemizygous	Proband
P4	36	M	Caucasian	0.30	0.10	OU	c.315-2A>G (p.?)	Hemizygous	Proband
P5	68	M	Caucasian	0.30	0.40	OU	c.1771-1G>A (p.?)	Hemizygous	Proband
P6	28	M	African-American	0.40	0.30	OU	Deletion of Exon 12†	Hemizygous	Proband
P7	57	M	Caucasian	0.00	0.20	OU	c.82del (Ser28Glnfs*32)	Hemizygous	Proband
P8	58	M	Caucasian	0.47	0.40	OU	c.1520A>G (p.His507Arg)	Hemizygous	Proband
P9	60	M	African-American	0.10	0.10	OU	*Not screened*	Hemizygous	Proband
P10	31	M	Iranian	0.10	0.00	OU	c.1237_1328del (p.Ser413Valfs*18)	Hemizygous	Proband
P11	77	M	Caucasian	0.40	0.60	OU	Deletion of Exons 6 and 7†	Hemizygous	Proband
P12	51	M	Caucasian	0.40	0.60	OU	c.1580_1584del (p.Leu527Cysfs*5)	Hemizygous	Proband
P13	52	M	Caucasian		0.10	OS	Deletion of Exons 9 and 10†	Hemizygous	Proband
P14	21	M	Caucasian	0.00	0.10	OU	c.1584_1587del (p.Val529Hisfs*7)	Hemizygous	Proband
P15	31	M	Caucasian/North-African	0.00	0.00	OU	c.819+1G>A (p.?)	Hemizygous	Proband
P16	10	M	Indian	0.10	0.10	OU	Deletion of entire *CHM* locus†	Hemizygous	Proband
Carrier									
C1	53	F	Caucasian	0.30	0.30	OU	c.1584_1587del (p.Val529Hisfs*7)	Heterozygous	Mother (P14)
C2	51	F	Caucasian	0.10	0.10	OU	c.1349G>T (Arg450Met)	Heterozygous	Sister (P3)
C3	76	F	African-America	0.10	1.00	OU	c.49+1G>A (p.?)	Heterozygous	Mother (P2)
C4	49	F	African-American	0.00	0.00	OU	*Not screened*	Heterozygous	
C5	49	F	African-American	0.00	0.00	OU	Deletion of Exon 12†	Heterozygous	Mother (P6)
C6	61	F	Caucasian	0.50	0.47	OU	c.757C>T (p.Arg253*)	Heterozygous	
C7	65	F	Caucasian	0.10	0.30	OU	c.1584_1587del (p.Val529Hisfs*7)	Heterozygous	
C8	54	F	Caucasian	0.00	0.17	OU	c.189G>C (p.Gln63His)	Heterozygous	
C9	29	F	Hispanic	0.00	0.00	OU	c.940G>A (p.Gly314Arg)	Heterozygous	

Abbreviations: P, patients; C, carrier; M, male; F, female; OD, right eye; OS, left eye; OU, both eyes; *, nonsense mutation.
Footnotes: ‡, GRCh38 assembly/NM_000390.3; †, failure of amplification by polymerase chain reaction (PCR).

5.2.1. Fundus imaging in CHM probands

CHM patients presented with patchy chorioretinal atrophy of various extent with islands of preserved retina in the posterior pole.

Advanced chorioretinal atrophy was seen as pale due to exposed sclera in color fundus images (**Figure 10**, white asterix). The choroidal vessel pattern was seen in areas with RPE atrophy in color fundus images and in NIR-AF images choroidal vessels were outlined by the diffuse signal emanating from residual choroidal pigment (**Figure 10B**: P7, P5, P15, P6).

Eight (8) patients (13 eyes) presented with central preserved RPE islands detected in NIR-AF images (**Figure 10B**: P7, P5, and P15 as green, yellow, and red asterisks). In 3 patients (6 eyes) NIR-AF areas presented as foci of more limited size. In color fundus photographs that were available for 23 eyes, 9 eyes exhibited islands of NIR-AF colocalized with pigmented areas in color fundus images. These islands were either densely pigmented (**Figure 10**: P5, green asterisk) or less compacted (**Figure 10**: P7, green asterisk).

In 19 out of 31 eyes the preserved RPE island was seen in NIR-AF and colocalized with a SW-AF signal in the same area (**Figure 10B** and **10C**: P7, P5, and P15; green and yellow asterisks in figure panels). In 12 eyes the preserved retina was seen as a large area of speckled SW-AF signal which was hypoautofluorescent in corresponding NIR-AF images (**Figure 10 B** and **10C;** P6; blue asterisk).

In 12 eyes (6 patients) areas of nummular pigment were seen in color images and NIR-AF images, but were void of signal in SW-AF images (**Figure 10B**, 1C: P7, P6, red asterisks). These areas were typically associated with thinning of outer retina in SD-OCT images.

SD-OCT scan analysis revealed, that areas of severe chorioretinal atrophy were defined by an absence of photoreceptor-attributable reflectivity bands (**Figure 10D**: P7, white asterisk and bracket). In areas of RPE loss and absent outer retinal bands, increased signal transmission into the choroid was observed, seen as vertical streaks extending posterior to RPE/Bruch's membrane (**Figure 10D**: P7, purple arrowheads). In some of these areas, the choroid had also atrophied. With severe outer retinal degeneration, the INL attributable band descended into the gap (**Figure 10D**: P6, red arrow). However, retinal islands with preserved NIR-AF and SW-AF signal were often associated with the presence of a visible but thinned ONL, and outer retinal layers that were discernible to variable extent (**Figure 10D**: P7, P5, P15, green bracket). P7 presented with outer retinal tubulations (ORT) in SD-OCT scans, that also exhibited NIR-AF signal but was devoid of SW-AF (**Figure 10D:** P7, red asterisk). Here, hyperreflectivity associated with the dense pigment reduced transmission of the SD-OCT signal into the choroid (**Figure 10D**: P7, red asterisk). Foci of the SW-AF signal in the absence of NIR-AF colocalized with thinned ONL and discontinuous or absent reflectivity of IZ, EZ, and ELM bands (**Figure 10C**: P5, AF blue arrowhead; D: P5, blue asterisk). Preserved retina in the foveal and parafoveal area as exhibited by P15 presented with increased central NIR-AF signal

and decreased foveal SW-AF, both of which are characteristic of the macula in healthy eyes (**Figure 10B, 10C**: P15). In addition, the SD-OCT image revealed relatively intact outer retinal layers (**Figure 10D**: P15, green bracket). An interesting observation was the speckled autofluorescence that characterized the extrafoveal region in the SW-AF image, as this brightly speckled macular area in the SW-AF image was hypoautofluorescent in the NIR-AF image. (**Figure 10B, 10C**: P15)

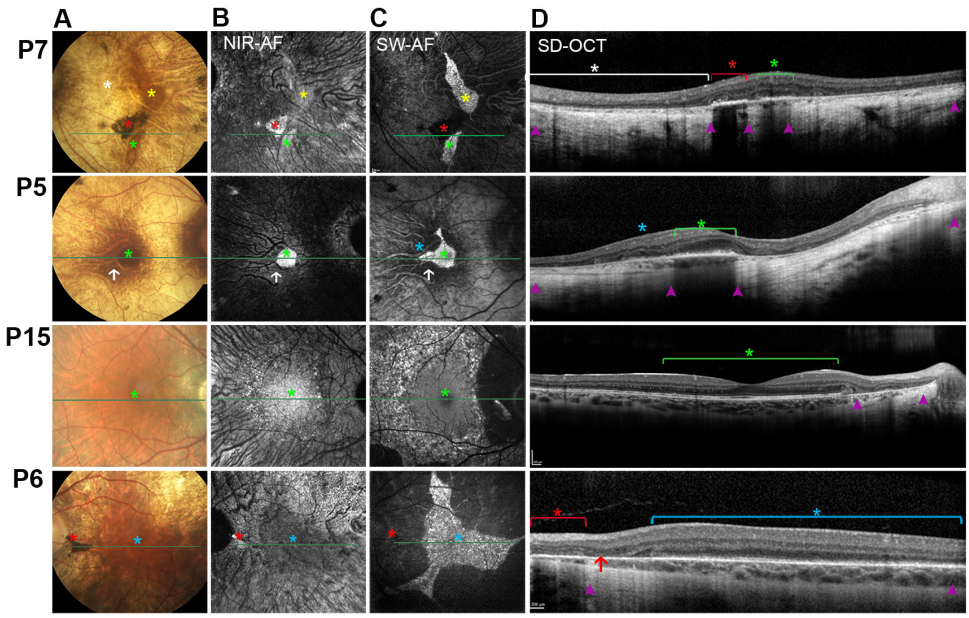

Figure 10. Multimodal fundus imaging of CHM probands (patients P7, P5, P15, and P6). Color fundus photographs (**A)** NIR-AF (**B**), SW-AF (**C**), and SD-OCT (**D**) reveal islands exhibiting NIR-AF and SW-AF signals (green and yellow asterisk); residual pigment and NIR-AF signal devoid of SW-AF (red asterisk); bare sclera (white asterisks); SW-AF signal in the absence of NIR-AF (blue asterisk, blue arrow); and hypertransmission of OCT signal (pink arrowhead). In P5, retained pigment in A exhibits weak NIR-AF but no SW-AF (white arrow). In P6, severe outer retinal degeneration exists with inner nuclear layer descent (red arrow). In SD-OCT scans (D) brackets indicate the corresponding area in the NIR-AF and SW-AF image. The horizontal axis and extent of the corresponding SD-OCT image are indicated by the green lines in A–C.

5.2.2. Fundus Imaging in CHM Carriers

All carriers presented with an alternating mosaic like pattern of AF mottling seen in both SW-AF and NIR-AF images extending throughout the posterior pole (18/18 eyes) (**Figure 11**). The foci of reduced NIR-AF signal in the mosaic pattern colocalized with reduced SW-AF (**Figure 11** B1, C1) One of the car-

riers (C3) had more advanced peripapillary and macular atrophic changes that were seen as areas of reduced SW-AF and NIR-AF signal (**Figure 11** carrier 3).

All carriers presented with hyperreflective deposits at the level of EZ and IZ in SD-OCT scans (**Figure 11**, carrier 1 and 2). In SW-AF and NIR-AF these aberrations were visible as bright hyperautofluorescence flecks (**Figure 11B**,**C** carriers 1 and 2).

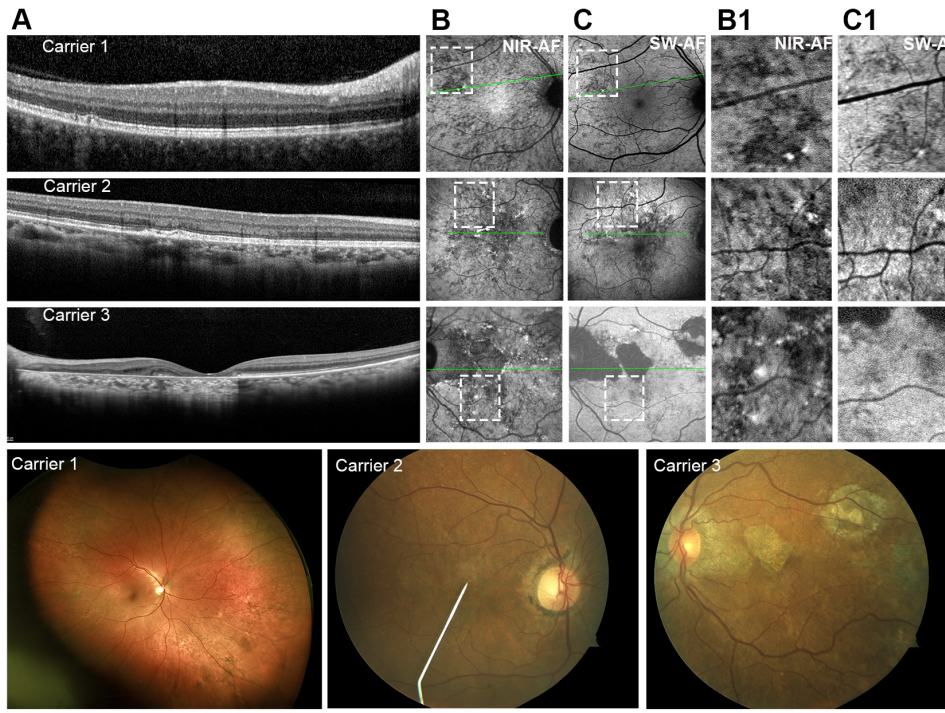

Figure 11. Multimodal imaging of choroideremia carriers (C1, C2, and C3). SD-OCT (A), NIR-AF (B), and SW-AF (C). Areas in the rectangles in B and C are expanded in B1 and C1, respectively. The horizontal axis and extent of the corresponding SD-OCT image are indicated by the green lines in B and C. Fundus color photos are presented in the lower panel (D)

5.2.3. qAF in CHM probands and carriers

To further characterize SW-AF in CHM, we analysed qAF levels in 6 probands (7 eyes; P1, P5, P7, P9, P10, and P15; age, 31–67 years) and 6 carriers (11 eyes; carriers 1, 4, 5, 7, 8, and 9; 12 eyes; age, 29–65 years). For probands we measured qAF levels in the foveal segment and for carriers in the classical qAF8 ring positioned circularly at 8° from fovea (**Figure 12C, 13C**).

To visualize the distribution of SW-AF intensities in relation to the central retinal islands, we generated qAF colormaps (scaled from 0–1200 qAF units) and compared CHM patients to age-matched healthy eyes. The qAF signal in

the macular area of CHM probands was nonuniform and profoundly reduced not only in chorioretinal areas but also in the area of preserved retina (**Figure 12 A,B**) compared to age-matched healthy eye (**Figure 12 C**). In CHM carriers color-coded qAF images revealed both an overall decrease in qAF and local increases and decreases associated with the mosaicism of the fundus (**Figsure 12A, 12B**: carriers 4, 1, and 5).

We also plotted qAF values in predetermined areas of macula to compare them to the healthy cohort. qAF intensities for CHM probands in foveal area and for the carriers in the circular qAF8 ring positioned at 8° from fovea were either within or below the range of the lower 95% CI in healthy eyes (**Figure 12**,**13 D**).

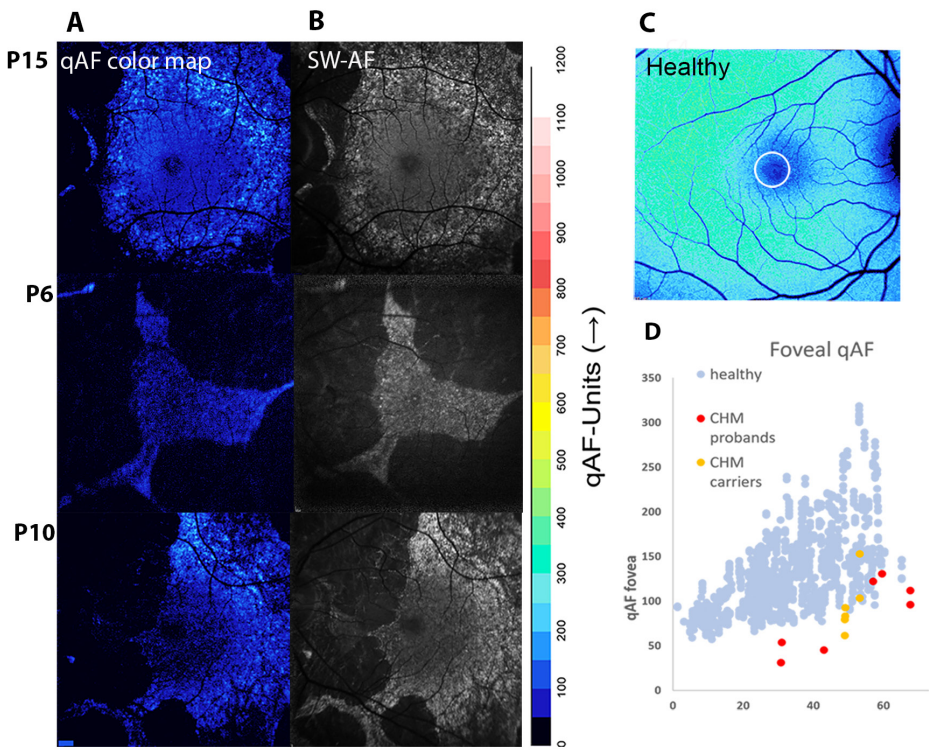

Figure 12. qAF color-coded images of P15, P6, and P10 (**A**). Corresponding SW-AF images (**B**). Healthy age-similar qAF color-coded image (**C**). qAF values acquired from foveal area (18 eccentricity; circle in C) and plotted as a function of age for healthy subjects (blue circles), CHM probands (P1, P5, P7, P9, P10, and P15; red circles), and CHM carriers (carriers 1, 3, 4, 7, 8, and 9; yellow circles) (**D**)

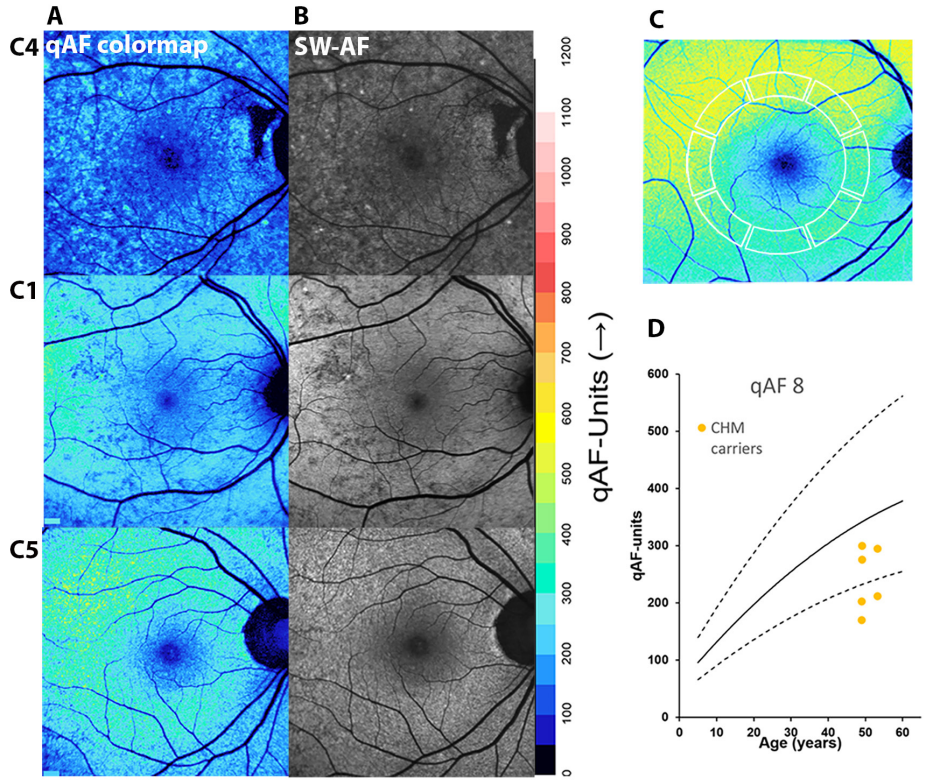

Figure 13. qAF in CHM carriers. qAF color-coded images of CHM carrier 4, carrier 1, and carrier 5 (**A**). Corresponding SW-AF images (**B**). Healthy (age 55 years) qAF color-coded image (**C**). qAF8 values (yellow circles) acquired from 8 concentric segments (78–98 eccentricity; outlined in C) and plotted as a function of age for carriers 1, 4, 5, 7, 8, and 9 (**D**). Mean (solid black line) 6 95% CIs (dashed lines).

5.2.4. Quantitation of NIR-AF in Patients and Carriers

To compare the levels of NIR-AF intensities in eyes with CHM to healthy eyes, we used a semiquantitative method to create horizontal NIR-AF profiles through the fovea of 9 probands (P6, P7, P9, P10, P11, P12, P14, P15, and P16; 18 eyes; age, 10.2–77.2 years) and 3 carriers (C7, C8, and C9; 6 eyes; age range, 29.3–64.7 years).

The intensity profiles (**Figure 14A, 14B**) revealed that for CHM probands, the mean NIR-AF intensity was below the 95% CI for healthy eyes (**Figure 14C**, green trace versus red and yellow). The NIR-AF profiles covered areas of atrophy as well as islands of preserved retina, therefore representing signal from exposed choroid and relatively preserved RPE. However even in the central positions of the profiles corresponding to preserved retina, the mean NIR-AF signal for CHM probands was lower compared to healthy cohort (**Figure 14**, C). In probands who presented with a preserved island exhibiting only SW-AF

and no NIR-AF signal the NIR-AF profiles showed even lower intensities (**Figure 14B**, yellow trace; 15C, NIR-AF) compared to probands with a preserved island emitting detectable NIR-AF signal (**Figure 14A**, red profile; **14C**, NIR-AF+). Profiles of the carriers (**Figure 14C**: blue trace) showed variability, with the central foveal values being below the healthy 95% CI (**Figure 14C**, below, green trace).

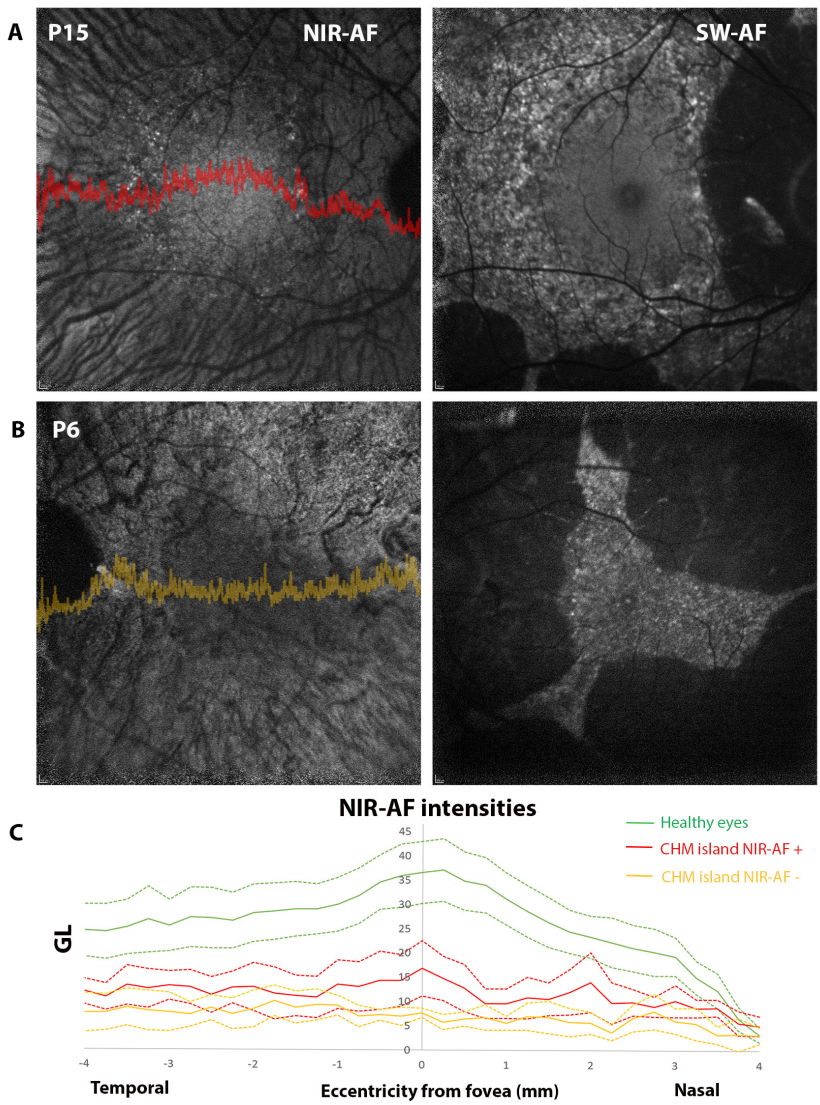

Figure 14. NIR-AF signal intensity profiles for CHM probands and carriers. NIR-AF images with profile overlay and SW-AF images for P15 (**A**) and P6 (**B**). Intensity profiles are presented as mean (solid line) and 95% CIs (dashed line).(**C**) Horizontal intensity profiles through the fovea are shown for 6 patients exhibiting a central NIR-AF signal (NIR-AFþ; red profile) and for 3 patients having reduced or absent central NIR-

AF signal (NIR-AF; yellow profile). Comparison is made to intensity profile constructed from 19 healthy eyes (green profile) (C, above). Horizontal profiles through the fovea are shown for 3 carriers (blue profile) and compared to healthy eyes (green profile) (C, below).

5.2.5. Retinal Thickness and Visual Acuity in Relation to NIR-AF Signal

Foveal thickness (FT) and subfoveal choroidal thickness (SFT) were measured in all 16 probands (31 eyes). In the group with detectable NIR-AF signal emitted from the retinal island, the average (±SD) FT and SFT were higher (FT, 191.6 µm ± 52.06; SFT, 148.42 µm ± 81.8) than in those with no NIR-AF signal originating from the central island (FT, 155.08µm ± 102.5; SFT, 124.6 µm ± 74.3); however, that difference was not statistically significant (P = 0.21 and P = 0.58, Wilcoxon-Mann-Whitney Test). The Bland-Altman analysis of the FT measurements obtained from the two observers revealed the mean of the differences to be 6.23 (±15.21, SD of the difference between the observers). The 95% limits of agreement between observers (estimated as ±1.96 ×SD) were -23.6 to 36.0, indicating that measurements by observer 1 could be 23.6 units below or 36 units above observer 2. In the case of choroidal thickness, the mean of the differences was 2.64 (±14.5) and the 95% limits of agreement between observers was -25.8 to 31.1. The logMAR-equivalent BCVA ranged from 0 to 0.87. The group with the preserved NIR-AF signal associated with a preserved retinal island (10 patients) had a better mean visual acuity (mean logMAR equivalent [±SD], 0.16 ± 0.1) compared to the group with absent NIR-AF signal (logMAR equivalent [±SD], 0.46 ± 0.2) (6 patients), and the difference proved to be statistically significant (P = 0.003, Wilcoxon-Mann-Whitney Test).

5.3. Photoreceptor Cells as a Source of Fundus Autofluorescence in Recessive Stargardt Disease (Study 3)

Accelerated bisretinoid formation is the hallmark of STGD1 due to the defective *ABCA4* gene. A generalized increase in retinal SW-AF signal (Burke et al. 2014) as well as hyperautofluorescent fleck formations are observed in STGD1. In this study SW-AF, NIR-AF and IR-R fundus images together with SD-OCT scans from 12 patients (6 female, 6 male; age range 9 to 61 years) with the diagnosis of STGD1 and expression of flecks were studied retrospectively by two independent graders (JRS, MP) using qualitative and quantitative approach.

Table 4. Demographic, clinical and genetic summary of the Stargardt disease patient cohort.

Patient	Age	Age of onset	Race/ Ethnicity	Iris color	BCVA		*ABCA4* Mutations	
					OD	OS	Allele 1	Allele 2
1	14	10	White	Green	20/70	20/80	p.[L541P/A1038V]	p.N1868I; c.768+358C>T‡
2	9	9	White	Hazel	20/200	20/200	p.W855*	p.T1526M
3	18	14	White	Blue	20/100	20/125	p.T972N	p.L2027F
4	23	18	White	Blue	20/30	20/30	p.C54Y	c.5196+1137G>A; ‡ c.1555-2745A>G‡
5	14	10	White	Blue	20/150	20/40	c.4773+3A>G	p.[L541P/A1038V]
6	12	8	White	Blue	20/300	20/200	c.5312+1G>A	p.R2030*
7	16	10	White	Blue	20/40	20/60	p.[L541P/A1038V]	p.L2027F
8	30	23	Indian	Brown	20/60	20/70	p.R653C	p.G1961E
9	61	52	White	Green	20/125	20/20	c.250_251insCAAA	p.N1868I
10	16	8	White	Brown	20/25	20/25	p.R1108C	p.Q1412*
11	41	18	White	Blue	20/200	20/150	p.G1961E	p.N1868I; c.2160+584A>G‡
12	55	50	White	Hazel	20/50	20/40	p.R2077W	p.N1868I

BCVA, best-corrected visual acuity; OD, right eye; OS, left eye; ‡, possibly pathogenic (pending functional validation studies)

5.3.1. Fundus flecks in SW-AF and NIR-AF images

In SW-AF images flecks were often distinctly hyperautofluorescent while being hypoautofluorescent (12/12 patients) in NIR-AF images (**Figure 15**, green rectangles; **Figure 16**). Other flecks were dark in NIR-AF images while being barely detectable in SW-AF images **(Figure 15** yellow arrows). We also observed that the fleck profiles in the NIR-AF images tended to be larger (**Figure 15**) whereas a halo of weaker autofluorescence surrounding the fleck was sometimes present in SW-AF (**Figure 15, 17**). In contrast to that some flecks in NIR-AF images exhibited a bright center and dark surround; these flecks could also be bright in SW-AF and were positioned more peripherally in the fundus (**Figure 15**, turquoise rectangle).

To further compare flecks in SW-AF and NIR-AF imaging modalities, we selected hyperautofluorescent flecks in a predetermined area of superior hemiretina in SW-AF images (total of 95 flecks; 19 eyes, 10 patients) and assessed them based on their appearance in NIR-AF images. As a result we found that out of these hyperAF flecks in SW-AF 7.3% were hyperautofluorescent in NIR-AF images, 7% appeared to be similar to neighbouring intensities and 85% were hypoautofluorescent. The latter included flecks having a bright center with a dark-surround. A chi-square test of independence showed that the differences in percentages were significant (X^2 (2, N=100) = 122.9, $p < 0.01$).

Flecks are a dynamic retinal finding and the AF signal shows transformation over time. Flecks can become darker in both SW-AF and NIR-AF imaging (**Figure 15**, red rectangles). Hypoautofluorescent flecks were most often seen in the central area adjacent to atrophy. Flecks were also visible in IR-R images (**Figure 15C, 16 C,E,G,I**) (12/12 patients); with this modality flecks could be hyper- or hyporeflective (**Figure 15; 16**).

Looking at the distribution of flecks in SW-AF and NIR-AF, flecks first appeared in central retina and over the course of the disease become more distributed toward periphery (8/11 patients) (**Figure 17, 18**) The spread of the flecks in SW-AF modality was led by hyperautofluorescent foci while in NIR-AF the advancement was seen as increase in hypoautofluorescent foci (9/9 patients) (**Figure 18**).

In some patients flecks showed a tendency to spread radially from the fovea to approximately 8° of eccentricity, beyond which a circumferential spread characterized the distribution (8/12 patients) (**Figure 17, 18**). Flecks are typically visualized within the 30° field in the clinical setting. Wide-field images show that flecks also form well beyond this range (12/12 patients) (**Figure 17**). Patients who were imaged as follow-ups (7/10) of 1 year, some flecks were observed to be hypoautofluorescent in NIR-AF images (**Figure 18** B) before any evidence of hyperautofluorescence in SW-AF images (**Figure 18** A versus C).

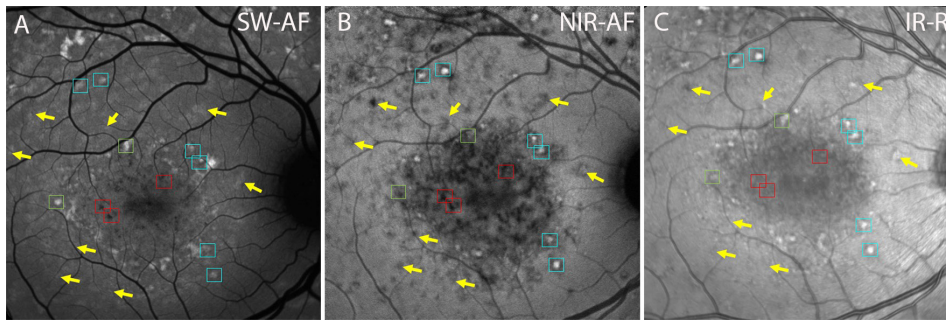

Figure 15. Fundus flecks in an STGD1 patient are viewed in short-wavelength autofluorescence (SW-AF) (**A**), near infrared autofluorescence (NIR-AF) (**B**) and infrared reflectance (IR-R) (**C**) images (Patient 5). Flecks can be hyperautofluorescent in SW-AF, hypoautofluorescent in NIR-AF and bright in IR-R images (green rectangles); bright in SW-AF, NIR-AF and IR-R images (turquoise rectangles); barely detectable in SW-AF, dark in NIR-AF and bright or not detectable in IR-R (yellow arrows). Flecks can be dark in all modalities (red rectangles).

5.3.2. Flecks in SD-OCT scans

For further structural evaluation of flecks, we analyzed SD-OCT images. Flecks seen in SW-AF, NIR (**Figure 16 A,B**) and IR-R (**Figure 16 C,E, G, I**) also co-localized with hyperreflective lesions in SD-OCT images; these lesions extended through photoreceptor-attributable OCT bands (12/12 patients) (**Figure 16 D, F, H, J**). Some flecks presented as a thickening at the level of interdigitation zone (IZ), others extended anterior to ellipsoid zone and external limiting membrane (ELM) making their way to outer nuclear layer (ONL). ONL thinning was observed as fleck height increased anteriorly (12/12 patients) (**Figure 16 D, H,** blue and red arrows).

Decreased transmission into the choroid was associated with most flecks, although other flecks that in SW-AF images exhibited fluorescence extinction were accompanied in SD-OCT images by increased transmission into the choroid (4/12 patients) (**Figure 16 A, B, H**, purple arrow).

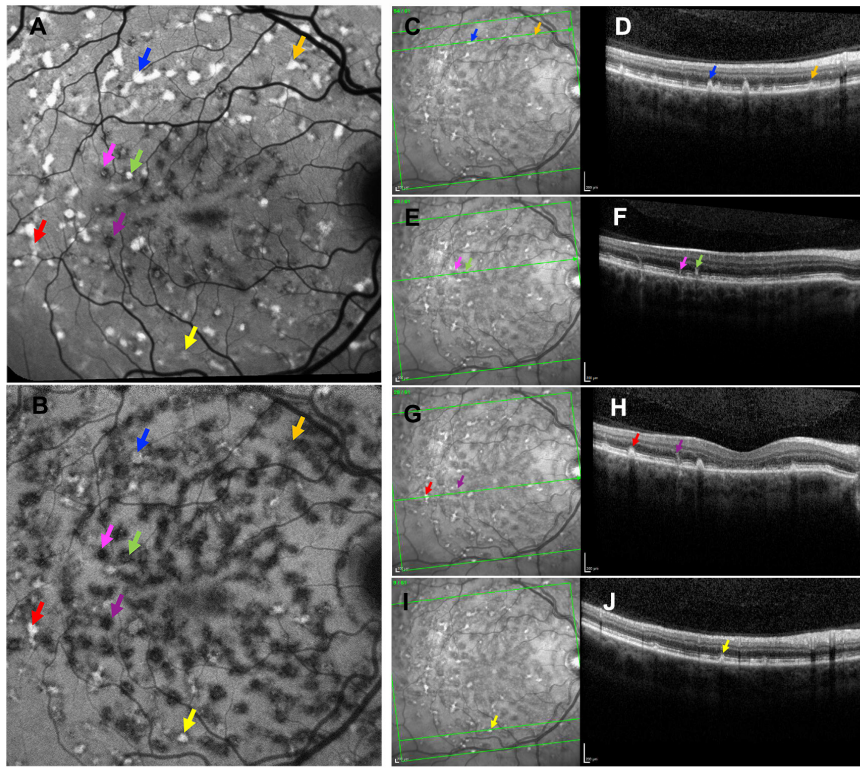

Figure 16. Retinal flecks in STGD1 imaged by short-wavelength autofluorescence (SW-AF) (**A**), near infrared autofluorescence (NIR-AF) (**B**) and IR-R (**C, E, G, I**) registered to images obtainedby spectral domain optical coherence tomography (**D, F, H, J**) (Patient 4). The horizontal axis and extent of SD-OCT image are indicated by horizontal green lines ending in arrows. Flecks are visible in SD-OCT images as hyperreflective radial lesions that occupy photoreceptor-attributable bands. Flecks are color-coded to indicate correspondence in successive imaging modalities

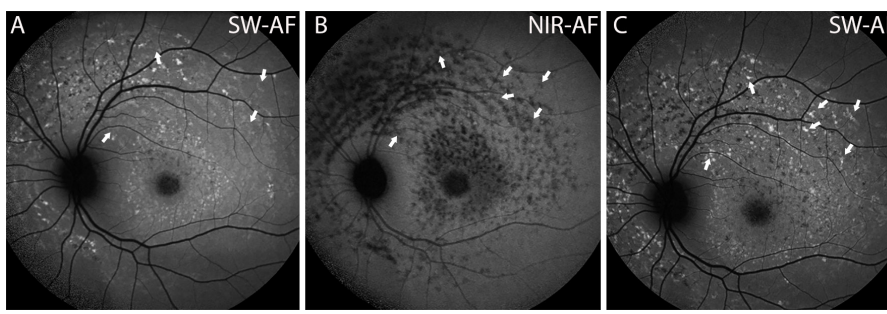

Figure 17. Spatial distribution of fundus flecks in serial images (Patient 3). Short-wavelength (SW-AF) (**A, C**) and near infrared (**B**) wide-field images. The SW-AF image in C was acquired 12 months after the SW-AF and NIR-AF images in A and B. Flecks (arrows) are hypoautofluorescent in NIR-AF images (**B**) while invisible or faintly visible in SW-AF images (**A**) before appearing hyperautofluorescent in SW-AF images after 12 months (**C**).

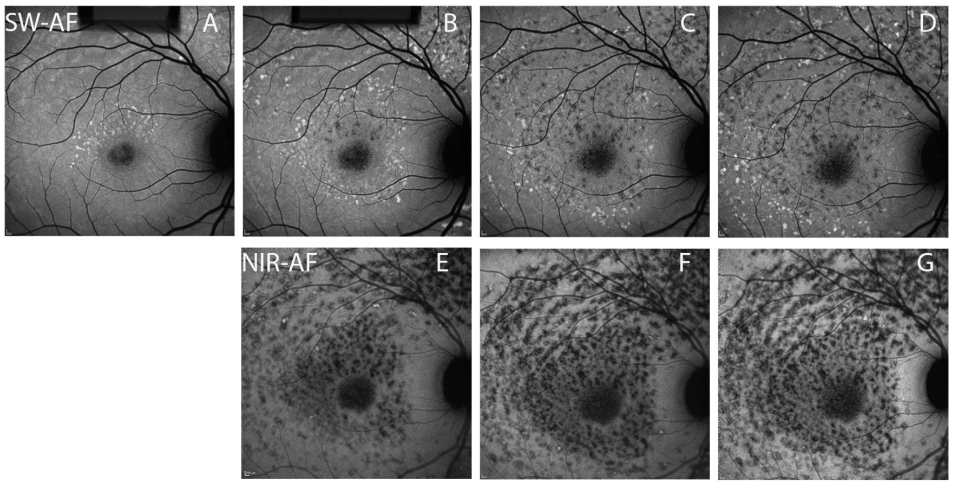

Figure 18. Progression of fleck formation in short wavelength (**A, B, C, D**) and near infrared (**E, F, G**) autofluorescence images (Patient 1). Serial images acquired at intervals of 13 months (**A** to **B,E**); 12 months (**B,E** to **C,F**); 6 months (**C,F to D, G**).

5.3.3. Quantitative autofluoresence and color coded images

The intensity of SW-AF signal was also examined in color-coded qAF images, where colors represent pixel grey level values in the scale of 0–1200. qAF images taken at intervals were examined to evaluate the brightness of flecks in time. **Figure 19** shows a patient (P1) imaged at 15-month and 18-month intervals. Flecks presented with more intensity in the superotemporal area of the macula with progression superiorly and later becoming more intense in inferior macula. This pattern of fleck evolution was seen in 5/10 patients (9/16 eyes). Flecks that transitioned to foci of intense autofluorescence (red/white foci) (**Figure 19A** left panel) were later reduced in brightness (8/10 patients) (**Figure 19A**, right panel, yellow and green foci). Notably the peripapillary area was spared from flecks and atrophy. The area of central atrophy revealed extinguished SW-AF intensities with gradations of color black to green.

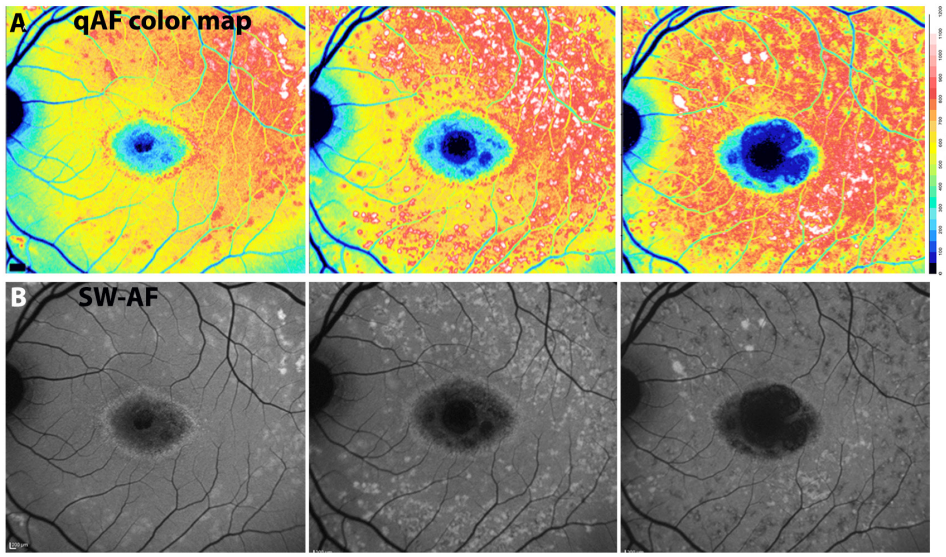

Figure 19. Flecks visualized in color-coded quantitative fundus autofluorescence (qAF) images (upper panel) shown together with the corresponding fundus autofluorescence (SW-AF; 488 nm) images (lower panel) of Patient 1. Serial images were acquired at a 15-month and 18-month interval. Lower qAF levels are coded in blue and higher qAF levels as red or white.

5.4. Insights into *PROM1*-Macular Disease Using Multimodal Imaging (Study 4)

5.4.1. Clinical and genetic data

Eighteen (18) subjects (36 eyes) with genetically confirmed diagnosis of *PROM1*-macular disease were analyzed in this study with the mean age being 42.8 years (range 5–66). Analysis of multimodal imaging included qualitative analysis SW-AF, NIR-AF and SD-OCT images, as well as quantitative analysis of those imaging modalities. A summary of the clinical, demographic and genetic characteristics of the cohort is presented in **Table 5**. Nine patients reported a family history consistent with autosomal dominant inheritance (**Figure 20**). Fifteen patients presented with central vision disturbance in the second or third decade of life; three were asymptomatic relatives (P8, P10 and P13) (**Table 5**). Five patients reported difficulty with night vision or photopsias. Full-field electroretinogram (ffERG) recordings were within normal limits in 6 of the 11 patients. Moderate attenuation of the 30 Hz flicker and single flash cone responses were detected in the remaining 5 patients (P1, P5, P16, P17 and P18).

Table 5. Demographic, clinical and genetic characteristics of patients with *PROM1*-associated maculopathy

Patient	Age (years)	Age of onset (years)	Year of presentation	Gender	Ethnicity	Snellen BCVA		Foveal sparing		FHx of retinal disease	*PROM1* variant	
						OD	OS	OD	OS		cDNA	Protein
1	55	50	2014	F	Caucasian	20/30	20/30	+	+	No	c.303+1G>A	p.(?)
2	46		2008	F	Hispanic	N/A	N/A	+	+	Yes	c.303+1G>A	p.(?)
3	33	25	2017	M	Caucasian	20/30	20/25	+	+	Yes	c.303+2T>C	p.(?)
4	66		2017	M	Caucasian	20/40	20/40	+	+	Yes	c.303+2T>C	p.(?)
5	58	35	2012	M	Caucasian	20/200	20/120	+	+	Yes	c.303+2T>C	p.(?)
6	45	44	2019	M	Asian	20/20	20/20	+	+	No	c.314A>G (homozygous)	p.(Tyr105Cys) homozygous
7	34	20	2011	F	Caucasian	20/200	20/40	-	-	Yes	c.400C>T	p.(Arg134Cys)
8	63	(asymptomatic)	2012	F	Caucasian	20/20	20/20	+	+	Yes	c.400C>T	p.(Arg134Cys)
9	59	20	2010	M	Caucasian	20/50	20/120	+	+	No	c.1117C>T	p.(Arg373Cys)
10	22	(asymptomatic)	2010	M	Caucasian	N/A	N/A	+	+	Yes	c.1117C>T	p.(Arg373Cys)
11	64	20	2019	M	Chinese	N/A	N/A	-	-	Yes	c.1117C>T	p.(Arg373Cys)
12	39	35	2019	F	Chinese	20/80	20/40	+	+	Yes	c.1117C>T	p.(Arg373Cys)
13	5	(asymptomatic)	2019	M	Chinese	20/20	20/20	+	+	Yes	c.1117C>T	p.(Arg373Cys)
14	40	37	2010	F	Hispanic	20/200	20/100	+	+		c.1117C>T	p.(Arg373Cys)
15	24	22	2020	F	Caucasian	20/25	20/25	+	+	No‡	c.1117C>T	p.(Arg373Cys)
16	44	40	2011	M	Caucasian	20/60	20/50	-	-	No	c.1354dupT	p.(Tyr452Leufs*13)
17	34	31	2017	M	Caucasian	20/100	20/100	+	+		c.2290A>T	p.(Lys764*)
18	32	27	2011	M	African-American	20/400	20/400	+	-	No	c.2373+5G>T	p.(?)

BCVA, best-corrected visual acuity, OD, right eye; OS, left eye; F, female; M, male; N/A, not acquired; FHx, family history; cDNA, complimentary DNA; ‡Father carries PROM1 variant but reported to be asymptomatic; Familial relationships: P4 is the father of P3, P8 is the mother of P7, P10 is the son of P9, P11 is the father of P12, P13 is the son of P12.

5.4.2. Retinal imaging

In 15 out of 18 patients the disease was confined to the macular area. In 3 patients fleck-like lesions or atrophic changes reached further to the posterior pole (P7, P8 and P11) (**Figure 20, 21**). None of the patients presented with bone spicules.

Patients presented with macular atrophy and RPE mottling in both SW-AF and NIR-AF images (**Figure 20, 21**). The most typical feature was granular hypoautofluorescence in the macular area, which was present in almost all eyes (36/38). Fleck-like formations were seen as small hyperautofluorescent foci surrounding central atrophy in SW-AF images in 30 eyes (**Figure 21A**, red arrow; P3, P6, P9, P15) and a hyperautofluorescent halo was seen in 20 eyes (20/38) (**Figure 21A**, blue arrow; P1, P9, P15, P17). NIR-AF imaging was available for 9 patients (18 eyes) and presented with decreased granular signal in the central macular area (**Figure 21 B**). Hyperautofluorescent foci were observed in only one subject (2/18 eyes) (**Figure 21B**, red arrow; P6) and a hyperautofluorescent halo was seen in 3 subjects (6/18 eyes) (**Figure 21B**, blue arrow; P9, P15, P17).

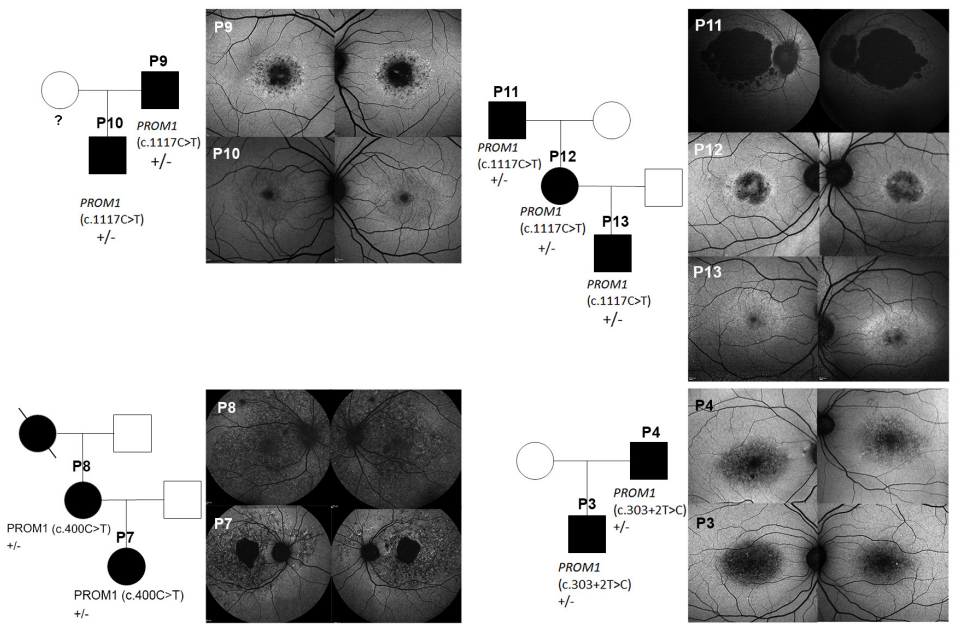

Figure 20: *PROM1*-macular dystrophy. Four pedigrees with dominant retinal disease inheritance patterns. Subjects with *PROM1*-macular dystrophy are shown in black. "-" is for pathogenic variants and "+" denotes a wild-type allele. Male, square; female, circle. Diagonal line denotes a deceased individual. Short-wavelength fundus autofluorescence (SW-AF) images of patients are shown next to each pedigree.

Thinning of outer retinal layers was observed in macular SD-OCT images. These changes varied from discontinuities in the EZ band (**Figure 21C** P3, P6) to total outer retinal atrophy (**Figure 21C** P1, P9, P15, P17). Increased transmission of SD-OCT signal into the choroid was commonly observed in the macular area, the extent of which varied (**Figure 21C**, yellow stars; P1, P9, P15, P17).

Areas of granular hypoautofluorescence in SW-AF and NIR-AF images corresponded to partial outer retinal degeneration (**Figure 21** A, C; P3, P6) while defined areas of hypoautofluorescence corresponded to complete loss of outer retinal layers and RPE in SD-OCT scans (**Figure 21** A, C; P9, P15). We evaluated presence of foveal sparing in SD-OCT, SW-AF and NIR-AF images and it was observed in 31 of 38 eyes.

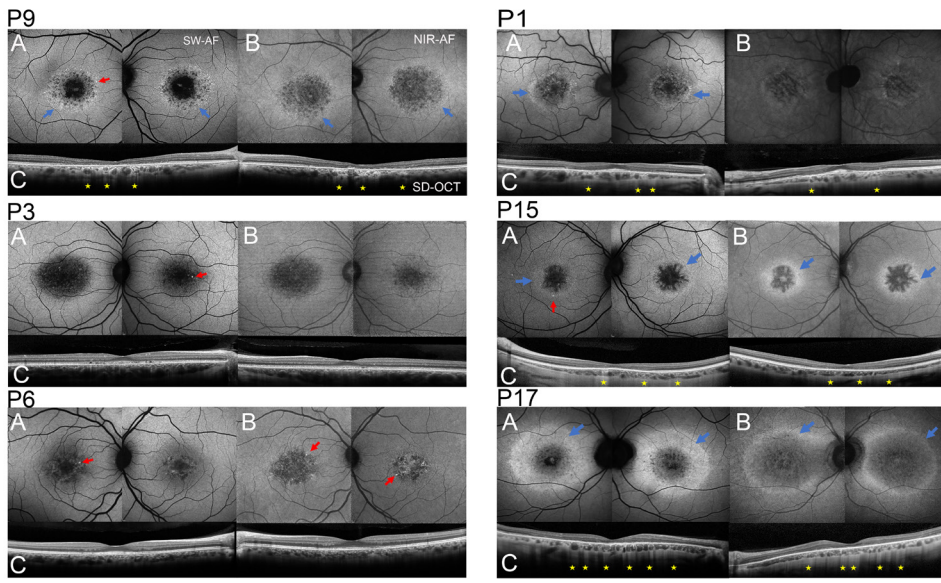

Figure 21: Short-wave fundus autofluorescence (SW-AF) (**A**), near infrared fundus autofluorescence (NIR-AF) (**B**) and spectral domain optical coherence tomography (SD-OCT) (**C**) in *PROM1* patients. Macular dystrophy presents as granular alterations in SW-AF and NIR-AF images. Loss of the ellipsoid (EZ) band is evident in the SD-OCT scans. Hyperautofluorescent foci are marked with a red arrow in SW-AF (**A,** P3, P6, P9, P15) and NIR-AF (**B** P6) images. Hyperautofluorescent halos are indicated with blue arrows in SW-AF (**A** P1, P9, P15, P17) and in NIR-AF (**B** P9, P15, P17) images. Advanced outer retinal disruption or atrophy is seen as hypertransmission into the choroid in SD-OCT images (**C**; P1, P9, P15, P17, yellow stars).

We analysed SW-AF intensities in 12 patients (20 eyes). qAF analysis revealed that in 18 eyes the values were within the 95% CI of healthy eyes. In one eye (P8 OS) qAF values were lower and in one eye (P17 OD) values were higher than the 95%CI (**Figure 22** A). Previously published qAF values of STGD1

(Burke et al. 2014) have been added to the graph to allow comparison with STGD4.

In addition comparison of qAF color-coded maps also demonstrated that there was no generalized increase of SW-AF levels in *PROM1* patients compared to healthy age-matched individuals. (**Figure 22B, C**) Centrally decreased qAF signal corresponded to areas of outer retinal atrophy (**Figure 22C**).

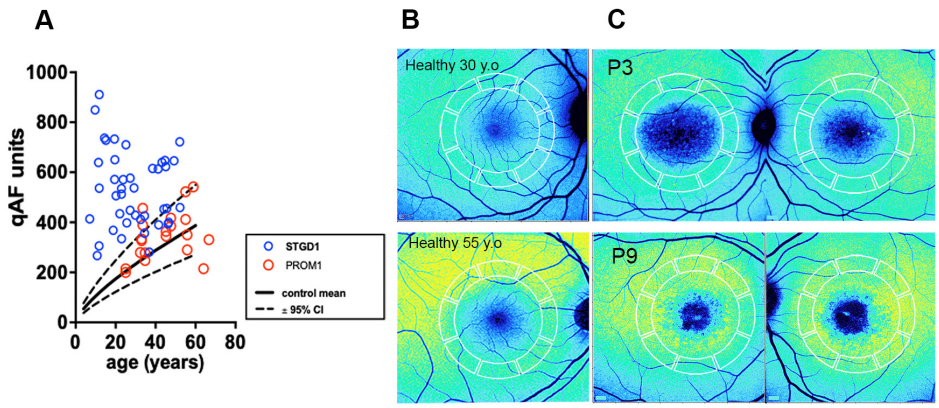

Figure 22: Quantitative fundus autofluorescence (qAF8) intensities recorded from *PROM1* patients are presented with previously published data acquired from STGD1 patients and reported in Burke *et al* al 2014 (Burke et al. 2014). qAF values acquired from *PROM1* patients (red circles) are plotted as a function of age together with mean (solid black line) and 95%CI (dashed lines) of the healthy control group. Values acquired from STGD1 patients are represented by blue circles (**A**). Color-coded maps of qAF distribution in healthy age-matched individuals (**B**) and *PROM1* patients (**C**). Only 2 of the 17 qAF8 values of *PROM1* patients were outside the 95% confidence intervals of the healthy controls; one eye above and the other eye below the range. In the color-coded images decreased SW-AF signal in the central macula corresponded to atrophic changes.

NIR-AF intensities were quantified in 8 patients (16 eyes) along a horizontal axis through the fovea (**Figure 23A**). The mean signal was reduced in central macula at an eccentricity of 0–2 mm nasally and temporally from fovea. Peripheral to this central area (2–4 mm eccentricity) however, mean NIR-AF intensity in PROM1 patients was comparable to that of healthy subjects (**Figure 24B**).

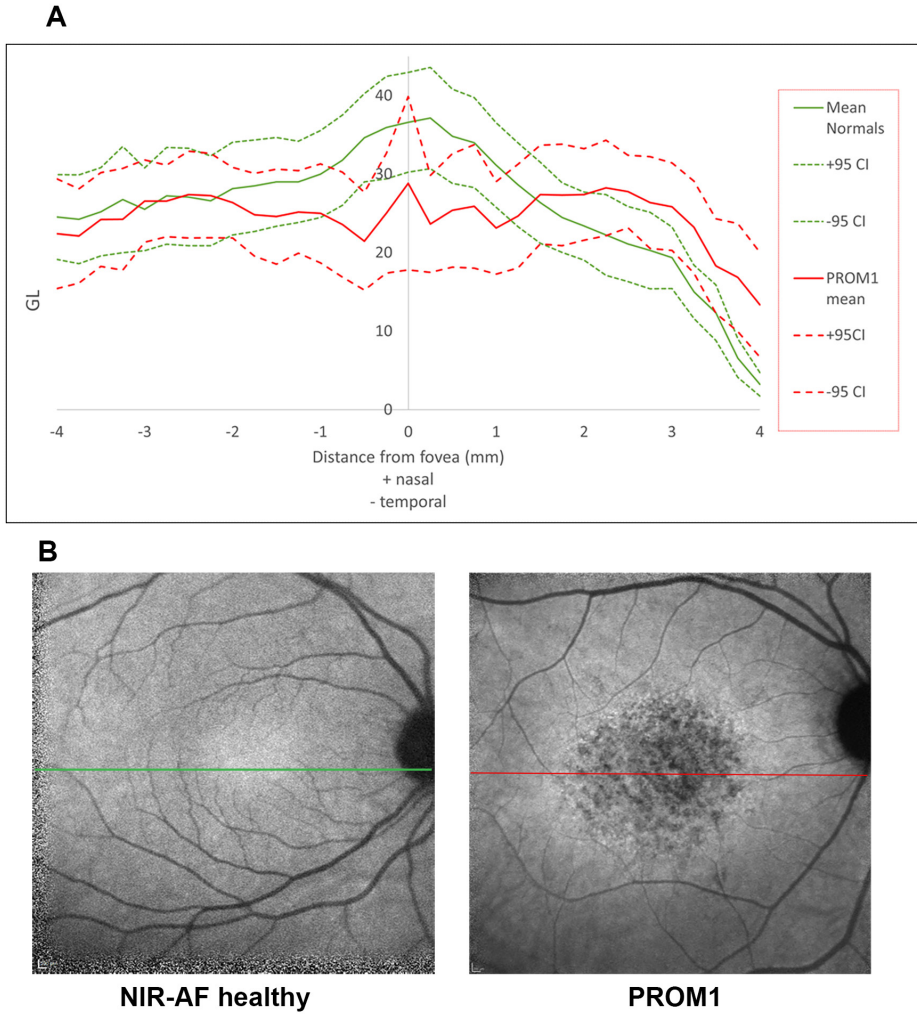

Figure 23: Quantitative NIR-AF analysis in *PROM1* patients. NIR-AF intensity profiles acquired from *PROM1* patients are plotted as mean (red solid line) and upper and lower 95% confidence intervals (CI) (dashed red lines) together with mean NIR-AF values of healthy subjects (green solid line) and corresponding 95% CI (dotted green line) (**A**). In *PROM1* patients the NIR-AF values are decreased in the central macula corresponding to the outer retinal disruption or atrophy seen in *PROM1* macular dystrophy, however the NIR-AF values in the adjacent macular area are comparable to those of healthy subjects (**A**). NIR-AF image of a healthy aged-matched eye (left) and *PROM1* patient (P9) (right) (**B**). The horizontal axes along which NIR-AF values were recorded are shown as green and red lines (**B**).

6. DISCUSSION

6.1. Origins of SW-AF and NIR-AF in cases of ABCA4 deficiency and albinism

In Study 1 we analyzed SW-AF and NIR-AF imaging in cases with varying levels of bisretinoid lipofuscin and RPE pigmentation.

Female carriers of ocular albinism presented with fundus mosaicism – a pattern of pigmented and hypopigmented RPE cells. This allowed for a unique study model to confirm how hypopigmented areas presented as dark hypoautofluorescence in NIR-AF images, while lack of RPE melanin was seen as increased SW-AF signal in the color coded maps of qAF.

STGD1 is macular dystrophy where the hallmark of pathological mechanism is the accelerated accumulation of bisretinoid lipofuscin due to the defective ABCA4 transporter protein (Eagle et al. 1980; Sparrow et al. 2013). Various imaging studies have shown increased SW-AF intensities in patients with STGD1 compared to healthy subjects (F. C. Delori, Staurenghi, et al. 1995; Cideciyan et al. 2004; Burke et al. 2014). The NIR-AF intensities in STGD1 have not been thoroughly studied. We analyzed the NIR-AF images of 25 subjects with STGD1 and found that in the perifoveal macular area without signs of macular atrophy the NIR-AF signal intensities were significantly higher than in healthy eyes (**Figure 8**).

To add to the clinical observation and better understand the origins of SW-AF and NIR-AF signal we also studied mice lines with varying pigmentation (albino, agouti and black coated) and also with different levels of bisretinoid lipofuscin accumulation (*Abca4* $^{-/-}$, *Abca4* $^{+/+}$, *Rdh8*$^{-/-}$*Abca4*$^{-/-}$).

In Study 1 we further confirmed the concept that melanin is the major contributor to the NIR-AF of the fundus. Analyzing the images of OA1 carriers revealed how hypopigmented areas corresponded to reduced NIR-AF. This together with further analysis of albino and agouti mice supports previous knowledge that NIR-AF signal originates mainly from RPE melanin (Keilhauer and Delori 2006).

Secondly we showed that NIR-AF signal is also increased as is the SW-AF signal in *ABCA4* patients (Cideciyan et al. 2007; Duncker, Lee, et al. 2013). This conclusion was supported by the finding that the NIR-AF signal in agouti *Abca4*$^{-/-}$ mice was elevated relative to the NIR-AF signal in agouti *Abca4*$^{+/+}$ mice. A possible explanation for that could be that the increase in lipofuscin in the RPE has a modulating effect on NIR-AF signal. Melanin has property of self-absorbance when melanosomes are packed tightly together. This property could be reduced when abundance of lipofuscin granules are separating the melanosomes from each other and the NIR-AF fluorescence would undergo less self-absorption. This mechanism however does not offer an explanation for the observation that in albino *Abca4*$^{-/-}$ mice, fundus NIR-AF intensities were elevated in tandem with increases in SW-AF even in the absence of melanin. It

has been proposed that bisretinoid could stimulate melanin synthesis (Poliakov et al. 2014), but our analysis of albino *Abca4-/-* versus albino wild-type mice, both of which are deficient in the tyrosinase gene required for melanin synthesis, showed a difference in NIR-AF intensities indicating that increased bisretinoid is not stimulating melanin synthesis.

Similarly, an increase in numbers of melanosomes paralleling a rise in NIR-AF intensity was not observed in pigmented *Abca4*$^{-/-}$ mice (Charbel Issa et al. 2013). An alternative explanation is that bisretinoid can contribute to the NIR-AF signal.

Another finding supporting this idea is that a hyperautofluorescent ring can be observed in the fundus of a patient with retinitis pigmentosa both in SW-AF and NIR-AF images even though there is no spatially corresponding pigmented ring seen in the fundus (Duncker, Tabacaru, et al. 2013). The hyperautofluorescent rings in NIR-AF images are unlikely to be a result of a change in transmission in the retinal layers that are anterior to the RPE (unmasking), because tissue absorption at wavelengths between 600 and 1300 nm is relatively low (Tsai, Chen, and Wang 2001). There are no pigmentary changes corresponding to the hyperautofluorescent NIR-AF ring in color fundus photographs and no increased reflectivity at the level of RPE in SD-OCT scans as is typical of pigment clumping at the borders of geographic atrophy in AMD (Rudolf et al. 2013; Fleckenstein et al. 2008).

Even in the light of those findings, melanin is still the major source of NIR-AF. As we saw from mice data, lower levels of RPE lipofuscin, such as those accounting for SW-AF in albino wild-type mice, do not make a detectable difference to NIR-AF intensities. That could be because the contribution of bisretinoid lipofuscin to the NIR-AF signal in the wild-type is minimal in comparison with melanin (**Figure 9**) (Gibbs et al. 2009). This observation is likely applicable to the healthy human eye.

A recent study that has been published by Taubitz et al. (published after Study 1) also showed a presence or NIR-AF signal in albino *Abca4*$^{-/-}$ mice that was weak compared to the high-intensity NIR-AF signal seen in pigmented *Abca4*$^{-/-}$ mice reasoning that oxidized melanin has increased NIR-AF properties. They also acknowledged that lipofuscin moiety of melanolipofuscin and subsequently lipofuscin granules can emit relevant levels of NIR-AF, potentially due to accumulation of melanin degradation products (Taubitz et al. 2019).

We also proposed in our study that SW-AF signal is attenuated by the presence of RPE melanin. When closely examining the SW-AF images acquired from OA1 carriers, we found that in the areas of less intense SW-AF signal appearing dark in the images corresponded spatially to bright focal areas in NIR-AF images, indicating that the SW-AF signal is attenuated by the presence of RPE melanin. Conversely, in the areas lacking melanin the SW-AF appeared brighter. This is in keeping with the observation that albino mice lacking melanin presented with elevated qAF intensities. Our HPLC quantitative analysis has shown that albino mice do not actually have increased bisretinoid levels. Therefore the finding that qAF is elevated in the albino mice can likely be

explained by increased irradiance: the lack of pigment allows more light to transmit through the iris and through the eye wall posterior to the iris leading to overall increase in intraocular light (van den Berg, IJspeert, and de Waard 1991; Coppens, Franssen, and van den Berg 2006).

In ocular albinism melanin is synthesized but melanosomes are grossly enlarged and reduced in number and the organization of melanin in the melanosomes is altered (Cortese et al. 2005; Schiaffino 2010; Falletta et al. 2014). This means that melanosomes of RPE are also aberrant, there is less light absorption in SW-AF imaging by melanin and that explains the elevated qAF values in hypopigmented RPE areas in OA1 carriers (**Figure 7)**.

In conclusion, the results of Study 1 confirmed that RPE melanin is a major source of NIR-AF signal, however increased levels of bisretinoid can begin to contribute to NIR-AF signal and SW-AF signal is modulated by variations in the levels of ocular pigment.

A limitation of this study was that the cohort of OA1 carriers was relatively small. The difference in NIR-AF intensity in agouti- versus black-coated mice may call into question the assumption that RPE cell melanin content does not vary in concert with the melanin concentration in other tissues, (e.g., iris, choroid, skin) (Weiter et al. 1986), this will require further research. The exact contribution of choroidal melanin to NIR-AF signal is not known but is believed to be minor in relation to RPE melanin. Some novel imaging techniques have aimed at detecting NIR-AF signal emitted specifically from RPE cells by using adaptive optics AF (Granger et al. 2018) or normalizing NIR-AF signal against IR-IR to reduce choroidal component of the signal, (Cideciyan, Swider, and Jacobson 2015), but further research in that field is still warranted.

6.2. Insights into disease process in choroideremia

Choroideremia presents with a typical posterior pole atrophy progressively encroaching the macula, however the central retina can be preserved until quite late, leaving a window of opportunity for therapeutic intervention. This preserved retinal island in the posterior pole declines in a logarithmic fashion with an estimated rate of 7–8% per year based on cross-sectional data (Jolly et al. 2016; Aylward et al. 2018). Different therapeutic interventions are targeted to stop this process and that is why retinal imaging modalities are crucial in monitoring the disease and evaluating retinal viability. SW-AF has been widely used to discriminate between the atrophic and viable retina in various retinal conditions (Rudolf et al. 2013; von Rückmann, Fitzke, and Bird 1995; Pichi et al. 2013). In choroideremia the residual islands with a preserved RPE are seen in SW-AF area with uniform or speckled signal, whereas areas with RPE atrophy are characterized by the loss of SW-AF signal (Jolly et al. 2016).

In Study 2 we presented the fundus images of 16 CHM probands. Preserved retinal islands of variable size were observed as seen in **Figure 10** (P15, P5, and P7). These islands were distinguished by the presence of SW-AF and NIR-AF

signals, intact or discontinuous IZ and EZ reflectivity bands attributable to photoreceptor cells, and the absence of hypertransmission into the choroid. These features indicate that RPE and photoreceptor cells were at least partially intact in those areas. In 19/31 eyes these preserved retinal areas were detected both in NIR-AF and SW-AF images (**Figures 10B** and **10C**: P7, P5, and P15; green and yellow asterisks in figure panels). However, in the remaining cases (12 eyes; 6 patients), there were more pigmented areas that were detectable in color and NIR-AF imaging but showed absence of signal in SW-AF images (**Figure 11B**, **11C**: P7, P6, red asterisks). In areas with preserved SW-AF signal, but no detectable NIR-AF signal, SD-OCT revealed thinned ONL and discontinuous or lost IZ, EZ, and ELM bands along with hypertransmission into the choroid **(Figure 11C**: P5, AF blue arrowhead; D: P5, blue asterisk). Our analysis of visual acuity showed better results in the group where there was presence of both NIR-AF and SW-AF signal in the central island compared to the group where SW-AF signal alone was detectable.

NIR-AF imaging in CHM subjects has not been widely published, but our results, showing that NIR-AF signal is not always detectable in retinal islands seen in SW-AF, are consistent with work by Birtel et al 2019 where they analysed NIR-AF in correlation to SW-AF and OCT in CHM and found a discrepancy between two AF imaging modalities with the central preserved islands being smaller in NIR-AF images than in SW-AF (Birtel et al. 2019). An article by Mucciolo et al. 2019 published after our Study 1, describing NIR-AF in young CHM subjects found that in areas with preserved NIR-AF and SW-AF signal the RPE-Bruchs membrane complex was continuous and hyperreflective, while in areas with only SW-AF signal the band was thinner, irregular and discontinuous showing hypertransmission (Mucciolo et al. 2019).

The presence of SW-AF signal without NIR-AF is not consistent with the common view that SW-AF signal originates only from the bisretinoid lipofuscin in the RPE. An alternative source of this signal could be the degenerating photoreceptor outer segments as seen in **Figure 10**, P6, where EZ-IZ layers have reduced reflectivity in the SD-OCT scan. We know that in healthy eyes, the fluorophores of SW-AF form in photoreceptor cells before phagocytic transfer to RPE (Sparrow and Yamamoto 2012). The likely contribution of degenerating photoreceptor cells to SW-AF has also been shown in other retinal diseases (Duncker, Greenberg, et al. 2014; Boudreault et al. 2017), as well as in our Study 3 analysing flecks in STGD1.

We also noted NIR-AF signal in the absence of SW-AF. In the case of P7 (**Figure 10** A–D), hyperpigmentation in color fundus images colocalized with a veil of AF in the NIR-AF images, an absence of SW-AF, thinned ONL, loss of photoreceptor attributable layer reflectivity, and the presence of an ORT, yet no hypertransmission into the choroid in the SD-OCT scan was detected. A zone having NIR-AF emission in P6 is also devoid of SW-AF (**Figure 10** B–D). This is an interesting discrepancy in AF findings between the two modalities. One explanation could be that these RPE cells still contain melanin, but have lost lipofuscin content. Another possible mechanism behind this finding could be

that increased melanin absorbs SW-AF light. As we described in Study 1 in albinism cases the presence of melanin in RPE cells can act as a modulator of SW-AF signal.

Choroideremia is an X-linked disease therefore females who are carriers of a pathogenic *CHM* variant can present with a typical retinal mosaic of alternating healthy and disease affected retina (**Figure 11**) (Murro et al. 2017; MacDonald, Russell, and Chan 2009; Coussa and Traboulsi 2012; T.L. Edwards et al. 2015). The reason for that is random X-chromosome inactivation leading to the expression of the mutated chromosome in some retinal cells and the extent of that can vary. Diffuse irregular hyper-and hypoautofluorescent changes have been described in SW-AF imaging modality (Wu et al. 2018), however NIR-AF imaging findings have not yet been analyzed in CHM carriers.

We analysed SW-AF and NIR-AF images in 6 CHM carriers and noted that patches of reduced AF in SW-AF images colocalized with reduced AF in NIR-AF images. The mosaicism seen in NIR-AF images could be a result of nonuniform melanin distribution associated with REP-1 dysfunction that represents an X-linked manifestation of altered RPE melanosome movement (Futter et al. 2004; Hume et al. 2001). This differs from our findings in Study 1, where we analyzed the pigment mosaicism in NIR-AF images of X-linked albinism carriers. Unlike in CHM carriers, patches of reduced signal in NIR-AF images of OA1 carriers colocalized with increased signal (not reduced signal) in the SW-AF modality (**Figure 6, 16**). It is also known that fundus changes in CHM carriers develop with age (Renner et al. 2009) and tend to progress (MacDonald, Russell, and Chan 2009). Random X-inactivation of REP-1 leading to melanosome dysfunctioning (Futter et al. 2004) is not sufficient to explain the SW-AF and NIR-AF characteristic findings in carriers, but rather a process involving melanin and lipofuscin in RPE cells. In this study we also aimed at measuring the signal intensities, an approach that has not been yet tried on CHM patients. We found that qAF intensities mapped to the fundus by scaled color-coding were profoundly reduced not only in CHM-affected patients but also in female CHM carriers. As demonstrated in CHM carrier 1 (**Figure 11A**), this qAF reduction was not attributable to outer retinal degeneration in SD-OCT scans (**Figure 11).**

The primary site of degenerative process has been under debate with the majority of studies supporting the concept that RPE cells are primarily affected (Jacobson et al. 2006; Flannery et al. 1990; Rodrigues et al. 1984; Mura et al. 2007; Hariri et al. 2017; L.W. Sun et al. 2016; Morgan et al. 2014) or happens independently in RPE and photoreceptor layers (Tolmachova et al. 2006; Mura et al. 2007; Flannery et al. 1990; Jacobson et al. 2006). That is consistent with outer retinal tubulations seen also in our study in CHM probands (**Figure 10**), that are considered a survival response of photoreceptors to RPE degeneration seen also often in age-related macular degeneration (Preti et al. 2018).

The absence of NIR-AF in the presence of SW-AF might seem contradictory as both signals mostly originate from RPE cells, however bisretinoid lipofuscin emission could also originate anterior to the RPE layer from photoreceptor outer

segments as occurs e.g. in Best vitelliform macular dystrophy (Duncker, Greenberg, et al. 2014).

Another interesting finding in this study was how NIR-AF signal intensities in CHM probands showed an overall decrease compared to healthy eyes even in areas with central preserved retina. Our results together with RPE depigmentation seen in young CHM probands (Mucciolo et al. 2019) could further confirm that RPE monolayer is affected in CHM early on. RPE cells have the capability to spread out and fill the gaps in the monolayer. RPE remodeling has been reported as part of the normal aging process where larger RPE compensate for adjacent cell loss (Ach et al. 2014). Remodeling of RPE monolayer through cell migration and spreading and concomitant thinning, could account for reduced NIR-AF signal originating in RPE as has been proposed by Birtel et al. (Birtel et al. 2019). Other studies have shown that there is an early thinning and polymegathism in the RPE monolayer in areas with normal photoreceptors (Aguilera et al. 2022). We have suggested a similar mechanism in our previous work regarding reticular pseudodrusen (Paavo et al. 2017).

Improved understanding of the patterns and sources of NIR-AF signal in choroideremia is a valuable addition to SW-AF imaging as the therapeutic trials need precise and sensitive methods to evaluate the viability of different cell types e.g. RPE prior and after treatment. NIR-AF imaging is also more comfortable for the patient due to its less disturbing dim red light.

A limitation of this study is the relatively small cohort, with age trending toward older subjects. The inclusion of children or young adults would have allowed us to evaluate retina at earlier stages of disease. Additionally, we did not have specimens that would have allowed us to correlate SW-AF, NIR-AF, and SD-OCT findings with histopathological changes. We correlated visual acuity with retinal thickness and the levels of NIR-AF signal, but wider functional tests such as microperimetry, combined with fundus autofluorescence could add valuable insight.

6.3. Photoreceptors as a source of fleck- related SW-AF signal and reduced NIR-AF signaling early RPE cell degeneration

Bisretinoid accumulation in the retinal pigmented epithelial (RPE) cells is a hallmark of STGD1 (Eagle et al. 1980; Birnbach et al. 1994; F. C. Delori, Staurenghi, et al. 1995). Cidecyan et al. have showed that new atrophic changes emerge within areas of intense SW-AF (Cideciyan et al. 2004). A conventional end-point for clinical trials and for monitoring STGD1 progression is focusing on the area of atrophy in SW-AF and SD-OCT findings (Fujinami, Zernant, et al. 2013; Strauss et al. 2019; Strauss et al. 2016), however RPE atrophy itself presents a stage where most therapeutic interventions will not be helpful anymore. In addition to atrophy, STGD1 usually presents with typical flecks in the macular area that later form in the periphery during the course of the disease.

Flecks are usually present even in the early disease stage and have a dynamic nature, therefore they present an interesting target for monitoring the disease progression and possible therapeutic effects. Retinal function at the location of flecks is one topic of interest. Some reports have exhibited decreased visual sensitivity over flecked areas (Verdina et al. 2012; Greenstein et al. 2008). More recent studies concluded that hyperautofluorescent flecks were associated with topographically normal function on perimetry and ffERG (Dhooge et al. 2021; Müller et al. 2019), however the accuracy of SW-AF imaging and microperimetry alignment is callenging in these studies. Another topic of interest is the origin of flecks. In previous literature the main hypothesis was that flecks were lipofuscin laden RPE cells (Eagle et al. 1980; Lopez et al. 1990).

In Study 3 we analyzed flecks and their AF properties and found that while flecks are mostly hyperautofluorescent in SW-AF, they spatially often correspond to foci of reduced NIR-AF signal (**Figure 15,17,18**). When observing flecks in time, we noted that the change from hyperautofluorescence to hypoautolfuorescence seems to happen earlier in NIR-AF images while hyperautofluorescence in SW-AF images is maintained longer (**Figure 18**). Based on those results and previous reports (Sparrow et al. 2015; Greenstein et al. 2017; S. Kellner et al. 2009), we propose that the fleck related increased SW-AF signal originates not only from the level of RPE but also anterior to that. Flecks could be a manifestation of degenerating photoreceptors, that are the source of intense SW-AF signal. Also we noted that fleck-formations in SD-OCT extended anteriorly through photoreceptor attributable layers interrupting rather than displacing those layers. ONL layer thinning was seen adjacent to those flecks that were taller (**Figure 16**). It has been previously shown that bisretinoid is produced in photoreceptor cell outer segments before phagocytosis by RPE (Sparrow et al. 2012). Our research group has previously proposed that SW-AF fundus autofluorescence does not just signal the status of RPE cells but, under some circumstances, can be indicative of the health of photoreceptor cells (Sparrow et al. 2015). Elevated SW-AF signal has been shown in different retinal conditions like AZOOR (Boudreault et al. 2017), acute macular neuroretinopathy (Gelman et al. 2012) and retinitis pigmentosa (Aizawa et al. 2010; Duncker, Lee, et al. 2013; Duncker, Tabacaru, et al. 2013; Popović, Jarc-Vidmar, and Hawlina 2005; Robson, El-Amir, et al. 2003; Schuerch et al. 2017) co-localizing with areas of photoreceptor degeneration.

A more recent histological study on a STGD1 mouse model by Fang et al. proposed an alternative explanation for fleck formation: flecks are degenerating RPE cells, that have been phagocytosed by macrophages in the subretinal space. Flecks that were hyperautofluorescent in SW-AF and NIR-AF corresponded to macrophages that contain lipofuscin, melanolipofuscin and melanin granules (Fang et al. 2020). However, an older report with *Rdh8−/−/Abca4−/−* mice using histology and imaging revealed that hyperautofluorescent foci in fundus AF images corresponded to photoreceptor cell rosettes in SD-OCT images and histological sections. The inner segment/outer segment–containing core of the rosette emitted an autofluorescence detected by fluorescence microscopy (Flynn

et al. 2014). The high intensity of AF signal in those foci could be explained by the fact that the bisretinoids in the photoreceptor outer segments are situated anterior to RPE cells, therefore they are not subject to absorbance by melanin and also being less compacted than in RPE they would undergo less self-absorption. This finding does not exclude the possibility that microglial/macrophage cells are present in association with the rosettes, but it is likely that AF is derived from outer segment debris (Zhao et al. 2018) that has accumulated extracellularly or within macrophages after phagocytosis.

In Study 3 we also noted that hyperreflective flecks in SD-OCT co-localized with foci of reduced NIR-AF signal. Since NIR-AF signal is mostly derived from RPE melanin, this could indicate a disease process in RPE cells. We also observed that flecks become hyperautofluorescent in SW-AF images after turning dark in NIR-AF. Histological studies have shown that alterations of the RPE are present many years before STGD1 fundus findings (Steinmetz et al. 1991). Given that both previous and recent studies have shown earlier hypo-autofluorescence in NIR-AF compared to SW-AF images, (Sparrow et al. 2015; Duncker, Marsiglia, et al. 2014; Müller et al. 2019) our fleck analysis supports the view that RPE degeneration can precede photoreceptors loss.

Therefore NIR-AF imaging could be a more sensitive diagnostic tool for early RPE atrophy. Another reason for utilizing NIR-AF imaging over SW-AF is the concern that excessive blue-light can exacerbate the phototoxicity associated with *ABCA4*-related disease (Cideciyan et al. 2007; Sparrow et al. 2012) and regular monitoring with NIR-AF could be a more safe option.

The limitation of this study is a rather small study cohort and the lack of histological and functional data.

6.4. Fundus autofluorescence of *PROM1*-macular disease

PROM1-macular disease also known as STGD4 is a rare inherited disease and shares similar clinical findings with STGD1. In Study 4 we used multimodal imaging to describe *PROM1*-macular disease.

Fifteen (15) study subjects presented with granular signal in SW-AF and NIR-AF images in the macular area that corresponed to outer retinal degeneration in SD-OCT images. Atrophic changes in central macula were better visualized with NIR-AF imaging, as SW-AF signal is absorbed by macular pigments in the fovea (**Figure 21, B**). Small hyperfluorescent foci surrounding the central retinal atrophy were observed in 30/38 eyes; these hyperautofluorescent foci were more visible in SW-AF images than NIR-AF images. Three patients presented with a more widespread retinal degeneration affecting the entire macula and advancing to posterior pole (**Figure 20** P7, P8, P11). The *PROM1*-associated disease process appears to affect the perifoveal region first and then advances to peripheral macular areas, while leaving the fovea intact until late-stage disease; foveal sparing was observed in 31/38 eyes. None of the patients presented with peripheral retinal changes like bone spicules.

PROM1-maculopathy is often compared to STGD1 and our cohort also presented with central macular atrophy with surrounding small hyperautofluorescent fleck-type foci (**Figure 21**). In STGD1 reduction or loss of ABCA4 protein leads to a defect in the visual cycle and to pathologically increased formation of bisretinoid fluorophores (Allikmets et al. 1997; F. C. Delori, Staurenghi, et al. 1995). These fluorophores subsequently accumulate in RPE, are the source of SW-AF (**Figure 22**) (Burke et al. 2014) and lead to cellular damage manifesting as STGD1 (Sparrow et al. 2013). However, despite the similarity in retinal findings between STGD1 and STGD4, qAF analysis of *PROM1*-macular disease showed that almost all eyes presented with SW-AF values comparable to healthy eyes **(Figure 22**). qAF has been shown to discriminate between retinal diseases sharing a similar clinical findings with STGD1 (Duncker, Tsang, Lee, et al. 2015), qAF may also be effective in distinguishing between *ABCA4* and *PROM1*-related macular dystrophy.

Our group has previously also observed that in *ABCA4*-disease high levels of lipofuscin not only present as elevated SW-AF signal, but an increase in NIR-AF signal is also observed (Duncker, Lee, et al. 2013) as we also showed in Study 2. To determine whether PROM1-macular dystrophy presents with distinctive findings regarding NIR-AF, we also measured the NIR-AF signal intensities in the patients. While the NIR-AF intensities in the foveal area were slightly reduced, in the perifoveal area NIR-AF signal was comparable to healthy eyes.

The study's limitation is that several participants were lacking some of the imaging modalities analyzed here. Nevertheless we believe the number of patients was enough to support our conclusions, especially regarding the SW-AF levels in *PROM1*-macular disease. We also acknowledge that the lack of longitudinal data does not allow us to follow the disease progression.

Our findings from Study 4 do not indicate that excessive accumulation of bisretinoid lipofuscin is a component of the *PROM1*-related disease process. That knowledge could be useful in developing future therapeutic targets for treating *PROM1*-retinal disease and also as a diagnostic tool in distinguishing STGD1 and STGD4 prior to genetic testing.

CONCLUSIONS

SW-AF and NIR-AF imaging have their strengths and weaknesses, but are valuable in both the clinical and research setting. The knowledge regarding SW-AF signal is much more extensive due to its widespread use. NIR-AF imaging has offered some valuable insights into retinal pathology in various studies, but is not so widely used in the clinical setting. SW-AF and NIR-AF images can be analyzed qualitatively, but quantifying the AF signal strength can add extra value in comparing patients and healthy subjects and detecting disease changes that influence the retinal fluorophores.

In Study 1 we further confirmed that melanin is the major source of NIR-AF signal (Keilhauer and Delori 2006) by analyzing ocular albinism carriers and mice models with varying fundus pigmentation. However we also noted that bisretinoid likely contributes to NIR-AF intensity in cases with excessive bisretinoid lipofuscin levels like in STGD1. We also showed that the presence of melanin has a modulating effect on the SW-AF signal used to detect bisretinoid lipofuscin and how the lack of melanin can increase the detectable SW-AF signal without an actual increase in bisretinoid levels.

While SW-AF and NIR-AF both present with a loss of signal in areas of RPE atrophy, NIR-AF could be a more sensitive tool for evaluating early RPE cell degeneration as we showed in choroideremia patients in Study 2 and in STGD1 patients in Study 3. That notion is also supported by other studies of STGD1 (Sparrow et al. 2015; Duncker, Marsiglia, et al. 2014) and CHM (Birtel et al. 2019). In Study 3 we analysed hyperautofluorescent flecks in SW-AF that corresponded to loss of signal in NIR-AF images. This finding indicates that SW-AF signal is not only specific to RPE cells, but degenerating photoreceptor cells are likely the aberrant source of SW-AF signal (Sparrow et al. 2015; Duncker, Marsiglia, et al. 2014). Both SW-AF and NIR-AF signal can be seen as easily accessible, non-invasive biomarkers for evaluating retinal health. In the era of developing new therapies for IRD it is important to understand the strengths and weaknesses of different imaging modalities when assessing viability of retinal cells.

Quantifying the AF signal intensity helps to further understand disease processes by evaluating the levels of retinal fluorophores. qAF can offer a means of evaluating therapeutic interventions in retinal conditions which manifest with abnormally low lipofuscin bisretinoid levels like in retinal dystrophies affecting the visual cycle or vitamin A deficiency (Lorenz et al. 2004; Lima de Carvalho, Tsang, and Sparrow 2022; Oh et al. 2020), or in cases like *ABCA4*-releated disease where there is abnormally high accumulation of the latter (Burke et al. 2014). qAF could also be helpful in the differential diagnosis of macular diseases that share clinical features (Duncker, Tsang, Lee, et al. 2015; Sparrow et al. 2016; Duncker, Tsang, Woods, et al. 2015). In Study 4 we showed that *PROM1*-macular dystrophy does not show elevated levels of SW-AF, thus differentiating it from phenotypically similar STGD1. That knowledge is valu-

able in differential diagnosis with inconclusive genetic testing or when developing therapeutic approaches for *PROM1*-disease.

A practical consideration is that patients with retinal conditions often experience increased light sensitivity and bright light used for SW-AF imaging is more uncomfortable than the dim red light of NIR-AF imaging. However the more concerning aspect is that some retinal degenerations may be more sensitive to short-wavelength light, especially conditions with excessive bisretinoid formation (Teussink et al. 2017; Paskowitz, LaVail, and Duncan 2006; Sparrow, Nakanishi, and Parish 2000). Such imaging-dependent effect has not been demonstrated and guidelines for ophthalmic instruments have been set to keep ocular radiation exposures within safe limits in the short-term (Sliney et al. 2005). When patients are imaged often and for a longer period of time, like in clinical trials, it would be safer to reduce the level of light exposure as much as possible. NIR-AF operating at longer wavelength light than SW-AF could reduce the potential risk of toxic effects due to repeated imaging.

Inherited retinal diseases have made their way to the frontline of the development of therapeutic approaches. Modern retinal imaging techniques are therefore especially important to help ophthalmologists make the correct diagnosis as well as to aid the researchers in studying the disease processes and evaluating possible therapeutic effects.

SUMMARY IN ESTONIAN

Funduse sinine ja lähi-infrapuna autofluorestsentsuuring autosoom-retsessiivse Stardgardti tõve, koroidereemia, *PROM1*-maakuli düstroofia ja okulaarse albinismi patsientidel

Sissejuhatus

Pärilikud võrkkestahaigused on juhtivaks nägemiskaotuse põhjuseks tööealise elanikkonna seas arenenud riikides (Liew, Michaelides, and Bunce 2014). Tegemist on kliiniliselt ja geneetiliselt väga heterogeense haiguste grupiga ning praeguseks on tõestatud enam kui 300 geenivea põhjuslik seos erinevate reetina düstroofiatega (https://web.sph.uth.edu/RetNet/), samas kui eraldiseisvana on enamasti tegemist väga haruldaste haigustega. Geeniviga võib põhjustada patoloogiat erinevates võrkkestarakkudes nagu näiteks kepikestes, kolvikestes või pigmentepiteeli rakkudes viies seeläbi nende kärbumiseni. Teistel juhtudel võib olla häiritud nägemistsükli toimimine või fototransdukstiooon (Georgiou 2020; Travis et al 2007, Solebo 2017). Enamasti on tegemist progresseeruvate haigustega, mis algavad lapseeas või varases täiskasvanueas ning võivad halvemal juhul viia täieliku nägemiskaotuseni. Geeniteraapia uuringud on andnud lootust seni parandamatute võrkkesta haiguste kulgu mõjutada. Tänaseks on heaks kiidetud siiski vaid ühe päriliku võrkkesta haiguse geenivea põhine ravimeetod (Wang 2020), kuid uuringud mitmete erinevate reetina düstroofiate ravimeetodite väljatöötamiseks on käimas.

Haiguste diagnoosimisel on lisaks molekulaargeneetilisele kinnitusele väga oluline ka fenotüübi kirjeldamine. Võrkkesta piltdiagnostika on mitte-invasiivne meetod võrkkesta haiguste uurimiseks ning on viimastel aastakümnetel teinud läbi suure arengu. Silmapõhja värvipilt aitab jäädvustada seda, mida näeb biomikroskoobiga uurides silmaarst. Uuemad kaamerad, kus on pildi loomiseks kasutusel skanneeerivad laserid, aitavad visualiseerida võrkkesta sellisel kujul, mida me tavaliselt silmaga ei näeks. Konfokaalne skanneeriv laseroftalmoskoop valgustab võrkkesta erineva lainepikkusega laserkiirtega ning salvestab tagasikiirgavat valgust luues seeläbi silmapõhjast pildi. Autofluorestsentsuuringul (AF) kasutatakse ära silmapõhja enda naturaalseid fluorofoore, millest peamised on bisretinoididest koosnev lipofustsiin ja pigment melaniin. Bisretinoide ergastatakse sinise spektri laserkiirega (sinine AF, 488 nm) ja melaniini lähi-infrapuna laserkiirega (lähipuna AF, 787 nm). Nende fluorofooride kogused ja jaotumine silmapõhjas muutuvad reetina haigusseisundite puhul. See võimaldab AF uuringuid kasutada silmapõhja haiguste diagnostikas ja monitoorimisel (Georgiou 2020, Boon 2008, Yung 2016).

Antud doktoritöös on AF uuringuga analüüsitud nelja erinevat võrrkesta haigust. Autosoom- retsessiivne Stargardti tõbi (STGD1) on levinuim juveniilne maakuli düstroofia, mille patogeneesi osaks on bisretinoididest koosneva lipofustsiini üleliigne kuhjumine võrkkestas (Allikmets 1997), mis viib fotoretsep-

torite ja pigmentepiteeli rakkude kärbumiseni (Cideciyan et al., 2004, Sparrow and Boulton, 2005). *PROM1*-maakuli düstroofia on STGD1-ga fenotüübilt sarnane, kuid palju haruldasem haigus (Maw et al 2000), mille patoloogilistest mehhanismidest on palju vähem teada. Koroidereemia on X-liiteline reetina düstroofia, mis avaldub silmapõhjas laialdaste progresseeruvate korioretinaalsete atroofia muutustena (Coussa and Traboulsi 2012). Okulaarne albinism on statsionaarne X-liiteline haigus, millega kaasneb sünnipärane silmapõhja melaniini vähesus. X-liiteliste haiguste puhul haigestuvad enamasti ainult mehed, kuid asümptomaatilistel naistel võib olla silmapõhjas haiguse kandjale omane tervetest ja mutantsetest rakkudest vahelduv mosaaikne leid (Moshiri et al. 2013).

Uurimistöö eesmärgid

1. Analüüsida reetina peamiste fluorofooride – bisretinoidi ja melaniini rolli sinise ja lähi-infrapuna AF signaali tekkes (Artikkel 1, 2 ja 3).
2. Kirjeldada AF uuringu tulemusi kvalitatiivselt ja kvantitatiivselt Stargardti haiguse, *PROM1*-maakuli düstroofia, koroidereemia ja okulaarse albinismi haigusjuhtudel (Artikkel 1,2,3,4).
3. Analüüsida sinise ja lähi-infrapuna autofluorestsents uuringu kliinilisi kasutusvõimalusi pärilike võrkkestahaiguste hindamisel (Artikkel 2,3,4).

Uuritavad ja meetodid

Doktoritöö aluseks on nii prospektiivsel kui ka retrospektiivsed läbilõikelised uuringud Columbia Ülikooli silmakliinikus geneetiliselt kinnitatud reetina düstroofia patsientidel. STGD1 grupp koosnes 25, koroidereemia grupp 16 patsiendist ja 9 haiguse kandjast ning okulaarse albinismi grupp 5 haiguse kandjast. PROM1-maakuli düstroofia uurimisgrupp koosnes 18 patsiendist. Kvantitatiivse autofluorestsentsuuringu võrdluseks olev tervete silmapõhja piltide kohort on kogutud juba varasemalt vabatahtlike (n=277) silmahaiguseta tervete uurimisel (Greenberg 2013).

Sinise AF ja lähi-infrapuna AF uuringu läbiviimiseks kasutati cSLO kaamerat (HRA2, Spectralis HRA + OCT, Heidelberg Engineering, Heidelberg, Germany), mille käigus teostati ka läbilõikeline SD-OCT uuring. SD-OCT uuringul saadakse võrkkesta kihtidest läbilõikelised pildid, mis aitavad AF uuringul nähtut korreleerida intraretinaaliste muutustega. Sinise ja lähipuna AF piltide analüüs oli nii kirjeldav kui ka kvantitatiivne, kus mõõtsime AF signaali tugevust spetsiaalselt arendatud tarkvara abil (Delori et al 2011). AF signaali tugevuse mõõtmine ning võrdlemine terve kontrollgrupiga võimaldab teha järeldusi silmapõhjas paiknevate fluorofooride sisalduse kohta ning anda informatsiooni reetinas toimuvate protsesside kohta.

Tulemused ja arutelu

Esimeses uuringus olid kaasatud okulaarse albinismi mutatsiooni naissoost kandjad (n=5, vanuse vahemik 13,5–34,6) ja STGD1 patsiendid (n=25, vanuse vahemik 8.3–51.5). Okulaarse albinismi kandjate silmapõhjas oli normipärase pigmentatsiooni ja hüpopigmentatsiooni mosaiikleid. Hüpopigmentatsiooni aladel puudus lähi-infrapuna AF signaal. Kvantitatiivsel AF signaali hindamisel selgus, et hüpopigmenteeritud alade sinise AF signaali tugevus oli kõrgem võrreldes tervete silmadega. Lisaks näitasime, et bisretoinididest koosneva lipofustsiini kõrgete tasemete korral tõuseb lisaks sinisele ka lähi-infrapuna AF signaal, olles keskmiselt kuni kolm korda kõrgem tervete silmadega võrreldes.

Teises uuringus moodustasid uuritavate rühma meessoost koroidereemia haiged (n=16, vanuse vahemik 10.2–77.2) ja koroidereemia mutatsiooni naissoost kandjad (n=9, vanusevahemik 29.3–75.5). Koroidereemia haigetel olid silmapõhjas laialdased korioretinaalse atroofia alad. Tsentraalselt säilunud võrkkesta ala oli tuvastatav sinisel AF uuringul kõikidel patsientidel, samas kui lähipuna AF uuringul oli vastav ala nähtav ainult 19 silmas 31-st.

Kolmandas uuringus hindasime STGD1 patsientide (n =12, vanuse vahemik 9–61) silmapõhjas avalduvate bisretinoididest koosnevate tähnide omadusi sinise ja lähi-infrapuna AF uuringuga. Analüüsil selgus, et tähnid olid peamiselt hüperautofluorestsentsed sinisel AF uuringul ja hüpoautofluorestsentsed lähipuna AF uuringul. Sinise AF uuringul hüperautofluorestsentest tähnidest 85% olid hüpoautofluorestsentsed lähipuna AF uuringul. Piltide analüüs ajas näitas, et tähnid kaotasid esmalt signaali lähipuna AF uuringul ja alles hiljem sinisel AF uuringul.

Neljandas uuringus analüüsisime *PROM1*-maakuli düstroofiaga patsiente (n=18, vanusevahemik 5–66). Maakuli degeneratiivsed muutused olid nähtavad nii sinise kui ka lähipuna AF uuringul. Kvantitatiivne sinise AF uuring näitas, et võrkkesta üldine AF signaali tugevus oli võrreldav tervete silmadega jäädes 95% usaldusvahemiku sisse, eristades seega *PROM1*-maakuli düsttroofiat fenotüübiliselt sarnasest STGD1 haigusest, mille puhul sinise AF signaal on tõusnud.

Uurimistöö järeldused

Sinine AF uuring on silmapõhja haiguste diagnostikas kasutusel olnud juba viimased aastakümned samas kui lähi-infrapuna AF uuring on kliinilises praktikas vähe levinud. Antud uurimistöö kinnitas teadmist, et lähi-infrapuna AF signaal pärineb peamiselt melaniinist ning sinise AF signaal bisretinoididest koosnevast lipofustsiinist. Samas näitasime esmakordselt kvantitatiivsel meetodil, et STGD1 patsientidel on lisaks sinisele AF signaalile tõusnud ka lähi-infrapuna AF signaali tugevus, mis viitab sellele, et lipofustsiini ulatuslik kuhjumine võrkkestas hakkab suurtes kogustes mõjutama ka lähi-infrapuna signaali (Uuring 1). Lisaks näitasime koroidereemia ja STGD1 patsientide põhjal, et lähi-infrapuna AF signaal hääbub degenereeruvas võrkkestas varasemalt kui sinine AF signaal, olles seega tundlikumaks biomarkeriks võrkkesta rakkude seisundi kohta

(Uuring 2,3). Sinise AF signaali kvantitatiivne analüüs näitas, et PROM1-maakuli düstroofia puhul ei ole lipofsustiini kuhjumine haigusele omane ning võimaldab seega eristada seda fenotüübiliselt sarnasest STGD1 (Uuring 4).

Antud uurimustöö aitab paremini mõista sinise ja lähipuna AF allikaid ning signaali muutumist võrkkesta rakkude kärbumise korral. Pärilikele võrkkesta haigustele suunatud uute terapeutiliste katsetuste valguses on AF uuring oluline meetod võrkkesta rakkude elujõulisuse hindamiseks enne ja pärast ravi. Melaniinist ja lipofustsiinist lähtuvat autofluorestsents signaali võib seega käsitleda kui mitte-invasiivsel moel jälgitavat biomarkerit võrkkesta rakkude seisundi hindamiseks. Kvantitatiivne autofluorestsents uuring annab võimaluse nende fluorofooride taseme muutusi jälgida ajas ja võrrelda tervete silmadega. Sinise spektriosa valgusel võib pikaajalise eksponeerimise korral olla fototoksiline toime võrkkesta rakkudele, seda eriti reetina düstroofiate korral, kus patoloogia osa on lipofustsiini kuhjumine (Teussink 2017, Sparrow 2000). Kuigi tänapäevaste kaamerate puhul võib AF uuringus kasutatavat lühiajalist sinise valguse mõju silmale pidada turvaliseks, siis lähi-infrapuna AF uuring võiks pakkuda paremat alternatiivi patsientidele, kelle monitooringuks korduv ja pikaajaline AF uuring on näidustatud.

REFERENCES

Ach, T., C. Huisingh, G. McGwin, J. D. Messinger, T. Zhang, M. J. Bentley, D. B. Gutierrez, Z. Ablonczy, R. T. Smith, K. R. Sloan, and C. A. Curcio. 2014. "Quantitative autofluorescence and cell density maps of the human retinal pigment epithelium." *Invest Ophthalmol Vis Sci* 55 (8): 4832–41. https://doi.org/10.1167/iovs.14-14802. https://www.ncbi.nlm.nih.gov/pubmed/25034602.

Adams, D. R., S. Menezes, R. Jauregui, Z. M. Valivullah, B. Power, M. Abraham, B. G. Jeffrey, A. Garced, R. P. Alur, D. Cunningham, E. Wiggs, M. A. Merideth, P. W. Chiang, S. Bernstein, S. Ito, K. Wakamatsu, R. M. Jack, W. J. Introne, W. A. Gahl, and B. P. Brooks. 2019. "One-year pilot study on the effects of nitisinone on melanin in patients with OCA-1B." *JCI Insight* 4 (2). https://doi.org/10.1172/jci.insight.124387. https://www.ncbi.nlm.nih.gov/pubmed/30674731.

Aguilera, N., T. Liu, A. J. Bower, J. Li, S. Abouassali, R. Lu, J. Giannini, M. Pfau, C. Bender, M. G. Smelkinson, A. Naik, B. Guan, O. Schwartz, A. Volkov, A. Dubra, Z. Liu, D. X. Hammer, D. Maric, R. Fariss, R. B. Hufnagel, B. G. Jeffrey, B. P. Brooks, W. M. Zein, L. A. Huryn, and J. Tam. 2022. "Widespread subclinical cellular changes revealed across a neural-epithelial-vascular complex in choroideremia using adaptive optics." *Commun Biol* 5 (1): 893. https://doi.org/10.1038/s42003-022-03842-7. https://www.ncbi.nlm.nih.gov/pubmed/36100689.

Ahn, J., J. T. Wong, and R. S. Molday. 2000. "The effect of lipid environment and retinoids on the ATPase activity of ABCR, the photoreceptor ABC transporter responsible for Stargardt macular dystrophy." *J Biol Chem* 275 (27): 20399–405. https://doi.org/10.1074/jbc.M000555200. https://www.ncbi.nlm.nih.gov/pubmed/10767284.

Aizawa, S., Y. Mitamura, A. Hagiwara, T. Sugawara, and S. Yamamoto. 2010. "Changes of fundus autofluorescence, photoreceptor inner and outer segment junction line, and visual function in patients with retinitis pigmentosa." *Clin Exp Ophthalmol* 38 (6): 597–604. https://doi.org/10.1111/j.1442-9071.2010.02321.x. https://www.ncbi.nlm.nih.gov/pubmed/20456441.

Aleman, T. S., G. Han, L. W. Serrano, N. M. Fuerst, E. S. Charlson, D. J. Pearson, D. C. Chung, A. Traband, W. Pan, G. S. Ying, J. Bennett, A. M. Maguire, and J. I. Morgan. 2017. "Natural History of the Central Structural Abnormalities in Choroideremia: A Prospective Cross-Sectional Study." *Ophthalmology* 124 (3): 359–373. https://doi.org/10.1016/j.ophtha.2016.10.022. https://www.ncbi.nlm.nih.gov/pubmed/27986385.

Allikmets, R. 1997. "A photoreceptor cell-specific ATP-binding transporter gene (ABCR) is mutated in recessive Stargardt macular dystrophy." *Nat Genet* 17 (1): 122. https://doi.org/10.1038/ng0997-122a. https://www.ncbi.nlm.nih.gov/pubmed/9288113.

Allikmets, R., N. Singh, H. Sun, N. F. Shroyer, A. Hutchinson, A. Chidambaram, B. Gerrard, L. Baird, D. Stauffer, A. Peiffer, A. Rattner, P. Smallwood, Y. Li, K. L. Anderson, R. A. Lewis, J. Nathans, M. Leppert, M. Dean, and J. R. Lupski. 1997. "A photoreceptor cell-specific ATP-binding transporter gene (ABCR) is mutated in recessive Stargardt macular dystrophy." *Nat Genet* 15 (3): 236–46. https://doi.org/10.1038/ng0397-236. https://www.ncbi.nlm.nih.gov/pubmed/9054934.

Anderson, D. H., and S. K. Fisher. 1979. "The relationship of primate foveal cones to the pigment epithelium." *J Ultrastruct Res* 67 (1): 23–32. https://doi.org/10.1016/s0022-5320(79)80014-3. https://www.ncbi.nlm.nih.gov/pubmed/109622.

Aylward, J. W., K. Xue, M. I. Patricio, J. K. Jolly, J. C. Wood, J. Brett, K. M. Jasani, and R. E. MacLaren. 2018. "Retinal Degeneration in Choroideremia follows an Exponential Decay Function." *Ophthalmology* 125 (7): 1122–1124. https://doi.org/10.1016/j.ophtha.2018.02.004. https://www.ncbi.nlm.nih.gov/pubmed/29580667.

Bakker, R., P. E. Wagstaff, C. C. Kruijt, E. Emri, C. D. M. van Karnebeek, M. B. Hoffmann, B. P. Brooks, C. J. F. Boon, L. Montoliu, M. M. van Genderen, and A. A. Bergen. 2022. "The retinal pigmentation pathway in human albinism: Not so black and white." *Prog Retin Eye Res* 91: 101091. https://doi.org/10.1016/j.preteyeres.2022.101091. https://www.ncbi.nlm.nih.gov/pubmed/35729001.

Bassi, M. T., M. V. Schiaffino, A. Renieri, F. De Nigris, L. Galli, M. Bruttini, M. Gebbia, A. A. Bergen, R. A. Lewis, and A. Ballabio. 1995. "Cloning of the gene for ocular albinism type 1 from the distal short arm of the X chromosome." *Nat Genet* 10 (1): 13–9. https://doi.org/10.1038/ng0595-13. https://www.ncbi.nlm.nih.gov/pubmed/7647783.

Ben-Shabat, S., C. A. Parish, H. R. Vollmer, Y. Itagaki, N. Fishkin, K. Nakanishi, and J. R. Sparrow. 2002. "Biosynthetic studies of A2E, a major fluorophore of retinal pigment epithelial lipofuscin." *J Biol Chem* 277 (9): 7183–90. https://doi.org/10.1074/jbc.M108981200. https://www.ncbi.nlm.nih.gov/pubmed/11756445.

Bhattacharya, S. K. 2009. "Retinal deimination in aging and disease." *IUBMB Life* 61 (5): 504–9. https://doi.org/10.1002/iub.184. https://www.ncbi.nlm.nih.gov/pubmed/19391158.

Biesemeier, A., U. Schraermeyer, and O. Eibl. 2011. "Chemical composition of melanosomes, lipofuscin and melanolipofuscin granules of human RPE tissues." *Exp Eye Res* 93 (1): 29–39. https://doi.org/10.1016/j.exer.2011.04.004. https://www.ncbi.nlm.nih.gov/pubmed/21524648.

Bille, J. F. 2019. "High Resolution Imaging in Microscopy and Ophthalmology: New Frontiers in Biomedical Optics.""

Birnbach, C. D., M. Järveläinen, D. E. Possin, and A. H. Milam. 1994. "Histopathology and immunocytochemistry of the neurosensory retina in fundus flavimaculatus." *Ophthalmology* 101 (7): 1211-9. https://doi.org/10.1016/s0161-6420(13)31725-4. https://www.ncbi.nlm.nih.gov/pubmed/8035984.

Birtel, J., T. Eisenberger, M. Gliem, P. L. Müller, P. Herrmann, C. Betz, D. Zahnleiter, C. Neuhaus, S. Lenzner, F. G. Holz, E. Mangold, H. J. Bolz, and P. Charbel Issa. 2018. "Clinical and genetic characteristics of 251 consecutive patients with macular and cone/cone-rod dystrophy." *Sci Rep* 8 (1): 4824. https://doi.org/10.1038/s41598-018-22096-0. https://www.ncbi.nlm.nih.gov/pubmed/29555955.

Birtel, J., A. P. Salvetti, J. K. Jolly, K. Xue, M. Gliem, P. L. Muller, F. G. Holz, R. E. MacLaren, and P. Charbel Issa. 2019. "Near-Infrared Autofluorescence in Choroideremia: Anatomic and Functional Correlations." *Am J Ophthalmol* 199: 19–27. https://doi.org/10.1016/j.ajo.2018.10.021. https://www.ncbi.nlm.nih.gov/pubmed/30713139.

Bittencourt, M. G., M. Hassan, M. S. Halim, R. Afridi, N. V. Nguyen, C. Plaza, A. N. T. Tran, M. I. Ahmed, Q. D. Nguyen, and Y. J. Sepah. 2019. "Blue light versus green light fundus autofluorescence in normal subjects and in patients with retinochoroidopathy secondary to retinal and uveitic diseases." *J Ophthalmic Inflamm Infect* 9 (1): 1. https://doi.org/10.1186/s12348-018-0167-2. https://www.ncbi.nlm.nih.gov/pubmed/30617430.

Bok, D. 1990. “Processing and transport of retinoids by the retinal pigment epithelium.” *Eye (Lond)* 4 (Pt 2): 326–32. https://doi.org/10.1038/eye.1990.44. https://www.ncbi.nlm.nih.gov/pubmed/2199240.

Bone, R. A., J. T. Landrum, L. Fernandez, and S. L. Tarsis. 1988. “Analysis of the macular pigment by HPLC: retinal distribution and age study.” *Invest Ophthalmol Vis Sci* 29 (6): 843–9. https://www.ncbi.nlm.nih.gov/pubmed/3372161.

Bonnin, P., Passot, and T. Triolaire-Cotten. 1976. “[Autofluorescence of papillary drusen in the diagnosis of false papillary edema].” *Bull Soc Ophtalmol Fr* 76 (4): 331–5. https://www.ncbi.nlm.nih.gov/pubmed/1028524.

Boon, C. J., B. Jeroen Klevering, J. E. Keunen, C. B. Hoyng, and T. Theelen. 2008. “Fundus autofluorescence imaging of retinal dystrophies.” *Vision Res* 48 (26): 2569–77. https://doi.org/10.1016/j.visres.2008.01.010. https://www.ncbi.nlm.nih.gov/pubmed/ 18289629.

Borrelli, E., M. Battista, B. Zuccaro, R. Sacconi, M. Brambati, L. Querques, F. Prascina, S. R. Sadda, F. Bandello, and G. Querques. 2020. “Spectrally Resolved Fundus Autofluorescence in Healthy Eyes: Repeatability and Topographical Analysis of the Green-Emitting Fluorophores.” *J Clin Med* 9 (8). https://doi.org/10.3390/jcm9082388. https://www.ncbi.nlm.nih.gov/pubmed/32726903.

Boudreault, K. A., K. Schuerch, J. Zhao, W. Lee, T. Cabral, L. A. Yannuzzi, S. H. Tsang, and J. R. Sparrow. 2017. “Quantitative Autofluorescence Intensities in Acute Zonal Occult Outer Retinopathy vs Healthy Eyes.” *JAMA Ophthalmol* 135 (12): 1330–1338. https://doi.org/10.1001/jamaophthalmol.2017.4499. https://www.ncbi.nlm.nih.gov/pubmed/29075777.

Boulton, M., and P. Dayhaw-Barker. 2001. “The role of the retinal pigment epithelium: topographical variation and ageing changes.” *Eye (Lond)* 15 (Pt 3): 384–9. https://doi.org/10.1038/eye.2001.141. https://www.ncbi.nlm.nih.gov/pubmed/11450762.

Boulton, M., F. Docchio, P. Dayhaw-Barker, R. Ramponi, and R. Cubeddu. 1990. “Age-related changes in the morphology, absorption and fluorescence of melanosomes and lipofuscin granules of the retinal pigment epithelium.” *Vision Res* 30 (9): 1291–303. https://doi.org/10.1016/0042-6989(90)90003-4. https://www.ncbi.nlm.nih.gov/pubmed/2219746.

Bringmann, A., S. Syrbe, K. Görner, J. Kacza, M. Francke, P. Wiedemann, and A. Reichenbach. 2018. “The primate fovea: Structure, function and development.” *Prog Retin Eye Res* 66: 49–84. https://doi.org/10.1016/j.preteyeres.2018.03.006. https://www.ncbi.nlm.nih.gov/pubmed/29609042.

Bueschbell, B., P. Manga, and A. C. Schiedel. 2022. “The Many Faces of G Protein-Coupled Receptor 143, an Atypical Intracellular Receptor.” *Front Mol Biosci* 9: 873777. https://doi.org/10.3389/fmolb.2022.873777. https://www.ncbi.nlm.nih.gov/pubmed/35495622.

Burke, T. R., T. Duncker, R. L. Woods, J. P. Greenberg, J. Zernant, S. H. Tsang, R. T. Smith, R. Allikmets, J. R. Sparrow, and F. C. Delori. 2014. “Quantitative fundus autofluorescence in recessive Stargardt disease.” *Invest Ophthalmol Vis Sci* 55 (5): 2841–52. https://doi.org/10.1167/iovs.13-13624. https://www.ncbi.nlm.nih.gov/pubmed/24677105.

Burke, T. R., G. A. Fishman, J. Zernant, C. Schubert, S. H. Tsang, R. T. Smith, R. Ayyagari, R. K. Koenekoop, A. Umfress, M. L. Ciccarelli, A. Baldi, A. Iannaccone, F. P. Cremers, C. C. Klaver, and R. Allikmets. 2012. “Retinal phenotypes in patients homozygous for the G1961E mutation in the ABCA4 gene.” *Invest Ophthalmol Vis*

Sci 53 (8): 4458–67. https://doi.org/10.1167/iovs.11-9166. https://www.ncbi.nlm.nih.gov/pubmed/22661473.

Carss, K. J., G. Arno, M. Erwood, J. Stephens, A. Sanchis-Juan, S. Hull, K. Megy, D. Grozeva, E. Dewhurst, S. Malka, V. Plagnol, C. Penkett, K. Stirrups, R. Rizzo, G. Wright, D. Josifova, M. Bitner-Glindzicz, R. H. Scott, E. Clement, L. Allen, R. Armstrong, A. F. Brady, J. Carmichael, M. Chitre, R. H. H. Henderson, J. Hurst, R. E. MacLaren, E. Murphy, J. Paterson, E. Rosser, D. A. Thompson, E. Wakeling, W. H. Ouwehand, M. Michaelides, A. T. Moore, N. IHR-BioResource Rare Diseases Consortium, A. R. Webster, and F. L. Raymond. 2017. "Comprehensive Rare Variant Analysis via Whole-Genome Sequencing to Determine the Molecular Pathology of Inherited Retinal Disease." *Am J Hum Genet* 100 (1): 75–90. https://doi.org/10.1016/j.ajhg.2016.12.003. https://www.ncbi.nlm.nih.gov/pubmed/28041643.

Cehajic-Kapetanovic, J., J. Birtel, M. E. McClements, M. E. Shanks, P. Clouston, S. M. Downes, P. Charbel Issa, and R. E. MacLaren. 2019. "Clinical and Molecular Characterization of PROM1-Related Retinal Degeneration." *JAMA Netw Open* 2 (6): e195752. https://doi.org/10.1001/jamanetworkopen.2019.5752. https://www.ncbi.nlm.nih.gov/pubmed/31199449.

Cella, W., V. C. Greenstein, J. Zernant-Rajang, T. R. Smith, G. Barile, R. Allikmets, and S. H. Tsang. 2009. "G1961E mutant allele in the Stargardt disease gene ABCA4 causes bull's eye maculopathy." *Exp Eye Res* 89 (1): 16–24. https://doi.org/10.1016/j.exer.2009.02.001. https://www.ncbi.nlm.nih.gov/pubmed/19217903.

Charbel Issa, P., A. R. Barnard, M. S. Singh, E. Carter, Z. Jiang, R. A. Radu, U. Schraermeyer, and R. E. MacLaren. 2013. "Fundus autofluorescence in the Abca4(-/-) mouse model of Stargardt disease – correlation with accumulation of A2E, retinal function, and histology." *Invest Ophthalmol Vis Sci* 54 (8): 5602–12. https://doi.org/10.1167/iovs.13-11688. https://www.ncbi.nlm.nih.gov/pubmed/23761084.

Charles, S. J., A. T. Moore, J. W. Grant, and J. R. Yates. 1992. "Genetic counselling in X-linked ocular albinism: clinical features of the carrier state." *Eye (Lond)* 6 (Pt 1): 75–9. https://doi.org/10.1038/eye.1992.15. https://www.ncbi.nlm.nih.gov/pubmed/1426406.

Chong, G. T., S. Farsiu, S. F. Freedman, N. Sarin, A. F. Koreishi, J. A. Izatt, and C. A. Toth. 2009. "Abnormal foveal morphology in ocular albinism imaged with spectral-domain optical coherence tomography." *Arch Ophthalmol* 127 (1): 37–44. https://doi.org/10.1001/archophthalmol.2008.550. https://www.ncbi.nlm.nih.gov/pubmed/19139336.

Cicinelli, M. V., A. Rabiolo, M. Brambati, C. Viganò, F. Bandello, and M. Battaglia Parodi. 2020. "Factors Influencing Retinal Pigment Epithelium-Atrophy Progression Rate in Stargardt Disease." *Transl Vis Sci Technol* 9 (7): 33. https://doi.org/10.1167/tvst.9.7.33. https://www.ncbi.nlm.nih.gov/pubmed/32832238.

Cideciyan, A. V., T. S. Aleman, M. Swider, S. B. Schwartz, J. D. Steinberg, A. J. Brucker, A. M. Maguire, J. Bennett, E. M. Stone, and S. G. Jacobson. 2004. "Mutations in ABCA4 result in accumulation of lipofuscin before slowing of the retinoid cycle: a reappraisal of the human disease sequence." *Hum Mol Genet* 13 (5): 525–34. https://doi.org/10.1093/hmg/ddh048. https://www.ncbi.nlm.nih.gov/pubmed/14709597.

Cideciyan, A. V., M. Swider, T. S. Aleman, M. I. Roman, A. Sumaroka, S. B. Schwartz, E. M. Stone, and S. G. Jacobson. 2007. "Reduced-illuminance autofluorescence imaging in ABCA4-associated retinal degenerations." *J Opt Soc Am A Opt Image*

Sci Vis 24 (5): 1457–67. https://doi.org/10.1364/josaa.24.001457. https://www.ncbi.nlm.nih.gov/pubmed/17429493.

Cideciyan, A. V., M. Swider, and S. G. Jacobson. 2015. "Autofluorescence imaging with near-infrared excitation:normalization by reflectance to reduce signal from choroidal fluorophores." *Invest Ophthalmol Vis Sci* 56 (5): 3393–406. https://doi.org/10.1167/iovs.15-16726. https://www.ncbi.nlm.nih.gov/pubmed/26024124.

Coppens, J. E., L. Franssen, and T. J. van den Berg. 2006. "Wavelength dependence of intraocular straylight." *Exp Eye Res* 82 (4): 688–92. https://doi.org/10.1016/j.exer.2005.09.007. https://www.ncbi.nlm.nih.gov/pubmed/16293245.

Corbeel, L., and K. Freson. 2008. "Rab proteins and Rab-associated proteins: major actors in the mechanism of protein-trafficking disorders." *Eur J Pediatr* 167 (7): 723–9. https://doi.org/10.1007/s00431-008-0740-z. https://www.ncbi.nlm.nih.gov/pubmed/18463892.

Cortese, K., F. Giordano, E. M. Surace, C. Venturi, A. Ballabio, C. Tacchetti, and V. Marigo. 2005. "The ocular albinism type 1 (OA1) gene controls melanosome maturation and size." *Invest Ophthalmol Vis Sci* 46 (12): 4358–64. https://doi.org/10.1167/iovs.05-0834. https://www.ncbi.nlm.nih.gov/pubmed/16303920.

Coussa, R. G., J. Kim, and E. I. Traboulsi. 2012. "Choroideremia: effect of age on visual acuity in patients and female carriers." *Ophthalmic Genet* 33 (2): 66–73. https://doi.org/10.3109/13816810.2011.623261. https://www.ncbi.nlm.nih.gov/pubmed/22060191.

Coussa, R. G., and E. I. Traboulsi. 2012. "Choroideremia: a review of general findings and pathogenesis." *Ophthalmic Genet* 33 (2): 57–65. https://doi.org/10.3109/13816810.2011.620056. https://www.ncbi.nlm.nih.gov/pubmed/22017263.

Creel, D. J., C. G. Summers, and R. A. King. 1990. "Visual anomalies associated with albinism." *Ophthalmic Paediatr Genet* 11 (3): 193–200. https://doi.org/10.3109/13816819009020979. https://www.ncbi.nlm.nih.gov/pubmed/2280977.

Cremers, F. P., S. A. Armstrong, M. C. Seabra, M. S. Brown, and J. L. Goldstein. 1994. "REP-2, a Rab escort protein encoded by the choroideremia-like gene." *J Biol Chem* 269 (3): 2111–7. https://www.ncbi.nlm.nih.gov/pubmed/8294464.

Cremers, F. P., F. Brunsmann, W. Berger, E. P. van Kerkhoff, T. J. van de Pol, B. Wieringa, I. H. Pawlowitzki, and H. H. Ropers. 1990. "Cloning of the breakpoints of a deletion associated with choroidermia." *Hum Genet* 86 (1): 61–4. https://doi.org/10.1007/BF00205174. https://www.ncbi.nlm.nih.gov/pubmed/1979308.

Cremers, F. P. M., W. Lee, R. W. J. Collin, and R. Allikmets. 2020. "Clinical spectrum, genetic complexity and therapeutic approaches for retinal disease caused by ABCA4 mutations." *Prog Retin Eye Res* 79: 100861. https://doi.org/10.1016/j.preteyeres.2020.100861. https://www.ncbi.nlm.nih.gov/pubmed/32278709.

Cukras, C. A., W. T. Wong, R. Caruso, D. Cunningham, W. Zein, and P. A. Sieving. 2012. "Centrifugal expansion of fundus autofluorescence patterns in Stargardt disease over time." *Arch Ophthalmol* 130 (2): 171–9. https://doi.org/10.1001/archophthalmol.2011.332. https://www.ncbi.nlm.nih.gov/pubmed/21987580.

da Costa, B. L., S. R. Levi, E. Eulau, Y. T. Tsai, and P. M. J. Quinn. 2021. "Prime Editing for Inherited Retinal Diseases." *Front Genome Ed* 3: 775330. https://doi.org/10.3389/fgeed.2021.775330. https://www.ncbi.nlm.nih.gov/pubmed/34901928.

De, S., and T. P. Sakmar. 2002. "Interaction of A2E with model membranes. Implications to the pathogenesis of age-related macular degeneration." *J Gen Physiol* 120 (2): 147–57. https://doi.org/10.1085/jgp.20028566. https://www.ncbi.nlm.nih.gov/pubmed/12149277.

Del Pozo-Valero, M., I. Martin-Merida, B. Jimenez-Rolando, A. Arteche, A. Avila-Fernandez, F. Blanco-Kelly, R. Riveiro-Alvarez, C. Van Cauwenbergh, E. De Baere, C. Rivolta, B. Garcia-Sandoval, M. Corton, and C. Ayuso. 2019. "Expanded Phenotypic Spectrum of Retinopathies Associated with Autosomal Recessive and Dominant Mutations in PROM1." *Am J Ophthalmol* 207: 204–214. https://doi.org/10.1016/j.ajo.2019.05.014. https://www.ncbi.nlm.nih.gov/pubmed/31129250.

Dellett, M., N. Sasai, K. Nishide, S. Becker, V. Papadaki, G. A. Limb, A. T. Moore, T. Kondo, and S. Ohnuma. 2014. "Genetic background and light-dependent progression of photoreceptor cell degeneration in Prominin-1 knockout mice." *Invest Ophthalmol Vis Sci* 56 (1): 164–76. https://doi.org/10.1167/iovs.14-15479. https://www.ncbi.nlm.nih.gov/pubmed/25414197.

Delori, F. C., C. K. Dorey, G. Staurenghi, O. Arend, D. G. Goger, and J. J. Weiter. 1995. "In vivo fluorescence of the ocular fundus exhibits retinal pigment epithelium lipofuscin characteristics." *Invest Ophthalmol Vis Sci* 36 (3): 718–29. https://www.ncbi.nlm.nih.gov/pubmed/7890502.

Delori, F. C., G. Staurenghi, O. Arend, C. K. Dorey, D. G. Goger, and J. J. Weiter. 1995. "In vivo measurement of lipofuscin in Stargardt's disease--Fundus flavimaculatus." *Invest Ophthalmol Vis Sci* 36 (11): 2327–31. https://www.ncbi.nlm.nih.gov/pubmed/7558729.

Delori, F., J. P. Greenberg, R. L. Woods, J. Fischer, T. Duncker, J. Sparrow, and R. T. Smith. 2011. "Quantitative measurements of autofluorescence with the scanning laser ophthalmoscope." *Invest Ophthalmol Vis Sci* 52 (13): 9379–90. https://doi.org/10.1167/iovs.11-8319. https://www.ncbi.nlm.nih.gov/pubmed/22016060.

Delori, François C. 1992. "Fluorophotometer for Noninvasive Measurement of RPE Lipofuscin." Noninvasive Assessment of the Visual System, Santa Fe, New Mexico, 1992/01/25.

Dhooge, P. P. A., E. H. Runhart, S. Lambertus, N. M. Bax, J. M. M. Groenewoud, B. J. Klevering, and C. B. Hoyng. 2021. "Correlation of Morphology and Function of Flecks Using Short-Wave Fundus Autofluorescence and Microperimetry in Patients With Stargardt Disease." *Transl Vis Sci Technol* 10 (3): 18. https://doi.org/10.1167/tvst.10.3.18. https://www.ncbi.nlm.nih.gov/pubmed/34003952.

Di Giosaffatte, N., M. Valiante, S. Tricarico, G. Parise, A. M. De Negri, G. Ricciotti, L. Florean, A. Paiardini, I. Bottillo, and P. Grammatico. 2022. "A Novel Hypothesis on Choroideremia-Manifesting Female Carriers: Could." *Genes (Basel)* 13 (7). https://doi.org/10.3390/genes13071268. https://www.ncbi.nlm.nih.gov/pubmed/35886051.

Docchio, F., M. Boulton, R. Cubeddu, R. Ramponi, and P. D. Barker. 1991. "Age-related changes in the fluorescence of melanin and lipofuscin granules of the retinal pigment epithelium: a time-resolved fluorescence spectroscopy study." *Photochem Photobiol* 54 (2): 247–53. https://doi.org/10.1111/j.1751-1097.1991.tb02013.x. https://www.ncbi.nlm.nih.gov/pubmed/1780361.

Duncker, T., J. P. Greenberg, R. Ramachandran, D. C. Hood, R. T. Smith, T. Hirose, R. L. Woods, S. H. Tsang, F. C. Delori, and J. R. Sparrow. 2014. "Quantitative fundus autofluorescence and optical coherence tomography in best vitelliform macular dystrophy." *Invest Ophthalmol Vis Sci* 55 (3): 1471–82. https://doi.org/10.1167/iovs.13-13834. https://www.ncbi.nlm.nih.gov/pubmed/24526438.

Duncker, T., W. Lee, S. H. Tsang, J. P. Greenberg, J. Zernant, R. Allikmets, and J. R. Sparrow. 2013. "Distinct characteristics of inferonasal fundus autofluorescence patterns in stargardt disease and retinitis pigmentosa." *Invest Ophthalmol Vis Sci* 54

(10): 6820–6. https://doi.org/10.1167/iovs.13-12895. https://www.ncbi.nlm.nih.gov/pubmed/24071957.

Duncker, T., M. Marsiglia, W. Lee, J. Zernant, S. H. Tsang, R. Allikmets, V. C. Greenstein, and J. R. Sparrow. 2014. "Correlations among near-infrared and short-wavelength autofluorescence and spectral-domain optical coherence tomography in recessive Stargardt disease." *Invest Ophthalmol Vis Sci* 55 (12): 8134–43. https://doi.org/10.1167/iovs.14-14848. https://www.ncbi.nlm.nih.gov/pubmed/25342616.

Duncker, T., G. E. Stein, W. Lee, S. H. Tsang, J. Zernant, S. Bearelly, D. C. Hood, V. C. Greenstein, F. C. Delori, R. Allikmets, and J. R. Sparrow. 2015. "Quantitative Fundus Autofluorescence and Optical Coherence Tomography in ABCA4 Carriers." *Invest Ophthalmol Vis Sci* 56 (12): 7274–85. https://doi.org/10.1167/iovs.15-17371. https://www.ncbi.nlm.nih.gov/pubmed/26551331.

Duncker, T., M. R. Tabacaru, W. Lee, S. H. Tsang, J. R. Sparrow, and V. C. Greenstein. 2013. "Comparison of near-infrared and short-wavelength autofluorescence in retinitis pigmentosa." *Invest Ophthalmol Vis Sci* 54 (1): 585–91. https://doi.org/10.1167/iovs.12-11176. https://www.ncbi.nlm.nih.gov/pubmed/23287793.

Duncker, T., S. H. Tsang, W. Lee, J. Zernant, R. Allikmets, F. C. Delori, and J. R. Sparrow. 2015. "Quantitative fundus autofluorescence distinguishes ABCA4-associated and non-ABCA4-associated bull's-eye maculopathy." *Ophthalmology* 122 (2): 345–55. https://doi.org/10.1016/j.ophtha.2014.08.017. https://www.ncbi.nlm.nih.gov/pubmed/25283059.

Duncker, T., S. H. Tsang, R. L. Woods, W. Lee, J. Zernant, R. Allikmets, F. C. Delori, and J. R. Sparrow. 2015. "Quantitative Fundus Autofluorescence and Optical Coherence Tomography in PRPH2/RDS- and ABCA4-Associated Disease Exhibiting Phenotypic Overlap." *Invest Ophthalmol Vis Sci* 56 (5): 3159–70. https://doi.org/10.1167/iovs.14-16343. https://www.ncbi.nlm.nih.gov/pubmed/26024099.

Eagle, R. C., A. C. Lucier, V. B. Bernardino, and M. Yanoff. 1980. "Retinal pigment epithelial abnormalities in fundus flavimaculatus: a light and electron microscopic study." *Ophthalmology* 87 (12): 1189–200. https://doi.org/10.1016/s0161-6420(80)35106-3. https://www.ncbi.nlm.nih.gov/pubmed/6165950.

Edwards, A. O., A. Miedziak, T. Vrabec, J. Verhoeven, T. S. Acott, R. G. Weleber, and L. A. Donoso. 1999. "Autosomal dominant Stargardt-like macular dystrophy: I. Clinical characterization, longitudinal follow-up, and evidence for a common ancestry in families linked to chromosome 6q14." *Am J Ophthalmol* 127 (4): 426–35. https://doi.org/10.1016/s0002-9394(98)00331-6. https://www.ncbi.nlm.nih.gov/pubmed/10218695.

Edwards, T. L., M. Groppe, J. K. Jolly, S. M. Downes, and R. E. MacLaren. 2015. "Correlation of retinal structure and function in choroideremia carriers." *Ophthalmology* 122 (6): 1274–6. https://doi.org/10.1016/j.ophtha.2014.12.036. https://www.ncbi.nlm.nih.gov/pubmed/25682176.

Eidinger, O., R. Leibu, H. Newman, L. Rizel, I. Perlman, and T. Ben-Yosef. 2015. "An intronic deletion in the PROM1 gene leads to autosomal recessive cone-rod dystrophy." *Mol Vis* 21: 1295–306. https://www.ncbi.nlm.nih.gov/pubmed/26702251.

Elsner, A. E., S. A. Burns, J. J. Weiter, and F. C. Delori. 1996. "Infrared imaging of sub-retinal structures in the human ocular fundus." *Vision Res* 36 (1): 191–205. https://doi.org/10.1016/0042-6989(95)00100-e. https://www.ncbi.nlm.nih.gov/pubmed/8746253.

Falk, T., N. R. Congrove, S. Zhang, A. D. McCourt, S. J. Sherman, and B. S. McKay. 2012. "PEDF and VEGF-A output from human retinal pigment epithelial cells

grown on novel microcarriers." *J Biomed Biotechnol* 2012: 278932. https://doi.org/10.1155/2012/278932. https://www.ncbi.nlm.nih.gov/pubmed/22547925.

Falletta, P., P. Bagnato, M. Bono, M. Monticone, M. V. Schiaffino, D. C. Bennett, C. R. Goding, C. Tacchetti, and C. Valetti. 2014. "Melanosome-autonomous regulation of size and number: the OA1 receptor sustains PMEL expression." *Pigment Cell Melanoma Res* 27 (4): 565–79. https://doi.org/10.1111/pcmr.12239. https://www.ncbi.nlm.nih.gov/pubmed/24650003.

Fang, Y., A. Tschulakow, T. Taubitz, B. Illing, A. Biesemeier, S. Julien-Schraermeyer, R. A. Radu, Z. Jiang, and U. Schraermeyer. 2020. "Fundus autofluorescence, spectral-domain optical coherence tomography, and histology correlations in a Stargardt disease mouse model." *FASEB J* 34 (3): 3693–3714. https://doi.org/10.1096/fj.201901784RR. https://www.ncbi.nlm.nih.gov/pubmed/31989709.

Fargeas, C. A., M. Florek, W. B. Huttner, and D. Corbeil. 2003. "Characterization of prominin-2, a new member of the prominin family of pentaspan membrane glycoproteins." *J Biol Chem* 278 (10): 8586–96. https://doi.org/10.1074/jbc.M210640200. https://www.ncbi.nlm.nih.gov/pubmed/12514187.

Federspiel, C. A., M. Bertelsen, and L. Kessel. 2018. "Vitamin A in Stargardt disease-an evidence-based update." *Ophthalmic Genet* 39 (5): 555–559. https://doi.org/10.1080/13816810.2018.1488174. https://www.ncbi.nlm.nih.gov/pubmed/29939824.

Feeney, L. 1978. "Lipofuscin and melanin of human retinal pigment epithelium. Fluorescence, enzyme cytochemical, and ultrastructural studies." *Invest Ophthalmol Vis Sci* 17 (7): 583–600. https://www.ncbi.nlm.nih.gov/pubmed/669890.

Feeney-Burns, L., E. S. Hilderbrand, and S. Eldridge. 1984. "Aging human RPE: morphometric analysis of macular, equatorial, and peripheral cells." *Invest Ophthalmol Vis Sci* 25 (2): 195–200. https://www.ncbi.nlm.nih.gov/pubmed/6698741.

Fishkin, N. E., J. R. Sparrow, R. Allikmets, and K. Nakanishi. 2005. "Isolation and characterization of a retinal pigment epithelial cell fluorophore: an all-trans-retinal dimer conjugate." *Proc Natl Acad Sci U S A* 102 (20): 7091–6. https://doi.org/10.1073/pnas.0501266102. https://www.ncbi.nlm.nih.gov/pubmed/15870200.

Fishman, G. A. 1976. "Fundus flavimaculatus. A clinical classification." *Arch Ophthalmol* 94 (12): 2061–7. https://doi.org/10.1001/archopht.1976.03910040721003. https://www.ncbi.nlm.nih.gov/pubmed/999551.

Flannery, J. G., A. C. Bird, D. B. Farber, R. G. Weleber, and D. Bok. 1990. "A histopathologic study of a choroideremia carrier." *Invest Ophthalmol Vis Sci* 31 (2): 229–36. https://www.ncbi.nlm.nih.gov/pubmed/2303326.

Fleckenstein, M., P. Charbel Issa, H. M. Helb, S. Schmitz-Valckenberg, R. P. Finger, H. P. Scholl, K. U. Loeffler, and F. G. Holz. 2008. "High-resolution spectral domain-OCT imaging in geographic atrophy associated with age-related macular degeneration." *Invest Ophthalmol Vis Sci* 49 (9): 4137–44. https://doi.org/10.1167/iovs.08-1967. https://www.ncbi.nlm.nih.gov/pubmed/18487363.

Flynn, E., K. Ueda, E. Auran, J. M. Sullivan, and J. R. Sparrow. 2014. "Fundus autofluorescence and photoreceptor cell rosettes in mouse models." *Invest Ophthalmol Vis Sci* 55 (9): 5643–52. https://doi.org/10.1167/iovs.14-14136. https://www.ncbi.nlm.nih.gov/pubmed/25015357.

Foote, K. G., N. Rinella, J. Tang, N. Bensaid, H. Zhou, Q. Zhang, R. K. Wang, T. C. Porco, A. Roorda, and J. L. Duncan. 2019. "Cone Structure Persists Beyond Margins of Short-Wavelength Autofluorescence in Choroideremia." *Invest Ophthalmol Vis Sci* 60 (14): 4931–4942. https://doi.org/10.1167/iovs.19-27979. https://www.ncbi.nlm.nih.gov/pubmed/31770433.

Freund, P. R., Y. V. Sergeev, and I. M. MacDonald. 2016. “Analysis of a large choroideremia dataset does not suggest a preference for inclusion of certain genotypes in future trials of gene therapy.” *Mol Genet Genomic Med* 4 (3): 344–58. https://doi.org/10.1002/mgg3.208. https://www.ncbi.nlm.nih.gov/pubmed/27247961.

Fry, L. E., M. I. Patrício, J. Williams, J. W. Aylward, H. Hewitt, P. Clouston, K. Xue, A. R. Barnard, and R. E. MacLaren. 2020. “Association of Messenger RNA Level With Phenotype in Patients With Choroideremia: Potential Implications for Gene Therapy Dose.” *JAMA Ophthalmol* 138 (2): 128–135. https://doi.org/10.1001/jamaophthalmol.2019.5071. https://www.ncbi.nlm.nih.gov/pubmed/31855248.

Fu, Y., and K. W. Yau. 2007. “Phototransduction in mouse rods and cones.” *Pflugers Arch* 454 (5): 805–19. https://doi.org/10.1007/s00424-006-0194-y. https://www.ncbi.nlm.nih.gov/pubmed/17226052.

Fujinami, K., N. Lois, A. E. Davidson, D. S. Mackay, C. R. Hogg, E. M. Stone, K. Tsunoda, K. Tsubota, C. Bunce, A. G. Robson, A. T. Moore, A. R. Webster, G. E. Holder, and M. Michaelides. 2013. “A longitudinal study of stargardt disease: clinical and electrophysiologic assessment, progression, and genotype correlations.” *Am J Ophthalmol* 155 (6): 1075–1088.e13. https://doi.org/10.1016/j.ajo.2013.01.018. https://www.ncbi.nlm.nih.gov/pubmed/23499370.

Fujinami, K., A. Oishi, L. Yang, G. Arno, N. Pontikos, K. Yoshitake, Y. Fujinami-Yokokawa, X. Liu, T. Hayashi, S. Katagiri, K. Mizobuchi, A. Mizota, K. Shinoda, N. Nakamura, T. Kurihara, K. Tsubota, Y. Miyake, T. Iwata, A. Tsujikawa, K. Tsunoda, and Japan Eye Genetics Consortium study group. 2020. “Clinical and genetic characteristics of 10 Japanese patients with PROM1-associated retinal disorder: A report of the phenotype spectrum and a literature review in the Japanese population.” *Am J Med Genet C Semin Med Genet* 184 (3): 656–674. https://doi.org/10.1002/ajmg.c.31826. https://www.ncbi.nlm.nih.gov/pubmed/32820593.

Fujinami, K., R. Singh, J. Carroll, J. Zernant, R. Allikmets, M. Michaelides, and A. T. Moore. 2014. “Fine central macular dots associated with childhood-onset Stargardt Disease.” *Acta Ophthalmol* 92 (2): e157–9. https://doi.org/10.1111/aos.12259. https://www.ncbi.nlm.nih.gov/pubmed/24020726.

Fujinami, K., J. Zernant, R. K. Chana, G. A. Wright, K. Tsunoda, Y. Ozawa, K. Tsubota, A. R. Webster, A. T. Moore, R. Allikmets, and M. Michaelides. 2013. “ABCA4 gene screening by next-generation sequencing in a British cohort.” *Invest Ophthalmol Vis Sci* 54 (10): 6662–74. https://doi.org/10.1167/iovs.13-12570. https://www.ncbi.nlm.nih.gov/pubmed/23982839.

Fulton, B. S., and R. R. Rando. 1987. “Biosynthesis of 11-cis-retinoids and retinyl esters by bovine pigment epithelium membranes.” *Biochemistry* 26 (24): 7938–45. https://doi.org/10.1021/bi00398a059. https://www.ncbi.nlm.nih.gov/pubmed/3427115.

Futter, C. E., J. S. Ramalho, G. B. Jaissle, M. W. Seeliger, and M. C. Seabra. 2004. “The role of Rab27a in the regulation of melanosome distribution within retinal pigment epithelial cells.” *Mol Biol Cell* 15 (5): 2264–75. https://doi.org/10.1091/mbc.e03-10-0772. https://www.ncbi.nlm.nih.gov/pubmed/14978221.

Gaillard, E. R., L. Zheng, J. C. Merriam, and J. Dillon. 2000. “Age-related changes in the absorption characteristics of the primate lens.” *Invest Ophthalmol Vis Sci* 41 (6): 1454–9. https://www.ncbi.nlm.nih.gov/pubmed/10798662.

Garner, A., and B. S. Jay. 1980. “Macromelanosomes in X-linked ocular albinism.” *Histopathology* 4 (3): 243–54. https://doi.org/10.1111/j.1365-2559.1980.tb02919.x. https://www.ncbi.nlm.nih.gov/pubmed/7390409.

Gelman, R., R. Chen, A. Blonska, G. Barile, and J. R. Sparrow. 2012. “Fundus autofluorescence imaging in a patient with rapidly developing scotoma.” *Retin Cases Brief Rep* 6 (4): 345–8. https://doi.org/10.1097/ICB.0b013e318260af5d. https://www.ncbi.nlm.nih.gov/pubmed/23293707.

Georgiou, M., K. Fujinami, and M. Michaelides. 2020. “Retinal imaging in inherited retinal diseases.” *Ann Eye Sci* 5. https://doi.org/10.21037/aes-20-81. https://www.ncbi.nlm.nih.gov/pubmed/33928237.

Georgiou, M., T. Kane, P. Tanna, Z. Bouzia, N. Singh, A. Kalitzeos, R. W. Strauss, K. Fujinami, and M. Michaelides. 2020. “Prospective Cohort Study of Childhood-Onset Stargardt Disease: Fundus Autofluorescence Imaging, Progression, Comparison with Adult-Onset Disease, and Disease Symmetry.” *Am J Ophthalmol* 211: 159–175. https://doi.org/10.1016/j.ajo.2019.11.008. https://www.ncbi.nlm.nih.gov/pubmed/31812472.

Gibbs, D., A. V. Cideciyan, S. G. Jacobson, and D. S. Williams. 2009. “Retinal pigment epithelium defects in humans and mice with mutations in MYO7A: imaging melanosome-specific autofluorescence.” *Invest Ophthalmol Vis Sci* 50 (9): 4386–93. https://doi.org/10.1167/iovs.09-3471. https://www.ncbi.nlm.nih.gov/pubmed/19324852.

Gomes, N. L., V. C. Greenstein, J. N. Carlson, S. H. Tsang, R. T. Smith, R. E. Carr, D. C. Hood, and S. Chang. 2009. “A comparison of fundus autofluorescence and retinal structure in patients with Stargardt disease.” *Invest Ophthalmol Vis Sci* 50 (8): 3953–9. https://doi.org/10.1167/iovs.08-2657. https://www.ncbi.nlm.nih.gov/pubmed/19324865.

Granger, C. E., Q. Yang, H. Song, K. Saito, K. Nozato, L. R. Latchney, B. T. Leonard, M. M. Chung, D. R. Williams, and E. A. Rossi. 2018. “Human Retinal Pigment Epithelium: In Vivo Cell Morphometry, Multispectral Autofluorescence, and Relationship to Cone Mosaic.” *Invest Ophthalmol Vis Sci* 59 (15): 5705–5716.https://doi.org/10.1167/iovs.18-24677. https://www.ncbi.nlm.nih.gov/pubmed/30513531.

Greenberg, J. P., T. Duncker, R. L. Woods, R. T. Smith, J. R. Sparrow, and F. C. Delori. 2013. “Quantitative fundus autofluorescence in healthy eyes.” *Invest Ophthalmol Vis Sci* 54 (8): 5684–93. https://doi.org/10.1167/iovs.13-12445. https://www.ncbi.nlm.nih.gov/pubmed/23860757.

Greenstein, V. C., J. Nunez, W. Lee, K. Schuerch, B. Fortune, S. H. Tsang, R. Allikmets, J. R. Sparrow, and D. C. Hood. 2017. “A Comparison of En Face Optical Coherence Tomography and Fundus Autofluorescence in Stargardt Disease.” *Invest Ophthalmol Vis Sci* 58 (12): 5227–5236. https://doi.org/10.1167/iovs.17-22532. https://www.ncbi.nlm.nih.gov/pubmed/29049723.

Greenstein, V. C., R. A. Santos, S. H. Tsang, R. T. Smith, G. R. Barile, and W. Seiple. 2008. “Preferred retinal locus in macular disease: characteristics and clinical implications.” *Retina* 28 (9): 1234–40. https://doi.org/10.1097/IAE.0b013e31817c1b47. https://www.ncbi.nlm.nih.gov/pubmed/18628727.

Greenstein, V. C., A. D. Schuman, W. Lee, T. Duncker, J. Zernant, R. Allikmets, D. C. Hood, and J. R. Sparrow. 2015. “Near-infrared autofluorescence: its relationship to short-wavelength autofluorescence and optical coherence tomography in recessive stargardt disease.” *Invest Ophthalmol Vis Sci* 56 (5): 3226–34. https://doi.org/10.1167/iovs.14-16050. https://www.ncbi.nlm.nih.gov/pubmed/26024107.

Group, Age-Related Eye Disease Study Research. 2000. “Risk factors associated with age-related macular degeneration. A case-control study in the age-related eye disease study: Age-Related Eye Disease Study Report Number 3.” *Ophthalmology* 107 (12): 2224–32. https://doi.org/10.1016/s0161-6420(00)00409-7. https://www.ncbi.nlm.nih.gov/pubmed/11097601.

Han, R. C., L. E. Fry, A. Kantor, M. E. McClements, K. Xue, and R. E. MacLaren. 2021. “Is subretinal AAV gene replacement still the only viable treatment option for choroideremia?” *Expert Opin Orphan Drugs* 9 (1): 13–24. https://doi.org/10.1080/21678707.2021.1882300. https://www.ncbi.nlm.nih.gov/pubmed/34040899.

Hariri, A. H., S. B. Velaga, A. Girach, M. S. Ip, P. V. Le, B. L. Lam, M. D. Fischer, E. M. Sankila, M. E. Pennesi, F. G. Holz, R. E. MacLaren, D. G. Birch, C. B. Hoyng, I. M. MacDonald, G. C. Black, S. H. Tsang, N. M. Bressler, M. Larsen, M. B. Gorin, A. R. Webster, S. R. Sadda, and Group Natural History of the Progression of Choroideremia Study. 2017. “Measurement and Reproducibility of Preserved Ellipsoid Zone Area and Preserved Retinal Pigment Epithelium Area in Eyes With Choroideremia.” *Am J Ophthalmol* 179: 110–117. https://doi.org/10.1016/j.ajo.2017.05.002. https://www.ncbi.nlm.nih.gov/pubmed/28499705.

Hassenstein, A., and C. H. Meyer. 2009. “Clinical use and research applications of Heidelberg retinal angiography and spectral-domain optical coherence tomography - a review.” *Clin Exp Ophthalmol* 37 (1): 130–43. https://doi.org/10.1111/j.1442-9071.2009.02017.x. https://www.ncbi.nlm.nih.gov/pubmed/19338610.

Hattar, S., H. W. Liao, M. Takao, D. M. Berson, and K. W. Yau. 2002. “Melanopsin-containing retinal ganglion cells: architecture, projections, and intrinsic photosensitivity.” *Science* 295 (5557): 1065–70. https://doi.org/10.1126/science.1069609. https://www.ncbi.nlm.nih.gov/pubmed/11834834.

Heath Jeffery, R. C., S. A. Mukhtar, I. L. McAllister, W. H. Morgan, D. A. Mackey, and F. K. Chen. 2021. “Inherited retinal diseases are the most common cause of blindness in the working-age population in Australia.” *Ophthalmic Genet* 42 (4): 431–439. https://doi.org/10.1080/13816810.2021.1913610. https://www.ncbi.nlm.nih. gov/pubmed/33939573.

Hendrickson, A., D. Possin, L. Vajzovic, and C. A. Toth. 2012. “Histologic development of the human fovea from midgestation to maturity.” *Am J Ophthalmol* 154 (5): 767–778.e2. https://doi.org/10.1016/j.ajo.2012.05.007. https://www.ncbi.nlm.nih.gov/pubmed/22935600.

Holz, F. G., F. Schütt, J. Kopitz, G. E. Eldred, F. E. Kruse, H. E. Völcker, and M. Cantz. 1999. “Inhibition of lysosomal degradative functions in RPE cells by a retinoid component of lipofuscin.” *Invest Ophthalmol Vis Sci* 40 (3): 737–43. https://www.ncbi.nlm.nih.gov/pubmed/10067978.

Hu, D. N., J. D. Simon, and T. Sarna. 2008. “Role of ocular melanin in ophthalmic physiology and pathology.” *Photochem Photobiol* 84 (3): 639–44. https://doi.org/10.1111/j.1751-1097.2008.00316.x. https://www.ncbi.nlm.nih.gov/pubmed/18346089.

Hu, D. N., G. P. Yu, S. A. McCormick, S. Schneider, and P. T. Finger. 2005. “Population-based incidence of uveal melanoma in various races and ethnic groups.” *Am J Ophthalmol* 140 (4): 612–7. https://doi.org/10.1016/j.ajo.2005.05.034. https://www.ncbi.nlm.nih.gov/pubmed/16226513.

Huang, A. S., L. A. Kim, and A. A. Fawzi. 2012. “Clinical characteristics of a large choroideremia pedigree carrying a novel CHM mutation.” *Arch Ophthalmol* 130 (9): 1184–9. https://doi.org/10.1001/archophthalmol.2012.1117. https://www.ncbi.nlm.nih.gov/pubmed/22965595.

Hume, A. N., L. M. Collinson, A. Rapak, A. Q. Gomes, C. R. Hopkins, and M. C. Seabra. 2001. “Rab27a regulates the peripheral distribution of melanosomes in melanocytes.” *J Cell Biol* 152 (4): 795–808. https://www.ncbi.nlm.nih.gov/pubmed/11266470.

Hussain, R. M., T. A. Ciulla, A. M. Berrocal, N. Z. Gregori, H. W. Flynn, and B. L. Lam. 2018. “Stargardt macular dystrophy and evolving therapies.” *Expert Opin Biol Ther* 18 (10): 1049–1059. https://doi.org/10.1080/14712598.2018.1513486. https://www.ncbi.nlm.nih.gov/pubmed/30129371.

Illing, M., L. L. Molday, and R. S. Molday. 1997. “The 220-kDa rim protein of retinal rod outer segments is a member of the ABC transporter superfamily.” *J Biol Chem* 272 (15): 10303–10. https://doi.org/10.1074/jbc.272.15.10303. https://www.ncbi.nlm.nih.gov/pubmed/9092582.

Imani, S., J. Cheng, M. D. Shasaltaneh, C. Wei, L. Yang, S. Fu, H. Zou, M. A. Khan, X. Zhang, H. Chen, D. Zhang, C. Duan, H. Lv, Y. Li, R. Chen, and J. Fu. 2018. “Genetic identification and molecular modeling characterization reveal a novel.” *Oncotarget* 9 (1): 122–141. https://doi.org/10.18632/oncotarget.22343. https://www.ncbi.nlm.nih.gov/pubmed/29416601.

Jacobson, S. G., A. V. Cideciyan, A. Sumaroka, T. S. Aleman, S. B. Schwartz, E. A. Windsor, A. J. Roman, E. M. Stone, and I. M. MacDonald. 2006. “Remodeling of the human retina in choroideremia: rab escort protein 1 (REP-1) mutations.” *Invest Ophthalmol Vis Sci* 47 (9): 4113–20. https://doi.org/10.1167/iovs.06-0424. https://www.ncbi.nlm.nih.gov/pubmed/16936131.

Jolly, J. K., H. Bridge, and R. E. MacLaren. 2019. “Outcome Measures Used in Ocular Gene Therapy Trials: A Scoping Review of Current Practice.” *Front Pharmacol* 10: 1076. https://doi.org/10.3389/fphar.2019.01076. https://www.ncbi.nlm.nih.gov/pubmed/ 31620003.

Jolly, J. K., T. L. Edwards, J. Moules, M. Groppe, S. M. Downes, and R. E. MacLaren. 2016. “A Qualitative and Quantitative Assessment of Fundus Autofluorescence Patterns in Patients With Choroideremia.” *Invest Ophthalmol Vis Sci* 57 (10): 4498–4503. https://doi.org/10.1167/iovs.15-18362. https://www.ncbi.nlm.nih.gov/pubmed/27750291.

Jolly, J. K., K. Xue, T. L. Edwards, M. Groppe, and R. E. MacLaren. 2017. “Characterizing the Natural History of Visual Function in Choroideremia Using Micro perimetry and Multimodal Retinal Imaging.” *Invest Ophthalmol Vis Sci* 58 (12): 5575–5583. https://doi.org/10.1167/iovs.17-22486. https://www.ncbi.nlm.nih.gov/pubmed/29084330.

Kaczmarek, J. C., P. S. Kowalski, and D. G. Anderson. 2017. “Advances in the delivery of RNA therapeutics: from concept to clinical reality.” *Genome Med* 9 (1): 60. https://doi.org/10.1186/s13073-017-0450-0. https://www.ncbi.nlm.nih.gov/pubmed/28655327.

Karim, B. O., K. J. Rhee, G. Liu, K. Yun, and S. R. Brant. 2014. “Prom1 function in development, intestinal inflammation, and intestinal tumorigenesis.” *Front Oncol* 4: 323. https://doi.org/10.3389/fonc.2014.00323. https://www.ncbi.nlm.nih.gov/pubmed/25452936.

Katz, M. L., C. M. Drea, G. E. Eldred, H. H. Hess, and W. G. Robison. 1986. “Influence of early photoreceptor degeneration on lipofuscin in the retinal pigment epithelium.” *Exp Eye Res* 43 (4): 561–73. https://doi.org/10.1016/s0014-4835(86)80023-9. https://www.ncbi.nlm.nih.gov/pubmed/3792460.

Katz, M. L., G. E. Eldred, and W. G. Robison. 1987. “Lipofuscin autofluorescence: evidence for vitamin A involvement in the retina.” *Mech Ageing Dev* 39 (1): 81–90. https://doi.org/10.1016/0047-6374(87)90088-1. https://www.ncbi.nlm.nih.gov/pubmed/ 3613689.

Katz, M. L., and M. Norberg. 1992. “Influence of dietary vitamin A on autofluorescence of leupeptin-induced inclusions in the retinal pigment epithelium.” *Exp Eye Res* 54 (2): 239–46. https://doi.org/10.1016/s0014-4835(05)80213-1. https://www.ncbi.nlm.nih.gov/pubmed/1559552.

Kaufman, Y., L. Ma, and I. Washington. 2011. “Deuterium enrichment of vitamin A at the C20 position slows the formation of detrimental vitamin A dimers in wild-type rodents.” *J Biol Chem* 286 (10): 7958–7965. https://doi.org/10.1074/jbc.M110.178640. https://www.ncbi.nlm.nih.gov/pubmed/21075840.

Kayatz, P., G. Thumann, T. T. Luther, J. F. Jordan, K. U. Bartz-Schmidt, P. J. Esser, and U. Schraermeyer. 2001. “Oxidation causes melanin fluorescence.” *Invest Ophthalmol Vis Sci* 42 (1): 241–6. https://www.ncbi.nlm.nih.gov/pubmed/11133875.

Kefalov, V. J. 2012. “Rod and cone visual pigments and phototransduction through pharmacological, genetic, and physiological approaches.” *J Biol Chem* 287 (3): 1635–41. https://doi.org/10.1074/jbc.R111.303008. https://www.ncbi.nlm.nih.gov/pubmed/22074928.

Keilhauer, C. N., and F. C. Delori. 2006. “Near-infrared autofluorescence imaging of the fundus: visualization of ocular melanin.” *Invest Ophthalmol Vis Sci* 47 (8): 3556–64. https://doi.org/10.1167/iovs.06-0122. https://www.ncbi.nlm.nih.gov/pubmed/16877429.

Kellner, S., U. Kellner, B. H. Weber, B. Fiebig, S. Weinitz, and K. Ruether. 2009. “Lipofuscin- and melanin-related fundus autofluorescence in patients with ABCA4-associated retinal dystrophies.” *Am J Ophthalmol* 147 (5): 895–902, 902.e1. https://doi.org/10.1016/j.ajo.2008.12.023. https://www.ncbi.nlm.nih.gov/pubmed/19243736.

Kellner, U., S. Kellner, and S. Weinitz. 2010. “Fundus autofluorescence (488 NM) and near-infrared autofluorescence (787 NM) visualize different retinal pigment epithelium alterations in patients with age-related macular degeneration.” *Retina* 30 (1): 6-15. https://doi.org/10.1097/iae.0b013e3181b8348b. https://www.ncbi.nlm.nih.gov/pubmed/20066766.

Khan, A. O., and H. J. Bolz. 2015. “Pediatric Cone-Rod Dystrophy with High Myopia and Nystagmus Suggests Recessive PROM1 Mutations.” *Ophthalmic Genet* 36 (4): 349–52. https://doi.org/10.3109/13816810.2014.886266. https://www.ncbi.nlm.nih.gov/pubmed/24547909.

Khan, K. N., F. Islam, A. T. Moore, and M. Michaelides. 2016. “Clinical and Genetic Features of Choroideremia in Childhood.” *Ophthalmology* 123 (10): 2158–65. https://doi.org/10.1016/j.ophtha.2016.06.051. https://www.ncbi.nlm.nih.gov/pubmed/27506488.

Khan, K. N., M. Kasilian, O. A. R. Mahroo, P. Tanna, A. Kalitzeos, A. G. Robson, K. Tsunoda, T. Iwata, A. T. Moore, K. Fujinami, and M. Michaelides. 2018. “Early Patterns of Macular Degeneration in ABCA4-Associated Retinopathy.” *Ophthalmology* 125 (5): 735–746. https://doi.org/10.1016/j.ophtha.2017.11.020. https://www.ncbi.nlm.nih.gov/pubmed/29310964.

Khan, K. N., E. C. Lord, G. Arno, F. Islam, K. J. Carss, F. Raymond, C. Toomes, M. Ali, C. F. Inglehearn, A. R. Webster, A. T. Moore, J. A. Poulter, and M. Michaelides. 2018. “DETAILED RETINAL IMAGING IN CARRIERS OF OCULAR ALBINISM.” *Retina* 38 (3): 620–628. https://doi.org/10.1097/IAE.0000000000001570. https://www.ncbi.nlm.nih.gov/pubmed/28234808.

Kim, H. J., and J. R. Sparrow. 2018. “Novel bisretinoids of human retina are lyso alkyl ether glycerophosphoethanolamine-bearing A2PE species.” *J Lipid Res* 59 (9):

1620–1629. https://doi.org/10.1194/jlr.M084459. https://www.ncbi.nlm.nih.gov/pubmed/29986955.

Kim, J. M., C. Lee, G. I. Lee, N. K. D. Kim, C. S. Ki, W. Y. Park, B. J. Kim, and S. J. Kim. 2017. "Identification of the PROM1 Mutation p.R373C in a Korean Patient With Autosomal Dominant Stargardt-like Macular Dystrophy." *Ann Lab Med* 37 (6): 536–539. https://doi.org/10.3343/alm.2017.37.6.536. https://www.ncbi.nlm.nih.gov/pubmed/28840994.

Kim, S. R., J. He, E. Yanase, Y. P. Jang, N. Berova, J. R. Sparrow, and K. Nakanishi. 2007. "Characterization of dihydro-A2PE: an intermediate in the A2E biosynthetic pathway." *Biochemistry* 46 (35): 10122–9. https://doi.org/10.1021/bi7009635. https://www.ncbi.nlm.nih.gov/pubmed/17685561.

Kim, S. R., Y. P. Jang, S. Jockusch, N. E. Fishkin, N. J. Turro, and J. R. Sparrow. 2007. "The all-trans-retinal dimer series of lipofuscin pigments in retinal pigment epithelial cells in a recessive Stargardt disease model." *Proc Natl Acad Sci U S A* 104 (49): 19273–8. https://doi.org/10.1073/pnas.0708714104. https://www.ncbi.nlm.nih.gov/pubmed/18048333.

Kim, S. R., K. Nakanishi, Y. Itagaki, and J. R. Sparrow. 2006. "Photooxidation of A2-PE, a photoreceptor outer segment fluorophore, and protection by lutein and zeaxanthin." *Exp Eye Res* 82 (5): 828–39. https://doi.org/10. 1016/j.exer.2005.10.004. https://www.ncbi.nlm.nih.gov/pubmed/16364293.

Kniazeva, M., M. F. Chiang, B. Morgan, A. L. Anduze, D. J. Zack, M. Han, and K. Zhang. 1999. "A new locus for autosomal dominant stargardt-like disease maps to chromosome 4." *Am J Hum Genet* 64 (5): 1394–9. https://doi.org/10.1086/302377. https://www.ncbi.nlm.nih.gov/pubmed/10205271.

Kniazeva, M. F., M. F. Chiang, G. R. Cutting, D. J. Zack, M. Han, and K. Zhang. 1999. "Clinical and genetic studies of an autosomal dominant cone-rod dystrophy with features of Stargardt disease." *Ophthalmic Genet* 20 (2): 71–81. https://doi.org/10.1076/opge.20.2.71.2287. https://www.ncbi.nlm.nih.gov/pubmed/10420191.

Kohno, H., Y. Chen, B. M. Kevany, E. Pearlman, M. Miyagi, T. Maeda, K. Palczewski, and A. Maeda. 2013. "Photoreceptor proteins initiate microglial activation via Toll-like receptor 4 in retinal degeneration mediated by all-trans-retinal." *J Biol Chem* 288 (21): 15326–41. https://doi.org/10.1074/jbc.M112.448712. https://www.ncbi.nlm.nih.gov/pubmed/23572532.

Kolb, H., E. Fernandez, and R. Nelson. 1995. "Webvision: The Organization of the Retina and Visual System."

Krock, B. L., J. Bilotta, and B. D. Perkins. 2007. "Noncell-autonomous photoreceptor degeneration in a zebrafish model of choroideremia." *Proc Natl Acad Sci U S A* 104 (11): 4600–5. https://doi.org/10.1073/pnas.0605818104. https://www.ncbi.nlm.nih.gov/pubmed/17360570.

Kwan, K. M., H. Otsuna, H. Kidokoro, K. R. Carney, Y. Saijoh, and C. B. Chien. 2012. "A complex choreography of cell movements shapes the vertebrate eye." *Development* 139 (2): 359–72. https://doi.org/10.1242/dev.071407. https://www.ncbi.nlm.nih.gov/pubmed/22186726.

Kwok, M. C., J. M. Holopainen, L. L. Molday, L. J. Foster, and R. S. Molday. 2008. "Proteomics of photoreceptor outer segments identifies a subset of SNARE and Rab proteins implicated in membrane vesicle trafficking and fusion." *Mol Cell Proteomics* 7 (6): 1053–66. https://doi.org/10.1074/mcp.M700571-MCP200. https://www.ncbi.nlm.nih.gov/pubmed/18245078.

Lam, B. L., J. L. Davis, and N. Z. Gregori. 2021. “Choroideremia Gene Therapy.” *Int Ophthalmol Clin* 61 (4): 185–193. https://doi.org/10.1097/IIO.0000000000000385. https://www.ncbi.nlm.nih.gov/pubmed/34584056.

Landrum, J. T., and R. A. Bone. 2001. “Lutein, zeaxanthin, and the macular pigment.” *Arch Biochem Biophys* 385 (1): 28–40. https://doi.org/10.1006/abbi.2000.2171. https://www.ncbi.nlm.nih.gov/pubmed/11361022.

Larijani, B., A. N. Hume, A. K. Tarafder, and M. C. Seabra. 2003. “Multiple factors contribute to inefficient prenylation of Rab27a in Rab prenylation diseases.” *J Biol Chem* 278 (47): 46798–804. https://doi.org/10.1074/jbc.M307799200. https://www.ncbi.nlm.nih.gov/pubmed/12941939.

Lee, T. K., K. E. McTaggart, P. A. Sieving, J. R. Heckenlively, A. V. Levin, J. Greenberg, R. G. Weleber, P. Y. Tong, E. F. Anhalt, B. R. Powell, and I. M. MacDonald. 2003. “Clinical diagnoses that overlap with choroideremia.” *Can J Ophthalmol* 38 (5): 364–72; quiz 372. https://doi.org/10.1016/s0008-4182(03)80047-9. https://www.ncbi.nlm.nih.gov/pubmed/12956277.

Lee, W., K. Noupuu, M. Oll, T. Duncker, T. Burke, J. Zernant, S. Bearelly, S. H. Tsang, J. R. Sparrow, and R. Allikmets. 2014. “The external limiting membrane in early-onset Stargardt disease.” *Invest Ophthalmol Vis Sci* 55 (10): 6139–49. https://doi.org/10.1167/iovs.14-15126. https://www.ncbi.nlm.nih.gov/pubmed/25139735.

Lee, W., J. Zernant, P. Y. Su, T. Nagasaki, S. H. Tsang, and R. Allikmets. 2022. “A genotype-phenotype correlation matrix for ABCA4 disease based on long-term prognostic outcomes.” *JCI Insight* 7 (2). https://doi.org/10.1172/jci.insight.156154. https://www.ncbi.nlm.nih.gov/pubmed/34874912.

Leibrock, C. S., T. Reuter, and T. D. Lamb. 1998. “Molecular basis of dark adaptation in rod photoreceptors.” *Eye (Lond)* 12 (Pt 3b): 511–20. https://doi.org/10.1038/eye.1998.139. https://www.ncbi.nlm.nih.gov/pubmed/9775211.

Liang, J., X. She, J. Chen, Y. Zhai, Y. Liu, K. Zheng, Y. Gong, H. Zhu, X. Luo, and X. Sun. 2019. “Identification of novel PROM1 mutations responsible for autosomal recessive maculopathy with rod-cone dystrophy.” *Graefes Arch Clin Exp Ophthalmol* 257 (3): 619–628. https://doi.org/10.1007/s00417-018-04206-w. https://www.ncbi.nlm.nih.gov/pubmed/30588538.

Liew, G., M. Michaelides, and C. Bunce. 2014. “A comparison of the causes of blindness certifications in England and Wales in working age adults (16–64 years), 1999–2000 with 2009–2010.” *BMJ Open* 4 (2): e004015. https://doi.org/10.1136/bmjopen-2013-004015. https://www.ncbi.nlm.nih.gov/pubmed/24525390.

Lima de Carvalho, J. R., S. H. Tsang, and J. R. Sparrow. 2022. “VITAMIN A DEFICIENCY MONITORED BY QUANTITATIVE SHORT WAVELENGTH FUNDUS AUTOFLUORESCENCE IN A CASE OF BARIATRIC SURGERY.” *Retin Cases Brief Rep* 16 (2): 218–221. https://doi.org/10.1097/ICB.0000000000000931. https://www.ncbi.nlm.nih.gov/pubmed/31599792.

Liu, J., Y. Itagaki, S. Ben-Shabat, K. Nakanishi, and J. R. Sparrow. 2000. “The biosynthesis of A2E, a fluorophore of aging retina, involves the formation of the precursor, A2-PE, in the photoreceptor outer segment membrane.” *J Biol Chem* 275 (38): 29354–60. https://doi.org/10.1074/jbc.M910191199. https://www.ncbi.nlm.nih.gov/pubmed/10887199.

Lois, N., A. S. Halfyard, A. C. Bird, and F. W. Fitzke. 2000. “Quantitative evaluation of fundus autofluorescence imaged “in vivo” in eyes with retinal disease.” *Br J Ophthalmol* 84 (7): 741–5. https://doi.org/10.1136/bjo.84.7.741. https://www.ncbi.nlm.nih.gov/pubmed/10873986.

Lois, N., A. S. Halfyard, A. C. Bird, G. E. Holder, and F. W. Fitzke. 2004. “Fundus autofluorescence in Stargardt macular dystrophy-fundus flavimaculatus.” *Am J Ophthalmol* 138 (1): 55–63. https://doi.org/10.1016/j.ajo.2004.02.056. https://www.ncbi.nlm.nih.gov/pubmed/15234282.

Lois, N., A. S. Halfyard, C. Bunce, A. C. Bird, and F. W. Fitzke. 1999. “Reproducibility of fundus autofluorescence measurements obtained using a confocal scanning laser ophthalmoscope.” *Br J Ophthalmol* 83 (3): 276–9. https://doi.org/10.1136/bjo.83.3.276. https://www.ncbi.nlm.nih.gov/pubmed/10365032.

Lois, N., G. E. Holder, C. Bunce, F. W. Fitzke, and A. C. Bird. 2001. “Phenotypic subtypes of Stargardt macular dystrophy-fundus flavimaculatus.” *Arch Ophthalmol* 119 (3): 359–69. https://doi.org/10.1001/archopht.119.3.359. https://www.ncbi.nlm.nih.gov/pubmed/11231769.

Lopez, P. F., I. H. Maumenee, Z. de la Cruz, and W. R. Green. 1990. “Autosomal-dominant fundus flavimaculatus. Clinicopathologic correlation.” *Ophthalmology* 97 (6): 798–809. https://doi.org/10.1016/s0161-6420(90)32508-3. https://www.ncbi.nlm.nih.gov/pubmed/2374685.

Lorenz, B., B. Wabbels, E. Wegscheider, C. P. Hamel, W. Drexler, and M. N. Preising. 2004. “Lack of fundus autofluorescence to 488 nanometers from childhood on in patients with early-onset severe retinal dystrophy associated with mutations in RPE65.” *Ophthalmology* 111 (8): 1585–94. https://doi.org/10.1016/j.ophtha.2004.01.033. https://www.ncbi.nlm.nih.gov/pubmed/15288992.

Lyle, W. M., J. O. Sangster, and T. D. Williams. 1997. “Albinism: an update and review of the literature.” *J Am Optom Assoc* 68 (10): 623–45. https://www.ncbi.nlm.nih.gov/pubmed/9354055.

Lyon, M. F. 1972. “X-chromosome inactivation and developmental patterns in mammals.” *Biol Rev Camb Philos Soc* 47 (1): 1–35. https://doi.org/10.1111/j.1469-185x.1972.tb00969.x. https://www.ncbi.nlm.nih.gov/pubmed/4554151.

MacDonald, I. M., L. Russell, and C. C. Chan. 2009. “Choroideremia: new findings from ocular pathology and review of recent literature.” *Surv Ophthalmol* 54 (3): 401–7. https://doi.org/10.1016/j.survophthal.2009.02.008. https://www.ncbi.nlm.nih.gov/pubmed/19422966.

Maeda, A., M. Golczak, T. Maeda, and K. Palczewski. 2009. “Limited roles of Rdh8, Rdh12, and Abca4 in all-trans-retinal clearance in mouse retina.” *Invest Ophthalmol Vis Sci* 50 (11): 5435–43. https://doi.org/10.1167/iovs.09-3944. https://www.ncbi.nlm.nih.gov/pubmed/19553623.

Mata, N. L., R. A. Radu, R. C. Clemmons, and G. H. Travis. 2002. “Isomerization and oxidation of vitamin a in cone-dominant retinas: a novel pathway for visual-pigment regeneration in daylight.” *Neuron* 36 (1): 69–80. https://doi.org/10.1016/s0896-6273(02)00912-1. https://www.ncbi.nlm.nih.gov/pubmed/12367507.

Maw, M. A., D. Corbeil, J. Koch, A. Hellwig, J. C. Wilson-Wheeler, R. J. Bridges, G. Kumaramanickavel, S. John, D. Nancarrow, K. Roper, A. Weigmann, W. B. Huttner, and M. J. Denton. 2000. “A frameshift mutation in prominin (mouse)-like 1 causes human retinal degeneration.” *Hum Mol Genet* 9 (1): 27–34. https://doi.org/10.1093/hmg/9.1.27. https://www.ncbi.nlm.nih.gov/pubmed/10587575.

McCulloch, D. L., M. F. Marmor, M. G. Brigell, R. Hamilton, G. E. Holder, R. Tzekov, and M. Bach. 2015. “ISCEV Standard for full-field clinical electroretinography (2015 update).” *Doc Ophthalmol* 130 (1): 1–12. https://doi.org/10.1007/s10633-014-9473-7. https://www.ncbi.nlm.nih.gov/pubmed/25502644.

McKay, B. S. 2019. “Pigmentation and vision: Is GPR143 in control?” *J Neurosci Res* 97 (1): 77–87. https://doi.org/10.1002/jnr.24246. https://www.ncbi.nlm.nih.gov/pubmed/29761529.

Mead, B., M. Berry, A. Logan, R. A. Scott, W. Leadbeater, and B. A. Scheven. 2015. “Stem cell treatment of degenerative eye disease.” *Stem Cell Res* 14 (3): 243–57. https://doi.org/10.1016/j.scr.2015.02.003. https://www.ncbi.nlm.nih.gov/pubmed/25752437.

Michaelides, M., M. C. Gaillard, P. Escher, L. Tiab, M. Bedell, F. X. Borruat, D. Barthelmes, R. Carmona, K. Zhang, E. White, M. McClements, A. G. Robson, G. E. Holder, K. Bradshaw, D. M. Hunt, A. R. Webster, A. T. Moore, D. F. Schorderet, and F. L. Munier. 2010. “The PROM1 mutation p.R373C causes an autosomal dominant bull’s eye maculopathy associated with rod, rod-cone, and macular dystrophy.” *Invest Ophthalmol Vis Sci* 51 (9): 4771–80. https://doi.org/10.1167/iovs.09-4561. https://www.ncbi.nlm.nih.gov/pubmed/20393116.

Michaelides, M., S. Johnson, A. Poulson, K. Bradshaw, C. Bellmann, D. M. Hunt, and A. T. Moore. 2003. “An autosomal dominant bull’s-eye macular dystrophy (MCDR2) that maps to the short arm of chromosome 4.” *Invest Ophthalmol Vis Sci* 44 (4): 1657–62. https://doi.org/10.1167/iovs.02-0941. https://www.ncbi.nlm.nih.gov/pubmed/12657606.

Molday, L. L., A. R. Rabin, and R. S. Molday. 2000. “ABCR expression in foveal cone photoreceptors and its role in stargardt macular dystrophy.” *Am J Ophthalmol* 130 (5): 689. https://doi.org/10.1016/s0002-9394(00)00756-x. https://www.ncbi.nlm.nih.gov/pubmed/11078864.

Molday, R. S., and K. Zhang. 2010. “Defective lipid transport and biosynthesis in recessive and dominant Stargardt macular degeneration.” *Prog Lipid Res* 49 (4): 476–92. https://doi.org/10.1016/j.plipres.2010.07.002. https://www.ncbi.nlm.nih.gov/pubmed/20633576.

Morgan, J. I., G. Han, E. Klinman, W. M. Maguire, D. C. Chung, A. M. Maguire, and J. Bennett. 2014. “High-resolution adaptive optics retinal imaging of cellular structure in choroideremia.” *Invest Ophthalmol Vis Sci* 55 (10): 6381–97. https://doi.org/10.1167/iovs.13-13454. https://www.ncbi.nlm.nih.gov/pubmed/25190651.

Moshiri, A., H. P. Scholl, M. V. Canto-Soler, and M. F. Goldberg. 2013. “Morphogenetic model for radial streaking in the fundus of the carrier state of X-linked albinism.” *JAMA Ophthalmol* 131 (5): 691–3. https://doi.org/10.1001/jamaophthalmol.2013.39. https://www.ncbi.nlm.nih.gov/pubmed/23519542.

Mucciolo, D. P., V. Murro, D. Giorgio, A. Sodi, I. Passerini, G. Virgili, and S. Rizzo. 2019. “Near-infrared autofluorescence in young choroideremia patients.” *Ophthalmic Genet* 40 (5): 421–427. https://doi.org/10.1080/13816810.2019.1666881. https://www.ncbi.nlm.nih.gov/pubmed/31544579.

Mura, M., C. Sereda, M. M. Jablonski, I. M. MacDonald, and A. Iannaccone. 2007. “Clinical and functional findings in choroideremia due to complete deletion of the CHM gene.” *Arch Ophthalmol* 125 (8): 1107–13. https://doi.org/10.1001/archopht.125.8.1107. https://www.ncbi.nlm.nih.gov/pubmed/17698759.

Murro, V., D. P. Mucciolo, I. Passerini, S. Palchetti, A. Sodi, G. Virgili, and S. Rizzo. 2017. “Retinal dystrophy and subretinal drusenoid deposits in female choroideremia carriers.” *Graefes Arch Clin Exp Ophthalmol* 255 (11): 2099–2111. https://doi.org/10.1007/s00417-017-3751-5. https://www.ncbi.nlm.nih.gov/pubmed/28752371.

Müller, P. L., J. Birtel, P. Herrmann, F. G. Holz, P. Charbel Issa, and M. Gliem. 2019. “Functional Relevance and Structural Correlates of Near Infrared and Short

Wavelength Fundus Autofluorescence Imaging in." *Transl Vis Sci Technol* 8 (6): 46. https://doi.org/10.1167/tvst.8.6.46. https://www.ncbi.nlm.nih.gov/pubmed/31879568.

Nõupuu, K., W. Lee, J. Zernant, V. C. Greenstein, S. Tsang, and R. Allikmets. 2016. "Recessive Stargardt disease phenocopying hydroxychloroquine retinopathy." *Graefes Arch Clin Exp Ophthalmol* 254 (5): 865–72. https://doi.org/10.1007/s00417-015-3142-8. https://www.ncbi.nlm.nih.gov/pubmed/26311262.

Nõupuu, K., W. Lee, J. Zernant, S. H. Tsang, and R. Allikmets. 2014. "Structural and genetic assessment of the ABCA4-associated optical gap phenotype." *Invest Ophthalmol Vis Sci* 55 (11): 7217–26. https://doi.org/10.1167/iovs.14-14674. https://www.ncbi.nlm.nih.gov/pubmed/25301883.

Oetting, W. S. 2002. "New insights into ocular albinism type 1 (OA1): Mutations and polymorphisms of the OA1 gene." *Hum Mutat* 19 (2): 85–92. https://doi.org/10.1002/humu.10034. https://www.ncbi.nlm.nih.gov/pubmed/11793467.

Oetting, W. S., and R. A. King. 1999. "Molecular basis of albinism: mutations and polymorphisms of pigmentation genes associated with albinism." *Hum Mutat* 13 (2): 99–115. https://doi.org/10.1002/(SICI)1098-1004(1999)13:2<99::AID-HUMU2>3.0.CO; 2-C. https://www.ncbi.nlm.nih.gov/pubmed/10094567.

Oh, J. K., J. R. Lima de Carvalho, J. Ryu, S. H. Tsang, and J. R. Sparrow. 2020. "Short-Wavelength and Near-Infrared Autofluorescence in Patients with Deficiencies of the Visual Cycle and Phototransduction." *Sci Rep* 10 (1): 8998. https://doi.org/10.1038/s41598-020-65763-x. https://www.ncbi.nlm.nih.gov/pubmed/32488013.

Ortonne, J. P. 2002. "Photoprotective properties of skin melanin." *Br J Dermatol* 146 Suppl 61: 7–10. https://doi.org/10.1046/j.1365-2133.146.s61.3.x. https://www.ncbi.nlm.nih.gov/pubmed/11966725.

Paavo, M., W. Lee, J. Merriam, S. Bearelly, S. Tsang, S. Chang, and J. R. Sparrow. 2017. "Intraretinal Correlates of Reticular Pseudodrusen Revealed by Autofluorescence and En Face OCT." *Invest Ophthalmol Vis Sci* 58 (11): 4769–4777. https://doi.org/10.1167/iovs.17-22338. https://www.ncbi.nlm.nih.gov/pubmed/28973322.

Palmisano, I., P. Bagnato, A. Palmigiano, G. Innamorati, G. Rotondo, D. Altimare, C. Venturi, E. V. Sviderskaya, R. Piccirillo, M. Coppola, V. Marigo, B. Incerti, A. Ballabio, E. M. Surace, C. Tacchetti, D. C. Bennett, and M. V. Schiaffino. 2008. "The ocular albinism type 1 protein, an intracellular G protein-coupled receptor, regulates melanosome transport in pigment cells." *Hum Mol Genet* 17 (22): 3487–501. https://doi.org/10.1093/hmg/ddn241. https://www.ncbi.nlm.nih.gov/pubmed/18697795.

Parish, C. A., M. Hashimoto, K. Nakanishi, J. Dillon, and J. Sparrow. 1998. "Isolation and one-step preparation of A2E and iso-A2E, fluorophores from human retinal pigment epithelium." *Proc Natl Acad Sci U S A* 95 (25): 14609–13. https://doi.org/10.1073/pnas.95.25.14609. https://www.ncbi.nlm.nih.gov/pubmed/9843937.

Park, S. P., F. S. Siringo, N. Pensec, I. H. Hong, J. Sparrow, G. Barile, S. H. Tsang, and S. Chang. 2013. "Comparison of fundus autofluorescence between fundus camera and confocal scanning laser ophthalmoscope-based systems." *Ophthalmic Surg Lasers Imaging Retina* 44 (6): 536-43. https://doi.org/10.3928/23258160-20131105-04. https://www.ncbi.nlm.nih.gov/pubmed/24221461.

Parker, M. A., L. R. Erker, I. Audo, D. Choi, S. Mohand-Said, K. Sestakauskas, P. Benoit, T. Appelqvist, M. Krahmer, C. Ségaut-Prévost, B. J. Lujan, A. Faridi, E. N. Chegarnov, P. N. Steinkamp, C. Ku, M. M. da Palma, P. O. Barale, S. Ayelo-Scheer, A. Lauer, T. Stout, D. J. Wilson, R. G. Weleber, M. E. Pennesi, J. A. Sahel, and P. Yang. 2022. "Three-Year Safety Results of SAR422459 (EIAV-ABCA4) Gene Therapy in Patients With ABCA4-Associated Stargardt Disease: An Open-Label

Dose-Escalation Phase I/IIa Clinical Trial, Cohorts 1–5." *Am J Ophthalmol* 240: 285–301. https://doi.org/10.1016/j.ajo.2022.02.013. https://www.ncbi.nlm.nih.gov/pubmed/35248547.

Parmann, R., S. H. Tsang, J. Zernant, R. Allikmets, V. C. Greenstein, and J. R. Sparrow. 2022. "Comparisons Among Optical Coherence Tomography and Fundus Autofluorescence Modalities as Measurements of Atrophy in ABCA4-Associated Disease." *Transl Vis Sci Technol* 11 (1): 36. https://doi.org/10.1167/tvst.11.1.36. https://www.ncbi.nlm.nih.gov/pubmed/35089312.

Paskowitz, D. M., M. M. LaVail, and J. L. Duncan. 2006. "Light and inherited retinal degeneration." *Br J Ophthalmol* 90 (8): 1060–6. https://doi.org/10.1136/bjo.2006.097436. https://www.ncbi.nlm.nih.gov/pubmed/16707518.

Piccolino, F. C., L. Borgia, E. Zinicola, M. Iester, and S. Torrielli. 1996. "Pre-injection fluorescence in indocyanine green angiography." *Ophthalmology* 103 (11): 1837–45. https://doi.org/10.1016/s0161-6420(96)30418-1. https://www.ncbi.nlm.nih.gov/pubmed/8942879.

Pichi, F., M. Morara, C. Veronese, P. Nucci, and A. P. Ciardella. 2013. "Multimodal imaging in hereditary retinal diseases." *J Ophthalmol* 2013: 634351. https://doi.org/10.1155/2013/634351. https://www.ncbi.nlm.nih.gov/pubmed/23710333.

Poliakov, E., N. V. Strunnikova, J. K. Jiang, B. Martinez, T. Parikh, A. Lakkaraju, C. Thomas, B. P. Brooks, and T. M. Redmond. 2014. "Multiple A2E treatments lead to melanization of rod outer segment-challenged ARPE-19 cells." *Mol Vis* 20: 285–300. https://www.ncbi.nlm.nih.gov/pubmed/24644403.

Ponjavic, V., M. Abrahamson, S. Andréasson, H. Van Bokhoven, F. P. Cremers, B. Ehinger, and G. Fex. 1995. "Phenotype variations within a choroideremia family lacking the entire CHM gene." *Ophthalmic Genet* 16 (4): 143–50. https://doi.org/10.3109/13816819509057855. https://www.ncbi.nlm.nih.gov/pubmed/8749050.

Popović, P., M. Jarc-Vidmar, and M. Hawlina. 2005. "Abnormal fundus autofluorescence in relation to retinal function in patients with retinitis pigmentosa." *Graefes Arch Clin Exp Ophthalmol* 243 (10): 1018–27. https://doi.org/10.1007/s00417-005-1186-x. https://www.ncbi.nlm.nih.gov/pubmed/15906064.

Pras, E., A. Abu, Y. Rotenstreich, I. Avni, O. Reish, Y. Morad, and H. Reznik-Wolf. 2009. "Cone-rod dystrophy and a frameshift mutation in the PROM1 gene." *Mol Vis* 15: 1709–16. https://www.ncbi.nlm.nih.gov/pubmed/19718270.

Preti, R. C., A. Govetto, R. G. A. Filho, L. Cabral Zacharias, S. Gianotti Pimentel, W. Y. Takahashi, M. L. R. Monteiro, J. P. Hubschman, and D. Sarraf. 2018. "OPTICAL COHERENCE TOMOGRAPHY ANALYSIS OF OUTER RETINAL TUBULATIONS: Sequential Evolution and Pathophysiological Insights." *Retina* 38 (8): 1518–1525. https://doi.org/10.1097/IAE.0000000000001810. https://www.ncbi.nlm.nih.gov/pubmed/28837535.

Quazi, F., S. Lenevich, and R. S. Molday. 2012. "ABCA4 is an N-retinylidene-phosphatidylethanolamine and phosphatidylethanolamine importer." *Nat Commun* 3: 925. https://doi.org/10.1038/ncomms1927. https://www.ncbi.nlm.nih.gov/pubmed/22735453.

Quazi, F., and R. S. Molday. 2014. "ATP-binding cassette transporter ABCA4 and chemical isomerization protect photoreceptor cells from the toxic accumulation of excess 11-cis-retinal." *Proc Natl Acad Sci U S A* 111 (13): 5024–9. https://doi.org/10.1073/pnas.1400780111. https://www.ncbi.nlm.nih.gov/pubmed/24707049.

Rabb, M. F., T. C. Burton, H. Schatz, and L. A. Yannuzzi. 1978. "Fluorescein angiography of the fundus: a schematic approach to interpretation." *Surv Ophthalmol* 22

(6): 387–403. https://doi.org/10.1016/0039-6257(78)90134-0. https://www.ncbi.nlm.nih.gov/pubmed/675501.

Radu, R. A., Y. Han, T. V. Bui, S. Nusinowitz, D. Bok, J. Lichter, K. Widder, G. H. Travis, and N. L. Mata. 2005. "Reductions in serum vitamin A arrest accumulation of toxic retinal fluorophores: a potential therapy for treatment of lipofuscin-based retinal diseases." *Invest Ophthalmol Vis Sci* 46 (12): 4393–401. https://doi.org/10.1167/iovs.05-0820. https://www.ncbi.nlm.nih.gov/pubmed/16303925.

Radu, R. A., J. Hu, Q. Yuan, D. L. Welch, J. Makshanoff, M. Lloyd, S. McMullen, G. H. Travis, and D. Bok. 2011. "Complement system dysregulation and inflammation in the retinal pigment epithelium of a mouse model for Stargardt macular degeneration." *J Biol Chem* 286 (21): 18593–601. https://doi.org/10.1074/jbc.M110.191866. https://www.ncbi.nlm.nih.gov/pubmed/21464132.

Radu, R. A., Q. Yuan, J. Hu, J. H. Peng, M. Lloyd, S. Nusinowitz, D. Bok, and G. H. Travis. 2008. "Accelerated accumulation of lipofuscin pigments in the RPE of a mouse model for ABCA4-mediated retinal dystrophies following Vitamin A supplementation." *Invest Ophthalmol Vis Sci* 49 (9): 3821–9. https://doi.org/10.1167/iovs.07-1470. https://www.ncbi.nlm.nih.gov/pubmed/18515570.

Radziwon, A., G. Arno, D. K Wheaton, E. M. McDonagh, E. L. Baple, K. Webb-Jones, D. G Birch, A. R. Webster, and I. M. MacDonald. 2017. "Single-base substitutions in the CHM promoter as a cause of choroideremia." *Hum Mutat* 38 (6): 704–715. https://doi.org/10.1002/humu.23212. https://www.ncbi.nlm.nih.gov/pubmed/28271586.

Ranjan, M., and S. R. Beedu. 2006. "Spectroscopic and biochemical correlations during the course of human lens aging." *BMC Ophthalmol* 6: 10. https://doi.org/10.1186/1471-2415-6-10. https://www.ncbi.nlm.nih.gov/pubmed/16519820.

Renner, A. B., B. S. Fiebig, E. Cropp, B. H. Weber, and U. Kellner. 2009. "Progression of retinal pigment epithelial alterations during long-term follow-up in female carriers of choroideremia and report of a novel CHM mutation." *Arch Ophthalmol* 127 (7): 907–12. https://doi.org/10.1001/archophthalmol.2009.123. https://www.ncbi.nlm.nih.gov/ pubmed/19597113.

Renner, A. B., U. Kellner, E. Cropp, M. N. Preising, I. M. MacDonald, J. A. van den Hurk, F. P. Cremers, and M. H. Foerster. 2006. "Choroideremia: variability of clinical and electrophysiological characteristics and first report of a negative electroretinogram." *Ophthalmology* 113 (11): 2066 e1–10. https://doi.org/10.1016/j.ophtha.2006.05.045. https://www.ncbi.nlm.nih.gov/pubmed/16935340.

Robson, A. G., A. El-Amir, C. Bailey, C. A. Egan, F. W. Fitzke, A. R. Webster, A. C. Bird, and G. E. Holder. 2003. "Pattern ERG correlates of abnormal fundus autofluorescence in patients with retinitis pigmentosa and normal visual acuity." *Invest Ophthalmol Vis Sci* 44 (8): 3544–50. https://doi.org/10.1167/iovs.02-1278. https://www.ncbi.nlm.nih.gov/pubmed/12882805.

Robson, A. G., J. D. Moreland, D. Pauleikhoff, T. Morrissey, G. E. Holder, F. W. Fitzke, A. C. Bird, and F. J. van Kuijk. 2003. "Macular pigment density and distribution: comparison of fundus autofluorescence with minimum motion photometry." *Vision Res* 43 (16): 1765–75. https://doi.org/10.1016/s0042-6989(03)00280-3. https://www.ncbi.nlm.nih.gov/pubmed/12818346.

Rodrigues, M. M., E. J. Ballintine, B. N. Wiggert, L. Lee, R. T. Fletcher, and G. J. Chader. 1984. "Choroideremia: a clinical, electron microscopic, and biochemical report." *Ophthalmology* 91 (7): 873–83. https://www.ncbi.nlm.nih.gov/pubmed/6089068.

Rosenberg, T., and M. Schwartz. 1998. “X-linked ocular albinism: prevalence and mutations – a national study.” *Eur J Hum Genet* 6 (6): 570–7. https://doi.org/10.1038/sj.ejhg.5200226. https://www.ncbi.nlm.nih.gov/pubmed/9887374.

Ross, Michael H., and Wojciech Pawlina. 2016. *Histology: a text and atlas: with correlated cell and molecular biology*. Seventh edition. ed. Philadelphia: Wolters Kluwer Health.

Rudolf, M., S. D. Vogt, C. A. Curcio, C. Huisingh, G. McGwin, A. Wagner, S. Grisanti, and R. W. Read. 2013. “Histologic basis of variations in retinal pigment epithelium autofluorescence in eyes with geographic atrophy.” *Ophthalmology* 120 (4): 821–8. https://doi.org/10.1016/j.ophtha.2012.10.007. https://www.ncbi.nlm.nih.gov/pubmed/23357621.

Saad, L., and I. Washington. 2016. “Can Vitamin A be Improved to Prevent Blindness due to Age-Related Macular Degeneration, Stargardt Disease and Other Retinal Dystrophies?” *Adv Exp Med Biol* 854: 355–61. https://doi.org/10.1007/978-3-319-17121-0_47. https://www.ncbi.nlm.nih.gov/pubmed/26427432.

Saari, J. C. 2000. “Biochemistry of visual pigment regeneration: the Friedenwald lecture.” *Invest Ophthalmol Vis Sci* 41 (2): 337–48. https://www.ncbi.nlm.nih.gov/pubmed/10670460.

---. 2012. “Vitamin A metabolism in rod and cone visual cycles.” *Annu Rev Nutr* 32: 125–45. https://doi.org/10.1146/annurev-nutr-071811-150748. https://www.ncbi.nlm.nih.gov/pubmed/22809103.

Sankila, E. M., R. Tolvanen, J. A. van den Hurk, F. P. Cremers, and A. de la Chapelle. 1992. “Aberrant splicing of the CHM gene is a significant cause of choroideremia.” *Nat Genet* 1 (2): 109–13. https://doi.org/10.1038/ng0592-109. https://www.ncbi.nlm.nih.gov/pubmed/1302003.

Schiaffino, M. V. 2010. “Signaling pathways in melanosome biogenesis and pathology.” *Int J Biochem Cell Biol* 42 (7): 1094–104. https://doi.org/10.1016/j.biocel.2010.03.023. https://www.ncbi.nlm.nih.gov/pubmed/20381640.

Schmidt, S. Y., and R. D. Peisch. 1986. “Melanin concentration in normal human retinal pigment epithelium. Regional variation and age-related reduction.” *Invest Ophthalmol Vis Sci* 27 (7): 1063–7. https://www.ncbi.nlm.nih.gov/pubmed/3721785.

Schmitz-Valckenberg, S., F. G. Holz, A. C. Bird, and R. F. Spaide. 2008. “Fundus autofluorescence imaging: review and perspectives.” *Retina* 28 (3): 385–409. https://doi.org/10.1097/IAE.0b013e318164a907. https://www.ncbi.nlm.nih.gov/pubmed/18327131.

Schmitz-Valckenberg, S., M. Pfau, M. Fleckenstein, G. Staurenghi, J. R. Sparrow, A. Bindewald-Wittich, R. F. Spaide, S. Wolf, S. R. Sadda, and F. G. Holz. 2021. “Fundus autofluorescence imaging.” *Prog Retin Eye Res* 81: 100893. https://doi.org/10.1016/j.preteyeres.2020.100893. https://www.ncbi.nlm.nih.gov/pubmed/32758681.

Schnur, R. E., M. Gao, P. A. Wick, M. Keller, P. J. Benke, M. J. Edwards, A. W. Grix, A. Hockey, J. H. Jung, K. K. Kidd, M. Kistenmacher, A. V. Levin, R. A. Lewis, M. A. Musarella, R. W. Nowakowski, S. J. Orlow, R. S. Pagon, D. A. Pillers, H. H. Punnett, G. E. Quinn, K. Tezcan, J. Wagstaff, and R. G. Weleber. 1998. “OA1 mutations and deletions in X-linked ocular albinism.” *Am J Hum Genet* 62 (4): 800–9. https://doi.org/10.1086/301776. https://www.ncbi.nlm.nih.gov/pubmed/9529334.

Schuerch, K., R. L. Woods, W. Lee, T. Duncker, F. C. Delori, R. Allikmets, S. H. Tsang, and J. R. Sparrow. 2017. “Quantifying Fundus Autofluorescence in Patients With Retinitis Pigmentosa.” *Invest Ophthalmol Vis Sci* 58 (3): 1843–1855. https://doi.org/10.1167/iovs.16-21302. https://www.ncbi.nlm.nih.gov/pubmed/28358950.

Seabra, M. C., M. S. Brown, and J. L. Goldstein. 1993. “Retinal degeneration in choroideremia: deficiency of rab geranylgeranyl transferase.” *Science* 259 (5093): 377–81. https://www.ncbi.nlm.nih.gov/pubmed/8380507.

Seabra, M. C., Y. K. Ho, and J. S. Anant. 1995. “Deficient geranylgeranylation of Ram/Rab27 in choroideremia.” *J Biol Chem* 270 (41): 24420–7. https://doi.org/10.1074/jbc.270.41.24420. https://www.ncbi.nlm.nih.gov/pubmed/7592656.

Sieving, P. A., J. H. Niffenegger, and E. L. Berson. 1986. “Electroretinographic findings in selected pedigrees with choroideremia.” *Am J Ophthalmol* 101 (3): 361–7. https://doi.org/10.1016/0002-9394(86)90832-9. https://www.ncbi.nlm.nih.gov/pubmed/ 3953730.

Simon, J. D., L. Hong, and D. N. Peles. 2008. “Insights into melanosomes and melanin from some interesting spatial and temporal properties.” *J Phys Chem B* 112 (42): 13201–17. https://doi.org/10.1021/jp804248h. https://www.ncbi.nlm.nih.gov/pubmed/18817437.

Simunovic, M. P., J. K. Jolly, K. Xue, T. L. Edwards, M. Groppe, S. M. Downes, and R. E. MacLaren. 2016. “The Spectrum of CHM Gene Mutations in Choroideremia and Their Relationship to Clinical Phenotype.” *Invest Ophthalmol Vis Sci* 57 (14): 6033–6039. https://doi.org/10.1167/iovs.16-20230. https://www.ncbi.nlm.nih.gov/pubmed/27820636.

Singer, D., K. Thamm, H. Zhuang, J. Karbanová, Y. Gao, J. V. Walker, H. Jin, X. Wu, C. R. Coveney, P. Marangoni, D. Lu, P. R. C. Grayson, T. Gulsen, K. J. Liu, S. Ardu, A. K. Wann, S. Luo, A. C. Zambon, A. M. Jetten, C. Tredwin, O. D. Klein, M. Attanasio, P. Carmeliet, W. B. Huttner, D. Corbeil, and B. Hu. 2019. “Prominin-1 controls stem cell activation by orchestrating ciliary dynamics.” *EMBO J* 38 (2). https://doi.org/10.15252/embj.201899845. https://www.ncbi.nlm.nih.gov/pubmed/30523147.

Sliney, D., D. Aron-Rosa, F. DeLori, F. Fankhauser, R. Landry, M. Mainster, J. Marshall, B. Rassow, B. Stuck, S. Trokel, T. M. West, M. Wolffe, and International Commission on Non-Ionizing Radiation Protection. 2005. “Adjustment of guidelines for exposure of the eye to optical radiation from ocular instruments: statement from a task group of the International Commission on Non-Ionizing Radiation Protection (ICNIRP).” *Appl Opt* 44 (11): 2162–76. https://doi.org/10.1364/ao.44.002162. https://www.ncbi.nlm.nih.gov/pubmed/15835362.

Sohocki, M. M., S. P. Daiger, S. J. Bowne, J. A. Rodriquez, H. Northrup, J. R. Heckenlively, D. G. Birch, H. Mintz-Hittner, R. S. Ruiz, R. A. Lewis, D. A. Saperstein, and L. S. Sullivan. 2001. “Prevalence of mutations causing retinitis pigmentosa and other inherited retinopathies.” *Hum Mutat* 17 (1): 42–51. https://doi.org/10.1002/1098-1004(2001)17:1<42::AID-HUMU5>3.0.CO;2-K. https://www.ncbi.nlm.nih.gov/pubmed/11139241.

Solebo, A. L., L. Teoh, and J. Rahi. 2017. “Epidemiology of blindness in children.” *Arch Dis Child* 102 (9): 853–857. https://doi.org/10.1136/archdischild-2016-310532. https://www.ncbi.nlm.nih.gov/pubmed/28465303.

Song, H., E. A. Rossi, L. Latchney, A. Bessette, E. Stone, J. J. Hunter, D. R. Williams, and M. Chung. 2015. “Cone and rod loss in Stargardt disease revealed by adaptive optics scanning light ophthalmoscopy.” *JAMA Ophthalmol* 133 (10): 1198–203. https://doi.org/10.1001/jamaophthalmol.2015.2443. https://www.ncbi.nlm.nih.gov/pubmed/26247787.

Sorsby, A., A. Franceschetti, R. Joseph, and J. B. Davey. 1952. “Choroideremia; clinical and genetic aspects.” *Br J Ophthalmol* 36 (10): 547–81. https://www.ncbi.nlm.nih.gov/pubmed/12978235.

Spaide, R. F., and C. A. Curcio. 2011. “Anatomical correlates to the bands seen in the outer retina by optical coherence tomography: literature review and model.” *Retina* 31 (8): 1609–19. https://doi.org/10.1097/IAE.0b013e3182247535. https://www.ncbi.nlm.nih.gov/pubmed/21844839.

Sparrow, J. R., A. Blonska, E. Flynn, T. Duncker, J. P. Greenberg, R. Secondi, K. Ueda, and F. C. Delori. 2013. “Quantitative fundus autofluorescence in mice: correlation with HPLC quantitation of RPE lipofuscin and measurement of retina outer nuclear layer thickness.” *Invest Ophthalmol Vis Sci* 54 (4): 2812–20. https://doi.org/10.1167/iovs.12-11490. https://www.ncbi.nlm.nih.gov/pubmed/23548623.

Sparrow, J. R., and M. Boulton. 2005. “RPE lipofuscin and its role in retinal patho biology.” *Exp Eye Res* 80 (5): 595–606. https://doi.org/10.1016/j.exer.2005.01.007. https://www.ncbi.nlm.nih.gov/pubmed/15862166.

Sparrow, J. R., T. Duncker, R. Woods, and F. C. Delori. 2016. “Quantitative Fundus Autofluorescence in Best Vitelliform Macular Dystrophy: RPE Lipofuscin is not Increased in Non-Lesion Areas of Retina.” *Adv Exp Med Biol* 854: 285–90. https://doi.org/10.1007/978-3-319-17121-0_38. https://www.ncbi.nlm.nih.gov/pubmed/26427423.

Sparrow, J. R., N. Fishkin, J. Zhou, B. Cai, Y. P. Jang, S. Krane, Y. Itagaki, and K. Nakanishi. 2003. “A2E, a byproduct of the visual cycle.” *Vision Res* 43 (28): 2983–90. https://www.ncbi.nlm.nih.gov/pubmed/14611934.

Sparrow, J. R., E. Gregory-Roberts, K. Yamamoto, A. Blonska, S. K. Ghosh, K. Ueda, and J. Zhou. 2012. “The bisretinoids of retinal pigment epithelium.” *Prog Retin Eye Res* 31 (2): 121–35. https://doi.org/10.1016/j.preteyeres.2011.12.001. https://www.ncbi.nlm.nih.gov/pubmed/22209824.

Sparrow, J. R., D. Hicks, and C. P. Hamel. 2010. “The retinal pigment epithelium in health and disease.” *Curr Mol Med* 10 (9): 802–23. https://www.ncbi.nlm.nih.gov/pubmed/21091424.

Sparrow, J. R., S. R. Kim, A. M. Cuervo, and U. Bandhyopadhyayand. 2008. “A2E, a pigment of RPE lipofuscin, is generated from the precursor, A2PE by a lysosomal enzyme activity.” *Adv Exp Med Biol* 613: 393–8. https://doi.org/10.1007/978-0-387-74904-4_46. https://www.ncbi.nlm.nih.gov/pubmed/18188969.

Sparrow, J. R., M. Marsiglia, R. Allikmets, S. Tsang, W. Lee, T. Duncker, and J. Zernant. 2015. “Flecks in Recessive Stargardt Disease: Short-Wavelength Autofluorescence, Near-Infrared Autofluorescence, and Optical Coherence Tomography.” *Invest Ophthalmol Vis Sci* 56 (8): 5029-39. https://doi.org/10.1167/iovs.15-16763. https://www.ncbi.nlm.nih.gov/pubmed/26230768.

Sparrow, J. R., K. Nakanishi, and C. A. Parish. 2000. “The lipofuscin fluorophore A2E mediates blue light-induced damage to retinal pigmented epithelial cells.” *Invest Ophthalmol Vis Sci* 41 (7): 1981–9. https://www.ncbi.nlm.nih.gov/pubmed/10845625.

Sparrow, J. R., C. A. Parish, M. Hashimoto, and K. Nakanishi. 1999. “A2E, a lipofuscin fluorophore, in human retinal pigmented epithelial cells in culture.” *Invest Ophthalmol Vis Sci* 40 (12): 2988–95. https://www.ncbi.nlm.nih.gov/pubmed/10549662.

Sparrow, J. R., H. R. Vollmer-Snarr, J. Zhou, Y. P. Jang, S. Jockusch, Y. Itagaki, and K. Nakanishi. 2003. “A2E-epoxides damage DNA in retinal pigment epithelial cells. Vitamin E and other antioxidants inhibit A2E-epoxide formation.” *J Biol Chem* 278

(20): 18207–13. https://doi.org/10.1074/jbc.M300457200. https://www.ncbi.nlm.nih.gov/pubmed/12646558.

Sparrow, J. R., Y. Wu, T. Nagasaki, K. D. Yoon, K. Yamamoto, and J. Zhou. 2010. "Fundus autofluorescence and the bisretinoids of retina." *Photochem Photobiol Sci* 9 (11): 1480–9. https://doi.org/10.1039/c0pp00207k. https://www.ncbi.nlm.nih.gov/pubmed/20862444.

Sparrow, J. R., and K. Yamamoto. 2012. "The bisretinoids of RPE lipofuscin: a complex mixture." *Adv Exp Med Biol* 723: 761–7. https://doi.org/10.1007/978-1-4614-0631-0_97. https://www.ncbi.nlm.nih.gov/pubmed/22183404.

Sparrow, J. R., J. Zhou, and B. Cai. 2003. "DNA is a target of the photodynamic effects elicited in A2E-laden RPE by blue-light illumination." *Invest Ophthalmol Vis Sci* 44 (5): 2245-51. https://www.ncbi.nlm.nih.gov/pubmed/12714667.

Staurenghi, G., S. Sadda, U. Chakravarthy, R. F. Spaide, and International Nomenclature for Optical Coherence Tomography (IN•OCT) Panel. 2014. "Proposed lexicon for anatomic landmarks in normal posterior segment spectral-domain optical coherence tomography: the IN•OCT consensus." *Ophthalmology* 121 (8): 1572-8. https://doi.org/10.1016/j.ophtha.2014.02.023. https://www.ncbi.nlm.nih.gov/pubmed/24755005.

Steinmetz, R. L., A. Garner, J. I. Maguire, and A. C. Bird. 1991. "Histopathology of incipient fundus flavimaculatus." *Ophthalmology* 98 (6): 953-6. https://doi. org/10.1016/s0161-6420(91)32197-3. https://www.ncbi.nlm.nih.gov/pubmed/1866150.

Strauss, R. W., X. Kong, A. Ho, A. Jha, S. West, M. Ip, P. S. Bernstein, D. G. Birch, A. V. Cideciyan, M. Michaelides, J. A. Sahel, J. S. Sunness, E. I. Traboulsi, E. Zrenner, S. Pitetta, D. Jenkins, A. H. Hariri, S. Sadda, H. P. N. Scholl, and ProgStar Study Group. 2019. "Progression of Stargardt Disease as Determined by Fundus Autofluorescence Over a 12-Month Period: ProgStar Report No. 11." *JAMA Ophthalmol* 137 (10): 1134–1145. https://doi.org/10.1001/jamaophthalmol.2019.2885. https://www.ncbi.nlm.nih.gov/pubmed/31369039.

Strauss, R. W., B. Muñoz, M. I. Ahmed, M. Bittencourt, E. M. Schönbach, M. Michaelides, D. Birch, E. Zrenner, A. M. Ervin, P. Charbel Issa, J. Kong, Y. Wolfson, M. Shah, S. Bagheri, S. West, H. P. N. Scholl, and for the ProgStar-4 Study Group. 2018. "The Progression of the Stargardt Disease Type 4 (ProgStar-4) Study: Design and Baseline Characteristics (ProgStar-4 Report No. 1)." *Ophthalmic Res* 60 (3): 185–194. https://doi.org/10.1159/000491791. https://www.ncbi.nlm.nih.gov/pubmed/30110705.

Strauss, R. W., B. Muñoz, Y. Wolfson, R. Sophie, E. Fletcher, M. G. Bittencourt, and H. P. Scholl. 2016. "Assessment of estimated retinal atrophy progression in Stargardt macular dystrophy using spectral-domain optical coherence tomography." *Br J Ophthalmol* 100 (7): 956-962. https://doi.org/10.1136/bjophthalmol-2015-307035. https://www.ncbi.nlm.nih.gov/pubmed/26568636.

Summers, C. G. 1996. "Vision in albinism." *Trans Am Ophthalmol Soc* 94: 1095-155. https://www.ncbi.nlm.nih.gov/pubmed/8981720.

Summers, C. G., J. E. Connett, A. M. Holleschau, J. L. Anderson, I. De Becker, B. S. McKay, and M. H. Brilliant. 2014. "Does levodopa improve vision in albinism? Results of a randomized, controlled clinical trial." *Clin Exp Ophthalmol* 42 (8): 713-21. https://doi.org/10.1111/ceo.12325. https://www.ncbi.nlm.nih.gov/pubmed/24641678.

Sun, H., R. S. Molday, and J. Nathans. 1999. "Retinal stimulates ATP hydrolysis by purified and reconstituted ABCR, the photoreceptor-specific ATP-binding cassette transporter responsible for Stargardt disease." *J Biol Chem* 274 (12): 8269-81.

https://doi.org/10.1074/jbc.274.12.8269. https://www.ncbi.nlm.nih.gov/pubmed/10075733.

Sun, H., and J. Nathans. 1997. "Stargardt's ABCR is localized to the disc membrane of retinal rod outer segments." *Nat Genet* 17 (1): 15–6. https://doi.org/10.1038/ng0997-15. https://www.ncbi.nlm.nih.gov/pubmed/9288089.

---. 2001. "Mechanistic studies of ABCR, the ABC transporter in photoreceptor outer segments responsible for autosomal recessive Stargardt disease." *J Bioenerg Biomembr* 33 (6): 523–30. https://doi.org/10.1023/a:1012883306823. https://www.ncbi.nlm.nih.gov/pubmed/11804194.

Sun, L. W., R. D. Johnson, V. Williams, P. Summerfelt, A. Dubra, D. V. Weinberg, K. E. Stepien, G. A. Fishman, and J. Carroll. 2016. "Multimodal Imaging of Photoreceptor Structure in Choroideremia." *PLoS One* 11 (12): e0167526. https://doi.org/10.1371/journal.pone.0167526. https://www.ncbi.nlm.nih.gov/pubmed/27936069.

Sundaramurthi, H., A. Moran, A. C. Perpetuini, A. Reynolds, and B. Kennedy. 2019. "Emerging Drug Therapies for Inherited Retinal Dystrophies." *Adv Exp Med Biol* 1185: 263–267. https://doi.org/10.1007/978-3-030-27378-1_43. https://www.ncbi.nlm.nih.gov/pubmed/31884622.

Sung, C. H., and J. Z. Chuang. 2010. "The cell biology of vision." *J Cell Biol* 190 (6): 953–63. https://doi.org/10.1083/jcb.201006020. https://www.ncbi.nlm.nih.gov/pubmed/20855501.

Syed, N., J. E. Smith, S. K. John, M. C. Seabra, G. D. Aguirre, and A. H. Milam. 2001. "Evaluation of retinal photoreceptors and pigment epithelium in a female carrier of choroideremia." *Ophthalmology* 108 (4): 711–20. https://www.ncbi.nlm.nih.gov/pubmed/11297488.

Syed, R., S. M. Sundquist, K. Ratnam, S. Zayit-Soudry, Y. Zhang, J. B. Crawford, I. M. MacDonald, P. Godara, J. Rha, J. Carroll, A. Roorda, K. E. Stepien, and J. L. Duncan. 2013. "High-resolution images of retinal structure in patients with choroideremia." *Invest Ophthalmol Vis Sci* 54 (2): 950–61. https://doi.org/10.1167/iovs.12-10707. https://www.ncbi.nlm.nih.gov/pubmed/23299470.

Tanna, P., R. W. Strauss, K. Fujinami, and M. Michaelides. 2017. "Stargardt disease: clinical features, molecular genetics, animal models and therapeutic options." *Br J Ophthalmol* 101 (1): 25–30. https://doi.org/10.1136/bjophthalmol-2016-308823. https://www.ncbi.nlm.nih.gov/pubmed/27491360.

Taubitz, T., Y. Fang, A. Biesemeier, S. Julien-Schraermeyer, and U. Schraermeyer. 2019. "Age, lipofuscin and melanin oxidation affect fundus near-infrared autofluorescence." *EBioMedicine* 48: 592–604. https://doi.org/10.1016/j.ebiom.2019.09.048. https://www.ncbi.nlm.nih.gov/pubmed/31648994.

Teussink, M. M., S. Lambertus, F. F. de Mul, M. B. Rozanowska, C. B. Hoyng, B. J. Klevering, and T. Theelen. 2017. "Lipofuscin-associated photo-oxidative stress during fundus autofluorescence imaging." *PLoS One* 12 (2): e0172635. https://doi.org/10.1371/journal.pone.0172635. https://www.ncbi.nlm.nih.gov/pubmed/28235055.

Theelen, T., T. T. Berendschot, C. J. Boon, C. B. Hoyng, and B. J. Klevering. 2008. "Analysis of visual pigment by fundus autofluorescence." *Exp Eye Res* 86 (2): 296–304. https://doi.org/10.1016/j.exer.2007.10.022. https://www.ncbi.nlm.nih.gov/pubmed/18096158.

Tolmachova, T., R. Anders, M. Abrink, L. Bugeon, M. J. Dallman, C. E. Futter, J. S. Ramalho, F. Tonagel, N. Tanimoto, M. W. Seeliger, C. Huxley, and M. C. Seabra. 2006. "Independent degeneration of photoreceptors and retinal pigment epithelium in conditional knockout mouse models of choroideremia." *J Clin Invest* 116 (2):

386–94. https://doi.org/10.1172/JCI26617. https://www.ncbi.nlm.nih.gov/pubmed/16410831.

Tolmachova, T., J. S. Ramalho, J. S. Anant, R. A. Schultz, C. M. Huxley, and M. C. Seabra. 1999. "Cloning, mapping and characterization of the human RAB27A gene." *Gene* 239 (1): 109-16. https://www.ncbi.nlm.nih.gov/pubmed/10571040.

Tolmachova, T., S. T. Wavre-Shapton, A. R. Barnard, R. E. MacLaren, C. E. Futter, and M. C. Seabra. 2010. "Retinal pigment epithelium defects accelerate photoreceptor degeneration in cell type-specific knockout mouse models of choroideremia." *Invest Ophthalmol Vis Sci* 51 (10): 4913–20. https://doi.org/10.1167/iovs.09-4892. https://www.ncbi.nlm.nih.gov/pubmed/20445111.

Travis, G. H., M. Golczak, A. R. Moise, and K. Palczewski. 2007. "Diseases caused by defects in the visual cycle: retinoids as potential therapeutic agents." *Annu Rev Pharmacol Toxicol* 47: 469–512. https://doi.org/10.1146/annurev.pharmtox.47.120505.105225. https://www.ncbi.nlm.nih.gov/pubmed/16968212.

Tsai, Cheng-Lun, Ji-Chung Chen, and Wen-Jwu Wang. 2001. "Near-infrared Absorption Property of Biological Soft Tissue Constituents." *Journal of Medical and Biological Engineering* 21: 7–14.

Tsang, S. H., and T. Sharma. 2018. "X-linked Ocular Albinism." *Adv Exp Med Biol* 1085: 49–52. https://doi.org/10.1007/978-3-319-95046-4_11. https://www.ncbi.nlm.nih.gov/pubmed/30578484.

Tsybovsky, Y., R. S. Molday, and K. Palczewski. 2010. "The ATP-binding cassette transporter ABCA4: structural and functional properties and role in retinal disease." *Adv Exp Med Biol* 703: 105–25. https://doi.org/10.1007/978-1-4419-5635-4_8. https://www.ncbi.nlm.nih.gov/pubmed/20711710.

Ueda, K., J. Zhao, H. J. Kim, and J. R. Sparrow. 2016. "Photodegradation of retinal bisretinoids in mouse models and implications for macular degeneration." *Proc Natl Acad Sci U S A* 113 (25): 6904–9. https://doi.org/10.1073/pnas.1524774113. https://www.ncbi.nlm.nih.gov/pubmed/27274068.

Vajaranant, T. S., G. A. Fishman, J. P. Szlyk, P. Grant-Jordan, M. Lindeman, and W. Seiple. 2008. "Detection of mosaic retinal dysfunction in choroideremia carriers electroretinographic and psychophysical testing." *Ophthalmology* 115 (4): 723–9. https://doi.org/10.1016/j.ophtha.2007.07.032. https://www.ncbi.nlm.nih.gov/pubmed/18201765.

van den Berg, T. J., J. K. IJspeert, and P. W. de Waard. 1991. "Dependence of intraocular straylight on pigmentation and light transmission through the ocular wall." *Vision Res* 31 (7–8): 1361–7. https://doi.org/10.1016/0042-6989(91)90057-c. https://www.ncbi.nlm.nih.gov/pubmed/1891824.

van den Hurk, J. A., W. Hendriks, D. J. van de Pol, F. Oerlemans, G. Jaissle, K. Rüther, K. Kohler, J. Hartmann, E. Zrenner, H. van Bokhoven, B. Wieringa, H. H. Ropers, and F. P. Cremers. 1997. "Mouse choroideremia gene mutation causes photoreceptor cell degeneration and is not transmitted through the female germline." *Hum Mol Genet* 6 (6): 851–8. https://doi.org/10.1093/hmg/6.6.851. https://www.ncbi.nlm.nih.gov/pubmed/9175730.

Verdina, T., S. H. Tsang, V. C. Greenstein, J. Zernant, A. Sodi, L. H. Lima, S. Chang, R. Allikmets, and U. Menchini. 2012. "Functional Analysis of Retinal Flecks in Stargardt Disease." *J Clin Exp Ophthalmol* 3. https://doi.org/10.4172/2155-9570.1000233. https://www.ncbi.nlm.nih.gov/pubmed/24409374.

von Rückmann, A., F. W. Fitzke, and A. C. Bird. 1995. "Distribution of fundus autofluorescence with a scanning laser ophthalmoscope." *Br J Ophthalmol* 79 (5): 407-

12. https://doi.org/10.1136/bjo.79.5.407. https://www.ncbi.nlm.nih.gov/pubmed/7612549.
---. 1997. “Fundus autofluorescence in age-related macular disease imaged with a laser scanning ophthalmoscope.” *Invest Ophthalmol Vis Sci* 38 (2): 478–86. https://www.ncbi.nlm.nih.gov/pubmed/9040481.
Wakamatsu, K., D. N. Hu, S. A. McCormick, and S. Ito. 2008. “Characterization of melanin in human iridal and choroidal melanocytes from eyes with various colored irides.” *Pigment Cell Melanoma Res* 21 (1): 97–105. https://doi.org/10.1111/j.1755-148X.2007.00415.x. https://www.ncbi.nlm.nih.gov/pubmed/18353148.
Wald, G. 1968. “The molecular basis of visual excitation.” *Nature* 219 (5156): 800–7. https://doi.org/10.1038/219800a0. https://www.ncbi.nlm.nih.gov/pubmed/4876934.
Wang, J., and D. Deretic. 2014. “Molecular complexes that direct rhodopsin transport to primary cilia.” *Prog Retin Eye Res* 38: 1–19. https://doi.org/10.1016/j.preteyeres.2013.08.004. https://www.ncbi.nlm.nih.gov/pubmed/24135424.
Wang, X., C. Yu, R. T. Tzekov, Y. Zhu, and W. Li. 2020. “The effect of human gene therapy for RPE65-associated Leber’s congenital amaurosis on visual function: a systematic review and meta-analysis.” *Orphanet J Rare Dis* 15 (1): 49. https://doi.org/10.1186/s13023-020-1304-1. https://www.ncbi.nlm.nih.gov/pubmed/32059734.
Wassell, J., S. Davies, W. Bardsley, and M. Boulton. 1999. “The photoreactivity of the retinal age pigment lipofuscin.” *J Biol Chem* 274 (34): 23828–32. https://doi.org/10.1074/jbc.274.34.23828. https://www.ncbi.nlm.nih.gov/pubmed/10446145.
Watt, B., G. van Niel, D. M. Fowler, I. Hurbain, K. C. Luk, S. E. Stayrook, M. A. Lemmon, G. Raposo, J. Shorter, J. W. Kelly, and M. S. Marks. 2009. “N-terminal domains elicit formation of functional Pmel17 amyloid fibrils.” *J Biol Chem* 284 (51): 35543–55. https://doi.org/10.1074/jbc.M109.047449. https://www.ncbi.nlm.nih.gov/pubmed/19840945.
Wavre-Shapton, S. T., T. Tolmachova, M. Lopes da Silva, C. E. Futter, and M. C. Seabra. 2013. “Conditional ablation of the choroideremia gene causes age-related changes in mouse retinal pigment epithelium.” *PLoS One* 8 (2): e57769. https://doi.org/10.1371/journal.pone.0057769. https://www.ncbi.nlm.nih.gov/pubmed/23460904.
Wawrocka, A., A. Skorczyk-Werner, K. Wicher, Z. Niedziela, R. Ploski, M. Rydzanicz, M. Sykulski, J. Kociecki, N. Weisschuh, S. Kohl, S. Biskup, B. Wissinger, and M. R. Krawczynski. 2018. “Novel variants identified with next-generation sequencing in Polish patients with cone-rod dystrophy.” *Mol Vis* 24: 326–339. https://www.ncbi.nlm.nih.gov/pubmed/29769798.
Webb, R. H., G. W. Hughes, and O. Pomerantzeff. 1980. “Flying spot TV ophthalmoscope.” *Appl Opt* 19 (17): 2991–7. https://doi.org/10.1364/AO.19.002991. https://www.ncbi.nlm.nih.gov/pubmed/20234539.
Weiland, J. D., and M. S. Humayun. 2014. “Retinal prosthesis.” *IEEE Trans Biomed Eng* 61 (5): 1412–24. https://doi.org/10.1109/TBME.2014.2314733. https://www.ncbi.nlm.nih.gov/pubmed/24710817.
Weiter, J. J., F. C. Delori, G. L. Wing, and K. A. Fitch. 1986. “Retinal pigment epithelial lipofuscin and melanin and choroidal melanin in human eyes.” *Invest Ophthalmol Vis Sci* 27 (2): 145–52. https://www.ncbi.nlm.nih.gov/pubmed/3943941.
Welch, R. J., X. Li, and C. L. Shields. 2018. “Mud-splattered fundus.” *Indian J Ophthalmol* 66 (4): 573. https://doi.org/10.4103/ijo.IJO_1003_17. https://www.ncbi.nlm. nih.gov/pubmed/29582825.

Weng, J., N. L. Mata, S. M. Azarian, R. T. Tzekov, D. G. Birch, and G. H. Travis. 1999. "Insights into the function of Rim protein in photoreceptors and etiology of Stargardt's disease from the phenotype in abcr knockout mice." *Cell* 98 (1): 13–23. https://doi.org/10.1016/S0092-8674(00)80602-9. https://www.ncbi.nlm.nih.gov/pubmed/10412977.

Westeneng-van Haaften, S. C., C. J. Boon, F. P. Cremers, L. H. Hoefsloot, A. I. den Hollander, and C. B. Hoyng. 2012. "Clinical and genetic characteristics of late-onset Stargardt's disease." *Ophthalmology* 119 (6): 1199–210. https://doi.org/10.1016/j.ophtha. 2012.01.005. https://www.ncbi.nlm.nih.gov/pubmed/22449572.

Wielgus, A. R., and T. Sarna. 2005. "Melanin in human irides of different color and age of donors." *Pigment Cell Res* 18 (6): 454-64. https://doi.org/10.1111/j.1600-0749.2005.00268.x. https://www.ncbi.nlm.nih.gov/pubmed/16280011.

Wing, G. L., G. C. Blanchard, and J. J. Weiter. 1978. "The topography and age relationship of lipofuscin concentration in the retinal pigment epithelium." *Invest Ophthalmol Vis Sci* 17 (7): 601-7. https://www.ncbi.nlm.nih.gov/pubmed/669891.

Wolfson, Y., E. Fletcher, R. W. Strauss, and H. P. N. Scholl. 2016. "Evidence of macular pigment in the central macula in albinism." *Exp Eye Res* 145: 468-471. https://doi.org/10.1016/j.exer.2015.10.006. https://www.ncbi.nlm.nih.gov/pubmed/26474496.

Wu, A. L., J. P. Wang, Y. J. Tseng, L. Liu, Y. C. Kang, K. J. Chen, A. N. Chao, L. K. Yeh, T. L. Chen, Y. S. Hwang, W. C. Wu, C. C. Lai, and N. K. Wang. 2018. "Multimodal Imaging of Mosaic Retinopathy in Carriers of Hereditary X-Linked Recessive Diseases." *Retina* 38 (5): 1047-1057. https://doi.org/10.1097/IAE.0000000000001629. https://www.ncbi.nlm.nih.gov/pubmed/28376043.

Wuthisiri, W., M. D. Lingao, J. E. Capasso, and A. V. Levin. 2013. "Lyonization in ophthalmology." *Curr Opin Ophthalmol* 24 (5): 389–97. https://doi.org/10.1097/ICU.0b013e3283641f91. https://www.ncbi.nlm.nih.gov/pubmed/23892913.

Yamamoto, K., K. D. Yoon, K. Ueda, M. Hashimoto, and J. R. Sparrow. 2011. "A novel bisretinoid of retina is an adduct on glycerophosphoethanolamine." *Invest Ophthalmol Vis Sci* 52 (12): 9084–90. https://doi.org/10.1167/iovs.11-8632. https://www.ncbi.nlm.nih.gov/pubmed/22039245.

Yang, Z., Y. Chen, C. Lillo, J. Chien, Z. Yu, M. Michaelides, M. Klein, K. A. Howes, Y. Li, Y. Kaminoh, H. Chen, C. Zhao, Y. T. Al-Sheikh, G. Karan, D. Corbeil, P. Escher, S. Kamaya, C. Li, S. Johnson, J. M. Frederick, Y. Zhao, C. Wang, D. J. Cameron, W. B. Huttner, D. F. Schorderet, F. L. Munier, A. T. Moore, D. G. Birch, W. Baehr, D. M. Hunt, D. S. Williams, and K. Zhang. 2008. "Mutant prominin 1 found in patients with macular degeneration disrupts photoreceptor disk morphogenesis in mice." *J Clin Invest* 118 (8): 2908–16. https://doi.org/10.1172/JCI35891. https://www.ncbi.nlm.nih.gov/pubmed/18654668.

Yang, Z., Y. Chen, C. Lillo, J. Chien, Z. Yu, M. Michaelides, M. Klein, K. A. Howes, Y. Li, Y. Kaminoh, H. Chen, C. Zhao, Y. Chen, Y. T. Al-Sheikh, G. Karan, D. Corbeil, P. Escher, S. Kamaya, C. Li, S. Johnson, J. M. Frederick, Y. Zhao, C. Wang, D. J. Cameron, W. B. Huttner, D. F. Schorderet, F. L. Munier, A. T. Moore, D. G. Birch, W. Baehr, D. M. Hunt, D. S. Williams, and K. Zhang. 2008. "Mutant prominin 1 found in patients with macular degeneration disrupts photoreceptor disk morphogenesis in mice." *J Clin Invest* 118 (8): 2908–16. https://doi.org/10.1172/JCI35891. https://www.ncbi.nlm.nih.gov/pubmed/18654668.

Young, R. W. 1971. “The renewal of rod and cone outer segments in the rhesus monkey.” *J Cell Biol* 49 (2): 303–18. https://doi.org/10.1083/jcb.49.2.303. https://www.ncbi.nlm.nih.gov/pubmed/19866760.

Young, R. W., and B. Droz. 1968. “The renewal of protein in retinal rods and cones.” *J Cell Biol* 39 (1): 169–84. https://doi.org/10.1083/jcb.39.1.169. https://www.ncbi.nlm.nih.gov/pubmed/5692679.

Yung, M., M. A. Klufas, and D. Sarraf. 2016. “Clinical applications of fundus autofluorescence in retinal disease.” *Int J Retina Vitreous* 2: 12. https://doi.org/10.1186/s40942-016-0035-x. https://www.ncbi.nlm.nih.gov/pubmed/27847630.

Zacchigna, S., H. Oh, M. Wilsch-Brauninger, E. Missol-Kolka, J. Jaszai, S. Jansen, N. Tanimoto, F. Tonagel, M. Seeliger, W. B. Huttner, D. Corbeil, M. Dewerchin, S. Vinckier, L. Moons, and P. Carmeliet. 2009. “Loss of the cholesterol-binding protein prominin-1/CD133 causes disk dysmorphogenesis and photoreceptor degeneration.” *J Neurosci* 29 (7): 2297-308. https://doi.org/10.1523/JNEUROSCI.2034-08.2009. https://www.ncbi.nlm.nih.gov/pubmed/19228982.

Zeitz, C., M. Nassisi, C. Laurent-Coriat, C. Andrieu, F. Boyard, C. Condroyer, V. Démontant, A. Antonio, M. E. Lancelot, H. Frederiksen, B. Kloeckener-Gruissem, S. El-Shamieh, X. Zanlonghi, I. Meunier, A. F. Roux, S. Mohand-Saïd, J. A. Sahel, and I. Audo. 2021. “CHM mutation spectrum and disease: An update at the time of human therapeutic trials.” *Hum Mutat* 42 (4): 323–341. https://doi.org/10.1002/humu.24174. https://www.ncbi.nlm.nih.gov/pubmed/33538369.

Zernant, J., C. Schubert, K. M. Im, T. Burke, C. M. Brown, G. A. Fishman, S. H. Tsang, P. Gouras, M. Dean, and R. Allikmets. 2011. “Analysis of the ABCA4 gene by next-generation sequencing.” *Invest Ophthalmol Vis Sci* 52 (11): 8479–87. https://doi.org/10.1167/iovs.11-8182. https://www.ncbi.nlm.nih.gov/pubmed/21911583.

Zhang, J., P. D. Kiser, M. Badiee, G. Palczewska, Z. Dong, M. Golczak, G. P. Tochtrop, and K. Palczewski. 2015. “Molecular pharmacodynamics of emixustat in protection against retinal degeneration.” *J Clin Invest* 125 (7): 2781–94. https://doi.org/10.1172/JCI80950. https://www.ncbi.nlm.nih.gov/pubmed/26075817.

Zhang, K., M. Kniazeva, M. Han, W. Li, Z. Yu, Z. Yang, Y. Li, M. L. Metzker, R. Allikmets, D. J. Zack, L. E. Kakuk, P. S. Lagali, P. W. Wong, I. M. MacDonald, P. A. Sieving, D. J. Figueroa, C. P. Austin, R. J. Gould, R. Ayyagari, and K. Petrukhin. 2001. “A 5-bp deletion in ELOVL4 is associated with two related forms of autosomal dominant macular dystrophy.” *Nat Genet* 27 (1): 89–93. https://doi.org/10.1038/83817. https://www.ncbi.nlm.nih.gov/pubmed/11138005.

Zhang, Q., F. Zulfiqar, X. Xiao, S. A. Riazuddin, Z. Ahmad, R. Caruso, I. MacDonald, P. Sieving, S. Riazuddin, and J. F. Hejtmancik. 2007. “Severe retinitis pigmentosa mapped to 4p15 and associated with a novel mutation in the PROM1 gene.” *Hum Genet* 122 (3–4): 293–9. https://doi.org/10.1007/s00439-007-0395-2. https://www.ncbi.nlm.nih.gov/pubmed/17605048.

Zhao, J., K. Ueda, M. Riera, H. J. Kim, and J. R. Sparrow. 2018. “Bisretinoids mediate light sensitivity resulting in photoreceptor cell degeneration in mice lacking the receptor tyrosine kinase Mer.” *J Biol Chem* 293 (50): 19400–19410. https://doi.org/10.1074/jbc.RA118.005949. https://www.ncbi.nlm.nih.gov/pubmed/30352873.

Zheng, W., R. E. Reem, S. Omarova, S. Huang, P. L. DiPatre, C. D. Charvet, C. A. Curcio, and I. A. Pikuleva. 2012. “Spatial distribution of the pathways of cholesterol homeostasis in human retina.” *PLoS One* 7 (5): e37926. https://doi.org/10.1371/journal.pone.0037926. https://www.ncbi.nlm.nih.gov/pubmed/22629470.

Zhong, J., B. You, K. Xu, X. Zhang, Y. Xie, and Y. Li. 2021. “genotypic and ocular phenotypic characterisation in a Chinese cohort with ocular albinism.” *Ophthalmic Genet* 42 (6): 717–724. https://doi.org/10.1080/13816810.2021.1958352. https://www.ncbi.nlm.nih.gov/pubmed/34346269.

Zhou, J., Y. P. Jang, S. R. Kim, and J. R. Sparrow. 2006. “Complement activation by photooxidation products of A2E, a lipofuscin constituent of the retinal pigment epithelium.” *Proc Natl Acad Sci U S A* 103 (44): 16182–7. https://doi.org/10.1073/pnas.0604255103. https://www.ncbi.nlm.nih.gov/pubmed/17060630.

Zhou, J., S. R. Kim, B. S. Westlund, and J. R. Sparrow. 2009. “Complement activation by bisretinoid constituents of RPE lipofuscin.” *Invest Ophthalmol Vis Sci* 50 (3): 1392–9. https://doi.org/10.1167/iovs.08-2868. https://www.ncbi.nlm.nih.gov/ pubmed/19029031.

Zinkernagel, M. S., and R. E. MacLaren. 2015. “Recent advances and future prospects in choroideremia.” *Clin Ophthalmol* 9: 2195–200. https://doi.org/10.2147/ OPTH.S65732. https://www.ncbi.nlm.nih.gov/pubmed/26648685.

ACKNOWLEDEMENTS

The current studies were carried out at the Department of Ophthalmology, Columbia University, during a research fellowship period. The analysis of the material and publication of articles also continued after that period.

This study was supported by the National Eye Institute grants EY12951, EY024091, and P30EY019007, and a grant from Research to Prevent Blindness to the Department of Ophthalmology, Columbia University

I wish to express my sincere gratitude to all the people who have helped me in my research work:

- My supervisor professor Janet R. Sparrow, who gave me the opportunity to work with her team at the Columbia University and provided an invaluable experience in the field of retinal imaging studies. I would also like to thank the members of prof. Sparrow's laboratory, especially Jin Zhao and Hye Jin Kim for their mice analysis that allowed a multidisciplinary approach by connecting clinical and basic research
- My supervisor dr Kuldar Kaljurand for the support and advice during my studies in the PhD program as well as in ophthalmology training in general
- My reviewers dr. Eeva-Marja Sankila and dr. Kalev Nõupuu for their thorough analysis and constructive commentary on the thesis
- My colleague and friend Winston Lee for training me in retinal imaging and for sharing his great scientific insight into inherited retinal disease
- My colleague and friend Rait Parmann for all his help in our shared projects
- Associate Professor Stephen H. Tsang from Columbia University Medical Center for his valuable teachings in the field of inherited retinal disease
- Professor Rando Allikmets and his laboratory members for all the collaboration, and Jana Zernant for being my personal guide in ocular genetics
- All the medical and research staff at Columbia University and co-authors with whom it was a pleasure to working with
- My colleagues from the Helsinki University Eye Hospital, especially dr. Sanna Seitsonen, who have given me the flexibility in clinical work to finish my PhD thesis
- My former colleagues in Tartu University Eye Clinic for valuable specialty training and my first mentor in research, Paula Reemann, who encouraged me in my early steps in research
- My great gratitude goes to my dear family, who have supported me in all my academic endeavours in Estonia and abroad, and to dear Rait who has been a great companion through these intense periods of finilizing my PhD

PUBLICATIONS

CURRICULUM VITAE

Name: Maarjaliis Paavo
Date of birth: 24 of January 1986, Tartu, Estonia
Address: Tenholantie 10, 00280 Helsinki
Contact: maarjaliis@hotmail.com

Education:

2005–2011	Faculty of Medicine, University of Tartu
1993–2005	Tartu Miina Härma Gymnasium
1992–1993	Tartu Kesklinna School

Professional experience:

11.09.2018–present	Helsinki Eye and Ear Hospital, Department of Retinal Disease
01.03.2017–15.06.2018	Columbia University Department of Ophthalmology, clinical research fellowship
01.10 2014–28.02.2017	Helsinki Eye and Ear Hospital
01.09.–30.09. 2014	Observership in Rotterdam Eye Clinic, Department of Oculoplastics
09.05.2014	European Board of Ophthalmology Diploma exam (fEBO)
01.09–31.12.2012	Turku University Hospital Eye Clinic clinical fellowship in glaucoma management
01.09.2011–31.08.2014	Ophthalmology Residency in the Tartu University Eye Clinic

Publications

Repo P, Järvinen RS, Sankila EM, et al. Identifying haplotypes in recessive inherited retinal dystrophies using whole-genome linked-read sequencing. *Clin Genet*. 2021;99(1):193–198. doi:10.1111/cge.13847

Lee W, Paavo M, Zernant J, et al. Modification of the *PROM1* disease phenotype by a mutation in *ABCA4*. *Ophthalmic Genet*. 2019;40(4):369–375. doi:10.1080/13816810.2019.1660382

Paavo M, Carvalho JRL Jr, Lee W, Sengillo JD, Tsang SH, Sparrow JR. Patterns and Intensities of Near-Infrared and Short-Wavelength Fundus Autofluorescence in Choroideremia Probands and Carriers. *Invest Ophthalmol Vis Sci*. 2019; 60(12):3752–3761. doi:10.1167/iovs.19-27366

Sparrow JR, Duncker T, Schuerch K, Paavo M, de Carvalho JRL Jr. Lessons learned from quantitative fundus autofluorescence. *Prog Retin Eye Res*. 2020; 74:100774. doi:10.1016/j.preteyeres.2019.100774

Jauregui R, Park KS, Tanaka AJ, et al. Spectrum of Disease Severity and Phenotype in Choroideremia Carriers. *Am J Ophthalmol*. 2019;207:77–86. doi:10.1016/j.ajo.2019.06.002

Lima de Carvalho JR Jr, Paavo M, Chen L, Chiang J, Tsang SH, Sparrow JR. Multimodal Imaging in Best Vitelliform Macular Dystrophy. *Invest Ophthalmol Vis Sci*. 2019; 60(6):2012–2022. doi:10.1167/iovs.19-26571

Sengillo JD, Cho GY, Paavo M, et al. Hyperautofluorescent Dots are Characteristic in Ceramide Kinase Like-associated Retinal Degeneration. *Sci Rep*. 2019;9(1):876. Published 2019 Jan 29. doi:10.1038/s41598-018-37578-4

Paavo M, Zhao J, Kim HJ, et al. Mutations in GPR143/OA1 and ABCA4 Inform Interpretations of Short-Wavelength and Near-Infrared Fundus Autofluorescence. *Invest Ophthalmol Vis Sci*. 2018;59(6):2459–2469. doi:10.1167/iovs.18-24213

Paavo M, Lee W, Allikmets R, Tsang S, Sparrow JR. Photoreceptor cells as a source of fundus autofluorescence in recessive Stargardt disease. J Neurosci Res. 2019; 97(1):98–106. doi:10.1002/jnr.24252

Paavo M, Lee W, Merriam J, et al. Intraretinal Correlates of Reticular Pseudodrusen Revealed by Autofluorescence and En Face OCT. Invest Ophthalmol Vis Sci. 2017;58(11):4769–4777. doi:10.1167/iovs.17-22338

Reemann P, Reimann E, Suutre S, et al. Expression of class II cytokine genes in children's skin. Acta Derm Venereol. 2014;94(4):386–392. doi:10.2340/00015555-1717

ELULOOKIRJELDUS

Nimi: Maarjaliis Paavo
Sünniaeg: 24. jaanaur 1986 Tartu, Eesti
Aadress: Tenholantie 10, 00280 Helsinki, Soome
Kontakt: maarjaliis@hotmail.com

Haridus:

2005–2011	Tartu Ülikool, arstiteaduskond, arstiõpe
1993–2005	Tartu Miina Härma Gümnaasium
1992–1993	Tartu Kesklinna Kool

Teadus-ja erialane tegevus:

11.09.2018–	Helsingi Ülikooli Keskhaigla, Silmakliinik, Võrkkestahaiguste osakond, eriarst
01.03.2017–15.06.2018	Columbia Ülikooli Silmahaiguste osakond, kliinilise teadustöö programm
01.10 2014–28.02.2017	Helsingi Ülikooli Keskhaigla, Silmakliinik
01.09.–30.09. 2014	Rotterdami Silmakliinik, okuloplastika praktika
09.05.2014	Euroopa oftalmoloogia eriala eksam (fEBO)
01.09–31.12.2012	Turu Ülikooli haigla, Silmakliinik, glaukoomi praktika
01.09.2011–31.08.2014	Tartu Ülikool, Silmakliinik, silmahaiguste resident

Publikatsioonid:

Repo P, Järvinen RS, Sankila EM, et al. Identifying haplotypes in recessive inherited retinal dystrophies using whole-genome linked-read sequencing. *Clin Genet*. 2021;99(1):193–198. doi:10.1111/cge.13847

Lee W, Paavo M, Zernant J, et al. Modification of the *PROM1* disease phenotype by a mutation in *ABCA4*. *Ophthalmic Genet*. 2019;40(4):369–375. doi:10.1080/13816810.2019.1660382

Paavo M, Carvalho JRL Jr, Lee W, Sengillo JD, Tsang SH, Sparrow JR. Patterns and Intensities of Near-Infrared and Short-Wavelength Fundus Autofluorescence in Choroideremia Probands and Carriers. *Invest Ophthalmol Vis Sci*. 2019; 60(12):3752–3761. doi:10.1167/iovs.19-27366

Sparrow JR, Duncker T, Schuerch K, Paavo M, de Carvalho JRL Jr. Lessons learned from quantitative fundus autofluorescence. *Prog Retin Eye Res*. 2020; 74:100774. doi:10.1016/j.preteyeres.2019.100774

Jauregui R, Park KS, Tanaka AJ, et al. Spectrum of Disease Severity and Phenotype in Choroideremia Carriers. *Am J Ophthalmol*. 2019;207:77–86. doi:10.1016/j.ajo.2019.06.002

Lima de Carvalho JR Jr, Paavo M, Chen L, Chiang J, Tsang SH, Sparrow JR. Multimodal Imaging in Best Vitelliform Macular Dystrophy. *Invest Ophthalmol Vis Sci*. 2019; 60(6):2012–2022. doi:10.1167/iovs.19-26571

Sengillo JD, Cho GY, Paavo M, et al. Hyperautofluorescent Dots are Characteristic in Ceramide Kinase Like-associated Retinal Degeneration. *Sci Rep*. 2019;9(1):876. Published 2019 Jan 29. doi:10.1038/s41598-018-37578-4

Paavo M, Zhao J, Kim HJ, et al. Mutations in GPR143/OA1 and ABCA4 Inform Interpretations of Short-Wavelength and Near-Infrared Fundus Autofluorescence. *Invest Ophthalmol Vis Sci*. 2018;59(6):2459–2469. doi:10.1167/iovs.18-24213

Paavo M, Lee W, Allikmets R, Tsang S, Sparrow JR. Photoreceptor cells as a source of fundus autofluorescence in recessive Stargardt disease. J Neurosci Res. 2019; 97(1):98–106. doi:10.1002/jnr.24252

Paavo M, Lee W, Merriam J, et al. Intraretinal Correlates of Reticular Pseudodrusen Revealed by Autofluorescence and En Face OCT. Invest Ophthalmol Vis Sci. 2017;58(11):4769–4777. doi:10.1167/iovs.17-22338

Reemann P, Reimann E, Suutre S, et al. Expression of class II cytokine genes in children's skin. Acta Derm Venereol. 2014;94(4):386–392. doi:10.2340/00015555-1717

DISSERTATIONES MEDICINAE UNIVERSITATIS TARTUENSIS

1. **Heidi-Ingrid Maaroos**. The natural course of gastric ulcer in connection with chronic gastritis and *Helicobacter pylori*. Tartu, 1991.
2. **Mihkel Zilmer**. Na-pump in normal and tumorous brain tissues: Structural, functional and tumorigenesis aspects. Tartu, 1991.
3. **Eero Vasar**. Role of cholecystokinin receptors in the regulation of behaviour and in the action of haloperidol and diazepam. Tartu, 1992.
4. **Tiina Talvik**. Hypoxic-ischaemic brain damage in neonates (clinical, biochemical and brain computed tomographical investigation). Tartu, 1992.
5. **Ants Peetsalu**. Vagotomy in duodenal ulcer disease: A study of gastric acidity, serum pepsinogen I, gastric mucosal histology and *Helicobacter pylori*. Tartu, 1992.
6. **Marika Mikelsaar**. Evaluation of the gastrointestinal microbial ecosystem in health and disease. Tartu, 1992.
7. **Hele Everaus**. Immuno-hormonal interactions in chronic lymphocytic leukaemia and multiple myeloma. Tartu, 1993.
8. **Ruth Mikelsaar**. Etiological factors of diseases in genetically consulted children and newborn screening: dissertation for the commencement of the degree of doctor of medical sciences. Tartu, 1993.
9. **Agu Tamm**. On metabolic action of intestinal microflora: clinical aspects. Tartu, 1993.
10. **Katrin Gross**. Multiple sclerosis in South-Estonia (epidemiological and computed tomographical investigations). Tartu, 1993.
11. **Oivi Uibo**. Childhood coeliac disease in Estonia: occurrence, screening, diagnosis and clinical characterization. Tartu, 1994.
12. **Viiu Tuulik**. The functional disorders of central nervous system of chemistry workers. Tartu, 1994.
13. **Margus Viigimaa**. Primary haemostasis, antiaggregative and anticoagulant treatment of acute myocardial infarction. Tartu, 1994.
14. **Rein Kolk**. Atrial versus ventricular pacing in patients with sick sinus syndrome. Tartu, 1994.
15. **Toomas Podar**. Incidence of childhood onset type 1 diabetes mellitus in Estonia. Tartu, 1994.
16. **Kiira Subi**. The laboratory surveillance of the acute respiratory viral infections in Estonia. Tartu, 1995.
17. **Irja Lutsar**. Infections of the central nervous system in children (epidemiologic, diagnostic and therapeutic aspects, long term outcome). Tartu, 1995.
18. **Aavo Lang**. The role of dopamine, 5-hydroxytryptamine, sigma and NMDA receptors in the action of antipsychotic drugs. Tartu, 1995.
19. **Andrus Arak**. Factors influencing the survival of patients after radical surgery for gastric cancer. Tartu, 1996.

20. **Tõnis Karki**. Quantitative composition of the human lactoflora and method for its examination. Tartu, 1996.
21. **Reet Mändar**. Vaginal microflora during pregnancy and its transmission to newborn. Tartu, 1996.
22. **Triin Remmel**. Primary biliary cirrhosis in Estonia: epidemiology, clinical characterization and prognostication of the course of the disease. Tartu, 1996.
23. **Toomas Kivastik**. Mechanisms of drug addiction: focus on positive reinforcing properties of morphine. Tartu, 1996.
24. **Paavo Pokk**. Stress due to sleep deprivation: focus on $GABA_A$ receptor-chloride ionophore complex. Tartu, 1996.
25. **Kristina Allikmets**. Renin system activity in essential hypertension. Associations with atherothrombogenic cardiovascular risk factors and with the efficacy of calcium antagonist treatment. Tartu, 1996.
26. **Triin Parik**. Oxidative stress in essential hypertension: Associations with metabolic disturbances and the effects of calcium antagonist treatment. Tartu, 1996.
27. **Svetlana Päi**. Factors promoting heterogeneity of the course of rheumatoid arthritis. Tartu, 1997.
28. **Maarike Sallo**. Studies on habitual physical activity and aerobic fitness in 4 to 10 years old children. Tartu, 1997.
29. **Paul Naaber**. *Clostridium difficile* infection and intestinal microbial ecology. Tartu, 1997.
30. **Rein Pähkla**. Studies in pinoline pharmacology. Tartu, 1997.
31. **Andrus Juhan Voitk**. Outpatient laparoscopic cholecystectomy. Tartu, 1997.
32. **Joel Starkopf**. Oxidative stress and ischaemia-reperfusion of the heart. Tartu, 1997.
33. **Janika Kõrv**. Incidence, case-fatality and outcome of stroke. Tartu, 1998.
34. **Ülla Linnamägi**. Changes in local cerebral blood flow and lipid peroxidation following lead exposure in experiment. Tartu, 1998.
35. **Ave Minajeva**. Sarcoplasmic reticulum function: comparison of atrial and ventricular myocardium. Tartu, 1998.
36. **Oleg Milenin**. Reconstruction of cervical part of esophagus by revascularised ileal autografts in dogs. A new complex multistage method. Tartu, 1998.
37. **Sergei Pakriev**. Prevalence of depression, harmful use of alcohol and alcohol dependence among rural population in Udmurtia. Tartu, 1998.
38. **Allen Kaasik**. Thyroid hormone control over β-adrenergic signalling system in rat atria. Tartu, 1998.
39. **Vallo Matto**. Pharmacological studies on anxiogenic and antiaggressive properties of antidepressants. Tartu, 1998.
40. **Maire Vasar**. Allergic diseases and bronchial hyperreactivity in Estonian children in relation to environmental influences. Tartu, 1998.
41. **Kaja Julge**. Humoral immune responses to allergens in early childhood. Tartu, 1998.

42. **Heli Grünberg**. The cardiovascular risk of Estonian schoolchildren. A cross-sectional study of 9-, 12- and 15-year-old children. Tartu, 1998.
43. **Epp Sepp**. Formation of intestinal microbial ecosystem in children. Tartu, 1998.
44. **Mai Ots**. Characteristics of the progression of human and experimental glomerulopathies. Tartu, 1998.
45. **Tiina Ristimäe**. Heart rate variability in patients with coronary artery disease. Tartu, 1998.
46. **Leho Kõiv**. Reaction of the sympatho-adrenal and hypothalamo-pituitary-adrenocortical system in the acute stage of head injury. Tartu, 1998.
47. **Bela Adojaan**. Immune and genetic factors of childhood onset IDDM in Estonia. An epidemiological study. Tartu, 1999.
48. **Jakov Shlik**. Psychophysiological effects of cholecystokinin in humans. Tartu, 1999.
49. **Kai Kisand**. Autoantibodies against dehydrogenases of α-ketoacids. Tartu, 1999.
50. **Toomas Marandi**. Drug treatment of depression in Estonia. Tartu, 1999.
51. **Ants Kask**. Behavioural studies on neuropeptide Y. Tartu, 1999.
52. **Ello-Rahel Karelson**. Modulation of adenylate cyclase activity in the rat hippocampus by neuropeptide galanin and its chimeric analogs. Tartu, 1999.
53. **Tanel Laisaar**. Treatment of pleural empyema — special reference to intrapleural therapy with streptokinase and surgical treatment modalities. Tartu, 1999.
54. **Eve Pihl**. Cardiovascular risk factors in middle-aged former athletes. Tartu, 1999.
55. **Katrin Õunap**. Phenylketonuria in Estonia: incidence, newborn screening, diagnosis, clinical characterization and genotype/phenotype correlation. Tartu, 1999.
56. **Siiri Kõljalg**. *Acinetobacter* – an important nosocomial pathogen. Tartu, 1999.
57. **Helle Karro**. Reproductive health and pregnancy outcome in Estonia: association with different factors. Tartu, 1999.
58. **Heili Varendi**. Behavioral effects observed in human newborns during exposure to naturally occurring odors. Tartu, 1999.
59. **Anneli Beilmann**. Epidemiology of epilepsy in children and adolescents in Estonia. Prevalence, incidence, and clinical characteristics. Tartu, 1999.
60. **Vallo Volke**. Pharmacological and biochemical studies on nitric oxide in the regulation of behaviour. Tartu, 1999.
61. **Pilvi Ilves**. Hypoxic-ischaemic encephalopathy in asphyxiated term infants. A prospective clinical, biochemical, ultrasonographical study. Tartu, 1999.
62. **Anti Kalda**. Oxygen-glucose deprivation-induced neuronal death and its pharmacological prevention in cerebellar granule cells. Tartu, 1999.
63. **Eve-Irene Lepist**. Oral peptide prodrugs – studies on stability and absorption. Tartu, 2000.

64. **Jana Kivastik**. Lung function in Estonian schoolchildren: relationship with anthropometric indices and respiratory symptomas, reference values for dynamic spirometry. Tartu, 2000.
65. **Karin Kull**. Inflammatory bowel disease: an immunogenetic study. Tartu, 2000.
66. **Kaire Innos**. Epidemiological resources in Estonia: data sources, their quality and feasibility of cohort studies. Tartu, 2000.
67. **Tamara Vorobjova**. Immune response to *Helicobacter pylori* and its association with dynamics of chronic gastritis and epithelial cell turnover in antrum and corpus. Tartu, 2001.
68. **Ruth Kalda**. Structure and outcome of family practice quality in the changing health care system of Estonia. Tartu, 2001.
69. **Annika Krüüner**. *Mycobacterium tuberculosis* – spread and drug resistance in Estonia. Tartu, 2001.
70. **Marlit Veldi**. Obstructive Sleep Apnoea: Computerized Endopharyngeal Myotonometry of the Soft Palate and Lingual Musculature. Tartu, 2001.
71. **Anneli Uusküla**. Epidemiology of sexually transmitted diseases in Estonia in 1990–2000. Tartu, 2001.
72. **Ade Kallas**. Characterization of antibodies to coagulation factor VIII. Tartu, 2002.
73. **Heidi Annuk**. Selection of medicinal plants and intestinal lactobacilli as antimicrobil components for functional foods. Tartu, 2002.
74. **Aet Lukmann**. Early rehabilitation of patients with ischaemic heart disease after surgical revascularization of the myocardium: assessment of health-related quality of life, cardiopulmonary reserve and oxidative stress. A clinical study. Tartu, 2002.
75. **Maigi Eisen**. Pathogenesis of Contact Dermatitis: participation of Oxidative Stress. A clinical – biochemical study. Tartu, 2002.
76. **Piret Hussar**. Histology of the post-traumatic bone repair in rats. Elaboration and use of a new standardized experimental model – bicortical perforation of tibia compared to internal fracture and resection osteotomy. Tartu, 2002.
77. **Tõnu Rätsep**. Aneurysmal subarachnoid haemorrhage: Noninvasive monitoring of cerebral haemodynamics. Tartu, 2002.
78. **Marju Herodes**. Quality of life of people with epilepsy in Estonia. Tartu, 2003.
79. **Katre Maasalu**. Changes in bone quality due to age and genetic disorders and their clinical expressions in Estonia. Tartu, 2003.
80. **Toomas Sillakivi**. Perforated peptic ulcer in Estonia: epidemiology, risk factors and relations with *Helicobacter pylori*. Tartu, 2003.
81. **Leena Puksa**. Late responses in motor nerve conduction studies. F and A waves in normal subjects and patients with neuropathies. Tartu, 2003.
82. **Krista Lõivukene**. *Helicobacter pylori* in gastric microbial ecology and its antimicrobial susceptibility pattern. Tartu, 2003.

83. **Helgi Kolk**. Dyspepsia and *Helicobacter pylori* infection: the diagnostic value of symptoms, treatment and follow-up of patients referred for upper gastrointestinal endoscopy by family physicians. Tartu, 2003.
84. **Helena Soomer**. Validation of identification and age estimation methods in forensic odontology. Tartu, 2003.
85. **Kersti Oselin**. Studies on the human MDR1, MRP1, and MRP2 ABC transporters: functional relevance of the genetic polymorphisms in the *MDR1* and *MRP1* gene. Tartu, 2003.
86. **Jaan Soplepmann**. Peptic ulcer haemorrhage in Estonia: epidemiology, prognostic factors, treatment and outcome. Tartu, 2003.
87. **Margot Peetsalu**. Long-term follow-up after vagotomy in duodenal ulcer disease: recurrent ulcer, changes in the function, morphology and *Helicobacter pylori* colonisation of the gastric mucosa. Tartu, 2003.
88. **Kersti Klaamas**. Humoral immune response to *Helicobacter pylori* a study of host-dependent and microbial factors. Tartu, 2003.
89. **Pille Taba**. Epidemiology of Parkinson's disease in Tartu, Estonia. Prevalence, incidence, clinical characteristics, and pharmacoepidemiology. Tartu, 2003.
90. **Alar Veraksitš**. Characterization of behavioural and biochemical phenotype of cholecystokinin-2 receptor deficient mice: changes in the function of the dopamine and endopioidergic system. Tartu, 2003.
91. **Ingrid Kalev**. CC-chemokine receptor 5 (CCR5) gene polymorphism in Estonians and in patients with Type I and Type II diabetes mellitus. Tartu, 2003.
92. **Lumme Kadaja**. Molecular approach to the regulation of mitochondrial function in oxidative muscle cells. Tartu, 2003.
93. **Aive Liigant**. Epidemiology of primary central nervous system tumours in Estonia from 1986 to 1996. Clinical characteristics, incidence, survival and prognostic factors. Tartu, 2004.
94. **Andres, Kulla**. Molecular characteristics of mesenchymal stroma in human astrocytic gliomas. Tartu, 2004.
95. **Mari Järvelaid**. Health damaging risk behaviours in adolescence. Tartu, 2004.
96. **Ülle Pechter**. Progression prevention strategies in chronic renal failure and hypertension. An experimental and clinical study. Tartu, 2004.
97. **Gunnar Tasa**. Polymorphic glutathione S-transferases – biology and role in modifying genetic susceptibility to senile cataract and primary open angle glaucoma. Tartu, 2004.
98. **Tuuli Käämbre**. Intracellular energetic unit: structural and functional aspects. Tartu, 2004.
99. **Vitali Vassiljev**. Influence of nitric oxide syntase inhibitors on the effects of ethanol after acute and chronic ethanol administration and withdrawal. Tartu, 2004.

100. **Aune Rehema**. Assessment of nonhaem ferrous iron and glutathione redox ratio as markers of pathogeneticity of oxidative stress in different clinical groups. Tartu, 2004.
101. **Evelin Seppet**. Interaction of mitochondria and ATPases in oxidative muscle cells in normal and pathological conditions. Tartu, 2004.
102. **Eduard Maron**. Serotonin function in panic disorder: from clinical experiments to brain imaging and genetics. Tartu, 2004.
103. **Marje Oona**. *Helicobacter pylori* infection in children: epidemiological and therapeutic aspects. Tartu, 2004.
104. **Kersti Kokk**. Regulation of active and passive molecular transport in the testis. Tartu, 2005.
105. **Vladimir Järv**. Cross-sectional imaging for pretreatment evaluation and follow-up of pelvic malignant tumours. Tartu, 2005.
106. **Andre Õun**. Epidemiology of adult epilepsy in Tartu, Estonia. Incidence, prevalence and medical treatment. Tartu, 2005.
107. **Piibe Muda**. Homocysteine and hypertension: associations between homocysteine and essential hypertension in treated and untreated hypertensive patients with and without coronary artery disease. Tartu, 2005.
108. **Külli Kingo**. The interleukin-10 family cytokines gene polymorphisms in plaque psoriasis. Tartu, 2005.
109. **Mati Merila**. Anatomy and clinical relevance of the glenohumeral joint capsule and ligaments. Tartu, 2005.
110. **Epp Songisepp**. Evaluation of technological and functional properties of the new probiotic *Lactobacillus fermentum* ME-3. Tartu, 2005.
111. **Tiia Ainla**. Acute myocardial infarction in Estonia: clinical characteristics, management and outcome. Tartu, 2005.
112. **Andres Sell**. Determining the minimum local anaesthetic requirements for hip replacement surgery under spinal anaesthesia – a study employing a spinal catheter. Tartu, 2005.
113. **Tiia Tamme**. Epidemiology of odontogenic tumours in Estonia. Pathogenesis and clinical behaviour of ameloblastoma. Tartu, 2005.
114. **Triine Annus**. Allergy in Estonian schoolchildren: time trends and characteristics. Tartu, 2005.
115. **Tiia Voor**. Microorganisms in infancy and development of allergy: comparison of Estonian and Swedish children. Tartu, 2005.
116. **Priit Kasenõmm**. Indicators for tonsillectomy in adults with recurrent tonsillitis – clinical, microbiological and pathomorphological investigations. Tartu, 2005.
117. **Eva Zusinaite**. Hepatitis C virus: genotype identification and interactions between viral proteases. Tartu, 2005.
118. **Piret Kõll**. Oral lactoflora in chronic periodontitis and periodontal health. Tartu, 2006.
119. **Tiina Stelmach**. Epidemiology of cerebral palsy and unfavourable neurodevelopmental outcome in child population of Tartu city and county, Estonia Prevalence, clinical features and risk factors. Tartu, 2006.

120. **Katrin Pudersell**. Tropane alkaloid production and riboflavine excretion in the field and tissue cultures of henbane (*Hyoscyamus niger* L.). Tartu, 2006.
121. **Külli Jaako**. Studies on the role of neurogenesis in brain plasticity. Tartu, 2006.
122. **Aare Märtson**. Lower limb lengthening: experimental studies of bone regeneration and long-term clinical results. Tartu, 2006.
123. **Heli Tähepõld**. Patient consultation in family medicine. Tartu, 2006.
124. **Stanislav Liskmann**. Peri-implant disease: pathogenesis, diagnosis and treatment in view of both inflammation and oxidative stress profiling. Tartu, 2006.
125. **Ruth Rudissaar**. Neuropharmacology of atypical antipsychotics and an animal model of psychosis. Tartu, 2006.
126. **Helena Andreson**. Diversity of *Helicobacter pylori* genotypes in Estonian patients with chronic inflammatory gastric diseases. Tartu, 2006.
127. **Katrin Pruus**. Mechanism of action of antidepressants: aspects of serotoninergic system and its interaction with glutamate. Tartu, 2006.
128. **Priit Põder**. Clinical and experimental investigation: relationship of ischaemia/reperfusion injury with oxidative stress in abdominal aortic aneurysm repair and in extracranial brain artery endarterectomy and possibilities of protection against ischaemia using a glutathione analogue in a rat model of global brain ischaemia. Tartu, 2006.
129. **Marika Tammaru**. Patient-reported outcome measurement in rheumatoid arthritis. Tartu, 2006.
130. **Tiia Reimand**. Down syndrome in Estonia. Tartu, 2006.
131. **Diva Eensoo**. Risk-taking in traffic and Markers of Risk-Taking Behaviour in Schoolchildren and Car Drivers. Tartu, 2007.
132. **Riina Vibo**. The third stroke registry in Tartu, Estonia from 2001 to 2003: incidence, case-fatality, risk factors and long-term outcome. Tartu, 2007.
133. **Chris Pruunsild**. Juvenile idiopathic arthritis in children in Estonia. Tartu, 2007.
134. **Eve Õiglane-Šlik**. Angelman and Prader-Willi syndromes in Estonia. Tartu, 2007.
135. **Kadri Haller**. Antibodies to follicle stimulating hormone. Significance in female infertility. Tartu, 2007.
136. **Pille Ööpik**. Management of depression in family medicine. Tartu, 2007.
137. **Jaak Kals**. Endothelial function and arterial stiffness in patients with atherosclerosis and in healthy subjects. Tartu, 2007.
138. **Priit Kampus**. Impact of inflammation, oxidative stress and age on arterial stiffness and carotid artery intima-media thickness. Tartu, 2007.
139. **Margus Punab**. Male fertility and its risk factors in Estonia. Tartu, 2007.
140. **Alar Toom**. Heterotopic ossification after total hip arthroplasty: clinical and pathogenetic investigation. Tartu, 2007.

141. **Lea Pehme**. Epidemiology of tuberculosis in Estonia 1991–2003 with special regard to extrapulmonary tuberculosis and delay in diagnosis of pulmonary tuberculosis. Tartu, 2007.
142. **Juri Karjagin**. The pharmacokinetics of metronidazole and meropenem in septic shock. Tartu, 2007.
143. **Inga Talvik**. Inflicted traumatic brain injury shaken baby syndrome in Estonia – epidemiology and outcome. Tartu, 2007.
144. **Tarvo Rajasalu**. Autoimmune diabetes: an immunological study of type 1 diabetes in humans and in a model of experimental diabetes (in RIP-B7.1 mice). Tartu, 2007.
145. **Inga Karu**. Ischaemia-reperfusion injury of the heart during coronary surgery: a clinical study investigating the effect of hyperoxia. Tartu, 2007.
146. **Peeter Padrik**. Renal cell carcinoma: Changes in natural history and treatment of metastatic disease. Tartu, 2007.
147. **Neve Vendt**. Iron deficiency and iron deficiency anaemia in infants aged 9 to 12 months in Estonia. Tartu, 2008.
148. **Lenne-Triin Heidmets**. The effects of neurotoxins on brain plasticity: focus on neural Cell Adhesion Molecule. Tartu, 2008.
149. **Paul Korrovits**. Asymptomatic inflammatory prostatitis: prevalence, etiological factors, diagnostic tools. Tartu, 2008.
150. **Annika Reintam**. Gastrointestinal failure in intensive care patients. Tartu, 2008.
151. **Kristiina Roots**. Cationic regulation of Na-pump in the normal, Alzheimer's and CCK_2 receptor-deficient brain. Tartu, 2008.
152. **Helen Puusepp**. The genetic causes of mental retardation in Estonia: fragile X syndrome and creatine transporter defect. Tartu, 2009.
153. **Kristiina Rull**. Human chorionic gonadotropin beta genes and recurrent miscarriage: expression and variation study. Tartu, 2009.
154. **Margus Eimre**. Organization of energy transfer and feedback regulation in oxidative muscle cells. Tartu, 2009.
155. **Maire Link**. Transcription factors FoxP3 and AIRE: autoantibody associations. Tartu, 2009.
156. **Kai Haldre**. Sexual health and behaviour of young women in Estonia. Tartu, 2009.
157. **Kaur Liivak**. Classical form of congenital adrenal hyperplasia due to 21-hydroxylase deficiency in Estonia: incidence, genotype and phenotype with special attention to short-term growth and 24-hour blood pressure. Tartu, 2009.
158. **Kersti Ehrlich**. Antioxidative glutathione analogues (UPF peptides) – molecular design, structure-activity relationships and testing the protective properties. Tartu, 2009.
159. **Anneli Rätsep**. Type 2 diabetes care in family medicine. Tartu, 2009.
160. **Silver Türk**. Etiopathogenetic aspects of chronic prostatitis: role of mycoplasmas, coryneform bacteria and oxidative stress. Tartu, 2009.

161. **Kaire Heilman**. Risk markers for cardiovascular disease and low bone mineral density in children with type 1 diabetes. Tartu, 2009.
162. **Kristi Rüütel**. HIV-epidemic in Estonia: injecting drug use and quality of life of people living with HIV. Tartu, 2009.
163. **Triin Eller**. Immune markers in major depression and in antidepressive treatment. Tartu, 2009.
164. **Siim Suutre**. The role of TGF-β isoforms and osteoprogenitor cells in the pathogenesis of heterotopic ossification. An experimental and clinical study of hip arthroplasty. Tartu, 2010.
165. **Kai Kliiman**. Highly drug-resistant tuberculosis in Estonia: Risk factors and predictors of poor treatment outcome. Tartu, 2010.
166. **Inga Villa**. Cardiovascular health-related nutrition, physical activity and fitness in Estonia. Tartu, 2010.
167. **Tõnis Org**. Molecular function of the first PHD finger domain of Autoimmune Regulator protein. Tartu, 2010.
168. **Tuuli Metsvaht**. Optimal antibacterial therapy of neonates at risk of early onset sepsis. Tartu, 2010.
169. **Jaanus Kahu**. Kidney transplantation: Studies on donor risk factors and mycophenolate mofetil. Tartu, 2010.
170. **Koit Reimand**. Autoimmunity in reproductive failure: A study on associated autoantibodies and autoantigens. Tartu, 2010.
171. **Mart Kull**. Impact of vitamin D and hypolactasia on bone mineral density: a population based study in Estonia. Tartu, 2010.
172. **Rael Laugesaar**. Stroke in children – epidemiology and risk factors. Tartu, 2010.
173. **Mark Braschinsky**. Epidemiology and quality of life issues of hereditary spastic paraplegia in Estonia and implemention of genetic analysis in everyday neurologic practice. Tartu, 2010.
174. **Kadri Suija**. Major depression in family medicine: associated factors, recurrence and possible intervention. Tartu, 2010.
175. **Jarno Habicht**. Health care utilisation in Estonia: socioeconomic determinants and financial burden of out-of-pocket payments. Tartu, 2010.
176. **Kristi Abram**. The prevalence and risk factors of rosacea. Subjective disease perception of rosacea patients. Tartu, 2010.
177. **Malle Kuum**. Mitochondrial and endoplasmic reticulum cation fluxes: Novel roles in cellular physiology. Tartu, 2010.
178. **Rita Teek**. The genetic causes of early onset hearing loss in Estonian children. Tartu, 2010.
179. **Daisy Volmer**. The development of community pharmacy services in Estonia – public and professional perceptions 1993–2006. Tartu, 2010.
180. **Jelena Lissitsina**. Cytogenetic causes in male infertility. Tartu, 2011.
181. **Delia Lepik**. Comparison of gunshot injuries caused from Tokarev, Makarov and Glock 19 pistols at different firing distances. Tartu, 2011.
182. **Ene-Renate Pähkla**. Factors related to the efficiency of treatment of advanced periodontitis. Tartu, 2011.

183. **Maarja Krass**. L-Arginine pathways and antidepressant action. Tartu, 2011.
184. **Taavi Lai**. Population health measures to support evidence-based health policy in Estonia. Tartu, 2011.
185. **Tiit Salum**. Similarity and difference of temperature-dependence of the brain sodium pump in normal, different neuropathological, and aberrant conditions and its possible reasons. Tartu, 2011.
186. **Tõnu Vooder**. Molecular differences and similarities between histological subtypes of non-small cell lung cancer. Tartu, 2011.
187. **Jelena Štšepetova**. The characterisation of intestinal lactic acid bacteria using bacteriological, biochemical and molecular approaches. Tartu, 2011.
188. **Radko Avi**. Natural polymorphisms and transmitted drug resistance in Estonian HIV-1 CRF06_cpx and its recombinant viruses. Tartu, 2011, 116 p.
189. **Edward Laane**. Multiparameter flow cytometry in haematological malignancies. Tartu, 2011, 152 p.
190. **Triin Jagomägi**. A study of the genetic etiology of nonsyndromic cleft lip and palate. Tartu, 2011, 158 p.
191. **Ivo Laidmäe**. Fibrin glue of fish (*Salmo salar*) origin: immunological study and development of new pharmaceutical preparation. Tartu, 2012, 150 p.
192. **Ülle Parm**. Early mucosal colonisation and its role in prediction of invasive infection in neonates at risk of early onset sepsis. Tartu, 2012, 168 p.
193. **Kaupo Teesalu**. Autoantibodies against desmin and transglutaminase 2 in celiac disease: diagnostic and functional significance. Tartu, 2012, 142 p.
194. **Maksim Zagura**. Biochemical, functional and structural profiling of arterial damage in atherosclerosis. Tartu, 2012, 162 p.
195. **Vivian Kont**. Autoimmune regulator: characterization of thymic gene regulation and promoter methylation. Tartu, 2012, 134 p.
196. **Pirje Hütt**. Functional properties, persistence, safety and efficacy of potential probiotic lactobacilli. Tartu, 2012, 246 p.
197. **Innar Tõru**. Serotonergic modulation of CCK-4- induced panic. Tartu, 2012, 132 p.
198. **Sigrid Vorobjov**. Drug use, related risk behaviour and harm reduction interventions utilization among injecting drug users in Estonia: implications for drug policy. Tartu, 2012, 120 p.
199. **Martin Serg**. Therapeutic aspects of central haemodynamics, arterial stiffness and oxidative stress in hypertension. Tartu, 2012, 156 p.
200. **Jaanika Kumm**. Molecular markers of articular tissues in early knee osteoarthritis: a population-based longitudinal study in middle-aged subjects. Tartu, 2012, 159 p.
201. **Kertu Rünkorg**. Functional changes of dopamine, endopioid and endocannabinoid systems in CCK2 receptor deficient mice. Tartu, 2012, 125 p.
202. **Mai Blöndal**. Changes in the baseline characteristics, management and outcomes of acute myocardial infarction in Estonia. Tartu, 2012, 127 p.

203. **Jana Lass**. Epidemiological and clinical aspects of medicines use in children in Estonia. Tartu, 2012, 170 p.
204. **Kai Truusalu**. Probiotic lactobacilli in experimental persistent *Salmonella* infection. Tartu, 2013, 139 p.
205. **Oksana Jagur**. Temporomandibular joint diagnostic imaging in relation to pain and bone characteristics. Long-term results of arthroscopic treatment. Tartu, 2013, 126 p.
206. **Katrin Sikk**. Manganese-ephedrone intoxication – pathogenesis of neurological damage and clinical symptomatology. Tartu, 2013, 125 p.
207. **Kai Blöndal**. Tuberculosis in Estonia with special emphasis on drug-resistant tuberculosis: Notification rate, disease recurrence and mortality. Tartu, 2013, 151 p.
208. **Marju Puurand**. Oxidative phosphorylation in different diseases of gastric mucosa. Tartu, 2013, 123 p.
209. **Aili Tagoma**. Immune activation in female infertility: Significance of autoantibodies and inflammatory mediators. Tartu, 2013, 135 p.
210. **Liis Sabre**. Epidemiology of traumatic spinal cord injury in Estonia. Brain activation in the acute phase of traumatic spinal cord injury. Tartu, 2013, 135 p.
211. **Merit Lamp**. Genetic susceptibility factors in endometriosis. Tartu, 2013, 125 p.
212. **Erik Salum**. Beneficial effects of vitamin D and angiotensin II receptor blocker on arterial damage. Tartu, 2013, 167 p.
213. **Maire Karelson**. Vitiligo: clinical aspects, quality of life and the role of melanocortin system in pathogenesis. Tartu, 2013, 153 p.
214. **Kuldar Kaljurand**. Prevalence of exfoliation syndrome in Estonia and its clinical significance. Tartu, 2013, 113 p.
215. **Raido Paasma**. Clinical study of methanol poisoning: handling large outbreaks, treatment with antidotes, and long-term outcomes. Tartu, 2013, 96 p.
216. **Anne Kleinberg**. Major depression in Estonia: prevalence, associated factors, and use of health services. Tartu, 2013, 129 p.
217. **Triin Eglit**. Obesity, impaired glucose regulation, metabolic syndrome and their associations with high-molecular-weight adiponectin levels. Tartu, 2014, 115 p.
218. **Kristo Ausmees**. Reproductive function in middle-aged males: Associations with prostate, lifestyle and couple infertility status. Tartu, 2014, 125 p.
219. **Kristi Huik**. The influence of host genetic factors on the susceptibility to HIV and HCV infections among intravenous drug users. Tartu, 2014, 144 p.
220. **Liina Tserel**. Epigenetic profiles of monocytes, monocyte-derived macrophages and dendritic cells. Tartu, 2014, 143 p.
221. **Irina Kerna**. The contribution of *ADAM12* and *CILP* genes to the development of knee osteoarthritis. Tartu, 2014, 152 p.

222. **Ingrid Liiv**. Autoimmune regulator protein interaction with DNA-dependent protein kinase and its role in apoptosis. Tartu, 2014, 143 p.
223. **Liivi Maddison**. Tissue perfusion and metabolism during intra-abdominal hypertension. Tartu, 2014, 103 p.
224. **Krista Ress**. Childhood coeliac disease in Estonia, prevalence in atopic dermatitis and immunological characterisation of coexistence. Tartu, 2014, 124 p.
225. **Kai Muru**. Prenatal screening strategies, long-term outcome of children with marked changes in maternal screening tests and the most common syndromic heart anomalies in Estonia. Tartu, 2014, 189 p.
226. **Kaja Rahu**. Morbidity and mortality among Baltic Chernobyl cleanup workers: a register-based cohort study. Tartu, 2014, 155 p.
227. **Klari Noormets**. The development of diabetes mellitus, fertility and energy metabolism disturbances in a Wfs1-deficient mouse model of Wolfram syndrome. Tartu, 2014, 132 p.
228. **Liis Toome**. Very low gestational age infants in Estonia. Tartu, 2014, 183 p.
229. **Ceith Nikkolo**. Impact of different mesh parameters on chronic pain and foreign body feeling after open inguinal hernia repair. Tartu, 2014, 132 p.
230. **Vadim Brjalin**. Chronic hepatitis C: predictors of treatment response in Estonian patients. Tartu, 2014, 122 p.
231. **Vahur Metsna**. Anterior knee pain in patients following total knee arthroplasty: the prevalence, correlation with patellar cartilage impairment and aspects of patellofemoral congruence. Tartu, 2014, 130 p.
232. **Marju Kase**. Glioblastoma multiforme: possibilities to improve treatment efficacy. Tartu, 2015, 137 p.
233. **Riina Runnel**. Oral health among elementary school children and the effects of polyol candies on the prevention of dental caries. Tartu, 2015, 112 p.
234. **Made Laanpere**. Factors influencing women's sexual health and reproductive choices in Estonia. Tartu, 2015, 176 p.
235. **Andres Lust**. Water mediated solid state transformations of a polymorphic drug – effect on pharmaceutical product performance. Tartu, 2015, 134 p.
236. **Anna Klugman**. Functionality related characterization of pretreated wood lignin, cellulose and polyvinylpyrrolidone for pharmaceutical applications. Tartu, 2015, 156 p.
237. **Triin Laisk-Podar**. Genetic variation as a modulator of susceptibility to female infertility and a source for potential biomarkers. Tartu, 2015, 155 p.
238. **Mailis Tõnisson**. Clinical picture and biochemical changes in blood in children with acute alcohol intoxication. Tartu, 2015, 100 p.
239. **Kadri Tamme**. High volume haemodiafiltration in treatment of severe sepsis – impact on pharmacokinetics of antibiotics and inflammatory response. Tartu, 2015, 133 p.

240. **Kai Part**. Sexual health of young people in Estonia in a social context: the role of school-based sexuality education and youth-friendly counseling services. Tartu, 2015, 203 p.
241. **Urve Paaver**. New perspectives for the amorphization and physical stabilization of poorly water-soluble drugs and understanding their dissolution behavior. Tartu, 2015, 139 p.
242. **Aleksandr Peet**. Intrauterine and postnatal growth in children with HLA-conferred susceptibility to type 1 diabetes. Tartu. 2015, 146 p.
243. **Piret Mitt**. Healthcare-associated infections in Estonia – epidemiology and surveillance of bloodstream and surgical site infections. Tartu, 2015, 145 p.
244. **Merli Saare**. Molecular Profiling of Endometriotic Lesions and Endometria of Endometriosis Patients. Tartu, 2016, 129 p.
245. **Kaja-Triin Laisaar**. People living with HIV in Estonia: Engagement in medical care and methods of increasing adherence to antiretroviral therapy and safe sexual behavior. Tartu, 2016, 132 p.
246. **Eero Merilind**. Primary health care performance: impact of payment and practice-based characteristics. Tartu, 2016, 120 p.
247. **Jaanika Kärner**. Cytokine-specific autoantibodies in AIRE deficiency. Tartu, 2016, 182 p.
248. **Kaido Paapstel**. Metabolomic profile of arterial stiffness and early biomarkers of renal damage in atherosclerosis. Tartu, 2016, 173 p.
249. **Liidia Kiisk**. Long-term nutritional study: anthropometrical and clinico-laboratory assessments in renal replacement therapy patients after intensive nutritional counselling. Tartu, 2016, 207 p.
250. **Georgi Nellis**. The use of excipients in medicines administered to neonates in Europe. Tartu, 2017, 159 p.
251. **Aleksei Rakitin**. Metabolic effects of acute and chronic treatment with valproic acid in people with epilepsy. Tartu, 2017, 125 p.
252. **Eveli Kallas**. The influence of immunological markers to susceptibility to HIV, HBV, and HCV infections among persons who inject drugs. Tartu, 2017, 138 p.
253. **Tiina Freimann**. Musculoskeletal pain among nurses: prevalence, risk factors, and intervention. Tartu, 2017, 125 p.
254. **Evelyn Aaviksoo**. Sickness absence in Estonia: determinants and influence of the sick-pay cut reform. Tartu, 2017, 121 p.
255. **Kalev Nõupuu**. Autosomal-recessive Stargardt disease: phenotypic heterogeneity and genotype-phenotype associations. Tartu, 2017, 131 p.
256. **Ho Duy Binh**. Osteogenesis imperfecta in Vietnam. Tartu, 2017, 125 p.
257. **Uku Haljasorg**. Transcriptional mechanisms in thymic central tolerance. Tartu, 2017, 147 p.
258. **Živile Riispere**. IgA Nephropathy study according to the Oxford Classification: IgA Nephropathy clinical-morphological correlations, disease progression and the effect of renoprotective therapy. Tartu, 2017, 129 p.

259. **Hiie Soeorg**. Coagulase-negative staphylococci in gut of preterm neonates and in breast milk of their mothers. Tartu, 2017, 216 p.
260. **Anne-Mari Anton Willmore**. Silver nanoparticles for cancer research. Tartu, 2017, 132 p.
261. **Ott Laius**. Utilization of osteoporosis medicines, medication adherence and the trend in osteoporosis related hip fractures in Estonia. Tartu, 2017, 134 p.
262. **Alar Aab**. Insights into molecular mechanisms of asthma and atopic dermatitis. Tartu, 2017, 164 p.
263. **Sander Pajusalu**. Genome-wide diagnostics of Mendelian disorders: from chromosomal microarrays to next-generation sequencing. Tartu, 2017, 146 p.
264. **Mikk Jürisson**. Health and economic impact of hip fracture in Estonia. Tartu, 2017, 164 p.
265. **Kaspar Tootsi**. Cardiovascular and metabolomic profiling of osteoarthritis. Tartu, 2017, 150 p.
266. **Mario Saare**. The influence of AIRE on gene expression – studies of transcriptional regulatory mechanisms in cell culture systems. Tartu, 2017, 172 p.
267. **Piia Jõgi**. Epidemiological and clinical characteristics of pertussis in Estonia. Tartu, 2018, 168 p.
268. **Elle Põldoja**. Structure and blood supply of the superior part of the shoulder joint capsule. Tartu, 2018, 116 p.
269. **Minh Son Nguyen**. Oral health status and prevalence of temporomandibular disorders in 65–74-year-olds in Vietnam. Tartu, 2018, 182 p.
270. **Kristian Semjonov**. Development of pharmaceutical quench-cooled molten and melt-electrospun solid dispersions for poorly water-soluble indomethacin. Tartu, 2018, 125 p.
271. **Janne Tiigimäe-Saar**. Botulinum neurotoxin type A treatment for sialorrhea in central nervous system diseases. Tartu, 2018, 109 p.
272. **Veiko Vengerfeldt**. Apical periodontitis: prevalence and etiopathogenetic aspects. Tartu, 2018, 150 p.
273. **Rudolf Bichele**. TNF superfamily and AIRE at the crossroads of thymic differentiation and host protection against *Candida albicans* infection. Tartu, 2018, 153 p.
274. **Olga Tšuiko**. Unravelling Chromosomal Instability in Mammalian Preimplantation Embryos Using Single-Cell Genomics. Tartu, 2018, 169 p.
275. **Kärt Kriisa**. Profile of acylcarnitines, inflammation and oxidative stress in first-episode psychosis before and after antipsychotic treatment. Tartu, 2018, 145 p.
276. **Xuan Dung Ho**. Characterization of the genomic profile of osteosarcoma. Tartu, 2018, 144 p.
277. **Karit Reinson**. New Diagnostic Methods for Early Detection of Inborn Errors of Metabolism in Estonia. Tartu, 2018, 201 p.

278. **Mari-Anne Vals**. Congenital N-glycosylation Disorders in Estonia. Tartu, 2019, 148 p.
279. **Liis Kadastik-Eerme**. Parkinson's disease in Estonia: epidemiology, quality of life, clinical characteristics and pharmacotherapy. Tartu, 2019, 202 p.
280. **Hedi Hunt**. Precision targeting of intraperitoneal tumors with peptide-guided nanocarriers. Tartu, 2019, 179 p.
281. **Rando Porosk**. The role of oxidative stress in Wolfram syndrome 1 and hypothermia. Tartu, 2019, 123 p.
282. **Ene-Ly Jõgeda**. The influence of coinfections and host genetic factor on the susceptibility to HIV infection among people who inject drugs. Tartu, 2019, 126 p.
283. **Kristel Ehala-Aleksejev**. The associations between body composition, obesity and obesity-related health and lifestyle conditions with male reproductive function. Tartu, 2019, 138 p.
284. **Aigar Ottas**. The metabolomic profiling of psoriasis, atopic dermatitis and atherosclerosis. Tartu, 2019, 136 p.
285. **Elmira Gurbanova**. Specific characteristics of tuberculosis in low default, but high multidrug–resistance prison setting. Tartu, 2019, 129 p.
286. **Van Thai Nguyeni**. The first study of the treatment outcomes of patients with cleft lip and palate in Central Vietnam. Tartu, 2019, 144 p.
287. **Maria Yakoreva**. Imprinting Disorders in Estonia. Tartu, 2019, 187 p.
288. **Kadri Rekker**. The putative role of microRNAs in endometriosis pathogenesis and potential in diagnostics. Tartu, 2019, 140 p.
289. **Ülle Võhma**. Association between personality traits, clinical characteristics and pharmacological treatment response in panic disorder. Tartu, 2019, 121 p.
290. **Aet Saar**. Acute myocardial infarction in Estonia 2001–2014: towards risk-based prevention and management. Tartu, 2019, 124 p.
291. **Toomas Toomsoo**. Transcranial brain sonography in the Estonian cohort of Parkinson's disease. Tartu, 2019, 114 p.
292. **Lidiia Zhytnik**. Inter- and intrafamilial diversity based on genotype and phenotype correlations of Osteogenesis Imperfecta. Tartu, 2019, 224 p.
293. **Pilleriin Soodla**. Newly HIV-infected people in Estonia: estimation of incidence and transmitted drug resistance. Tartu, 2019, 194 p.
294. **Kristiina Ojamaa**. Epidemiology of gynecological cancer in Estonia. Tartu, 2020, 133 p.
295. **Marianne Saard**. Modern Cognitive and Social Intervention Techniques in Paediatric Neurorehabilitation for Children with Acquired Brain Injury. Tartu, 2020, 168 p.
296. **Julia Maslovskaja**. The importance of DNA binding and DNA breaks for AIRE-mediated transcriptional activation. Tartu, 2020, 162 p.
297. **Natalia Lobanovskaya**. The role of PSA-NCAM in the survival of retinal ganglion cells. Tartu, 2020, 105 p.

298. **Madis Rahu**. Structure and blood supply of the postero-superior part of the shoulder joint capsule with implementation of surgical treatment after anterior traumatic dislocation. Tartu, 2020, 104 p.
299. **Helen Zirnask**. Luteinizing hormone (LH) receptor expression in the penis and its possible role in pathogenesis of erectile disturbances. Tartu, 2020, 87 p.
300. **Kadri Toome**. Homing peptides for targeting of brain diseases. Tartu, 2020, 152 p.
301. **Maarja Hallik**. Pharmacokinetics and pharmacodynamics of inotropic drugs in neonates. Tartu, 2020, 172 p.
302. **Raili Müller**. Cardiometabolic risk profile and body composition in early rheumatoid arthritis. Tartu, 2020, 133 p.
303. **Sergo Kasvandik**. The role of proteomic changes in endometrial cells – from the perspective of fertility and endometriosis. Tartu, 2020, 191 p.
304. **Epp Kaleviste**. Genetic variants revealing the role of STAT1/STAT3 signaling cytokines in immune protection and pathology. Tartu, 2020, 189 p.
305. **Sten Saar**. Epidemiology of severe injuries in Estonia. Tartu, 2020, 104 p.
306. **Kati Braschinsky**. Epidemiology of primary headaches in Estonia and applicability of web-based solutions in headache epidemiology research. Tartu, 2020, 129 p.
307. **Helen Vaher**. MicroRNAs in the regulation of keratinocyte responses in *psoriasis vulgaris* and atopic dermatitis. Tartu, 2020, 242 p.
308. **Liisi Raam**. Molecular Alterations in the Pathogenesis of Two Chronic Dermatoses – Vitiligo and Psoriasis. Tartu, 2020, 164 p.
309. **Artur Vetkas**. Long-term quality of life, emotional health, and associated factors in patients after aneurysmal subarachnoid haemorrhage. Tartu, 2020, 127 p.
310. **Teele Kasepalu**. Effects of remote ischaemic preconditioning on organ damage and acylcarnitines' metabolism in vascular surgery. Tartu, 2020, 130 p.
311. **Prakash Lingasamy**. Development of multitargeted tumor penetrating peptides. Tartu, 2020, 246 p.
312. **Lille Kurvits.** Parkinson's disease as a multisystem disorder: whole transcriptome study in Parkinson's disease patients' skin and blood. Tartu, 2021, 142 p.
313. **Mariliis Põld.** Smoking, attitudes towards smoking behaviour, and nicotine dependence among physicians in Estonia: cross-sectional surveys 1982–2014. Tartu, 2021, 172 p.
314. **Triin Kikas**. Single nucleotide variants affecting placental gene expression and pregnancy outcome. Tartu, 2021, 160 p.
315. **Hedda Lippus-Metsaots**. Interpersonal violence in Estonia: prevalence, impact on health and health behaviour. Tartu, 2021, 172 p.

316. **Georgi Dzaparidze.** Quantification and evaluation of the diagnostic significance of adenocarcinoma-associated microenvironmental changes in the prostate using modern digital pathology solutions. Tartu, 2021, 132 p.
317. **Tuuli Sedman.** New avenues for GLP1 receptor agonists in the treatment of diabetes. Tartu, 2021, 118 p.
318. **Martin Padar.** Enteral nutrition, gastrointestinal dysfunction and intestinal biomarkers in critically ill patients. Tartu, 2021, 189 p.
319. **Siim Schneider.** Risk factors, etiology and long-term outcome in young ischemic stroke patients in Estonia. Tartu, 2021, 131 p.
320. **Konstantin Ridnõi.** Implementation and effectiveness of new prenatal diagnostic strategies in Estonia. Tartu, 2021, 191 p.
321. **Risto Vaikjärv.** Etiopathogenetic and clinical aspects of peritonsillar abscess. Tartu, 2021, 115 p.
322. **Liis Preem.** Design and characterization of antibacterial electrospun drug delivery systems for wound infections. Tartu, 2022, 220 p.
323. **Keerthie Dissanayake.** Preimplantation embryo-derived extracellular vesicles: potential as an embryo quality marker and their role during the embryo-maternal communication. Tartu, 2022, 203 p.
324. **Laura Viidik.** 3D printing in pharmaceutics: a new avenue for fabricating therapeutic drug delivery systems. Tartu, 2022, 139 p.
325. **Kasun Godakumara.** Extracellular vesicle mediated embryo-maternal communication – A tool for evaluating functional competency of preimplantation embryos. Tartu, 2022, 176 p.
326. **Hindrek Teder.** Developing computational methods and workflows for targeted and whole-genome sequencing based non-invasive prenatal testing. Tartu, 2022, 138 p.
327. **Jana Tuusov.** Deaths caused by alcohol, psychotropic and other substances in Estonia: evidence based on forensic autopsies. Tartu, 2022, 157 p.
328. **Heigo Reima.** Colorectal cancer care and outcomes – evaluation and possibilities for improvement in Estonia. Tartu, 2022, 146 p.
329. **Liisa Kuhi.** A contribution of biomarker collagen type II neoepitope C2C in urine to the diagnosis and prognosis of knee osteoarthritis. Tartu, 2022, 157 p.
330. **Reeli Tamme.** Associations between pubertal hormones and physical activity levels, and subsequent bone mineral characteristics: a longitudinal study of boys aged 12–18. Tartu, 2022, 118 p.
331. **Deniss Sõritsa.** The impact of endometriosis and physical activity on female reproduction. Tartu, 2022, 152 p.
332. **Mohammad Mehedi Hasan.** Characterization of follicular fluid-derived extracellular vesicles and their contribution to periconception environment. Tartu, 2022, 194 p.
333. **Priya Kulkarni.** Osteoarthritis pathogenesis: an immunological passage through synovium-synovial fluid axis. Tartu, 2022, 268 p.

334. **Nigul Ilves.** Brain plasticity and network reorganization in children with perinatal stroke: a functional magnetic resonance imaging study. Tartu, 2022, 169 p.
335. **Marko Murruste.** Short- and long-term outcomes of surgical management of chronic pancreatitis. Tartu, 2022, 180 p.
336. **Marilin Ivask.** Transcriptomic and metabolic changes in the WFS1-deficient mouse model. Tartu, 2022, 158 p.
337. **Jüri Lieberg.** Results of surgical treatment and role of biomarkers in pathogenesis and risk prediction in patients with abdominal aortic aneurysm and peripheral artery disease. Tartu, 2022, 160 p.
338. **Sanna Puusepp.** Comparison of molecular genetics and morphological findings of childhood-onset neuromuscular disorders. Tartu, 2022, 216 p.
339. **Khan Nguyen Viet.** Chemical composition and bioactivity of extracts and constituents isolated from the medicinal plants in Vietnam and their nanotechnology-based delivery systems. Tartu, 2023, 172 p.
340. **Getnet Balcha Midekessa.** Towards understanding the colloidal stability and detection of Extracellular Vesicles. Tartu, 2023, 172 p.
341. **Kristiina Sepp.** Competency-based and person-centred community pharmacy practice – development and implementation in Estonia. Tartu, 2023, 242 p.
342. **Linda Sõber.** Impact of thyroid disease and surgery on patient's quality of voice and swallowing. Tartu, 2023, 114 p.
343. **Anni Lepland.** Precision targeting of tumour-associated macrophages in triple negative breast cancer. Tartu, 2023, 160 p.
344. **Sirje Sammul.** Prevalence and risk factors of arterial hypertension and cardiovascular mortality: 13-year longitudinal study among 35- and 55-year-old adults in Estonia and Sweden. Tartu, 2023, 158 p.